Investigation of operating parameters in a vertical stirred mill

By:

Garren Chad Edwards

BSc. Eng. (Chemical), University of Cape Town

A thesis submitted to the University of Cape Town as fulfillment of the requirement for the degree of

Master of Science in Chemical Engineering

Supervised by: André van der Westhuizen

Department of Chemical Engineering

University of Cape Town

February 2016

Plagiarism Declaration

I declare that this thesis, submitted in fulfilment for a degree of Master of Science in Chemical Engineering at the University of Cape Town, is my own work. I understand the meaning of plagiarism, and all work that is not mine has been properly acknowledged.

Garren Chad Edwards

Acknowledgments

First and foremost I would like to thank my parents and my siblings Dale, Toni-lee and Devon! Chenéy – I thank you for always being patient through the duration of my MSc.

I thank the CMR lab staff for the duration of my MSc. A special mention for Rubin, who has helped me for a large portion of my experiments. My supervisor, Andre, I thank you for your input and setting up of this project. Your attention to all detail is astounding; I hope this characteristic of you will rub off on me more in the future.

Finally I would like to thank Lonmin and Tharisa Minerals for their input into this project.

Table of Contents

Abstract

Due to the depletion of coarser grained ores, more mineralogically complex ores are being treated. These complex ores usually have finer grained valuable minerals. Liberation of these finer grained valuable minerals lies in grinding finer. Grinding to these fine sizes is energy intensive and using standard ball mills are energy inefficient at these sizes (P80 < 75μm). Therefore, stirred mills are becoming increasingly prevalent in the mineral processing industry. In order to optimize these mills, the effects and mechanisms of the significant variables need to be understood.

This project investigated operating parameters against performance in a laboratory scale vertical stirred mill (Deswik mill), in an ultrafine grinding (UFG) application of MG2 reef in the bushveld igneous complex. The operating variables that were investigated are stirrer speed, solids concentration, media size and media filling. The Kwade stress energy model was tested on the grinding results. The grinding performance was quantified in two ways, i.e. grinding efficiency and grinding rate. The grinding performance for this study was also investigated through a statistical analysis. The experiments was designed using a face centred central composite design (FCCD) and the results was statistically analysed using a design of experiments (DOE) software.

The results show that the Kwade stress energy model is applicable to this mill and can be very useful to find the most efficient operating conditions for this system. The best energy utilization conditions occur at the optimum stress energies range of $1 \cdot 10^{-3}$ Nm – $3 \cdot 10^{-3}$ Nm.

$$\frac{Rate_{SA}}{EU_{SA}} \; \alpha \; \frac{P_m}{\left(\dot{m}_p \cdot \tau_{grind}\right)}$$

The efficiency, rate and power draw was taken to be the main indicators of performance in a vertical stirred mill, and can be linked as shown by the proportionality equation above. The effect that the operating variables have on these performance indicators was shown to vary over the course of the grinding process.

The following table shows where the best efficiencies and grinding rates occurs using a one variable at a time approach:

Variable	Best Efficiency	Lowest Power	Fastest Rate	Highest Power
Stirrer speed	8 m/s	8 m/s	12 m/s	12 m/s
Solids concentration	40 % Solids	40 % Solids	20 % Solids	20 % Solids
Mill filling	65 % (shifting to 75 % at higher Ecs)	65 %	75 %	75 %
Grinding media size	1.5 mm	1.5 mm	1.5 mm	3.0 mm

It was observed that there is a trade-off between efficiency and grinding rate in terms of stirrer speed and solids concentration.

Regression models for efficiency, rate and power draw was developed to explore the design space. The regression models was optimised to obtain a high efficiency and low rate and again optimised to obtain a high rate and low efficiency. Based on the optimisation results a high power draw coincided with having a high rate, and a low power draw coincided with a high efficiency. The regression optimisation results was as expected and follows the best efficiency and best rate results observed in the one variable approach with the exception of solids concentration that factors in the low efficiency and low rate in the analyses.

The following table shows the variables ranking, and is based on the variables sensitivity to change at 10 kWh/t, using the regression model developed:

Variable Ranking	Δ P80 (Efficiency) [μm]	Δ Rate [m²/kg/min]	Δ P [W]
Stirrer Speed	1.93 **(2)**	3.57 **(2)**	44.94 **(1)**
Solids concentration	2.62 **(1)**	5.89 **(1)**	9.16 **(4)**
Grinding media size	1.40 **(3)**	1.19 **(4)**	11.93 **(3)**
Mill filling	0.00 **(4)**	1.75 **(3)**	24.63 **(2)**

Based on the range of the variables investigated in this study and the lack of optimum turn around points, a broader range of the operating parameters is recommended for future studies as shown below:

Variable	Investigated	Recommended
Stirrer speed	8 m/s – 12 m/s	4 m/s – 16 m/s
% Solids	20 % - 40 %	10 % - 80 %
% Mill filling	65 % - 85 %	40 % - 90 %
Media size	1.5 mm – 3.0 mm	1 mm – 6 mm

It is also recommended that a comparative study between a vertical and horizontal stirred mill be done, as horizontal stirred mills are more prevalent in the South African minerals processing industry.

List of Figures

List of Tables

List of Symbols

SF	Stress frequency	[s^{-1}]
$SN/SN_F/SN_M$	Stress numbers	[-]
SE/SE_{GM}	Stress energies or stress intensities	[Nm]
N_C	Number of media contacts	[-]
P_S	Probability of being struck by media	[-]
N_P	Number of particles in stirred mill	[-]
$t_c/t_{grind}/t$	Residence time	[s]
ν_t/n	Speed of stirrer	[m/s]
E_{CS}	Specific energies	[kWh/t]
P80	Size through which 80 % product particles pass	[um]
F80	Size through which 80 % feed particles pass	[um]
ϱ_{GM}	Density of grinding media	[kg/m^3]
ϱ	Density of slurry	[kg/m^3]
d_{GM}	Media diameter	[m]
ϕ_{GM}	Mill filling	[-]
ε	Media voidage	[-]
c_V	Solids concentration	[-]
D_{discs}	Diameter of stirrer disks	[m]
P/P_m	Power of mill	[W]
m_p	Mass of product	[kg/s]
ν_E	Energy transfer factor	[-]
$c_{L,I}$	Energy loss factors	[-]

1. INTRODUCTION

Comminution is a physical process, and in a mineral processing context it is the crushing and grinding of larger ore particles into smaller particles using specialised crushing and grinding equipment. This is done to liberate or unlock the valuable minerals from the unwanted or gangue minerals, so that the valuable minerals can be separated from the gangue minerals through the exploitation of its physical and chemical properties. The adequate liberation of valuable minerals has become harder in recent years due to the depletion of high grade and coarse grained ore bodies. Low grade and fine grained ore bodies are now regularly mined and poses significant challenges to the traditional comminution stages in terms of liberation of valuable minerals.

Tumbling mills are the dominant grinding comminution equipment in both coarser and finer grinding due to their ability to process large throughputs. Tumbling mills are energy intensive and are energy inefficient at fine and ultrafine grinding levels as such an alternative grinding technology to ball mills was developed and adapted from other industries namely stirred mills.

Stirred mills have found wide acceptance in mineral processing operations due to the improved efficiencies over tumbling mills. Stirred mills can be categorised into two main types: horizontal stirred mills and vertical stirred mills. Although the geometry of these stirred mills differs, the breakage mechanisms are thought to be similar. The introduction of stirred mills into the South African platinum industry has brought its benefits, and assessing the most important variables of stirred mills will lead to a more energy efficient operation. A number of researchers (Mankosa et al., 1989; Zheng et al., 1996; Kwade et al., 1996; Jankovic, 2003; He et al., 2006) have identified and assessed important variables in the operation of vertical and horizontal stirred mills.

In favour of energy efficiency and increased liberation benefits, stirred mills have become the preferred comminution device in fine and ultrafine grinding circuits.

1.1 Research objectives

The aim of this thesis is to investigate the effect and influence of a selection of operating parameters on the performance (energy efficiency and grinding rate) of a vertically stirred mill. The key operating parameters studied during this project are:

- Stirrer speed
- Grinding media mill filling
- Grinding media size
- Solids concentration on a mass basis

The objectives of the study are:

- To initially determine if ultrafine grinding has an effect on the flotation response for this ore, and if so
- Test the stress energy methodology in a vertical stirred mill (a methodology that describes the effect of different operating variables into one concept, i.e. stress energy – which was developed in a horizontal stirred mill (Kwade et al., 1996))
- Determine the relationships between key operating parameters on the stress energies, product size, energy efficiency (energy utilization) and grinding rates in the stirred mill
- Determine the most energy efficient and best grinding rate conditions in the design space

1.2 Hypotheses

The hypotheses are listed below and explained using grinding performance (grinding efficiency and grinding rate):

Stirrer speed

- An increase in stirrer speed would result in an increase in mill efficiency, followed by an optimum, then decrease in mill efficiency.
- The power draw will increase as the mill speed is increased.
- The grinding rate would increase as the mill speed is increased.
  Explanation:
    - The mill speed controls media motion and this in turn affects the collision rate and energy transfer between media and particles in the stirred mill. The frequency and energy of collisions in the mill increases as the speed increases until a point is reached where more energy is used to break particles than is necessary, and energy is wasted. There is an optimum mill efficiency.
    - Increasing the stirrer speed would increase the mechanical energy consumption.
    - The rate continues to increase due to the increase in collision frequency and energy at high speeds.

Solids concentration

- An increase in solids concentration would result in an increase in grinding efficiency, followed by an optimum, then a decrease in both efficiency.
- An increase in solids concentration would result in an increase in power draw.
- An increase in solids concentration would result in an increase in grinding rate, followed by an optimum, then a decrease in rate.
  Explanation:
    - At low slurry densities there are more media on media collisions due to a low solid particle content (low efficiency and low rate). At high slurry densities there are more particle on particle collisions and a dampening effect occurs between media and particles causing a loss in energy. The suspension viscosity also increases which leads to more viscous heat losses and the media velocity is limited due to this increase in viscosity. By this reasoning there is an optimum performance in terms of efficiency and rate between low and high slurry densities.

- As the stirred mill load increases due to an increase in solids concentration, the power draw will increase.

Media size

- At low energy inputs larger media are more energy efficient, while at high energy inputs smaller media are more energy efficient, because the optimum media size decreases as the product particle size decreases.

Mill filling

- An increase in mill filling would result in an increase in efficiency, followed by an optimum, then decrease in efficiency, because the grinding media mill filling affects the media – particle collision rate.
- An increase in mill filling would result in an increase in power draw, because the mass in the mill increases.
- An increase in mill filling would result in an increase in rate, followed by an optimum, then decrease in rate, because the grinding media mill filling affects the media – particle collision rate.

  Explanation:
  - An increase in the frequency of media on particle collisions would result when increasing the media load, but if the media load is too high (>80%), more media on media collisions would take place and energy is wasted.
  - There is an optimum for both energy efficiency and grinding rate.

1.3 Thesis structure

The research objectives and hypotheses are proposed to outline the central themes of this thesis. Overall, the scope of this thesis is to investigate the effect of the most important operating parameters in a vertically stirred mill. It is with this in mind that stirred mills are reviewed in Chapter 2. This includes looking at different types of stirred mills, the effects of operating parameters and fundamental models developed for stirred mills. The experimental chapter, Chapter 3, describes the equipment and materials used and outlines the procedures used to test the hypotheses and research objectives. Chapter 4 presents the research results and then discusses the findings in relation to literature and the validity of the hypotheses and objectives. The conclusions, Chapter 5, concludes and consolidates the theme of this thesis, and recommendations for further work are presented.

2. LITERATURE REVIEW

Comminution is a process whereby material is reduced from a coarser feed size to a finer product size (Kwade, 2004). Once the valuable minerals are liberated it is separated from the unwanted or gangue minerals through various downstream separation processes such as flotation, leaching, gravity separation, magnetic separation etc.

The first stage in comminution is the crushing of the ore followed by grinding. Depending on the wanted product particle size, different crushing and grinding equipment are used. The focus of this study is the investigation of operating parameters in a vertical stirred media mill which is normally used for grinding of F80's < 75 μm.

The need to grind finer in the minerals industry has arisen due to the depletion of coarser grained ore bodies and the subsequent increased treatment of finer disseminated and more mineralogically complex ore bodies (Partyka & Yan, 2007). This has led to the emergence of a new grinding technology being used in the mineral processing industry, stirred media mills. Stirred mills can be regarded as relatively new to the minerals processing industry, however it has been used extensively in the ceramic, paint and pharmaceutical industries (Jankovic, 2003). These mills attempt to grind finer than tumbling mills and liberate the valuables in finer grained ore bodies. Conventional tumbling mills are energy inefficient at P80 grind sizes of < 75 μm when compared to stirred mills. Jankovic (2003) presents a comparison schematic between stirred mills and ball mills which is shown in Figure 2.1, it illustrates that stirred mills are more energy efficient than tumbling mills when grinding to P80 particle sizes of < 100 μm.

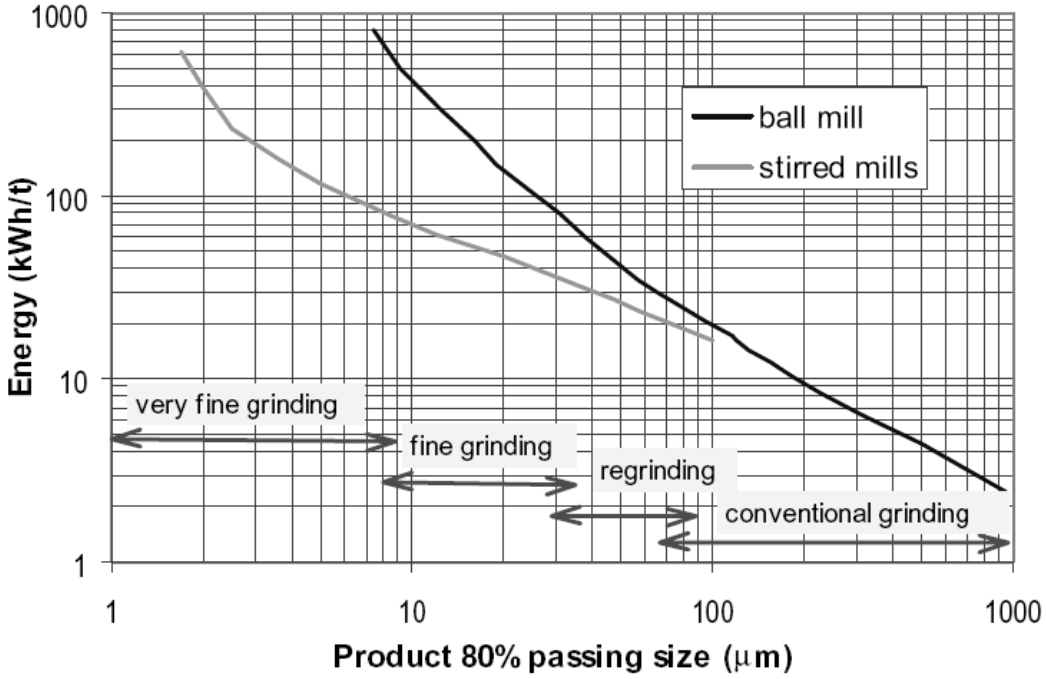

Figure 2.1: Schematic showing energy consumption versus product size (P80) comparison for stirred milling and conventional ball milling (Jankovic, 2003)

2.1 Stirred media mills

Stirred mills consist of a fixed cylinder, fitted with a stirrer/agitator placed in this cylindrical chamber. The grinding chamber is filled with media and mineral slurry containing the particles to be ground. The operating conditions in the mineral processing industry are different to that of the other industries where stirred mills are used (ceramic, paint, pharmaceutical and food industries) however the principles of the mill operation remain the same.

Rule (2011), at the time, listed all the stirred mill operations in the South African PGM industry, shown in Table 2.1. The stirred mills in the table below will be discussed in more detail in the following sections, i.e. the Deswik mill, Metso SMD and IsaMill™.

Table 2.1: Stirred mill installations in the South African PGM industry (Rule, 2011)

Operator	Operation	number of stirred mills	type	installed power kW	application
PGM Concentrators					
Anglo Platinum/JVs	WLTR	1	IsaMill™ M10000	2600	UFG/MIG
	Waterval UG2	2	IsaMill™ M10000	6000	MIG
	Mogalakwena South	3	IsaMill™ M10000	9000	MIG
	Mogalakwena North	4	IsaMill™ M10000	12000	MIG
	Waterval	4	IsaMill™ M10000	12000	MIG
	Amandelbult	4	IsaMill™ M10000	12000	MIG
	Amandelbult	1	IsaMill™ M3000	1500	UFG
	Mogalkwena North	1	IsaMill™ M10000	3000	UFG
	Waterval	1	IsaMill™ M10000	3000	UFG
	Mototolo	1	Metso SMD™ 355	355	UFG
RBR	BRPM	1	IsaMill™ M10000	3000	MIG
Lonmin	Eastern Platinum C	1	IsaMill™ M3000	1000	UFG
	Eastern Platinum A/B	1	Metso SMD™ 355	355	UFG
Platmin	Boynton	1	IsaMill™ M3000	1500	MIG
PGM Tailings retreatment					
Impala	Rustenburg TRP	2	Metso SMD™ 355	710	UFG
Platinum Mile	Paardekraal TRP	2	Metso SMD™ 355	710	UFG
	Paardekraal TRP	2	Deswik-2000 litre	1065	UFG/MIG
Chromite tailings retreatment					
Aquarius/JV	RK1 chromite tails	1	Deswik-1000 litre	500	MIG
Sylvania	Steelpoort	2	Metso SMD™ 185/18.5	203.5	UFG/MIG
	Lannex	1	Metso SMD™ 185/18.5	185	UFG/MIG
	Lannex	1	Kings	75	MIG
	Millsell	2	Metso SMD™ 185/18.5	203.5	UFG/MIG
Tharisa	Brits chrome TRP	1	Deswik-500 litre	220	MIG

2.1.1 Knelson-Deswik mill (now FLSmidth vertical stirred mill)

Knelson-Deswik mills are vertical stirred mills with perforated discs designed for fine grinding applications. Figure 2.2 shows a typical Knelson-Deswik mill. It was originally designed for use in the pigment industry in South Africa during the mid 1990's. The feed enters the bottom of the mill and the product exits the top of the mill through media retention screens and into the product launder.

According to Rahal et al. (2011) process and mill variables related to the Knelson-Deswik range includes:

- Feed material size no coarser than 300 μm – 400 μm.
- Slurry density of 1.2 kg/L – 1.5 kg/L for open circuit grinding, which was obtained through empirical testing of a wide range of materials.
- Slurry flow rate is dependent on the grinding application.
- The mill has the highest grinding efficiency when operated at a mill speed of between 10 m/s – 12 m/s. The Knelson-Deswik is a "medium" speed stirred mill and falls between the "low" and "high" range of stirred mills operating at <3m/s and >15m/s respectively as shown in Table 2.2.
- Media load varies between 65 % and 80 %.

Table 2.2: Comparison of power intensity and tip speed for different stirred mill technologies (Rahal et al., 2011)

Type	*Power Intensity (kW/m^3)*	*Tip Speed (m/s)*
Tower Mill (Vertimill™)	20-40	< 3
Vertical Pin Stirred Mill	50-100	< 3
Knelson-Deswik Mill	240-765	10-12
Horizontal Stirred Mills	300-1000	> 15

Figure 2.2: Knelson-Deswik Stirred Mill

2.1.2 Stirred Media Detritor (SMD)

Stirred Media Detritors (SMD's) are manufactured and sold by Metso Minerals Ltd. The mill is a vertical stirred pin mill as shown in Figure 2.3. These mills operate at low impeller speeds of < 3 m/s.

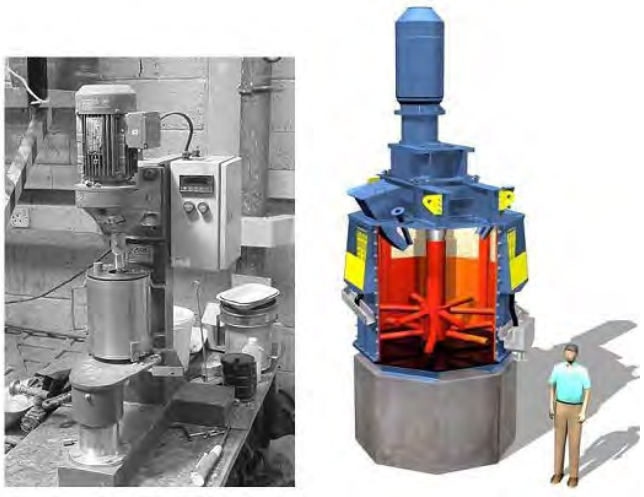

Figure 2.3: Lab scale and Industrial Scale SMD mills

The feed particle size to SMD's should be less than 250 μm and the product particle size can be ground to less than 5 μm. The feed enters through a port at the top of the mill and is directed to the bottom, where it enters the mill below the stirring vortex. The product exits the mill through media retention screens situated around the top of the mill and into an external launder. The typical solids concentration for SMD's should be between 30 % - 60 % solids with an optimum grinding efficiency occurring between 40 % - 50 % solids (Metso, 2015). Some advantages of the SMD's include (Metso, 2015):

- Low operating costs
    - Low wear and low maintenance
- The power intensity is high enough to induce proper grinding but not high enough for the need of a cooling jacket around the stirred mill

2.1.3 IsaMill™

The IsaMill™ was developed by Mt. Isa Mines and Netzsch-Feinmahltechnik GmbH during the 1990's, to grind the fine grained ore at the Mt. Isa mines. Since then IsaMills™ have been installed in many operations around the world. The IsaMill™ is a horizontal high speed mill with perforated discs as shown in Figure 2.4. The IsaMill™ grinding media motion and flow is shown in Figure 2.5.

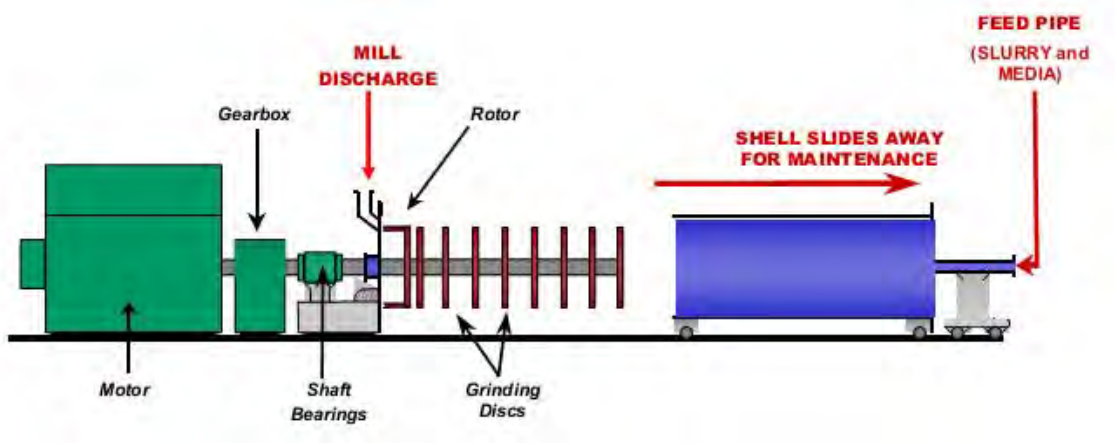

Figure 2.4: IsaMill™ layout (Burford and Clark, 2007)

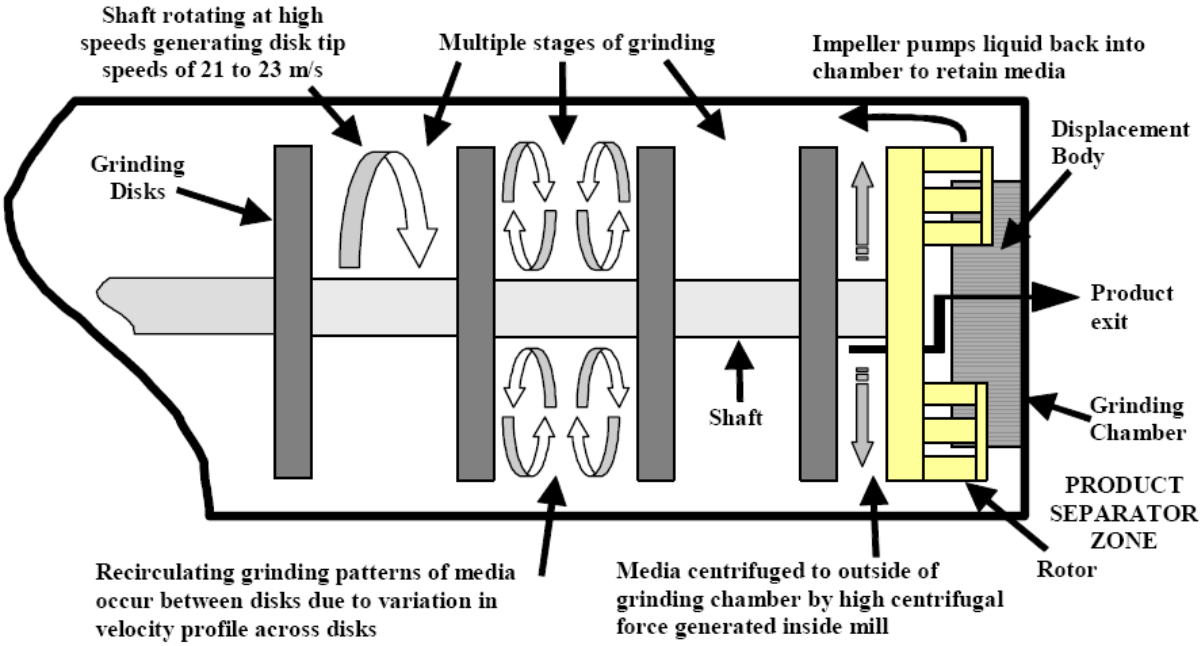

Figure 2.5: IsaMill™ grinding mechanism (Burford and Clark, 2007)

The advantage the IsaMill™ has over other stirred mills is its capability of stirring at high speeds and having a product separator inside the stirred mill. The high speeds allow the IsaMill™ to have higher power intensities and faster grinding times than vertical stirred mills of the same volume. The product separator keeps the media inside the mill with no need for additional media retention screens.

2.2 Operating parameters of stirred milling

As early as 1971, 44 variables were identified that affected performance in a stirred media mill (Blecher et al, 1996**)**. The optimisation of energy utilisation in stirred media mills is dependent on the complex interactions between these variables. The significant variables can be categorised as mill configuration or process state (Rahal et al, 2011). Figure 2.6 shows some critical operating variables in stirred media mills.

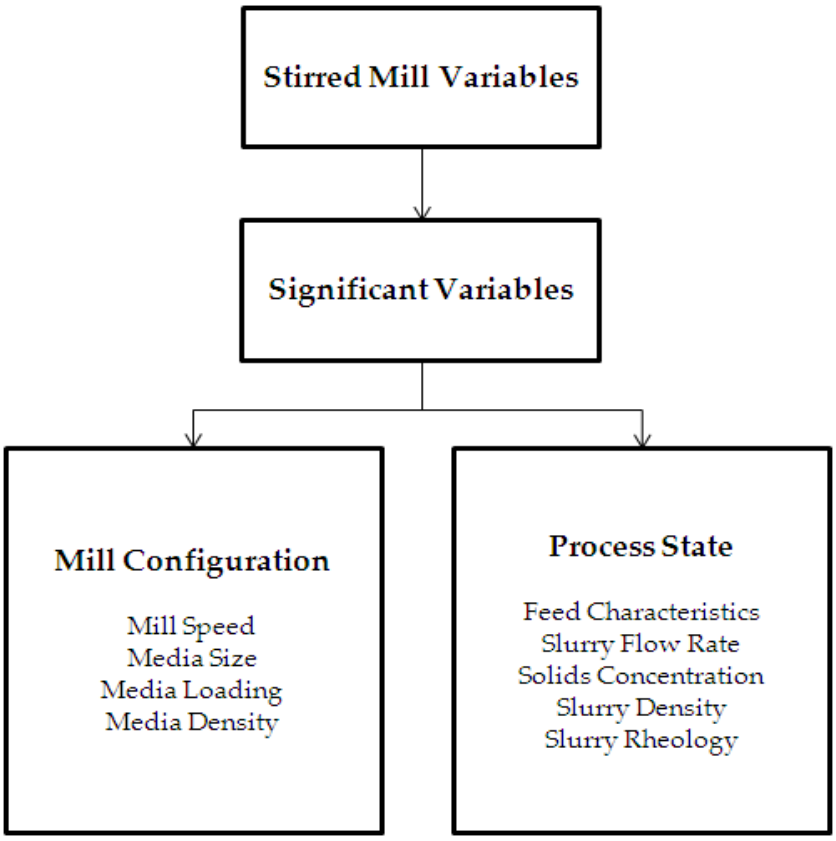

Figure 2.6: Critical operating variables of stirred media mills (Rahal et al, 2011)

The sections that follow will highlight the importance of the operating parameters of stirred mills to be investigated in this study.

2.2.1 Stirrer speed and the effect it has on media motion

Stirrer speed has been shown to affect the energy efficiency and energy input in stirred mills. Determining the optimum stirrer speed is crucial for ensuring that the stirred mill is running efficiently. The ranges of stirrer speeds that have been tested in literature vary from study to study depending on the stirred mill arrangement and impellors used. The typical ranges of vertical mill speeds studied using pin-type impellors are: 200 – 330 rpm by Mankosa et al. (1986), 200 – 1350 rpm by Mankosa et al. (1989), 260 – 1000 rpm by Zheng et al. (1996) and 450, 1000 – 1500 rpm by Jankovic (2003). The speed ranges of horizontal stirred mills using perforated disc-type impellors are higher than that of the vertical stirred mill pin-type impellors. Typical horizontal stirred mill speeds studied are: 2130 – 4370 rpm by Bel Fadhel and Frances (2001) and 1500 – 2500 rpm by Outtara and Frances (2003).

When stirrer speed is increased the energy input and product fineness are increased, but energy efficiency declines (Zheng et al, 1996). This agrees with the work by Mankosa et al. (1989), which shows a decrease in product fineness with decreasing stirrer speed at a constant energy input, and that low stirrer speeds are more energy efficient than high stirrer speeds. The work by Jankovic (2003) highlights that the best efficiency occurs at low stirrer speeds too. In the study by Bel Fadhel and Frances (2001), they showed using horizontal stirred mills that lower speeds operate more efficiently than higher speeds. Again in the work by Outtara and Frances (2003), they show that lower stirrer speeds are more energy efficient than the higher stirrer speeds. Increasing the stirrer speed leads to higher collision rates and collision energies between the media and the particles. This leads to a faster grind time but at the cost of energy efficiency. Regardless of the orientation of the stirred mill it is always observed that lower stirrer speeds are more energy efficient than higher stirrer speeds.

The stirrer speed and impellor type also directly affects the flow fields and motion of grinding media in stirred mills. The media motion and flow fields in stirred mills are complex and have been studied using DEM (discrete element method), CFD (computational fluid dynamics) and PEPT (positron emission particle tracking).

To understand the complex fundamental mechanisms in stirred media mills better, the motion of media and slurry in stirred media mills needs to be investigated. Blecher et al. (1996) numerically developed and investigated the flow fields in a horizontal stirred mill for a laminar stirred and homogenous Newtonian fluid, and studied its effects on the motion and trajectories of single grinding beads. The work by Blecher et al. (1996) is a simplistic model for the complex motion fields in stirred mills. Important factors such as particle-particle interactions, particle-media interactions, the effect of

a particle size distribution and turbulence amongst others on the flow fields have been ignored, but serves as a good reference for the continual study on the fundamental mechanisms in stirred mills. During this work they noted that there exist two high energy intensive zones where most grinding would take place, a zone around the stirred discs with high tangential and radial velocity gradients and a zone near the chamber wall with a high axial fluid transport gradient. These zones are shown in Figure 2.7. From this work a characteristic motion index was developed that explains a single bead motion in horizontal stirred media mills, and describes the mean ratio between centrifugal and inertial forces of a single bead.

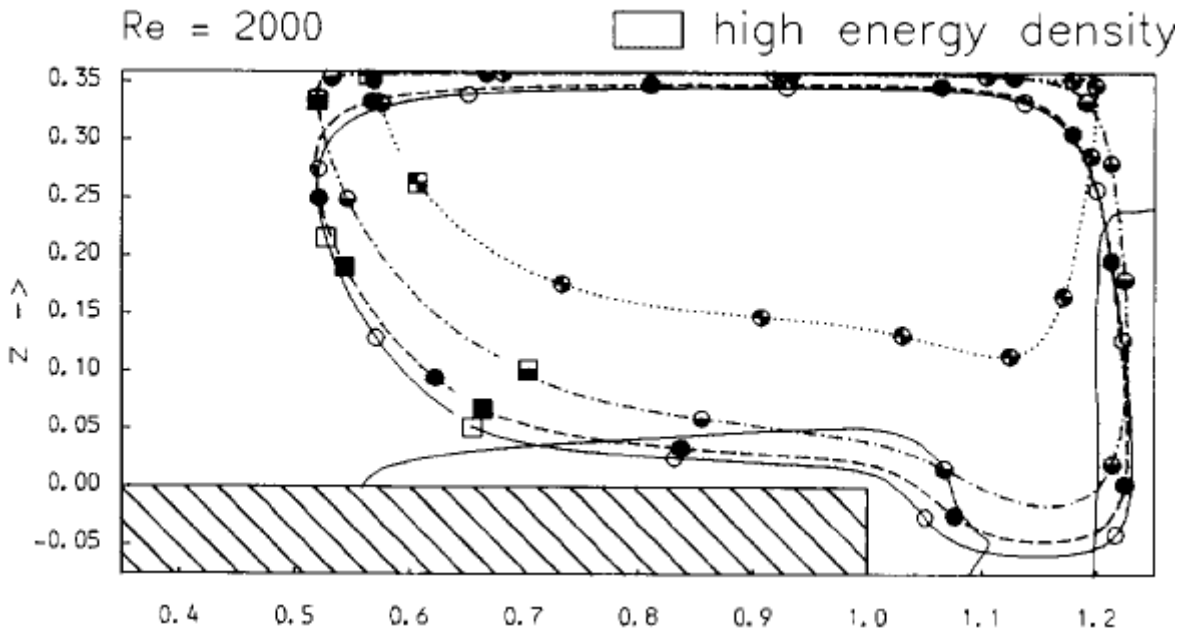

Figure 2.7: High energy density zones in horizontal stirred mill (Blecher et al., 1996)

The advent of more powerful computers has led to better numerical and simulation results for the motion of media in stirred mills. Sinnot et al. (2006) examined media motion, energy consumption and the collision environment using a DEM simulation approach in vertical stirred mills. Jayasundara et al. (2006, 2008, 2009, 2010, and 2011) studied the effects of different parameters on media and slurry motion in a horizontal stirred mill using DEM models, combined DEM-CFD models and PEPT as validation (van der Westhuizen et al, 2011). The complex motion of media in stirred mills will be continually investigated due to all the interactions of the parameters that occur in a stirred mill in both orientations and different stirrer types.

2.2.2 Media size

Media plays an important role in the grinding efficiency of stirred mills. The most important media factors are size, density and hardness. Typical media sizes used in stirred mill operations are less than < 6 mm.

Media size is claimed to be an important parameter in fine grinding. The following studies shows that the grinding result is strongly affected by the media size (Mankosa et al., 1986; Blecher et al., 1996; Kwade et al., 1996; Bel Fadhel and Frances, 2001). Mankosa et al. (1986) studied the effects of media size in a low-speed vertical stirred mill with a pin-type stirrer on coal. The energy-specific breakage rate (tons/kWh) was found to be at an optimum when the media/feed particle ratio was 20:1, where a monosize feed was used. This study shows that the media selection needs to be made in conjunction with the feed size. Blecher et al. (1996) showed that when the grinding media are small, the media tend to follow the flow streamlines and enter zones of high energy density (Figure 2.7) because of higher drag forces, as compared to larger media which have a higher inertial force. This means that smaller media has a higher probability to influence the grinding result, as smaller media enters into the high energy zones more frequently than larger media. Kwade et al. (1996) studied the comminution of limestone in a horizontal stirred mill with a perforated disc stirrer. Their results show that at low specific energies larger media yield a finer product (d50), whereas at high specific energies smaller media yields a finer product (d50). As the product becomes finer with increasing energy input, the media size influences the grinding result and having a combination of small and larger media in the mill would be beneficial. Bel Fadhel and Frances (2001), studied the comminution of gibbsite in a horizontally stirred mill with a disc stirrer and the results agree with the work of Kwade et al. (1996). The work shows that at low specific energies larger media are preferable, while at high specific energies smaller media are preferable. However, from this work, the mean ratio of media/feed size was found to be between 20 and 200 which conflicts with the work by Mankosa et al. (1986). This is possibly due to different feed conditions and different stirred mill geometries.

From the review above, it follows that selecting the best grinding media size is dependent on the feed size, the required product size and the specific energy input.

2.2.3 Media density and elasticity

The grinding media are the carriers of energy in a stirred mill and transfer the energy to the feed particles during a collision. The transfer of energy depends on the kinetic energy of the media. The density and elasticity of the media play an important role in the transfer of energy from the stirrer to the feed particles during a collision. More dense media have more stored energy due to its higher mass, and less elastic media transfer more energy during collisions.

Zheng et al. (1996) showed that more dense media (steel at density of 7.8 g/cm^3) generates finer product particles but are less energy efficient than less dense (glass at density of 2.5 g/cm^3) media due to an increase in mill energy consumption. Becker et al. (2001) showed the effect of grinding media density and elasticity on specific energy in a horizontal stirred mill with discs using limestone and fused corundum as feed. In the study the Young's Modulus (a measure of stiffness of an elastic material) is shown to have an impact on the energy supplied to the stirred mill. Media with a high Young's Modulus have a higher transferrable energy compared to media with a lower Young's Modulus.

Extensive research focused on grinding media has recommended that media used in high energy stirred mills have the following structural and physical combinations (Graves and Boehm, 2007):

- High hardness and fracture toughness
- Fine grain structure and high surface stability
- Low friction coefficient

If constant grinding media bead mass is retained, media size and media density are obviously linked and the selection of the type of media will play an important role in the performance of the grinding in a stirred mill. In mineral processing operations zirconia based ceramic grinding media are typically used as it satisfies the above recommendations.

2.2.4 Solids concentration and slurry rheology

Solids concentration and particle size distribution have a major effect on the slurry rheology in fine grinding. The surface properties dominate the system when the particles are of ultrafine sizes and the solids concentration is high (He et al., 2004). In mineral processing, the solids concentration is traditionally controlled by the addition or removal of water. At low solids concentrations the particles have a low chance to be trapped between the grinding media, while at higher solids concentrations the probability of being trapped is increased. Zheng at al. (1996) shows that there is an optimum solids concentration for which energy efficiency is a maximum. Their results show that as the solids concentration increases the energy efficiency increases to an optimum, then decreases as the solids concentration is further increased. Jankovic (2003) showed results that are in accordance with the results obtained by Zheng et al. (1996), in that an increase in solids concentration results in an increase in stirred mill efficiency. However Jankovic (2003) speculates that a maximum efficiency occurs as the tested solids concentration range was not high enough. In the work by Mankosa et al. (1989), it is seen that as the solids concentration is increased the torque increases. Their result is expected as power (and torque) is proportional to the slurry concentration when the power number of the system is constant. However at very high solids concentrations and very fine sizes the viscosity controls the power draw and torque of the system (Zheng et al., 1996).

2.2.5 Media filling

The grinding media filling refers to the bulk volume fraction of grinding media in the stirred mill. The media filling has a direct impact on the power draw in the stirred mill. Van der Westhuizen et al. (2010) noted the existence of an optimum mill filling in horizontal stirred mills. In vertical stirred mills Weller and Gao (1999) suggested that as long as the media covers a minimum number of stirrers, an increase in the mill filling would increase the grinding volume, but the efficiency in the grinding volume would not increase. The limit on media filling in vertical stirred mills is fixed by the minimum height of the media separation zone at the top of the mill or the position of the top stirrer to the product outlet (Weller and Gao, 1999).

2.3 Breakage mechanisms in stirred mills

Breakage in comminution occurs through three different mechanisms i.e. abrasion, cleavage and fracture (more commonly known as abrasion, impact and compression respectively). This is shown in Figure 2.8 and all these mechanisms occur in the grinding process but normally one mechanism is dominant in the process. Tuzun et al. (1995) observed that 1st order breakage occurs in a vertical stirred mill using a feed of 100% passing 100μm and grinding down to median size of 2μm. 1st order breakage in stirred mills is also observed in the work of Yue and Klein (2005), however below a P80 of 10μm a non-linear relationship is observed which suggests a change in the grinding mechanism. Hogg (1999) developed a theoretical model and suggested that abrasion is a dominant mechanism in ultrafine grinding and developed a combined abrasion – fracture model to describe the breakage in stirred mills. Hogg (1999) shows that abrasion increases the grinding process and leads to an appearance of a non-first-order breakage function in ultrafine grinding.

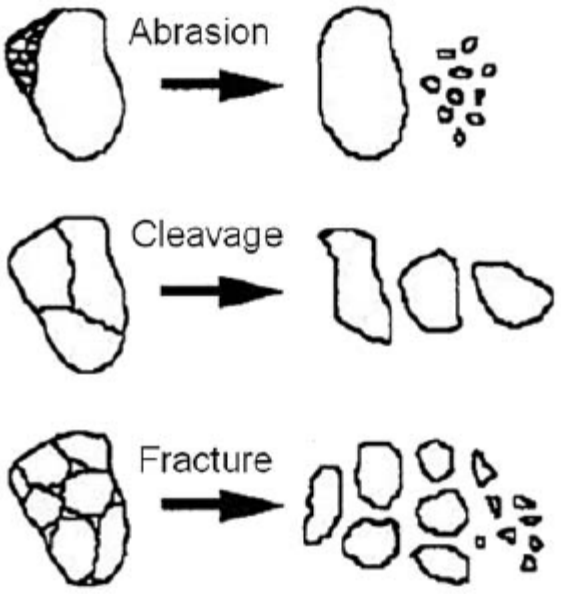

Figure 2.8: Mechanisms of breakage (Hennart et al., 2009)

2.4 Stress models and energy considerations

2.4.1 Introduction

Energy input is required to reduce coarse particles to fine and ultrafine particles as shown in Figure 2.9. Finer particles contain less internal flaws and become more uniform in structure so the energy required to break finer particles are greater than that of coarser particles. The required specific energy input is affected by the mill design, macroscopic conditions and also on the properties of the individual particles (Wang and Forssberg, 2007).

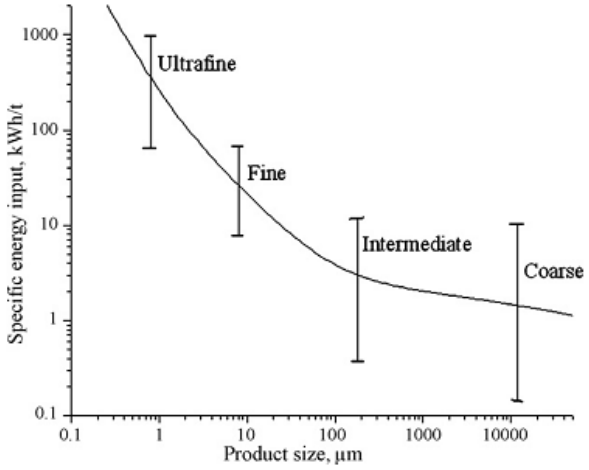

Figure 2.9: Required specific energy for size reduction (Wang & Forssberg, 2007)

The description, selection and design of comminution processes are based mainly on practical experience and empirical relations (Kwade, 2004). Kwade (2004) has developed physical grinding models for stirred media mills called stress models. These stress models were developed to explain the physical processes in horizontal stirred media mills as opposed to looking at it as a "black-box". There are two ways in which the grinding process can be looked at in these stress models: the mill related stress model and product related stress model (Kwade, 2004).

2.4.2 Mill related stress model

The mill related stress model explains how the mill stresses the particles, how frequent a stress event takes place and which energy is available at the stress events. This stress model describes what occurs in the mill from the mills perspective. Mill characteristic numbers are defined and are independent of product particle size and properties. The grinding behaviour of the mill is described by Kwade (2004) as:

- The type of stress event (impact, shear or compression) and number of particles stressed at one event,
- The number of stress events supplied by the mill per unit time i.e. frequency of stress events SF_M, and
- The energy which is supplied by the mill at each stress event i.e. stress energy, SE

The product of the frequency of stress events, SF_M, and mean comminution time, t_c, is defined as the total number of stress events, SN_M. The mean comminution time to achieve a certain product quality and with it the total number of stress events, SN_M, are a function of stress energy, SE, and the breakage behaviour of the product (Kwade, 2004). The stress energy is not constant at all stress events and is defined as the transfer of energy at a stress event. The stress energy can be described as a distribution.

Figure 2.10 shows a frequency distribution of stress energy. The distribution describes the stress frequency and how often the stressing occurs at a given stress energy.

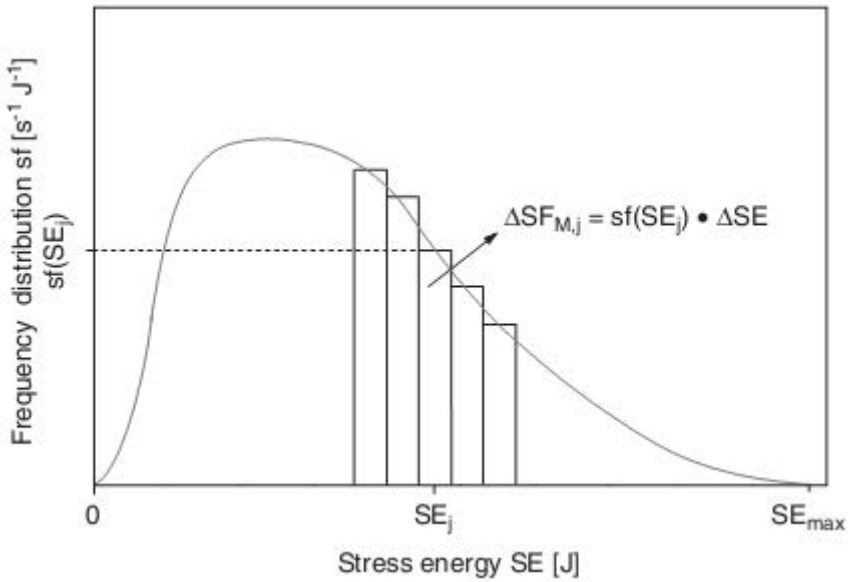

Figure 2.10: Qualitative frequency distribution of the stress energy (Kwade, 2004)

2.4.3 Product related stress model

The product related stress model explains how the particle is stressed, the frequency of particle stresses and the intensity at which the particle is stressed. This stress model describes what occurs in the mill from the particles perspective. In order to describe the grinding of a particle, the number and size of the particles need to be considered. The grinding principle is described by Kwade (2004) and is determined by:

- How the feed and resulting particles are stressed (shear, impact or compression),
- How often the feed and resulting particles are stressed i.e. the number of stress events of the feed particle, SN_F, and
- How high the specific energy at each stress event is i.e. SE

In comminution processes the feed and fragment particles are stressed with different stress energies at different times and the SN_F and SE are thus characterised by distributions because of these intermittent collisions (Kwade, 2004).

2.4.4 Relation between stress models and specific energy input

The total energy transferred to the particles can be estimated by the summation of stress energies of all individual stress events. This is represented by the area beneath the curve in Figure 2.10. The specific energy transferred to the product particles, $E_{CS,P}$, is determined by relating the stress energy to total mass of product, m_P. This relationship is shown in equation 2.1 below:

$$\frac{\sum_{i=1}^{SN_M} SE_i}{m_{P,tot}} = \frac{\sum_{j=1}^{n} SE_j \cdot \Delta SF_{M,j}}{m_{P,tot}} \cdot t_c = \frac{SN_M \cdot \overline{SE}}{m_{P,tot}} = E_{cs,p} = \upsilon_E \cdot E_{cs,M} \tag{2.1}$$

Where:

- SN_M – Stress number
- SE – Stress energy
- SF_M – Stress frequency
- $m_{P,tot}$ – Total mass of product
- t_c – Residence time
- υ_E – Energy transfer factor
- E_{cs} – Specific energy

The energy transferred to the particles is proportionally related to the energy consumed by the mill by an energy transfer factor, or energy efficiency, ν_E.

The stress number of the grinding process can be defined as:

$$SN_M = \frac{N_c P_s}{N_p} \tag{2.2}$$

Where:

- N_C – Number of media contacts,
- P_S – Probability that a particle can be struck, and
- N_P – Number of product particles in the mill

The stress number for the grinding crystalline materials is shown in equation 2.3 after substituting proportional conditions for N_C, P_S, and N_P (Kwade, 1999). From equation 2.3 a relative stress number can be calculated and the influence of operating parameters on the stress number can be investigated.

$$SN_M \; \alpha \; \frac{\varphi_{GM}(1-\epsilon)}{(1-\varphi_{GM}(1-\epsilon))c_v} \cdot \frac{nt_c}{d_{GM}^2} \tag{2.3}$$

Where:

- SN_M – Stress number
- φ_{GM} – Mill filling
- ε – Voidage
- c_v – Solids concentration
- n – Stirrer speed
- t_c – Residence time
- d_{GM} – Grinding media size

2.4.5 Application of stress models in stirred mills

2.4.5.1 Energy transfer in stirred media mills

The transfer of energy in stirred mills can occur in different ways as shown in Figure 2.11. The most important transfer of energy takes place between the grinding media and the particles as shown by C, D and E in Figure 2.11.

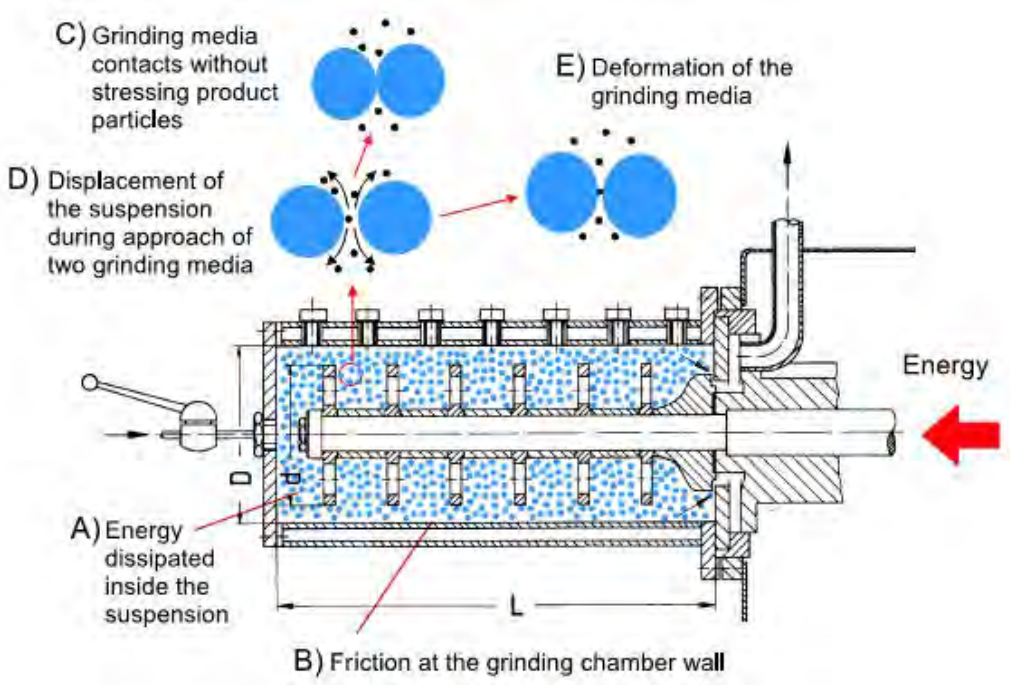

Figure 2.11: Energy dissipation in a stirred mill (Kwade, 2004)

Based on the energy transfer in stirred mills, the energy transfer factor in stirred mills can be defined by equation 2.4, where $c_{L,i}$ are the loss factors defined in Figure 2.11:

$$v_E = \prod_{i=a}^{E}(1 - c_{L,i}) \tag{2.4}$$

Where:

- v_E – Energy transfer factor
- $c_{L,I}$ – Energy loss factors

2.4.5.2 Stress model in horizontal stirred media mills

The stress energy in horizontal stirred media mills developed by Kwade et al. (1996) can be described by equation 2.5:

$$SE\ \alpha\ SE_{GM} = d_{GM}^3(\rho_{GM} - \rho)v_t^2 \tag{2.5}$$

Where:

- SE_{GM} – Stress Energy of the Grinding Media
- d_{GM} – Diameter of Grinding Media
- v_t – Stirrer Tip Speed
- ϱ_{GM} – Density of Grinding Media
- ϱ – Slurry Density

Based on the assumptions by Kwade et al. (1996), equation 2.5 is only valid if:

- The viscosity of the suspension is not too high;
- The tangential velocity is proportional to the stirrer tip speed
- The geometry of the mill is not changed, and
- The young's modulus of the product material is low compared to the young's modulus of the grinding media (Becker et al, 2001);

Figure 2.12 shows that stress energy can be used to describe the effect of the grinding media operating parameters of diameter, density and stirrer tip speed at constant solids concentration and media filling, to obtain an optimum grind size (Kwade, 1996). To operate a stirred mill most effectively, the mill should operate at the optimum stress intensity.

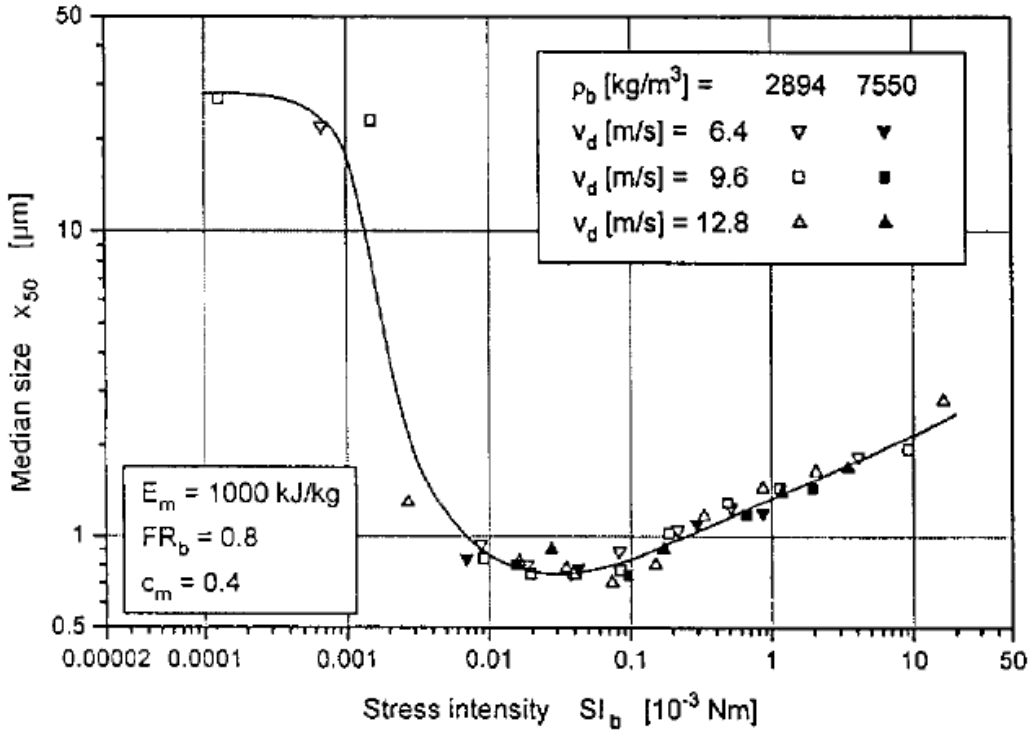

Figure 2.12: Relationship between specific energy, stress energy and median product particle size (d50) (Kwade et al., 1996)

Stender et al. (2004) using the stress models, have shown how stirred mills of varying size but at the same operating conditions have different optimum stress intensities, as shown in Figure 2.13. Mills of varying size have different energy transfer coefficients and energy efficiencies, and these energy transfer coefficients should be considered when scaling up stirred media mills.

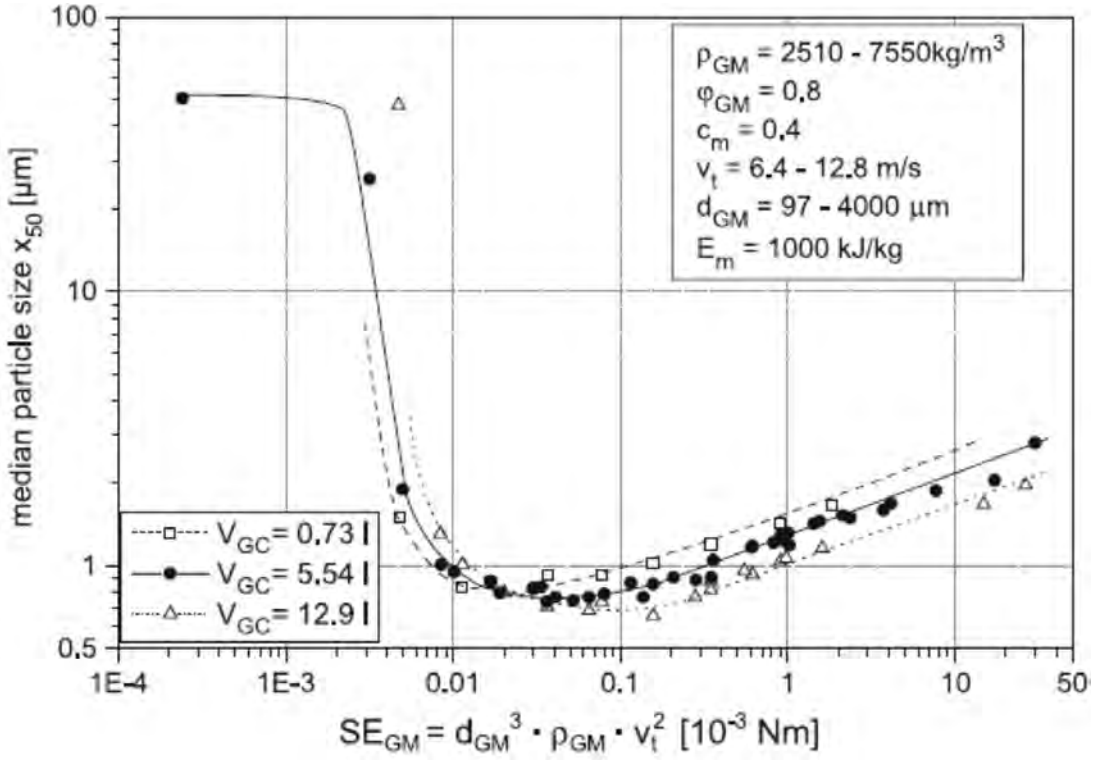

Figure 2.13: Stress energy versus median product particle size (d50) for mills of varying size (Stender et al., 2004)

2.4.5.3 Stress model in vertical stirred mills

Jankovic (2001) looked at media stress energy in vertical stirred mills, using limestone. He noted that due to height, gravitational acceleration needed to be considered. An additional relationship of stress energy was developed for vertical stirred mills, taking gravitational acceleration into account. The relationship is shown below:

$$SE_{GM} = d_{GM}^2(\rho_{GM} - \rho)gh \tag{2.6}$$

Where:

- g – Gravitational Acceleration
- h – Media Height

The total stress energy in vertical stirred mills is the sum of both stress energy expressions. In vertical stirred mills at lower stirrer speeds the gravitational

component dominates whereas at high stirrer speeds the centrifugal component dominates (Jankovic, 2001). Figure 2.14 shows the stress energy versus particle size for vertical stirred mills. The same characteristic stress energy trend is seen like the horizontal stirred mills shown in Kwade et al., 1996.

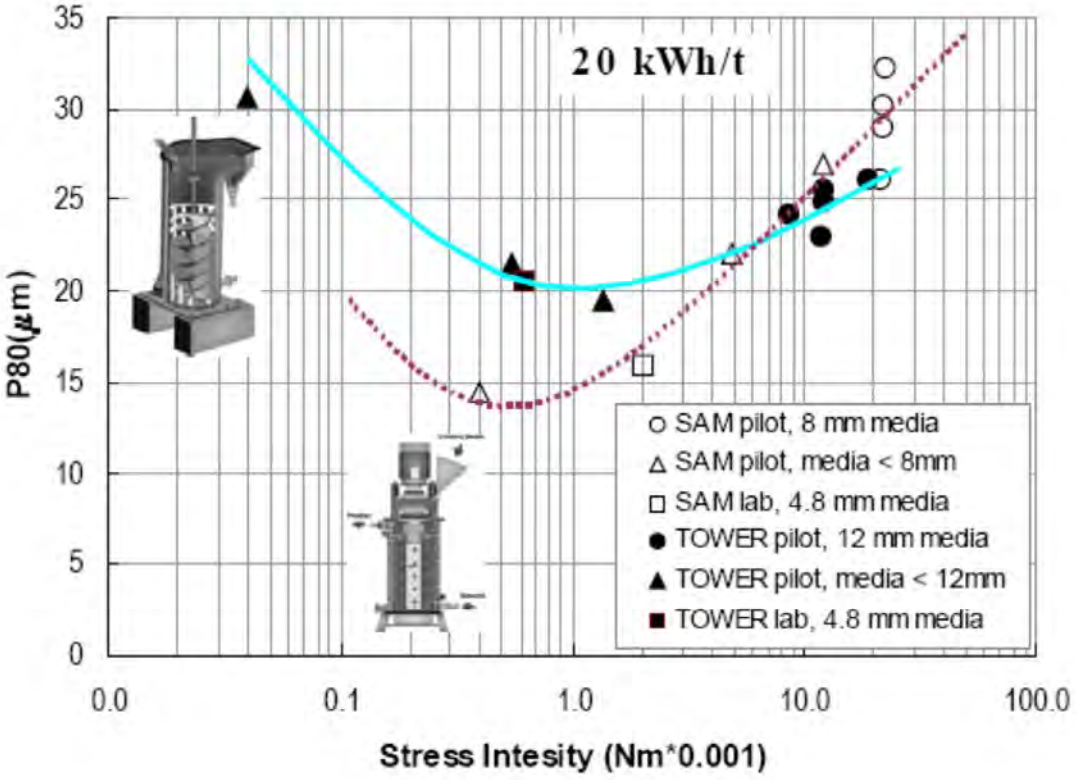

Figure 2.14: Stress energy versus particle size for vertical stirred mills (Jankovic, 2001)

2.4.6 Conclusion

The work conducted by Kwade et al. (1996) and Jankovic (2001) provides useful physical models that describe the stress energy of grinding media in stirred mills which is proportional to the total stress energy of the system. By using the models the optimum stress energy of the particles can be determined. The stress models are therefore useful in the optimisation process of a stirred mill.

2.5 Effects of fine grinding on froth flotation

During the froth flotation process the surface properties of minerals involved in the process are exploited, resulting in the separation of the wanted minerals from the gangue minerals. If the minerals are not adequately liberated, and locked in or attached to the gangue, it can lead to low recovery due to minerals reporting to the tails, or low grade due to the locked minerals reporting to the concentrate.

Stirred mills are used in two main areas of application in a typical PGM concentrator – mainstream inert grinding (MIG), P80 < 45 μm (Rule, 2011), to mainly improve recovery, and ultrafine grinding (UFG), P80 < 25 μm (Rule, 2011), to mainly improve concentrate grade.

In fine grinding operations ceramic media is used as opposed to steel media, as it is metallurgically inert in flotation. Steel releases iron into solution and causes the precipitation/adsorption of iron hydroxides onto the mineral surfaces (Rule, 2011).

Figure 2.15(A) shows a typical recovery versus particle size curve for flotation plants, where coarser and finer particles are floated together. Figure 2.15(B) shows a conceptual depiction where fine particles are treated without coarser particles.

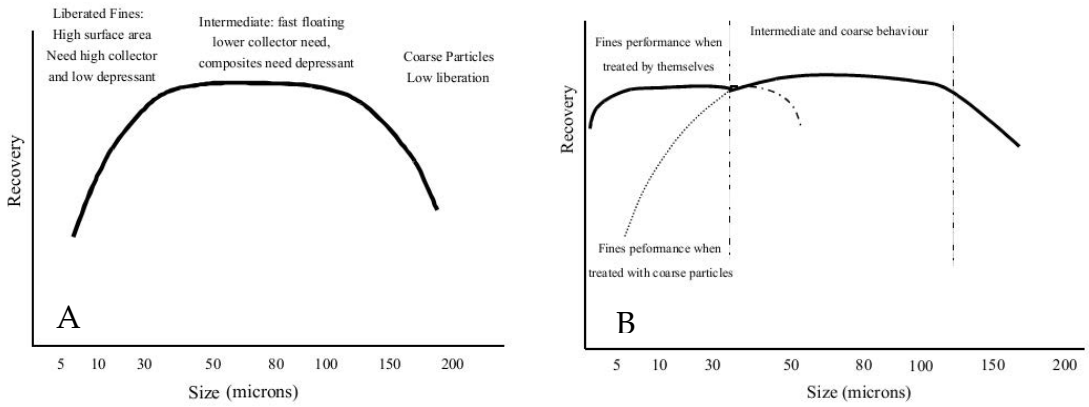

Figure 2.15: A – Conventional recovery versus particle size curve, B – Fines treated alone (Pease et al., 2006)

The figures show the benefits of grinding finer and treating the fines separately.

2.6 Conclusion

As ore become more complex and the valuable mineral grain sizes become smaller, the means to recover these minerals lie in grinding finer. Grinding to the sizes needed to liberate theses minerals is energy intensive and using the standard mineral processing technology of ball mills is energy inefficient. The ability of stirred mills to grind to these sizes at better energy efficiencies than ball mills sees stirred mills becoming more prevalent in the mineral processing industry. The research focus to date has mainly been on the operating conditions, mill configuration, energy requirements and breakage mechanisms.

Common stirred milling technologies used in South Africa is the Isamill, SMD and Knelson-Deswik mill (FLSmidth). This study will focus on a three litre Knelson-Deswik mill. A key focus of this study is the optimisation of energy requirements based on the stress model approach developed by Kwade et al. (1996) and determining the effect of the chosen operating variables on the material used in the test work.

3. RESEARCH METHODOLOGY

3.1 Introduction

This chapter describes all the equipment and methods used to conduct successful experiments.

3.2 Experimental materials and methods

All experiments were conducted in a Deswik laboratory scale vertical stirred milling rig as shown in Figure 3.1.

Figure 3.1: Stirred mill and ancillary equipment

3.2.1 Grinding equipment

The grinding takes place in the three litre vertical grinding chamber shown in Figure 3.2. The grinding chamber body is made of stainless steel and lined with polyurethane. The grinding chamber has a media retention screen of 1 mm attached above the grinding chamber, to keep the grinding media within the stirred vessel. At the top of the grinding chamber is a product launder for discharging the product slurry. The stirred mill also has a water cooling jacket to maintain the temperature of the slurry, if needed.

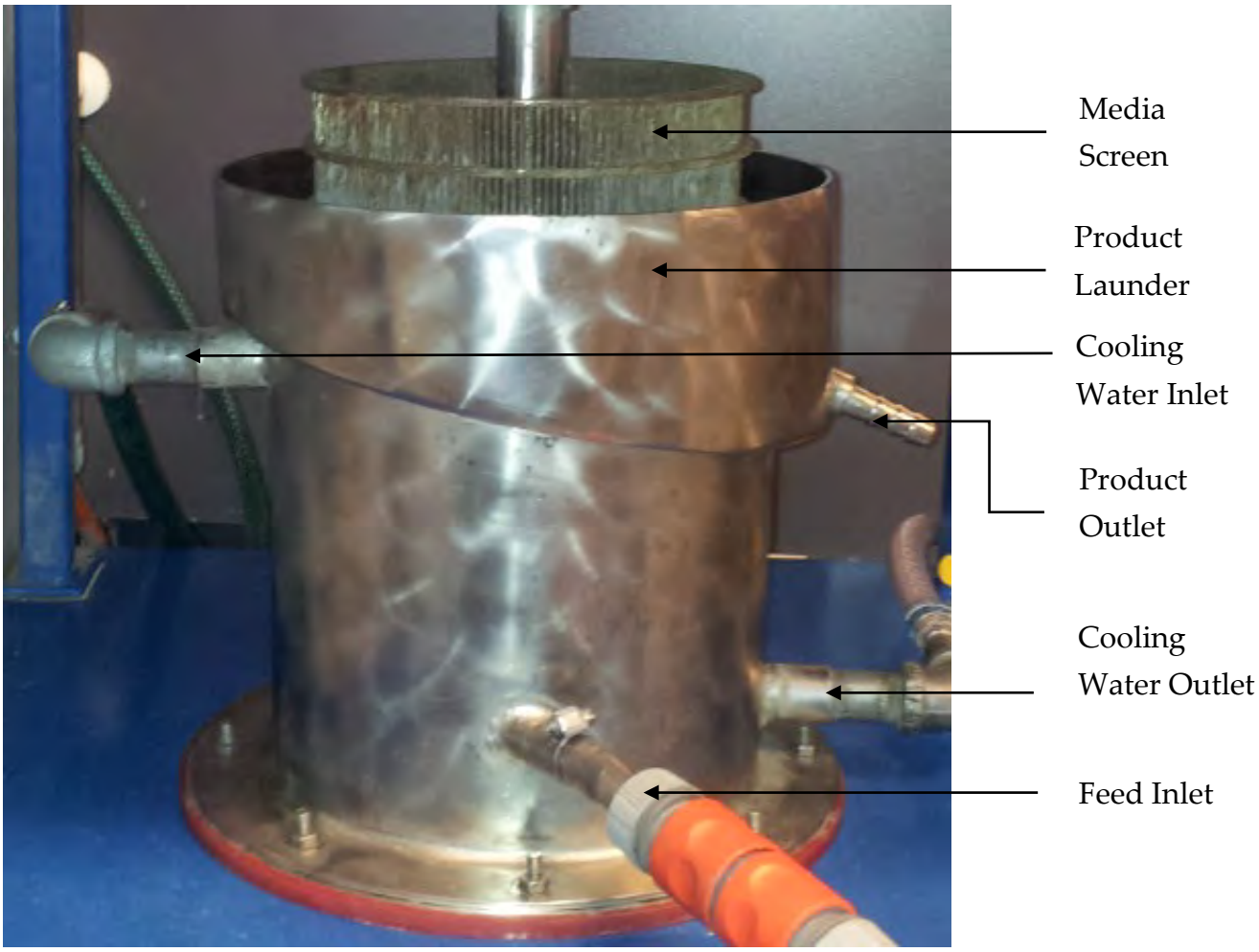

Figure 3.2: Grinding chamber

The grinding impellor is placed in the grinding chamber, and consists of a 25 mm diameter stainless steel shaft connected to a 3 kW electric motor, as shown in Figure 3.3. There are five grinding disc spacers of 50 mm diameter and four larger 120 mm grinding discs made of polyurethane.

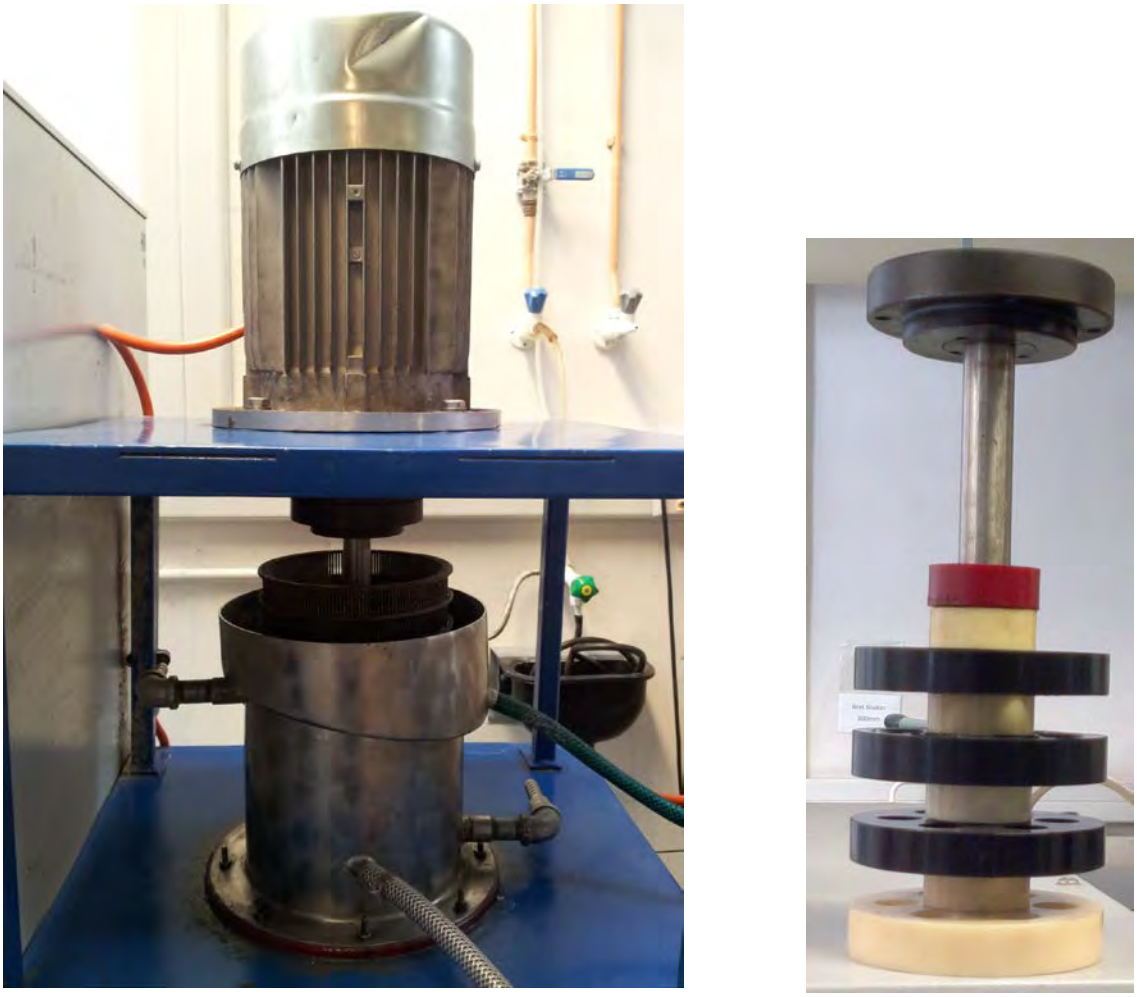

Figure 3.3: Stirred mill and grinding impellor

The ancillary equipment connected to the rig are the feed and product tanks, a peristaltic pump, control panel and fluke power meter as shown in Figure 3.4.

Figure 3.4: Setup showing tanks and pump

3.2.2 Mill instrumentation

The mill power, mixing tank agitator and pump speed are controlled via a touch screen control panel which communicates with the PLC to make changes to the system. The control panel is shown in Figure 3.5. The secondary feed tank is controlled via a variable speed drive not connected to the main control panel. A Fluke 1735 3-Phase power logger was used to log the power over the duration of the experiments, and a Lutron DT-2236 tachometer was used to measure the stirrer speed. These devices are shown in Figure 3.6.

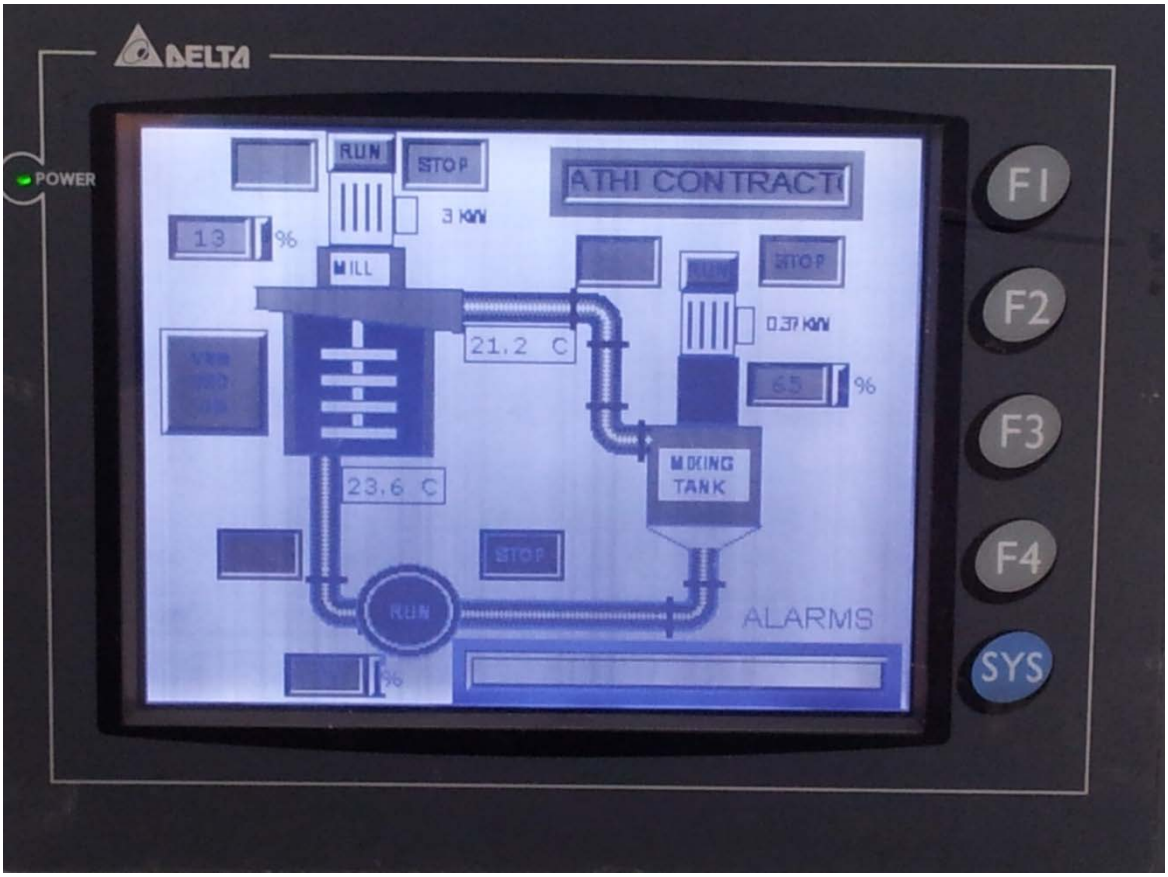

Figure 3.5: Control panel

Figure 3.6: Tachometer and Fluke power logger

3.2.2.1 Stirrer speed calibration

The disc stirrer speed was adjusted using the percentage of mill speed, which is the control input for stirrer speed. The mill stirrer speed, rpm's or m/s, were obtained using the digital tachometer. Figure 3.7 shows the outcome of this calibration.

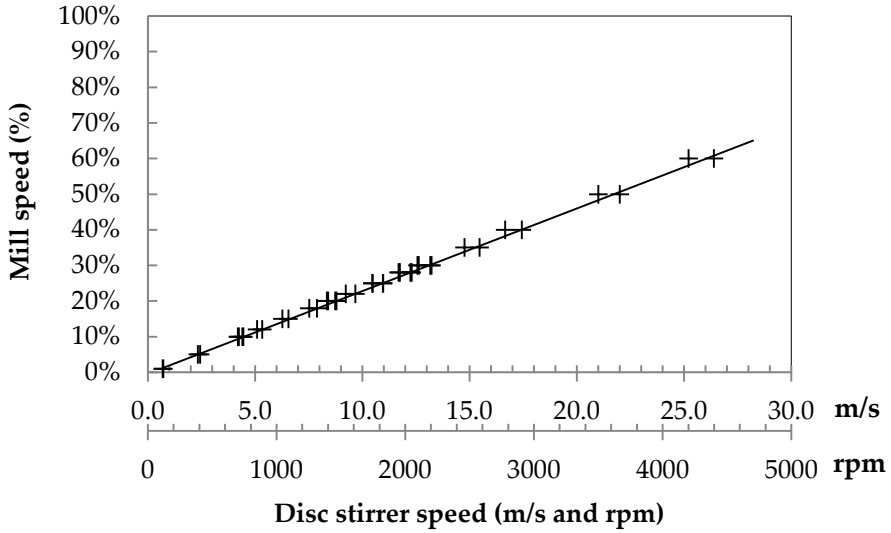

Figure 3.7: Stirrer disc speed calibration

3.2.2.2 Power calibration

The stirred mill electrical power was measured using a Fluke 1735 Power Logger. The Power Logger consists of four current clamps, four voltage probes and the device itself, which were connected to the mill motor. All electrical information needed to calculate the power was logged on the device, and uploaded to a PC for analysis.

The no load electrical power conditions were logged at experiment conditions before each experiment. The mill was then charged with media and slurry, and the gross electrical power logged. The net power for each experiment is the difference between the gross electrical power and the no load electrical power.

$$\text{Net Power} = \text{Gross Power} - \text{No Load Power} \quad (3.1)$$

3.2.3 Operation of mill

The experimental setup is shown in Figure 3.8. At the start of each experiment a no load power test was conducted. The power was measured using the Fluke 1735 Power Logger, after which the grinding media was added to the mill. For the duration of the experiment the gross power was recorded. The net power was then calculated from the difference between the no load and gross power. The slurry was prepared in the feed tank to the correct % solids by mass. After the slurry was well mixed a feed sample of 100 ml was taken, the slurry density measured and the feed flow rate measured. The experiments were run in pass mode for between 8 – 10 passes. A total of 8 – 10 100 ml samples were collected from the mill product for particle size analysis, using a Malvern Mastersizer 2000. All collected samples were subjected to a particle size analysis. The samples were collected after four – five residence times. The feed flow rate was kept constant and was on average 1.13 L/min. The slurry was then pumped through the stirred mill, once the slurry had exited the mill for approximately 15 seconds the product line was diverted to the product tank. When the feed tank was empty the grinding was stopped and the product and feed lines for the system were swapped, making the feed tank now the product tank, and the product tank now the feed tank. The same process was repeated for each successive pass.

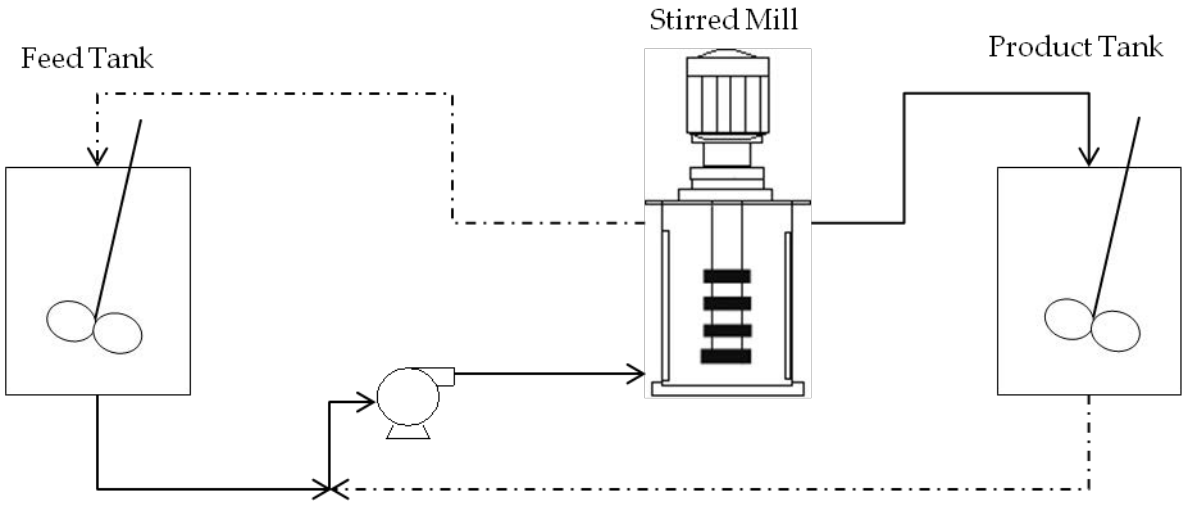

Figure 3.8: Experimental Setup

3.2.4 Batch flotation procedure

A 3 L flotation cell was used for the batch flotation tests. A total of 8 experiments were completed i.e. 4 experiments at different grinds completed in duplicate. The % solids of the flotation feed were maintained at 20 % - 25 %. The impeller speed and air flow rates were 1200 rpm and 7 L/min respectively.

The reagent conditions used are shown in Table 3.1. The collector, SIBX, was added to the feed tank ahead of grinding, allowing for sufficient conditioning of newly ground particles during the grinding process. The depressant, Sendep 30, was added to the flotation cell with slurry and conditioned for 2 min thereafter the frother, DOW 250, was added and conditioned for 1 min.

Table 3.1: Reagent Conditions

SIBX	220 g/t
DOW 250	40 g/t
Sendep 30	76 g/t

Four concentrates were collected at 15 second intervals for 0 -2 min, 2 – 6 min, 6 – 12 min and 12 – 20 min. The concentrates were collected in containers from the flotation cell product launder. The tailings were collected after the last concentrate was collected. The wet concentrates and tailings were filtered and dried and the dry masses were recorded. The grinding feed samples collected before flotation were analysed for particle size distribution using a Malvern Mastersizer 2000. The concentrate and tailings samples collected were analysed for nickel and copper to serve as a proxy for the PGM responses in a base metal sulphide type ore.

The recovery and grade of nickel and copper were calculated as follows:

$$Recovery\ (\%) = \frac{\%\ of Ni/Cu\ in\ Concentrate \times Mass\ of\ Concentrate}{\%\ of Ni/Cu\ in\ Feed \times Mass\ of\ Feed} \qquad (3.2)$$

$$Grade\ (\%) = \frac{\%\ of Ni/Cu\ in\ Concentrate \times Mass\ of\ Concentrate}{Mass\ of\ Concentrate} \qquad (3.3)$$

The cumulative grades and recoveries were calculated and reported.

3.2.5 Material used

The ore used for the study was the MG2 seam of the MG reef layers from the bushveld igneous complex, which is a dominantly chromitite rich ore. A flotation cleaner tails stream was used in this study. Approximately 300 kg of material was received and the material was prepared for experiments by mixing and splitting out representative feed samples of ten 30 kg batches. The batches were in turn split down to the masses needed for the grinding experiments. Figure 3.9 shows the average particle size distribution of the feed samples. The d80 and d50 values of the feed were 38.67 µm and 15.55 µm respectively.

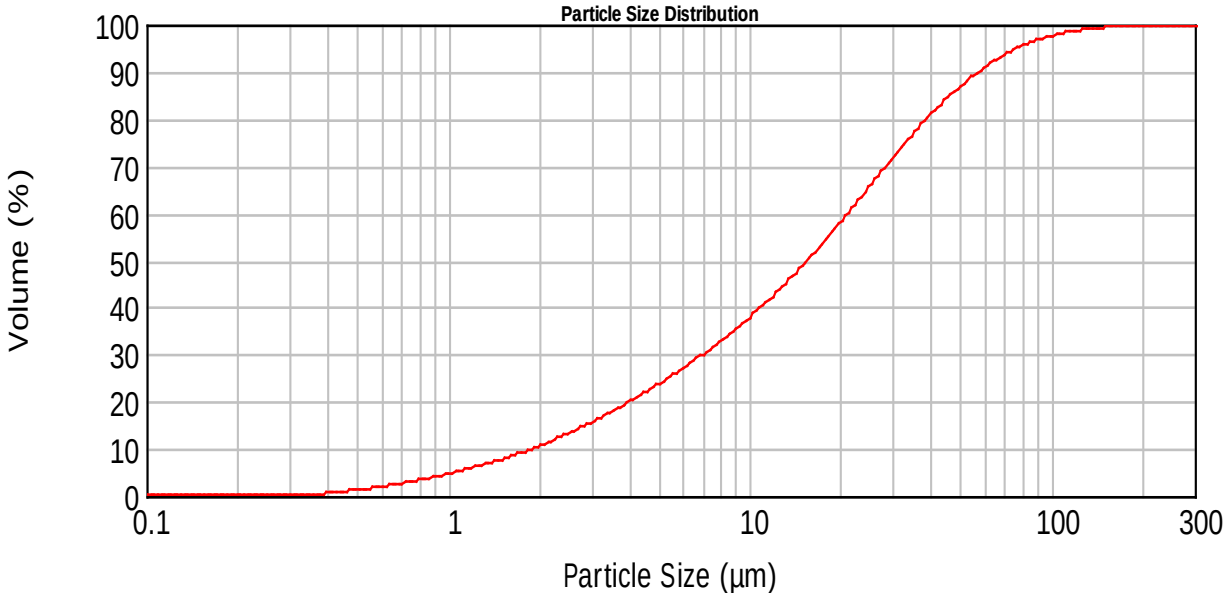

Figure 3.9: Feed PSD

3.2.6 Particle size characterisation

All feed and product samples were analysed by laser diffraction using a Malvern Mastersizer 2000. The system consists of a laser, used to generate a source of light, and a set of detectors for the detection of the scattered light from the particles being analysed. A diffraction model is then used to analyse the data collected by the detectors. The Malvern Mastersizer uses the Mie theory to determine the particle sizes. The Mie theory predicts the intensity of the scattered light off the particle surface and the refracted and transmitted light through the particle to determine the volume of the particle. It allows for accurate results over a broad size range (0.02 μm – 2000 μm).

The Malvern Mastersizer 2000 was calibrated for the material used, by varying the dispersant dosages, the stirrer and pump speeds, the duration of ultrasonic bath sound, the refractive index and the absorption. The conditions for the standard operating procedure, SOP, that gave the least error on the fitted data and residual for the system was chosen as the SOP to be used for the particle size characterisation.

3.3 Design of experiments

The operating variables investigated during this project are shown in Table 3.2. The stirrer speed, % solids, and mill filling were chosen to cover the range of operating settings outlined by Rahal et al. (2011) in a Deswik mill. The media size range was chosen on the basis of typical fine grinding media sizes used in the minerals processing industry.

Table 3.2: Experimental Conditions

	Low (-1)	Centre (0)	High (1)
Stirrer Speed (m/s)	8 (1273 rpm)	10 (1591 rpm)	12 (1909 rpm)
% Solids (c_m / c_v)	20 % c_m / 7.5 % c_v	30 % c_m / 12.4 % c_v	40 % c_m / 17.9 % c_v
Media Size (mm)	1.5	2.0	3.0
Mill Filling (%)	65	75	85

A design of experiments approach was used in setting up the experimental test work. An irregular four factor factorial design was chosen in order to construct a predictive model for the variables investigated. This design was chosen as it minimises the number of experiments and looks only at one factor and two factor interactions. To determine if there was any curvature in the system, a response surface design was added to the factorial design. This means that centre points were added, between the high and low parameter settings, to the experimental design. The experimental design now investigates any curvature between the parameter settings. This design is called a face-centred central composite design.

The experiments were carried out in the following random order:

Table 3.3: face centred central composite design (FCCD)

	Run Number	Stirrer Speed v_t (m/s)	% solids	Media Size d_{GM} (mm)	Mill Filling MF (%)
Block 1: Resolution V Irregular Design	1	-1	-1	-1	-1
	2	1	1	-1	-1
	3	-1	1	1	-1
	4	-1	1	-1	1
	5	1	1	-1	1
	6	1	1	1	-1
	7	1	-1	-1	1
	8	1	-1	1	1
	9	1	-1	1	-1
	10	-1	1	1	1
	11	-1	-1	-1	1
	12	-1	-1	1	-1
Block 2: Augmentation to FCCD	13	0	0	0	0
	14	0	0	0	0
	15	0	0	-1	0
	16	0	0	0	1
	17	1	0	0	0
	18	0	1	0	0
	19	-1	0	0	0
	20	0	-1	0	0
	21	0	0	0	-1
	22	0	0	1	0

In total 22 experiments were carried out using the design of experiments approach. The data from these experiments were analysed statistically using Design-Expert software.

From the factorial design, all of the stress energy data obtained was approximately in the $1 \cdot 10^{-3}$ Nm – $10 \cdot 10^{-3}$ Nm range.

Cenobead zirconium silicate (CZS) grinding media of sizes 1.5 mm, 2.0 mm, 3.0 mm and a density of 4.1 g/cm^3 were used for the design experiments. Cenobead CZM media of 1.0 mm and 5.0 mm, with a density of 3.7 g/cm^3, were used in the stress energy high-low experiments.

The two additional experiments completed are outlined below in Table 3.4:

Table 3.4 Extra experiments

	v_t (m/s)	% solids	d_{GM} (mm)	MF (%)
SE$_{LOW}$	6 m/s	30 %	1 mm	65 %
SE$_{HIGH}$	13 m/s	30 %	5 mm	65 %

4. RESULTS & DISCUSSION

4.1 Flotation trials

A stirred milling test followed by four batch flotation tests were carried out. This was done to determine if improved liberation has an impact on the flotation response on this particular ore type and stream i.e. MG cleaner flotation tails.

Figure 4.1 shows the PSD's of samples used during the flotation campaign.

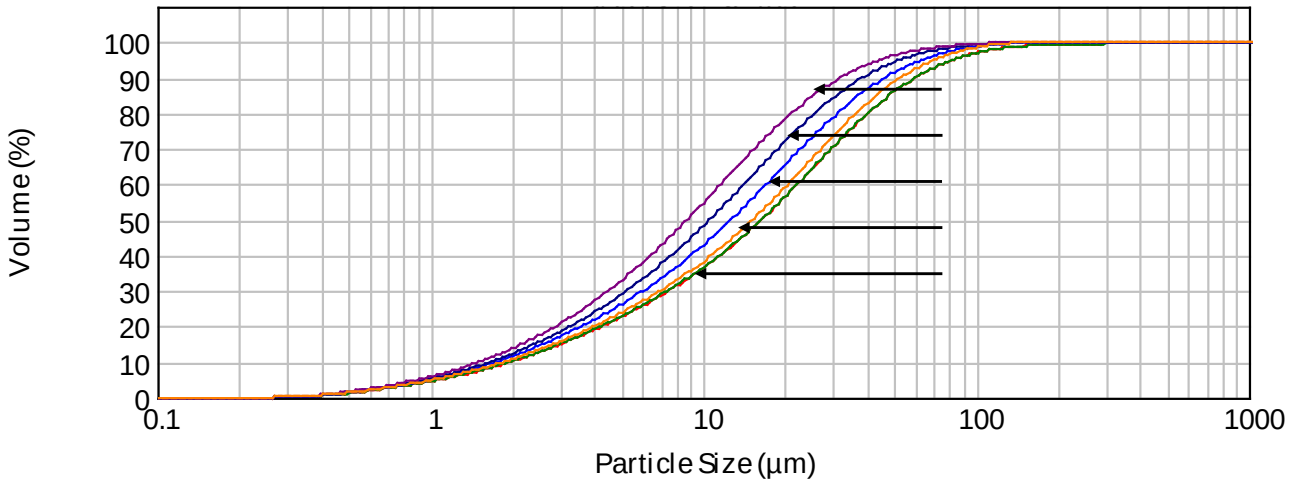

Figure 4.1: Particle size distributions of feeds for flotation at different grinds

Figure 4.2 and Figure 4.3 show the recoveries of nickel and copper respectively, which serve as proxies for PGM's recoveries. The flotation was completed at four different P80 grinds 36.60 µm, 31.10 µm, 25.68 µm and 21.15 µm. It was observed that the recoveries of both nickel and copper follow the same trends with the highest recoveries at a P80 grind of 31.10 µm. The recoveries decrease in the following P80 grind order: 31.10 µm, 25.68 µm, 21.15 µm and 36.60 µm. It was observed that the coarsest grind, which involved mostly surface cleaning had the lowest recovery. This could be because the particles are not sufficiently liberated, and it follows that some level of increased liberation is required for this process stream. However, at the finest grind (highest level of liberation) the recovery drops most likely due to a number of flotation related aspects which include froth stabilities, reagent additions amongst others.

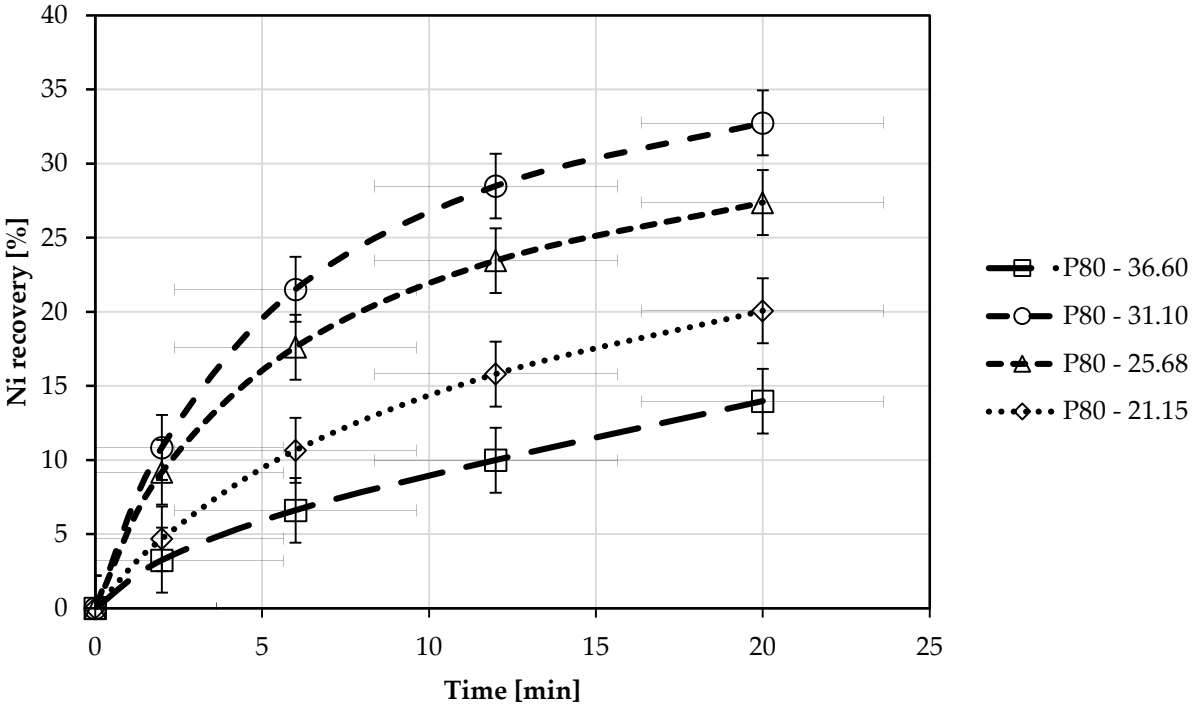

Figure 4.2: Ni recovery [%] versus flotation time

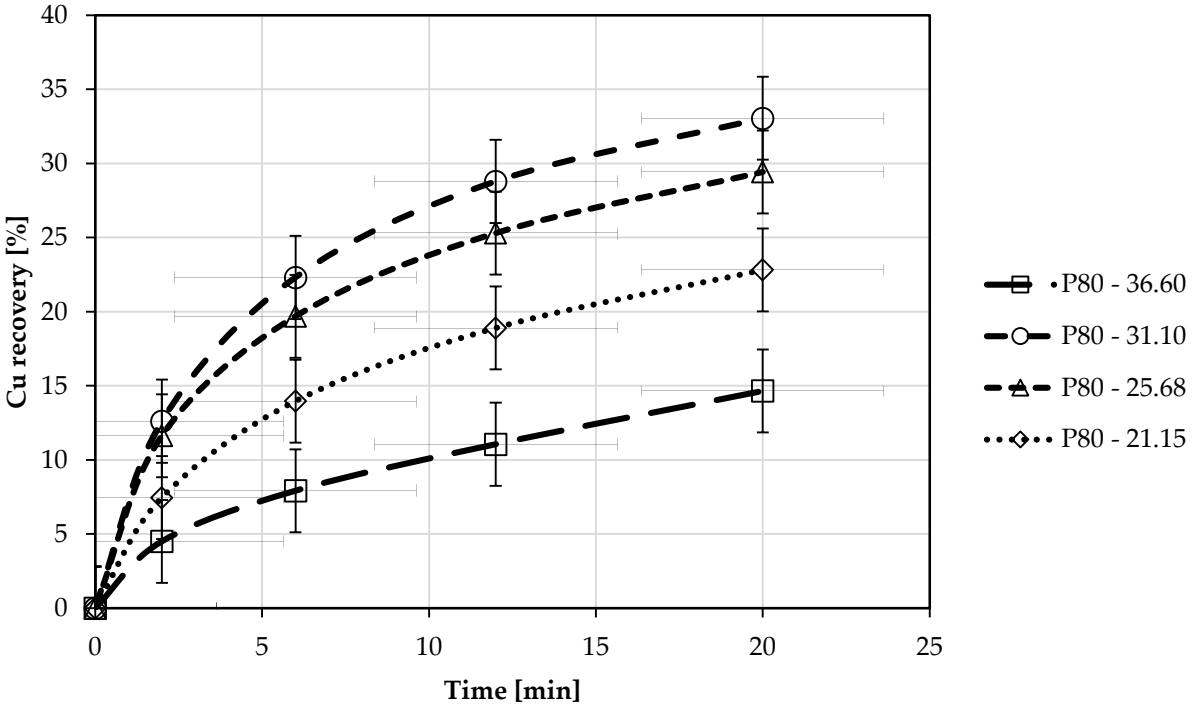

Figure 4.3: Cu recovery [%] versus flotation time

Figure 4.4 and Figure 4.5 shows the grade recovery curves for both nickel and copper respectively. In both cases the best grade recovery curve are found at the P80 of 21.15 μm followed by the P80's 25.68 μm, 31.10 μm and 36.60 μm. It follows from the grade – recovery curves, that the finer grinds have the highest grades at the same recoveries, but that their final recoveries are lower due to lower flotation kinetics.

It should be noted here, that the reagent additions were used in a "g/t" basis and not a surface area basis. When grinding finer, a higher "g/t" reagent addition should be added in order to achieve a similar "g/m²" due to a larger surface area present. Higher reagent additions could potentially improve the recoveries at finer grinds.

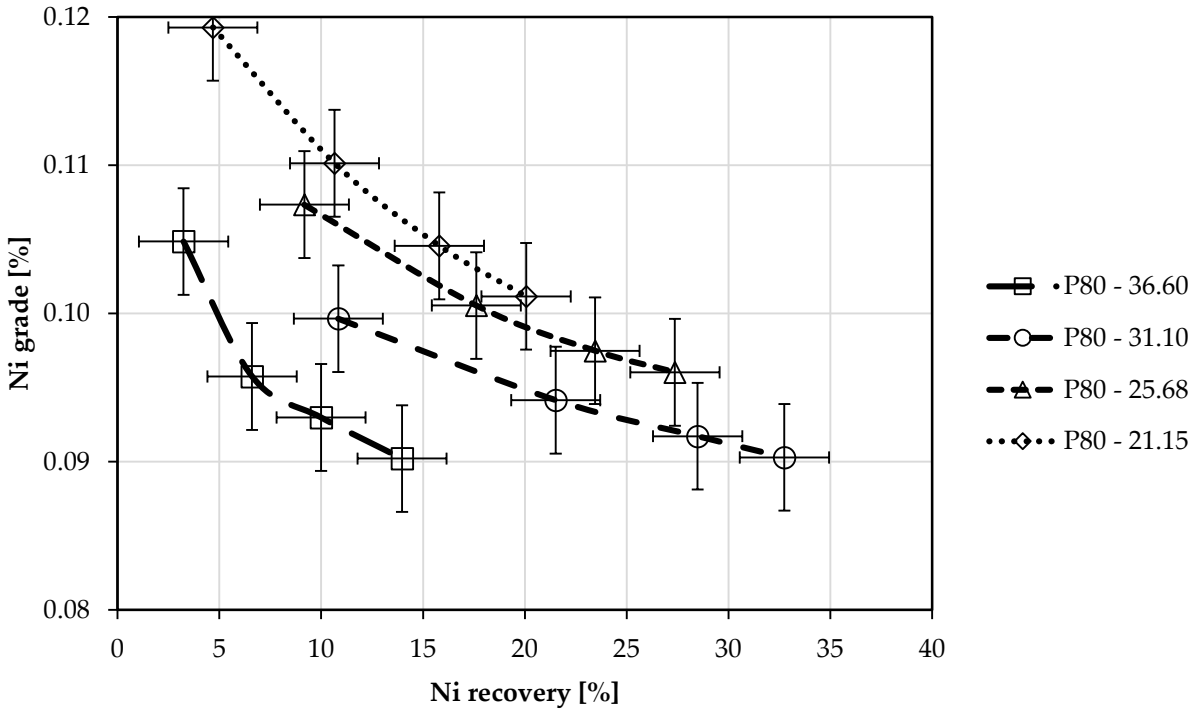

Figure 4.4: Ni grade - recovery curves

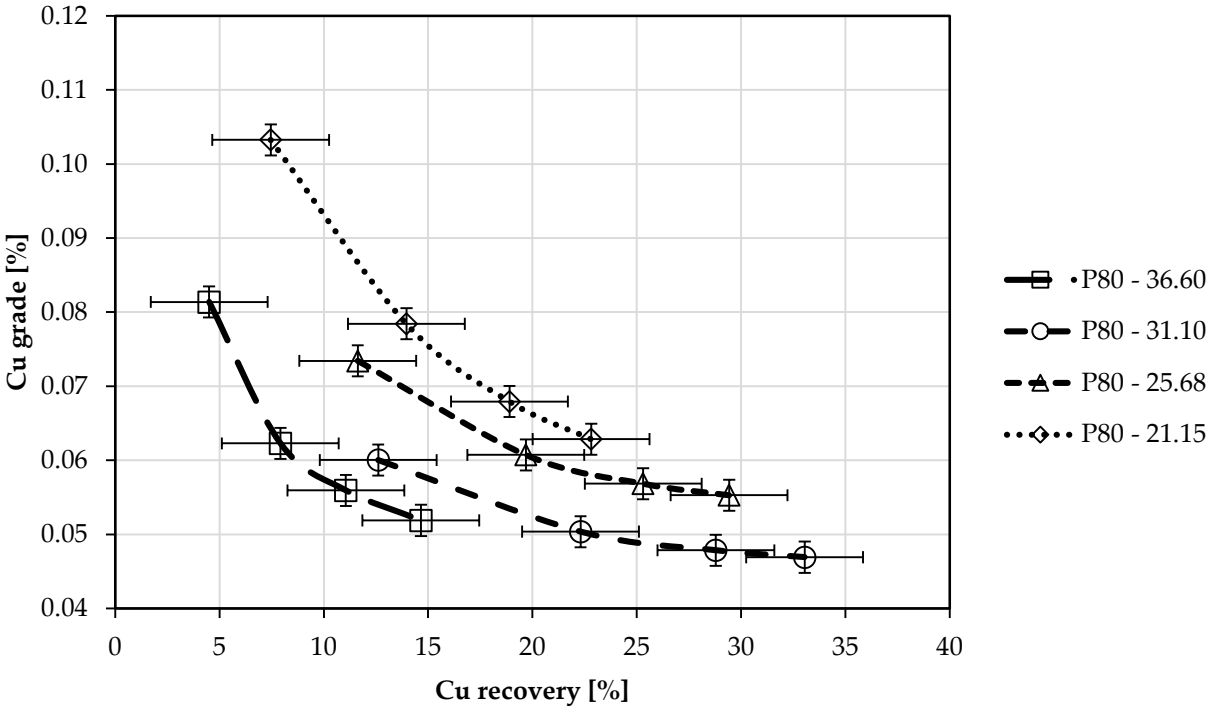

Figure 4.5: Cu grade - recovery curves

Based on the flotation responses it is clear that fine grinding does have an impact on flotation responses of this ore (improved liberation leading to a higher grade at the same recovery). The stirred mill operating parameters outlined in Chapter 3 are investigated next using the stress energy model.

4.2 Stress energy analysis

4.2.1 Stress energy in vertical stirred mills

The concept of stress energy was introduced and discussed in Chapter 2. The maximum stress energies for the grinding media were calculated for all experiments using equation 2.5 developed by Kwade et al. (1996), outlined in Chapter 2, and presented here again.

$$SE\ \alpha\ SE_{GM} = d_{GM}^3(\rho_{GM} - \rho)v_t^2 \quad (2.5)$$

Where:

- SE_{GM} – Stress Energy of the Grinding Media
- d_{GM} – Diameter of Grinding Media
- v_t – Stirrer Tip Speed
- ϱ_{GM} – Density of Grinding Media
- ϱ – Slurry Density

The gravitational effect present in vertical stirred mills was not investigated during this study because of the high speeds used. When operating at high speeds the centrifugal forces would be more dominant than the gravitational force (Jankovic, 2001).

The optimum stress energy is the energy which is just enough to fracture a particle. If the stress energy is too high the particles will be fractured but with energy losses. If the stress energy is too low the particles may only be fractured after a high number of impacts. From this there exists an optimum stress energy, where the energy is just enough to fracture the particle.

The aim of this exercise is to validate the stress energy model on a platinum bearing South African ore. The results and discussion of the stress energies investigations are presented in this section.

4.2.2 Stress energy considerations

4.2.2.1 Stress energy versus particle size

The stress energy is defined in two ways: the mill related stress model, and the product related stress model outlined in Chapter 2.4. The outcome from these viewpoints are the stress model equations. From these the interactions in the stirred mill can be explained. Figure 4.6 shows the stress energy plots first explored by Kwade et al. (1996) using limestone as feed in a horizontal stirred mill. Optimum stress energies were found where the stress energies decreases slightly as the energy input is increased. Figure 4.7 shows the work of Jankovic (2003) using a zinc concentrate in a vertical stirred mill with pin stirrers. The figures show identical trends and demonstrates that the stress energy model can be used for both vertical and horizontal stirred mills.

Figure 4.8 shows the stress energy plots at 65% mill filling and an optimum is observed for each energy input (the line through the optimums gives an indication of where the optimum stress energies can be achieved). Smaller P80's are achieved as the energy inputs increases from 10 to 30 kWh/t. This is expected as the particles are exposed to a higher power intensity and/or longer grinding times. These stress energy trends are very similar to those first depicted by Kwade et al. (1996) and Jankovic (2003). Optimum stress energies in the range $1 \cdot 10^{-3}$ Nm – $3 \cdot 10^{-3}$ Nm are observed for the energy inputs. Also, as found by Kwade et al. (1996), the optimum stress energy decreases with increasing energy input, or decreases very slightly in a narrow stress energy range as in the work by Jankovic (2003).

At high energy inputs the mill content particles require less stress energy (SE_{GM}) for fracture. As given in equation 2.5 (stress energy equation), the stress energy of the grinding media is dependent on the diameter of grinding media, d_{GM}^3, the stirrer tip speed, v_t^2, the grinding media density, ϱ_{GM}, and the slurry density, ϱ. Different combinations of these variables can result in the same optimum stress energy. Knowing the optimum stress energy for a particular target grind size is essential when targeting the best energy efficiency and setting up the operating parameters of the process. When operating the stirred mill outside the optimum stress energy range, it is evident from the results presented that the grinding becomes less energy efficient.

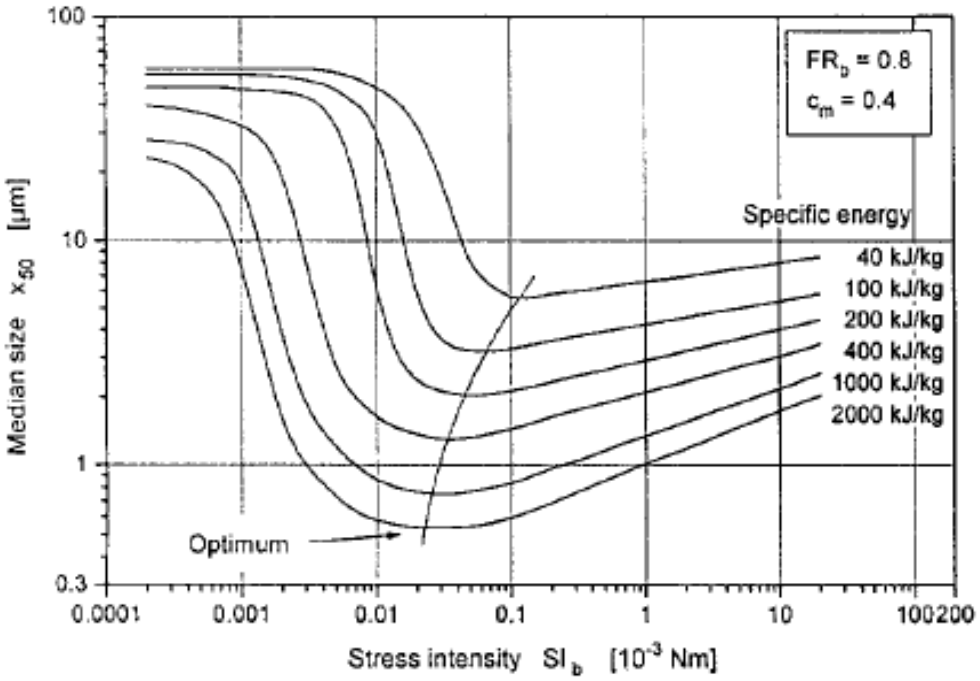

Figure 4.6: Product fineness as a function of stress intensity at varying specific energies in a horizontal stirred mill with discs (Kwade et al., 1996)

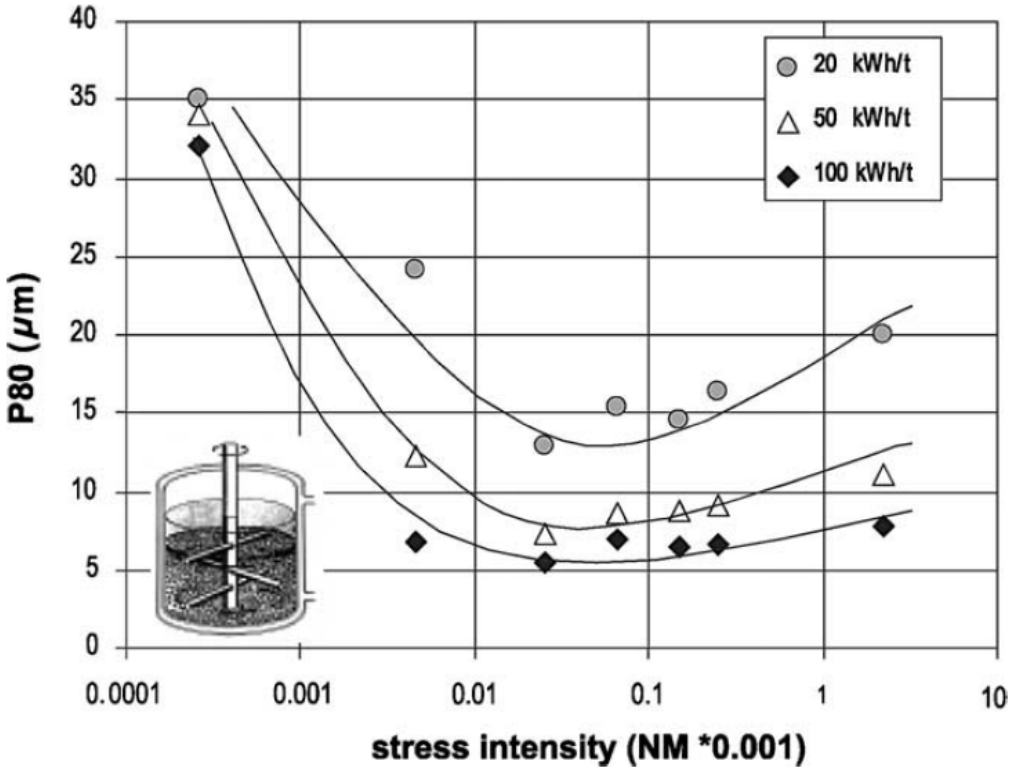

Figure 4.7: Stress energy versus particle size for vertical stirred mills with pin stirrers using zinc concentrate (Jankovic, 2003)

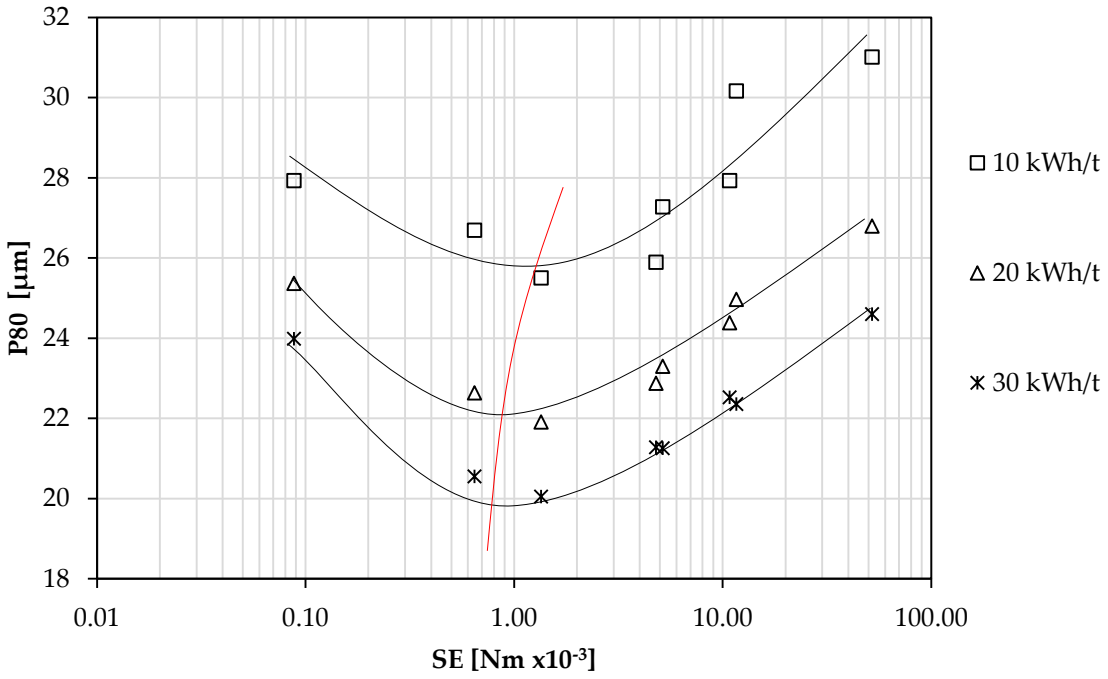

Figure 4.8: Stress energy plots at 65% mill filling

4.2.2.2 Stress energy versus specific energy input

Figure 4.9 shows the required energy input versus stress energy at grind sizes of 20 µm, 25 µm and 30 µm. Optimum stress energies are observed at the target grinds of 20 µm, 25 µm and 30 µm where the specific energy is at a minimum (as shown by the line through where the optima can be achieved). It is seen that the optimum stress energies decreases as the required target grind is decreased. This is similar to the works of Kwade et al. (1996) and Jankovic (2003). It should be noted that stirred milling is a dynamic process and a particle and its fragments would experience different stress energies in the range from stress energies of near zero to the maximum stress energy the grinding media can impart in the stirred mill for the duration of the grind. The optimum stress energies in Figure 4.8 and Figure 4.9 are the maximum stress energies the grinding media can impart to the particle. To obtain a targeted grind, there exists a minimum specific energy input at which the stress energy is at an optimum, as shown in Figure 4.9. Conversely, when operating at a particular specific energy input there exists a minimum P80 grindsize where the stress energy is at an optimum as shown in Figure 4.8.

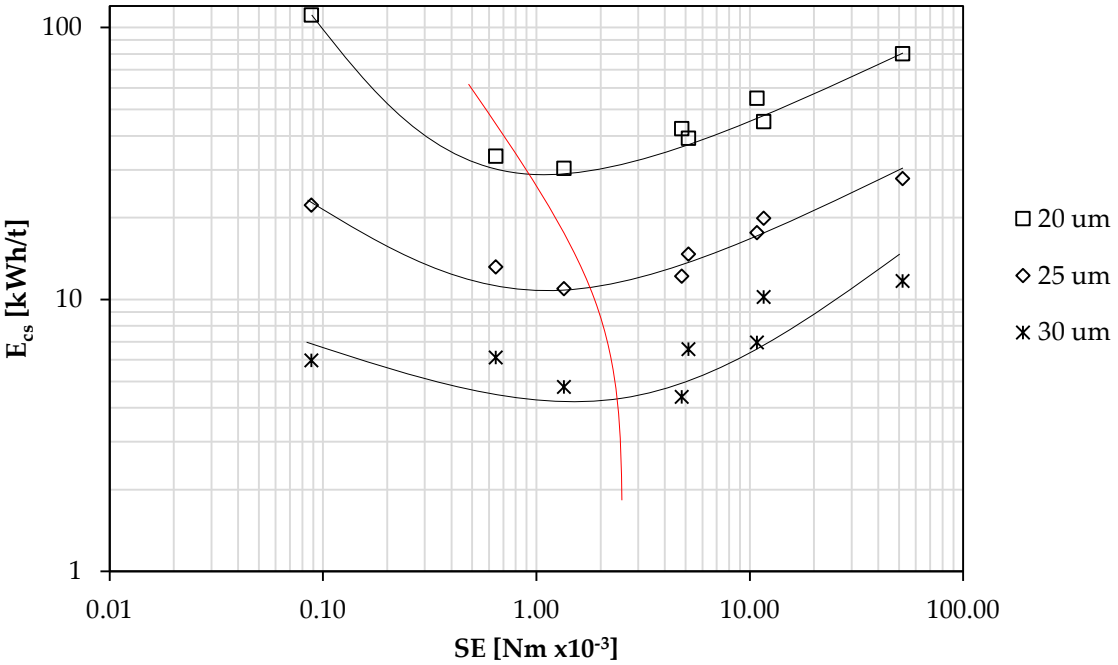

Figure 4.9: Stress energy versus kWh/t at P80's of 20 µm, 25 µm and 30 µm

4.2.2.3 Stress energy versus energy utilization

Figure 4.10 shows the efficiency (refer to Chapter 4.3) versus stress energy. It is observed that the maximum efficiency in the process occurs in the $1 \cdot 10^{-3}$ Nm – $3 \cdot 10^{-3}$ Nm range. It is noted that as the energy input increases the efficiency of the grinding process decreases. This figure complements Figure 4.8 and Figure 4.9. In all the stress energy figures it is seen that the best efficiency performance occurs at the optimum stress energies (as shown by the lines through the stress energy curves where the optima can be achieved).

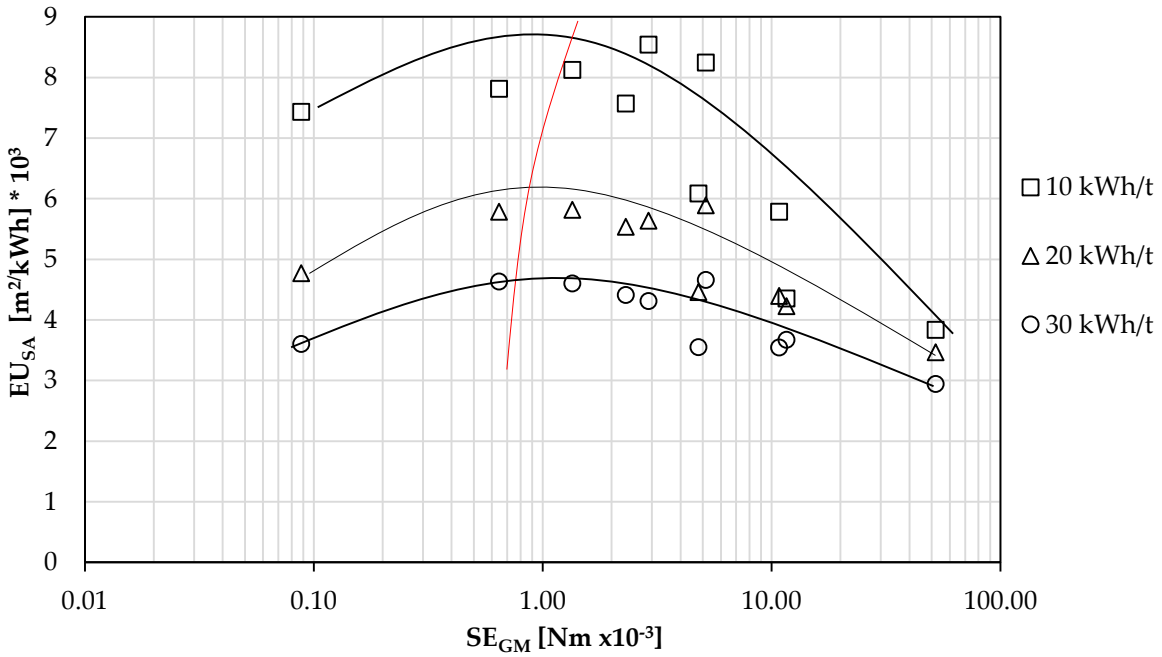

Figure 4.10: Energy utilisation versus SE_{GM}

4.2.2.4 Stress energy and stress numbers

Figure 4.12 shows the stress energy versus stress number (calculated using equation 2.3, shown here).

$$SN\ \alpha\ \frac{\varphi_{GM}(1-\epsilon)}{(1-\varphi_{GM}(1-\epsilon))c_v} \cdot \frac{nt_c}{d_{GM}^2} \qquad (2.3)$$

Where:

- SN_M – Stress number
- φ_{GM} – Mill filling
- ε – Voidage
- c_v – Solids concentration
- n – Stirrer speed
- t_c – Residence time
- d_{GM} – Grinding media size

The stress number is influenced by the mill filling, the solids concentration, media size, stirrer speed and grinding time. The stress number gives an indication of the number of times a particle is struck by grinding media. Figure 4.11 shows the relative number of stress events that occur in the stirred mill at different stress energies to grind to a median size of 2 µm. As the stress energy is decreased the number of stresses increases to maintain the required grindsize. Figure 4.12 shows the stress energy

versus stress number for a P80 grindsize of 25 μm at 65 % mill filling. This figure is similar to the one produced by Kwade (1999). It is observed that as the stress energy decreases, the number of stresses increases. This is expected; to fragment particles at lower stress energies to the same degree as at higher stress energies, the number of particle collisions or stress events needs to be increased. The number of stresses is related to the residence time or specific energy input of the stirred mill, the longer the particle has in the milling environment the more likely a high number of stresses occurs. To obtain a targeted grind at a low residence time or specific energy input, a high stress energy will be needed. To obtain the same targeted grind at a low stress energy, the residence time or specific energy would need to be increased. It is expected that this outcome is the same for all degrees of grinding.

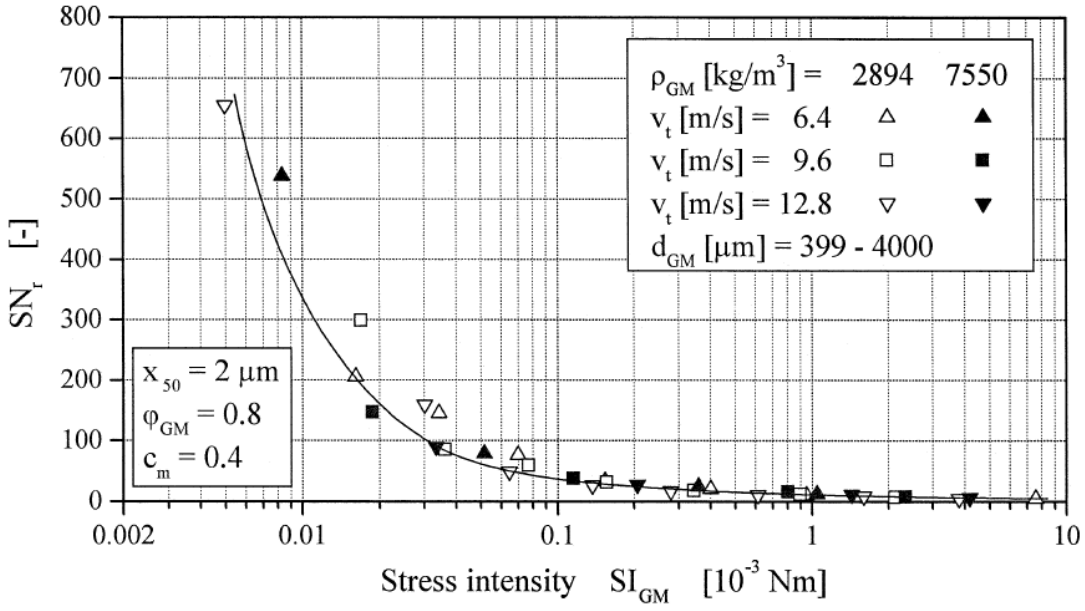

Figure 4.11: SN_r versus SE for median particle size of 2 μm (Kwade, 1999)

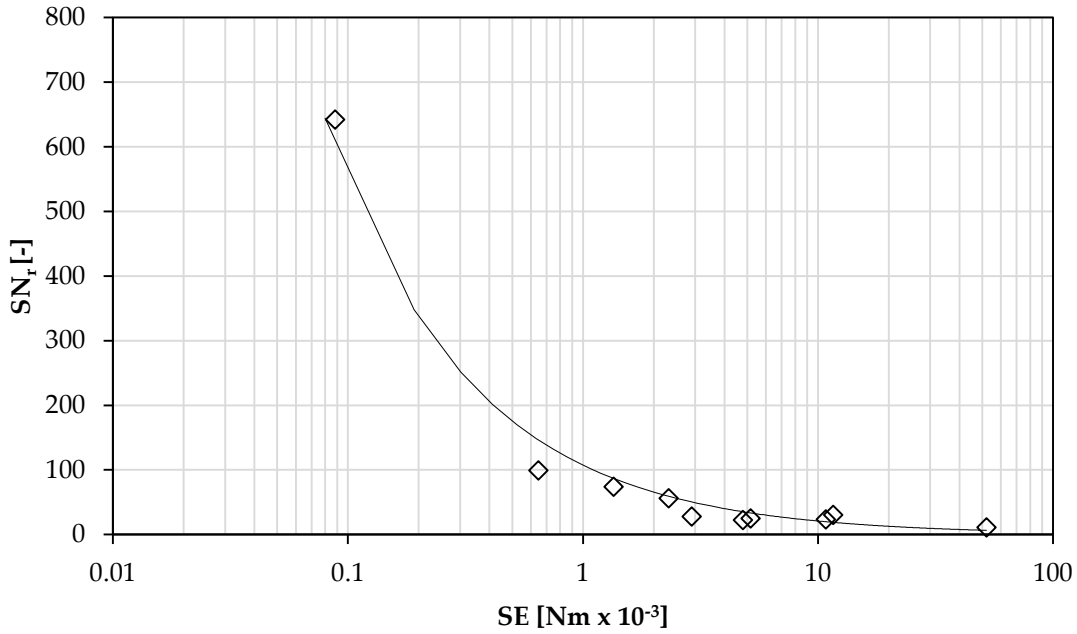

Figure 4.12: SN_r versus SE for P80's of 25 μm

The results for the stress energy analysis are in agreement with the past findings of Kwade et al. (1996) and Jankovic (2001). In their work, optimum stress energies for varying operating conditions and specific energy inputs were observed. It can be concluded that knowing the optimum grinding media stress energies (SE_{GM}) in a stirred mill system is important, because operating at the optimum grinding media stress energies would lead to operating at the optimum energy utilization. However when the stress energy is low, a high number of stresses (long residence time or high specific energy) is needed to maintain a targeted grind as opposed to a higher stress energy that needs less particle stresses to maintain the targeted grind.

It can be concluded that the stress energy model can be used when operating a vertical stirred mill using disc stirrers.

4.3 Operating variable analysis

The operating parameters of any process have an influence on the performance of the process. Understanding process operating parameters are important if the process is to be understood and optimised. In comminution, the process operating parameters have an influence on the power drawn by the mill, the grinding rate and the efficiency of the process.

The influence of stirred mill operating parameters have been investigated by others over a number of years as outlined in Chapter 2. However, most of these studies look at how one variable influences the performance of the stirred mill at a time. The interactions that multiple variables have on the power draw, grinding rate and efficiency in stirred mills have not been investigated in much detail. The influence of grinding media size, stirrer tip speed, solids concentration of the feed slurry, and mill filling of the grinding chamber on a volume basis are investigated in a vertical stirred mill with discs using the traditional one variable at a time approach here and in Chapter 4.4 looking at the effects of the influence of multiple variables on the stirred mill performance.

In this section, data extracted from the grinding experiments are analysed by only varying one variable at a time. By doing so, the effects of the changing variable can be monitored and observations can be made into this variables influence on the rate, power drawn and efficiency. The one variable at a time data is obtained using the mid-points of the design variables as outlined in Chapter 3.

Figure 4.13 shows how the specific surface area of the experiment samples (obtained from Malvern Mastersizer) are related to the P80 of the experiment samples. This trend is expected, when the product becomes finer the specific surface area increases. Figure 4.14 shows the specific surface areas versus specific comminution energy, this figure shows a large variation in surface areas at input energies. It comes to reason that at given energy inputs the efficiencies are different, for example at 20 kWh/t the surface area varies between ~0.45 m^2/g – ~0.55 m^2/g.

The efficiency in this project is defined in three different ways:

1. The P80 of the product samples at a given energy input is used as an efficiency indicator, where having a low P80 for a given set of operating parameters at the same energy input is considered a good efficiency. The P80 linked with energy input is a common efficiency indicator in minerals processing operations.

2. The second efficiency indicator (EU_{SA} – Energy utilization on a surface area basis) is defined as the change in surface area (m^2/g), obtained from the Malvern Mastersizer, from fresh feed to product at an input energy of "x" kWh/t. This is also shown in equation 4.1, and the EU_{SA} is used as an indicator for the efficiency of the whole system.

$$EU_{SA} = \frac{SA_{product} - SA_{feed}}{\text{"x" kWh/t}} \tag{4.1}$$

3. The third efficiency indicator ($EU_{10\mu m}$ – Energy utilization of particles passing 10 μm) was defined at the percent new passing 10 μm from feed to product at an energy input of "x" kWh/t. This is shown in equation 4.2, and the $EU_{10\mu m}$ is used as an indicator for the efficiency of the material passing 10 μm.

$$EU_{10\mu m} = \frac{(\%\ \text{Passing 10 } \mu m)_{product} - (\%\ \text{Passing 10 } \mu m)_{feed}}{\text{"x" kWh/t}} \tag{4.2}$$

The grinding rate is defined in two ways:

1. As shown in equation 4.3, the change in surface area (SA) between the feed and product over the residence time taken to obtain the product surface area from the feed surface area.

$$Rate_{SA} = \frac{SA_{product} - SA_{feed}}{\tau_{grind}} \tag{4.3}$$

2. The rate is also defined in terms of the percent new passing 10 μm from the feed to product over the grinding residence time as shown in equation in 4.4.

$$Rate_{10\mu m} = \frac{(\%\ \text{Passing 10 } \mu m)_{product} - (\%\ \text{Passing 10 } \mu m)_{feed}}{\tau_{grind}} \tag{4.4}$$

The generation of new surface area or new % passing a certain size produced in the stirred mill per unit time can be obtained by multiplying the above rates by the mass present in the mill.

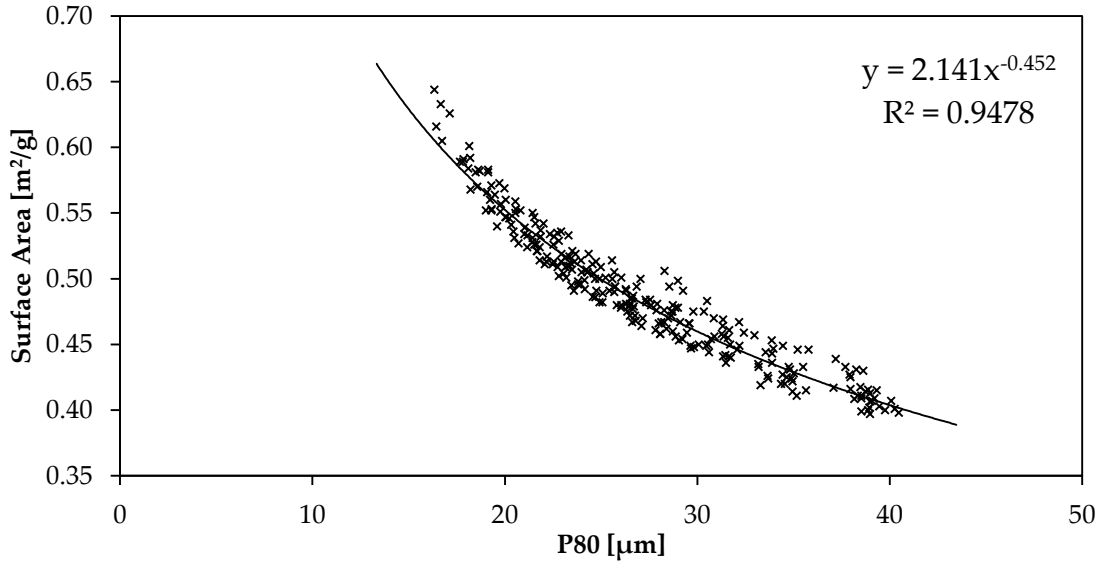

Figure 4.13: Specific surface area [m²/g] vs P80 [µm]

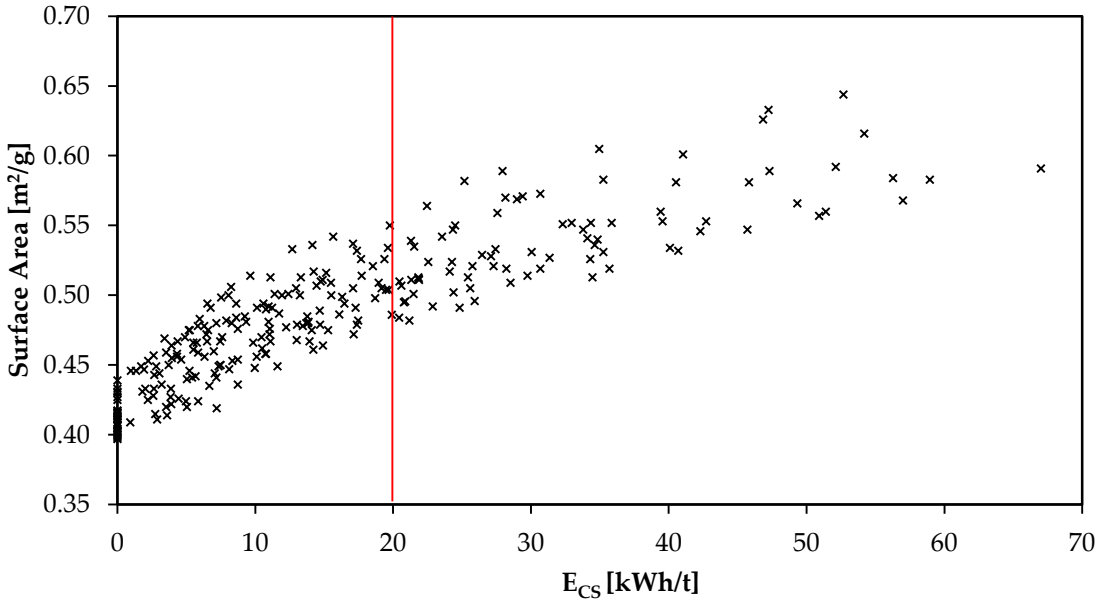

Figure 4.14: Surface area vs energy input

The figures used to obtain the energy inputs, grinding times, P80's and surface areas can be found in the Appendix.

4.3.1 The effect of stirrer speed on efficiency, power and rate

The stirrer speed is an important variable that influences the motion of the grinding media in the stirred mill and the energy imparted to the particles. The media motion in turn influences how the grinding media imparts energy to the particles, i.e. the stress frequency and stress energy. Stirrer speed also has a direct influence on the level of turbulence (dimensionless Reynolds number) and Power number in the stirred mill. This means that the stirrer speed has an influence on the efficiency and grinding rate in the stirred mill. The stirrer speeds tested were 8 m/s (1273 rpm), 10 m/s (1591 rpm) and 12 m/s (1909 rpm). The % mill filling, % solids and grinding media size were kept constant at the centre point conditions of 75 % mill filling, 30 % solids and 2.0 mm respectively.

Figure 4.15 and Figure 4.16 shows the signature plots (P80 versus specific energy input) and the PSD's at varying speeds at 10 kWh/t respectively. From the signature plots in Figure 4.15, it is seen that 8 m/s produces the finest grind size at a given energy input. It is observed from Figure 4.16 that the PSD's become finer as the stirrer speed is decreased. The PSD's of all stirrer speeds can be seen in the Figure B.2, in the appendix.

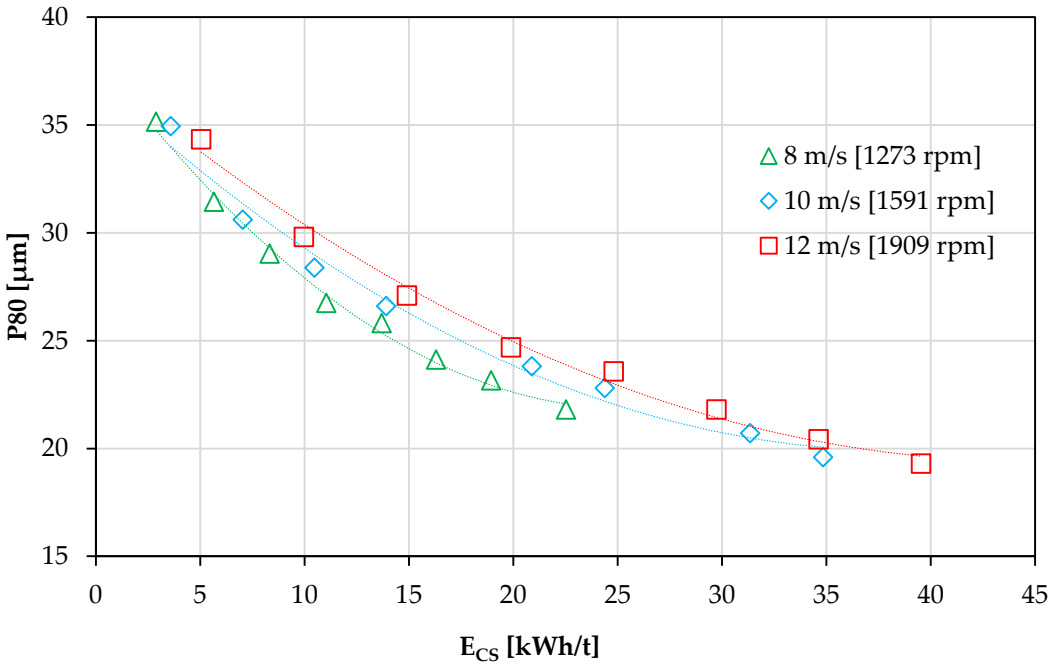

Figure 4.15: P80 versus specific energy input for varying stirrer speeds

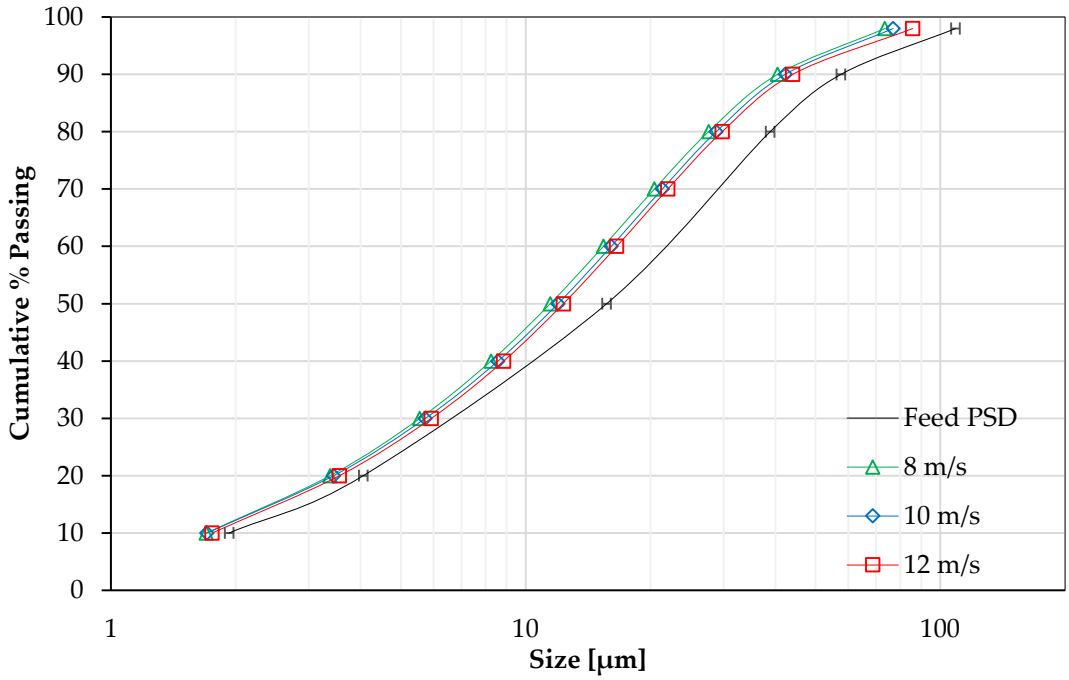

Figure 4.16: PSD's at 10 kWh/t energy inputs at varying stirrer speeds

4.3.1.1 Efficiency

Figure 4.17 and Figure 4.18 shows the stirrer tip speed at energy inputs of 10 kWh/t, 20 kWh/t and 30 kWh/t. It is observed in Figure 4.17 that the smallest P80 grinds occur at 8 m/s for all energy inputs. 8 m/s was the most efficient speed tested as confirmed by Figure 4.18 and Figure 4.19, showing the energy utilisations. Figure 4.18 also shows that the comminution efficiency decreases as the energy input is increased. This result agrees with work carried out by Mankosa et al (1989), Zheng et al. (1996), Bel Fadhel and Frances (2001), Jankovic (2003) and Ouattara and Frances (2013) in that lower stirrer speeds are more energy efficient. This also confirmed in Figure 4.15 and Figure 4.16, and shows that the grinding becomes more efficient at lower speeds versus higher stirrer speeds. It is clear from the results that at higher energy inputs, a change in the stirrer speed has a low impact on the comminution result and efficiency during this study.

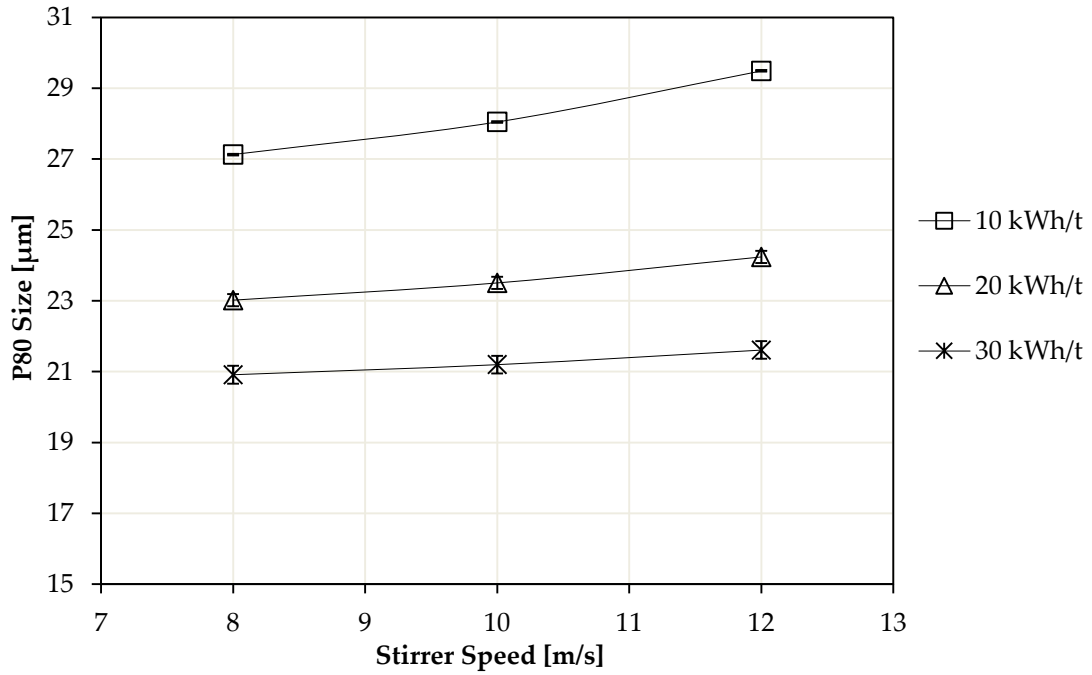

Figure 4.17: P80 versus Stirrer speed

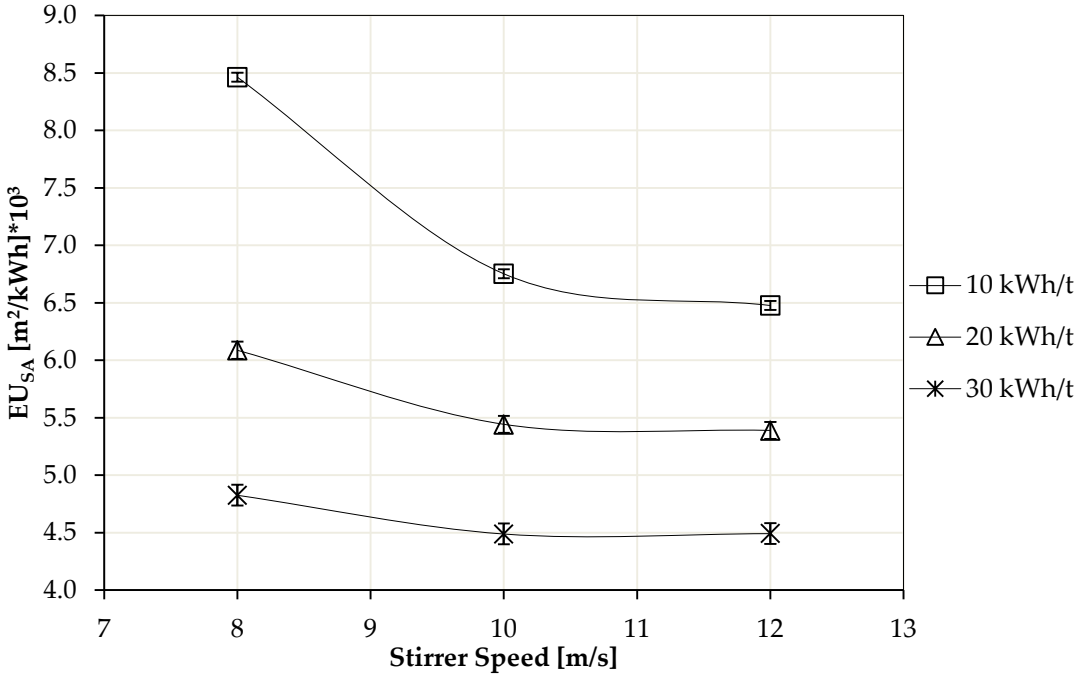

Figure 4.18: EUSA (Energy Utilisation) versus Stirrer speed

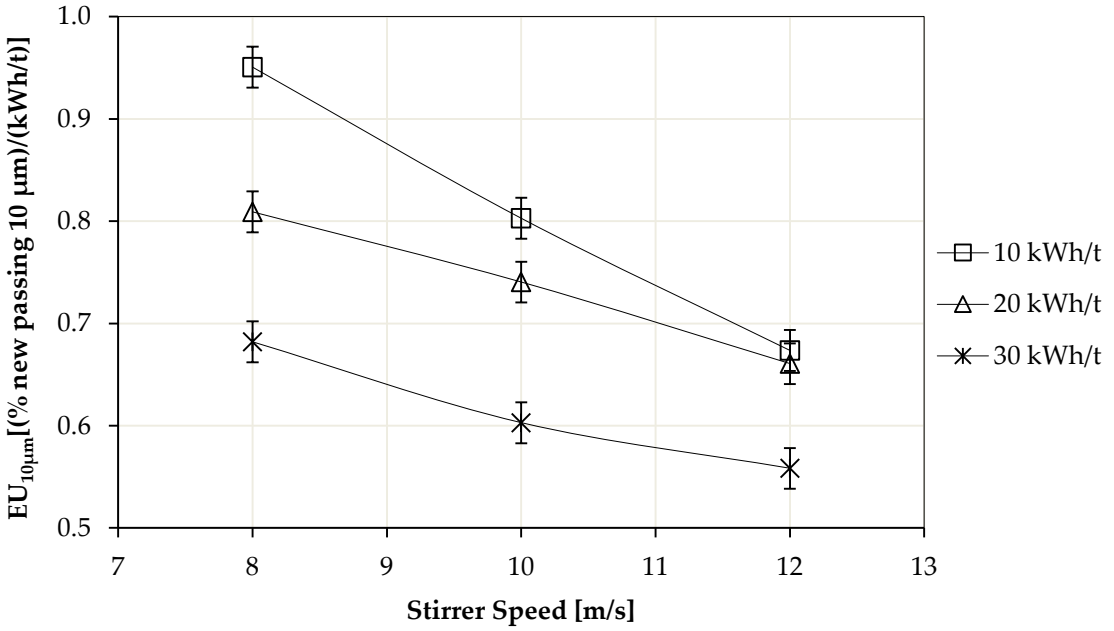

Figure 4.19: $EU_{10\mu m}$ (Energy Utilisation) versus % Stirrer speed (% new passing 10 µm)

At low speeds the transfer of energy is more efficient. As the speed of the stirrer is increased, more turbulence in the mill contents is expected due to increased velocities in the flow fields. This leads to an increase in the number of stress events, it will also however lead to more energy being lost through heat generation in the slurry, media deformation and media-media collisions and a lower efficiency is expected. The best efficiency would occur when the stress energy is just sufficient enough to propagate cracks in the particles and break the intra-particle forces (Bel Fadhel and Frances, 2001; Kwade et al., 1996). The optimum efficiency in this case occurs at the lowest stirrer speed (8 m/s). It is speculated that at even lower stirrer speeds (<< 8 m/s) the efficiency (energy utilisation) would decrease as the available stress energy would be less than what is needed to fracture the particles.

4.3.1.2 Power

Figure 4.20 shows the stirrer tip speed versus power draw. As expected the power draw increases as the tip speed is increased from 8 m/s to 12 m/s. The result of power draw increasing with stirrer speed is well known (Zheng et al., 1996; Gao et al., 1996; Jayasundara et al., 2010) as stirrer speed is the main driver of energy transfer in stirred mills. It directly transfers the electrical and mechanical energy to the contents of the mill.

The dimensionless power number (N_{Po}) equation (equation 4.5) for turbulent stirred tanks, predicts that the $P_m \alpha v_t^3$. Equation 4.5 is valid in stirred tanks where Reynolds numbers are greater than 100000 (i.e. the system is in the turbulent flow regime). The power draw in this study shows that $P_m \alpha v_t^{1.4}$. This is close to the proportionality shown by Gao et al. (1996), who showed that $P_m \alpha v_t^{1.55}$. A reason for the different proportionalities between the power number and the actual power, could be the grinding media influence on the power number affecting the density of the fluid inside the vessel (ϱ_{slurry} and ϱ_{media}).

$$N_{Po} = \frac{P_m}{D_{discs}^5 v_t^3 \rho_{slurry}} \tag{4.5}$$

Where:

- N_{Po} – Power number
- P_m – Power of the mill
- D_{discs} – Diameter of the discs
- ϱ_{slurry} – Slurry density

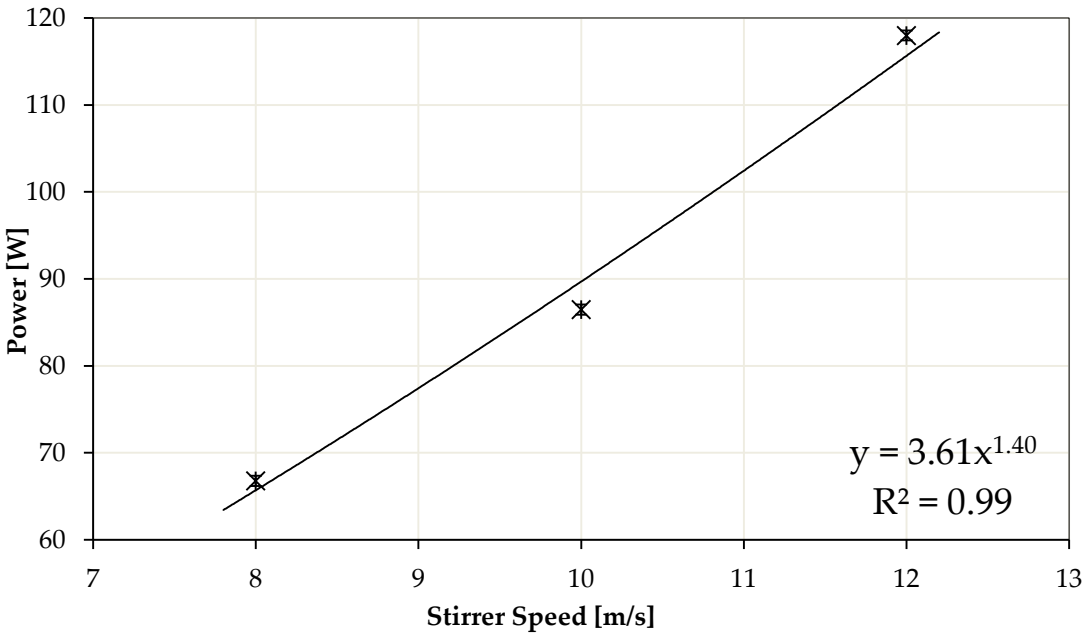

Figure 4.20: Power draw versus stirrer speed

4.3.1.3 Rate

At low stirrer speeds less energy is transferred to the particles at each collision event, while at higher stirrer speeds more energy is transferred (see stress energy equation 2.5). The rate of transfer of energy and number of stress events is dependent on the stirrer speed. From equation 2.2 it is seen that the number of contacts, N_C, the number of particles in the system, N_P, and the probability that a particle is stressed, P_S, influences the stress frequency i.e. the number of stress events.

$$SN = \frac{N_c P_s}{N_p} \tag{2.2}$$

Where:

- N_C – Number of media contacts,
- P_S – Probability that a particle can be struck, and
- N_P – Number of product particles in the mill

The number of contacts between the media and particles is directly proportional to the stirrer speed, number of grinding media and the residence time of the particles (Kwade, 1999). So at a constant residence time, t, and a constant number of grinding media (constant mill filling), when increasing the stirrer speed, v_t, the number of media – particle contacts would increase, and as a consequence the stress number (SN) increases. An increase in the number of particle stresses would lead to a higher chance for a faster rate.

The effect of grinding rate was evaluated at stirrer speeds of 8 m/s, 10 m/s and 12 m/s. The grinding rate increases with an increase in stirrer speed for all energy inputs. The fastest grinding rate occurs at 12 m/s and is shown in Figure 4.21 and Figure 4.22. As stated previously, when the speed of the stirrer is increased the transferrable energy to the grinding media is increased and the number of media – particle contacts increases. This results in a faster grinding rate in the mill. From these results it can be concluded that an increase in stirrer speeds would lead to an increase in grinding rates. The fastest rate also coincides with the highest power draw, showing that the rate is directly influenced by the power input. This is confirmed through Figure 4.23, which shows the PSD's at varying speeds after four passes (constant residence time) and it is observed that the 12 m/s curve has the finest PSD.

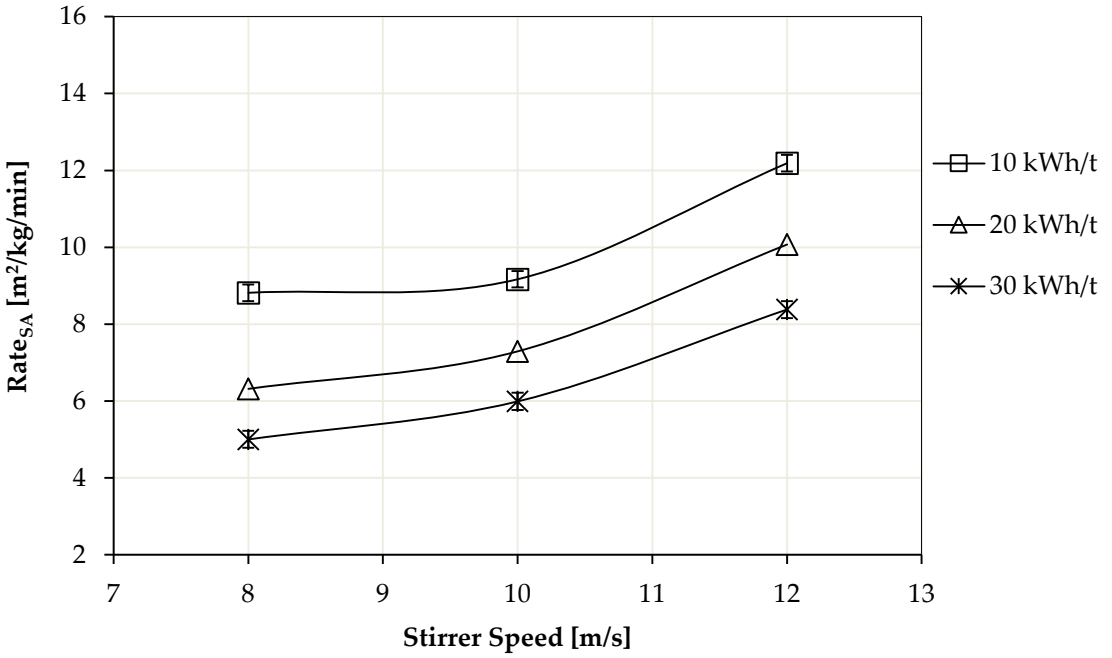

Figure 4.21: Grinding rates versus stirrer speed at varying E_{cs}

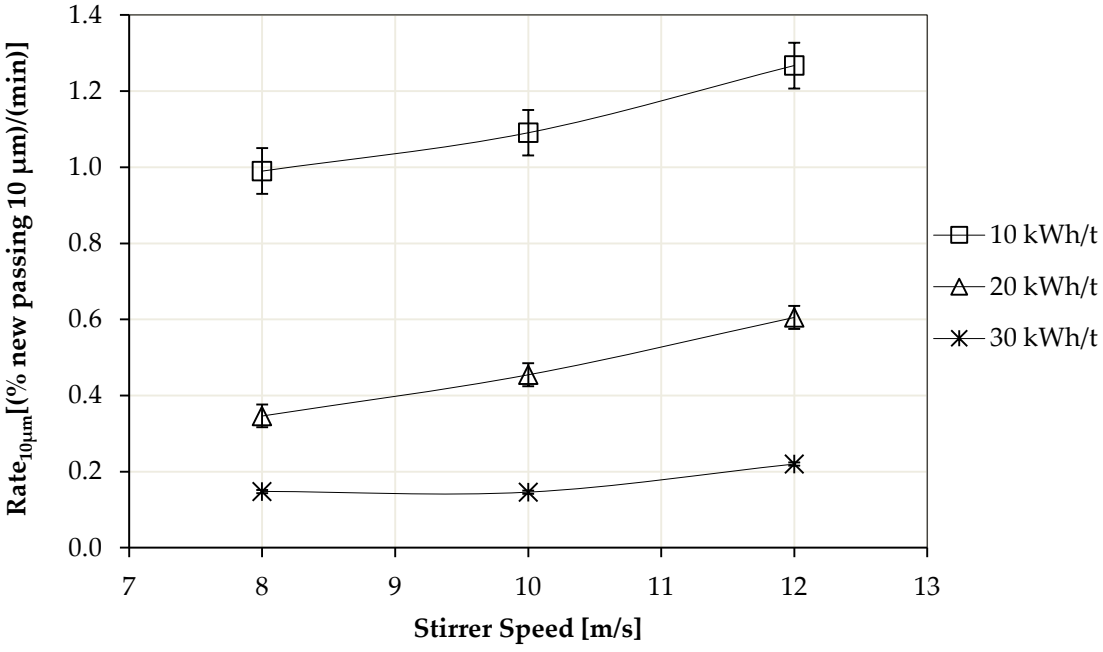

Figure 4.22: Grinding rates versus stirrer speed (% new passing 10 µm)

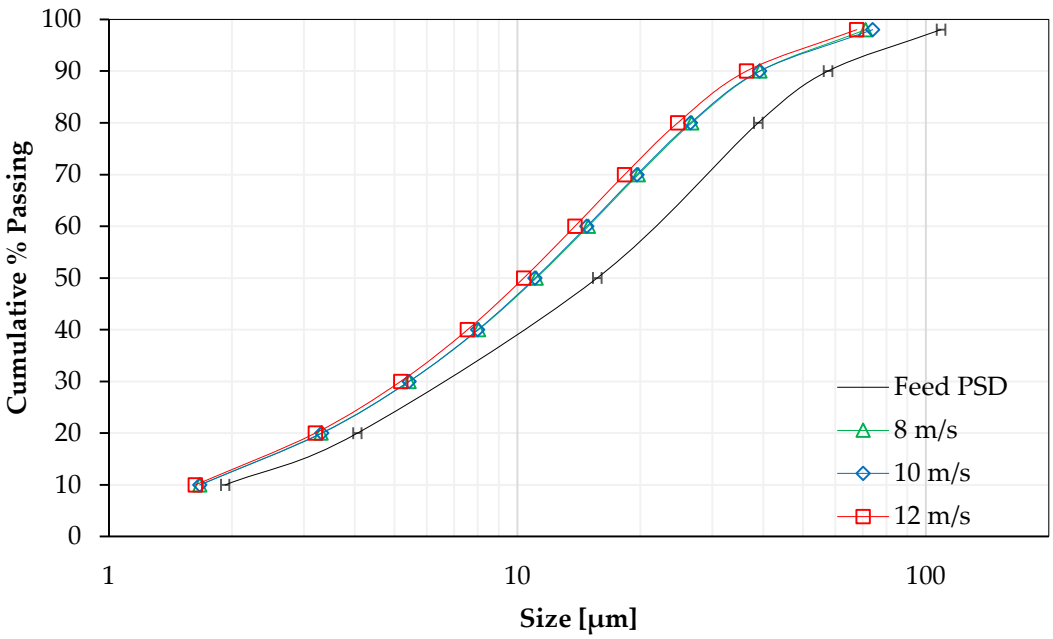

Figure 4.23: PSD's at varying speeds after pass 4

From the stirrer speed results it can be concluded that the best efficiencies occur at 8 m/s while the best rates occurs at 12 m/s.

4.3.2 The effect of solids concentration on efficiency, power and rate

The solids concentration is a very important factor in fine grinding as it directly relates to the product fineness and energy consumption (Zheng et al., 1996). During this study solid concentrations of 20 %, 30 % and 40 % by weight were investigated. The stirrer speed, % mill filling and grinding media size were kept constant at centre point conditions of 10 m/s, 75 % mill filling and 2.0 mm respectively. Figure 4.24 and Figure 4.25 show the signature plots and PSD's at 10 kWh/t respectively.

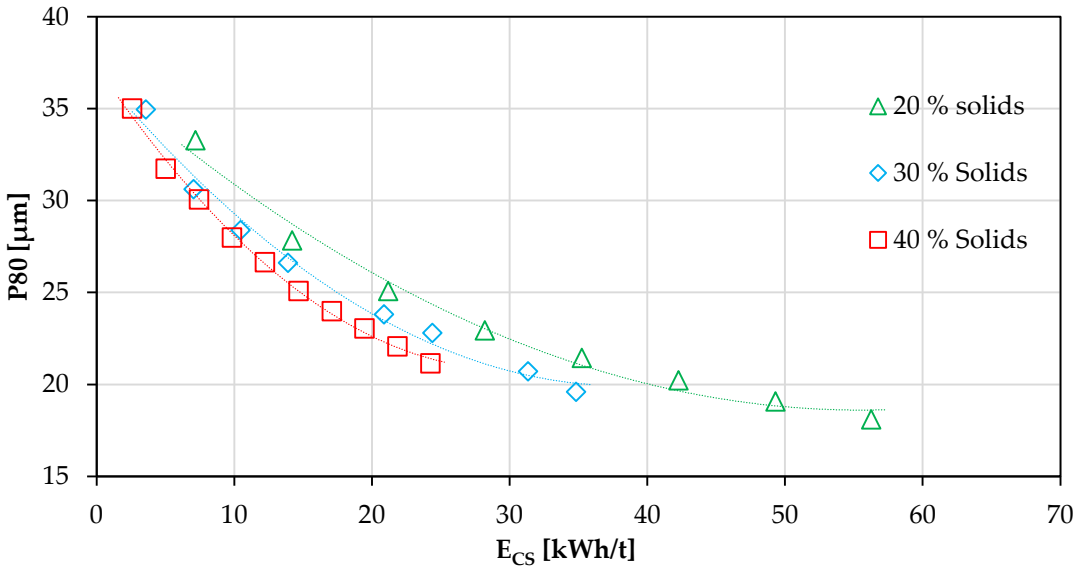

Figure 4.24: P80 size versus specific energy input at varying % solids

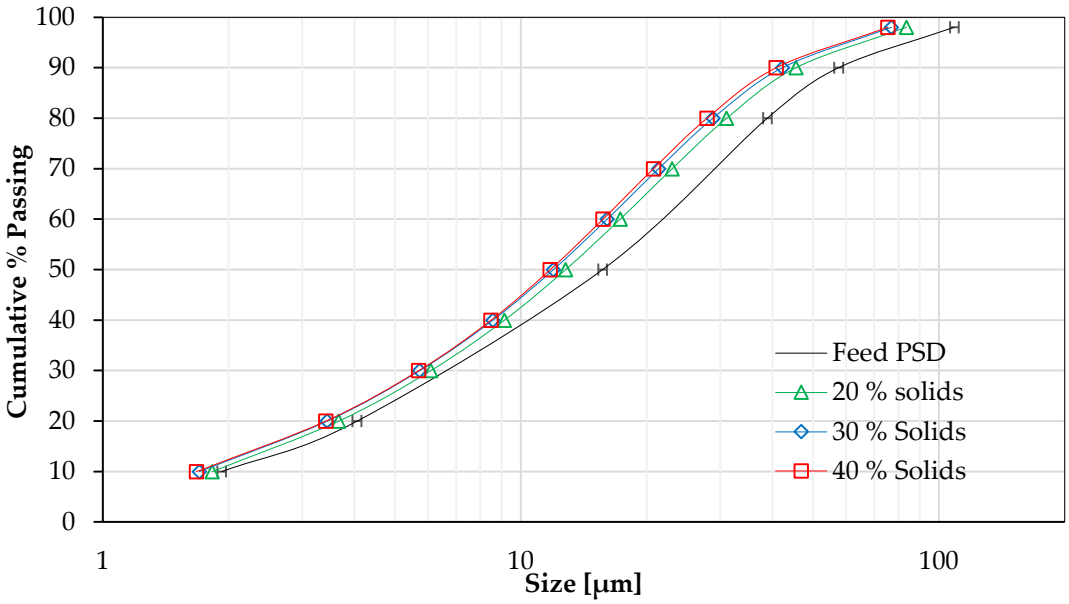

Figure 4.25: PSD's at 10 kWh/t energy inputs at varying % solids

4.3.2.1 Efficiency

Figure 4.26, Figure 4.27 and Figure 4.28 shows the % solids by mass versus P80 size and energy utilisations at 10 kWh/t, 20 kWh/t and 30 kWh/t respectively. At all energy inputs the most efficient solids concentration is at 40 % solids. This is confirmed through the plots in Figure 4.24, which show that at 40 % solids, less energy is required to grind to a given grind size. Figure 4.25 shows the PSD's at varying % solids at an energy input of 10 kWh/t. This figure complements the efficiency curves and signature plots as it shows that the finest PSD is obtained at 40 % solids. The full PSD's for all solids concentrations can be seen in Figure B.4, in Appendix B.

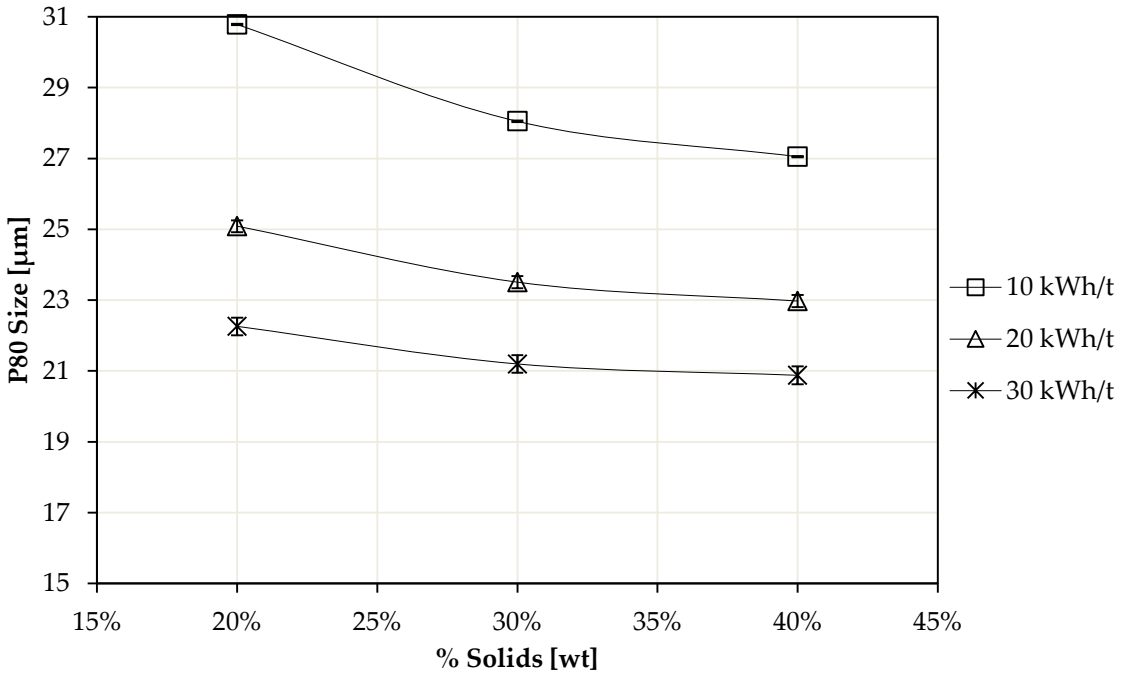

Figure 4.26: P80 versus % solids

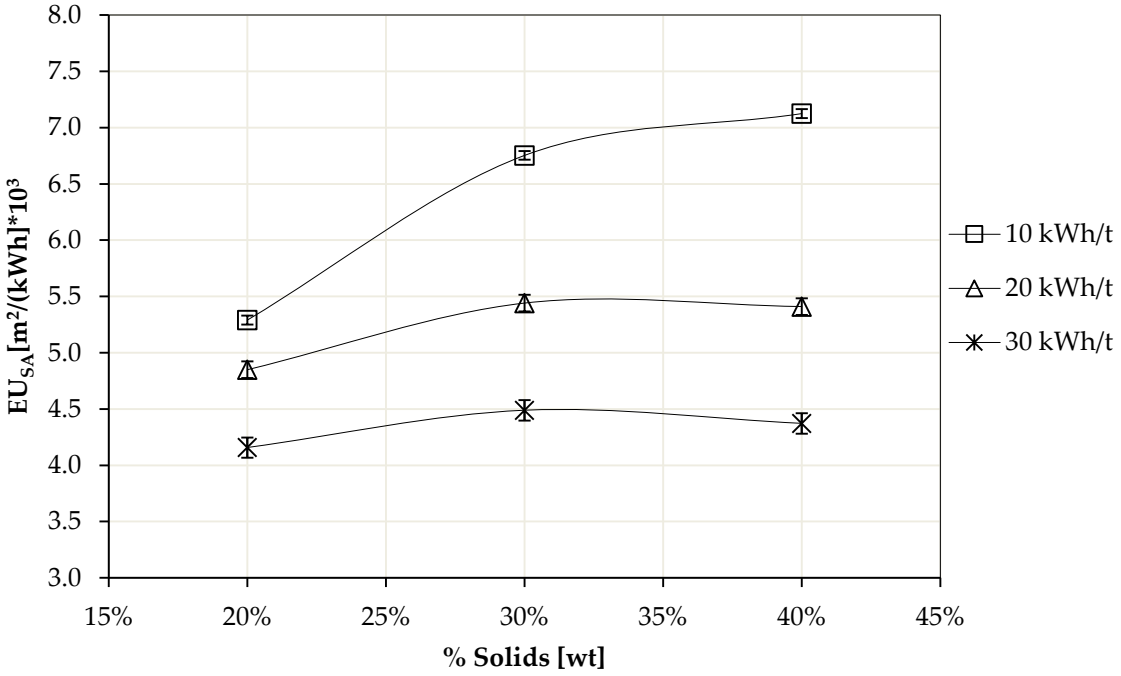

Figure 4.27: EU_{SA} (Energy Utilisation) versus % solids

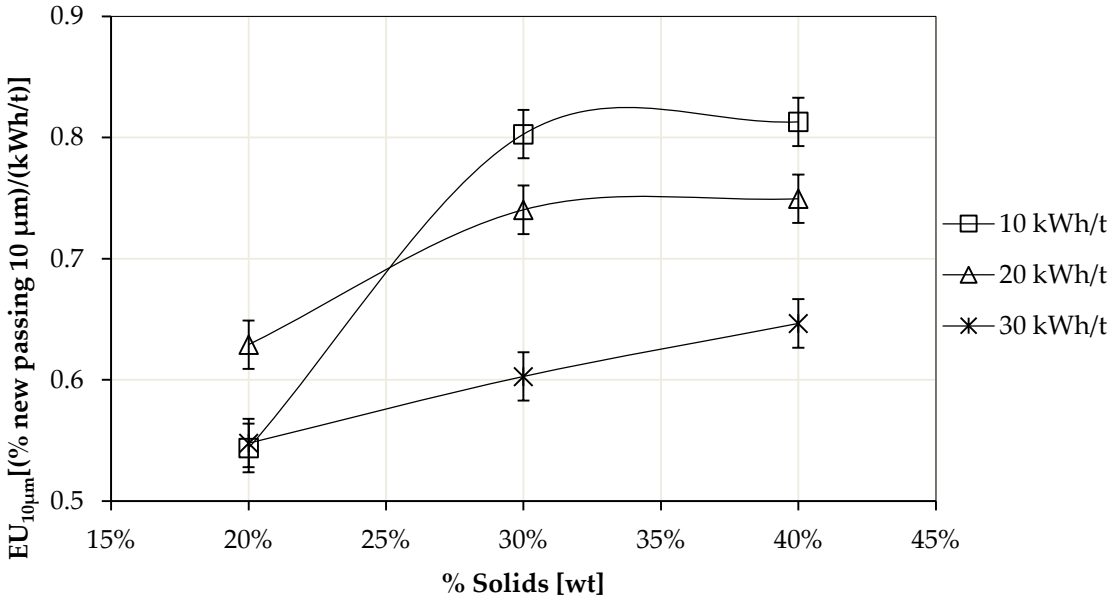

Figure 4.28: $EU_{10\mu m}$ (Energy Utilisation) versus % solids (% new passing 10 μm)

At the low solids concentration of 20 % there are fewer particles to fracture in the mill chamber due to the low solids content. This leads to more media – media collisions, and wasted energy. As the % solids increases from 20 % - 40 %, so does the number of

effective stress events (more media – particle collisions) leading to a more efficient use of energy. Figure 4.29 and Figure 4.30 shows solids concentration versus efficiency, which is taken from Zheng et al. (1996) and Bernhardt et al. (1999) respectively, they observed that there is an optimum solids concentration and then a decrease in efficiency at higher concentrations. Like Zheng et al. (1996) and Bernhardt et al. (1999), it can be assumed that for this work that there is an optimum solids concentration for the ore tested during this project however it falls outside the range tested.

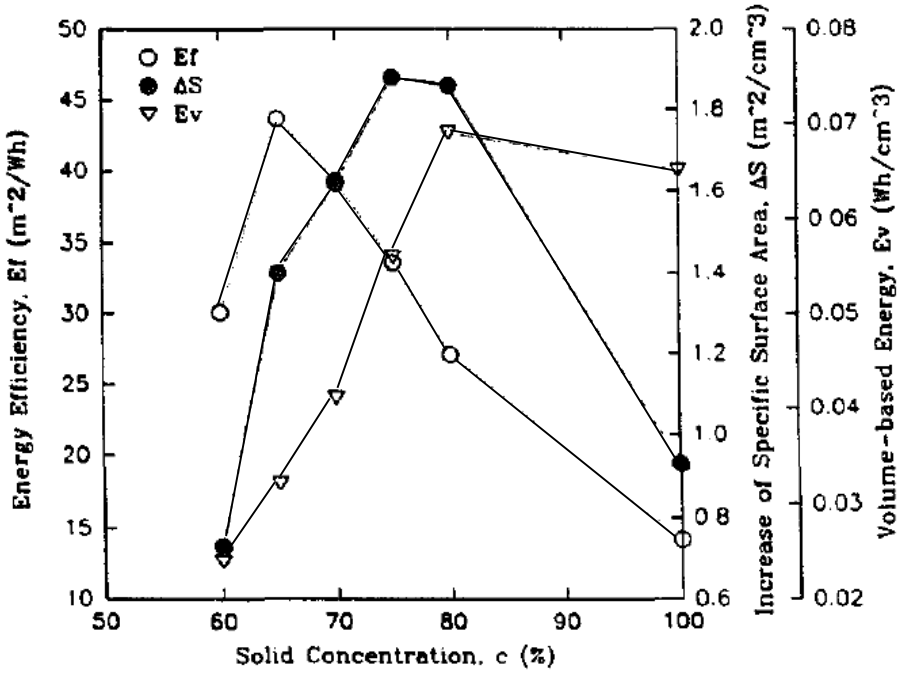

Figure 4.29: Energy efficiency versus solids concentration (Zheng et al., 1996)

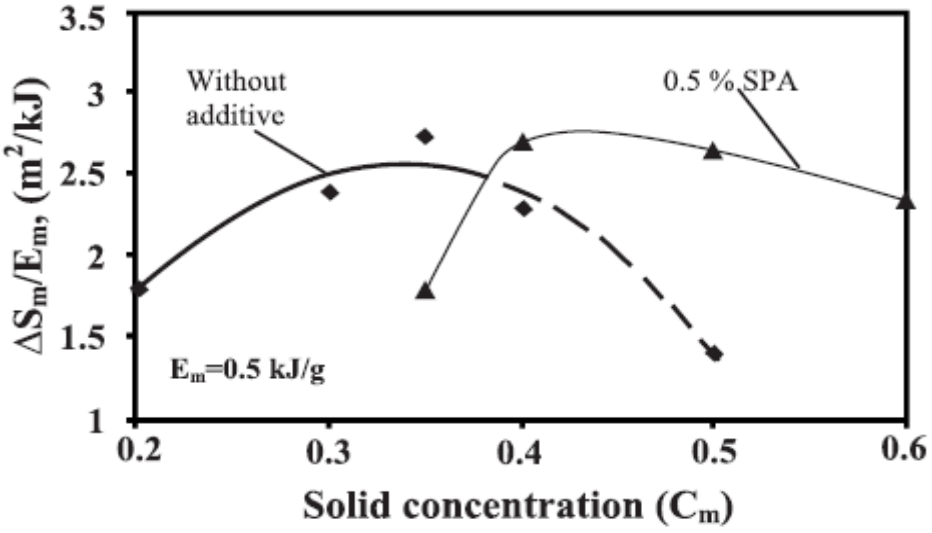

Figure 4.30: Energy efficiency versus solids concentration (Bernhardt et al., 1999)

4.3.2.2 Power

As the solids concentration is increased from 20 % - 40 %, the density and viscosity increases and a higher power draw is expected. However, in this study the power draw decreased as the solids concentration was increased. Figure 4.31 shows the % solids by mass versus power draw. It is observed that the power draw decreases as the % solids is increased from 20 % solids to 40 % solids. Jankovic (2003) found similar results to the results in this study in a low speed vertical stirred mill using pins. He attributed the drop in power when increasing the solids concentration to buoyancy affects in a vertical stirred mill and an increase in the number of particles. It can be speculated that at low solids concentrations the power draw is controlled more by the resistance (friction) between the grinding media and slurry suspension. As the solids concentration is increased the media becomes coated and a lubrication effect is observed which lowers the friction between system particles. These results are in contrast to the result found by Gao et al. (1996), who used a horizontal mill with perforated discs with dolomite as feed, shown in Figure 4.32. They found that as the solids concentration increases the power draw increases. However they were working at a much higher solids concentration of 65 % - 85 % solids and were using a viscosity modifier.

Solids concentrations higher than 40 % was not tested due to feed pump limitations. At higher solids concentrations (> 40 % solids), it is expected that the slurry would become more viscous (as seen in Figure 4.33 the viscosity increases linearly, courtesy of Ruwona (2015) who used the same ore to test viscosity effects in stirred milling). The power draw of the system would increase as a consequence to a higher viscosity. Higher % solids would lead to a drop in efficiency and it is also well known that as the % solids is increased, an increase in viscosity occurs which leads to viscous heat losses (He et al., 2006). Media motion is also hampered due to the higher viscosity of the slurry which leads to a drop in efficiency (He et al., 2006). At higher solids concentrations, an increase in particle – particle interactions can lead to a dampening or cushioning effect between the media and particles. As a result of high solids concentrations, stress energies would decrease due to a smaller difference between the media density and slurry density.

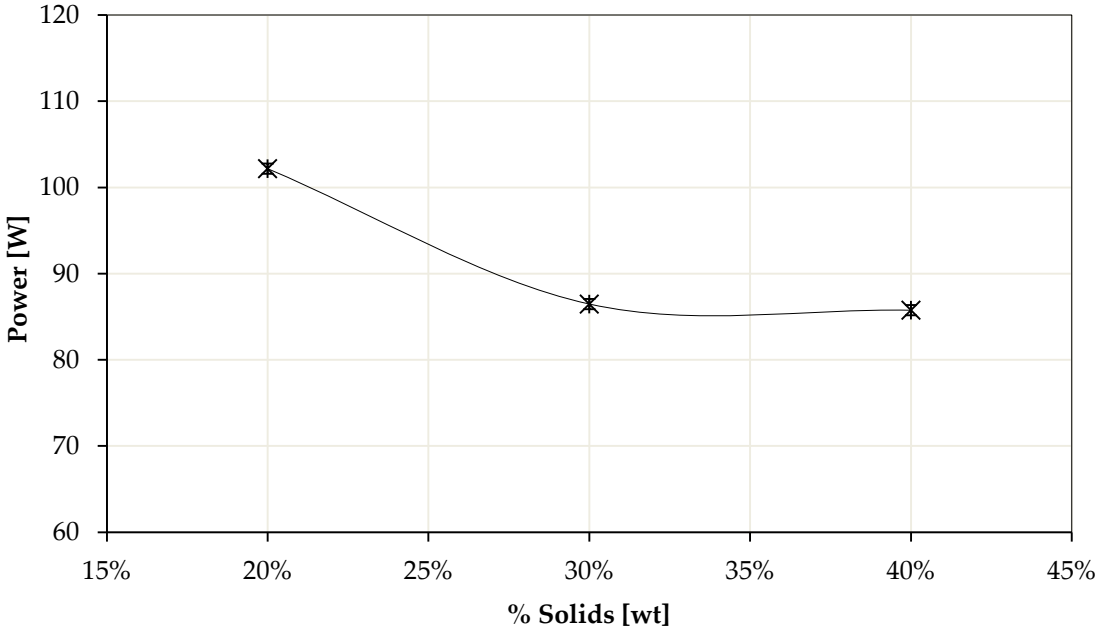

Figure 4.31: Power draw versus % solids

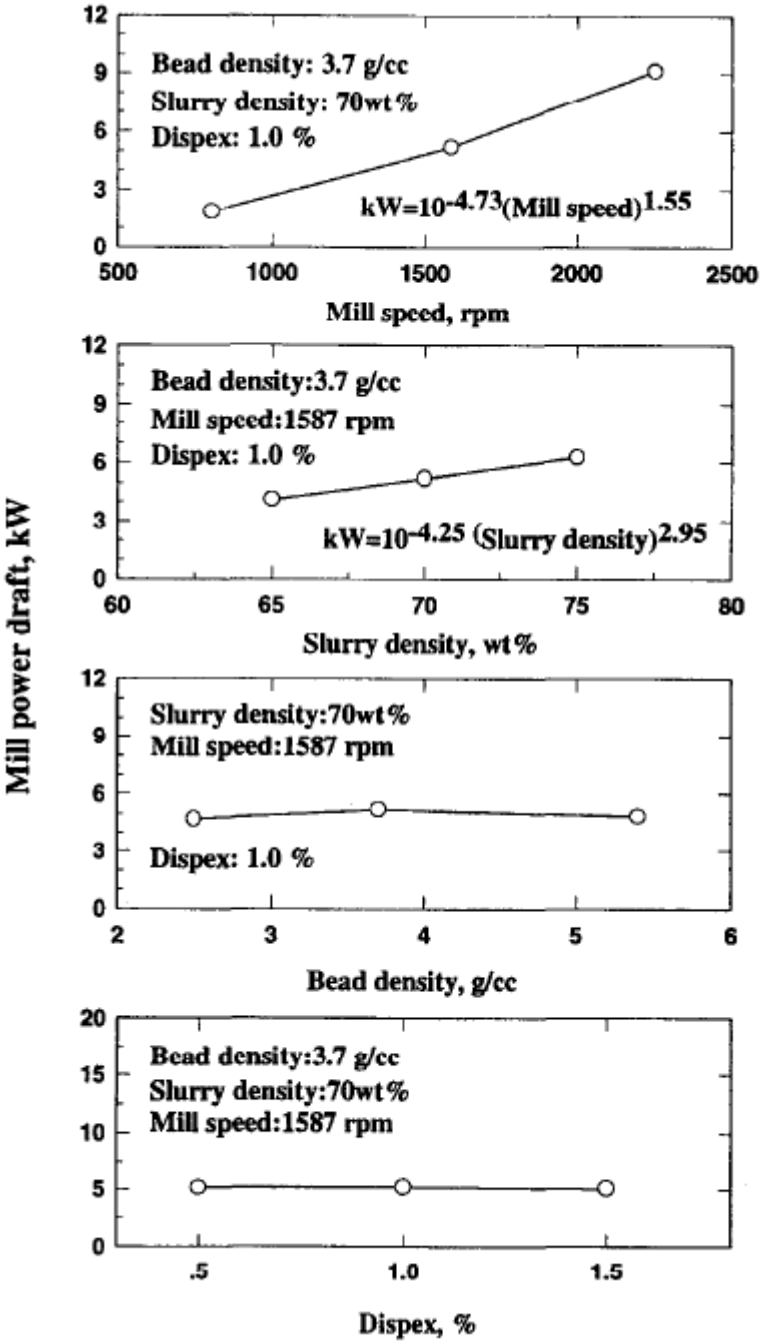

Figure 4.32: Effect of mill speed, slurry density, media density and dispersant on power draw in a horizontal stirred mill with perforated disc stirrers (Gao et al., 1996)

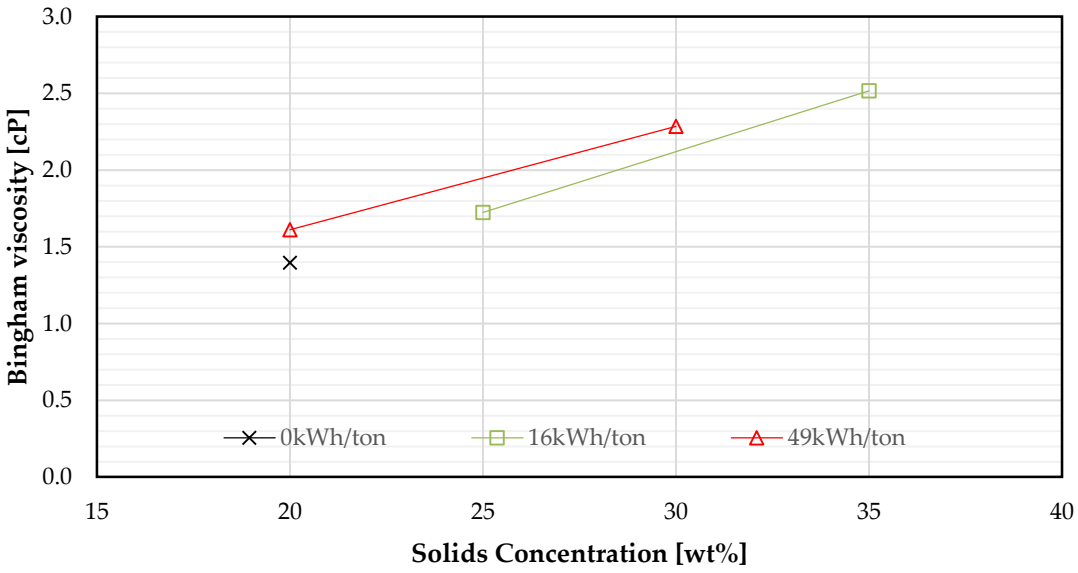

Figure 4.33: Bingham viscosity versus solids concentration (courtesy of Ruwona, 2015)

4.3.2.3 Rate

The grinding rates were evaluated at solids concentrations of 20 %, 30 % and 40 %. From equation 4.5, which was defined in this study (where $Rate_{SA}$ and EU_{SA} were defined in equations 4.1 and 4.3 respectively), it is seen that the rate is proportional to the power draw of the system. It is also seen that as the mass flow ($\dot{m}_p$) increases (the solids concentration), the rate decreases and as previously seen the efficiency increases (Figure 4.27). Figure 4.34 and Figure 4.35 confirms that the fastest rate occurs at a solids concentration of 20 % for all energy inputs, this is confirmed by the similar power draw, which coincides with the solids concentration at which the highest power draw was observed. The number of particles in the stirred mill is inversely proportional to stress number (from equation 2.2), so a lower number of particles in the mill (20 % solids concentration) would therefore have a higher stress number i.e. a higher chance for particle collisions and breakage events to occur. Figure 4.34 and Figure 4.35 also shows the generation of new surface area and new mass passing 10 µm. These results show that as the solids in the stirred mill is increased, the speed rate decreases but the generation of new mass/surface area increases or remains relatively constant. The solids throughput or solids concentration is therefore vital in terms of generation of new mass/surface area in stirred mill operations. Figure 4.36 shows the PSD's at varying solids concentrations after four passes (constant residence time) and shows

that the fineness of grind increases with decreasing solids concentration in this study. This figure also confirms that the fastest rate occurs at 20 % solids.

$$\frac{Rate_{SA}}{EU_{SA}} \alpha \frac{P_m}{(\dot{m}_p \cdot \tau_{grind})} \tag{4.5}$$

Where:

- $Rate_{SA}$ – Rate on a surface area basis
- EU_{SA} – Energy efficiency on a surface area basis
- P_m – Power of the mill
- m_p – Mass in the mill
- τ_{grind} – Residence time

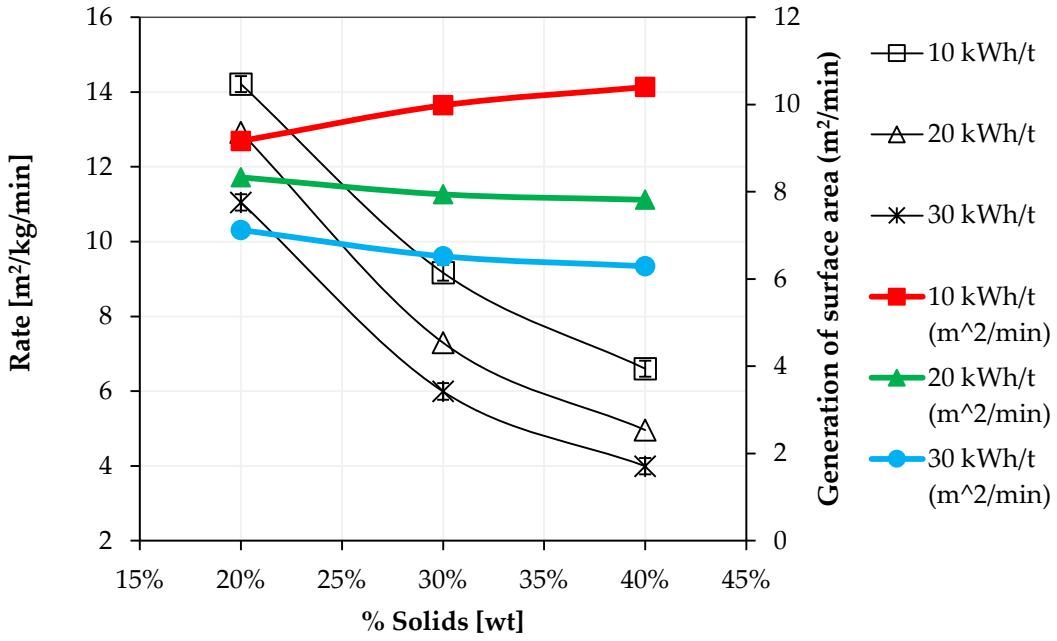

Figure 4.34: Grinding rates versus % solids at varying E_{cs}

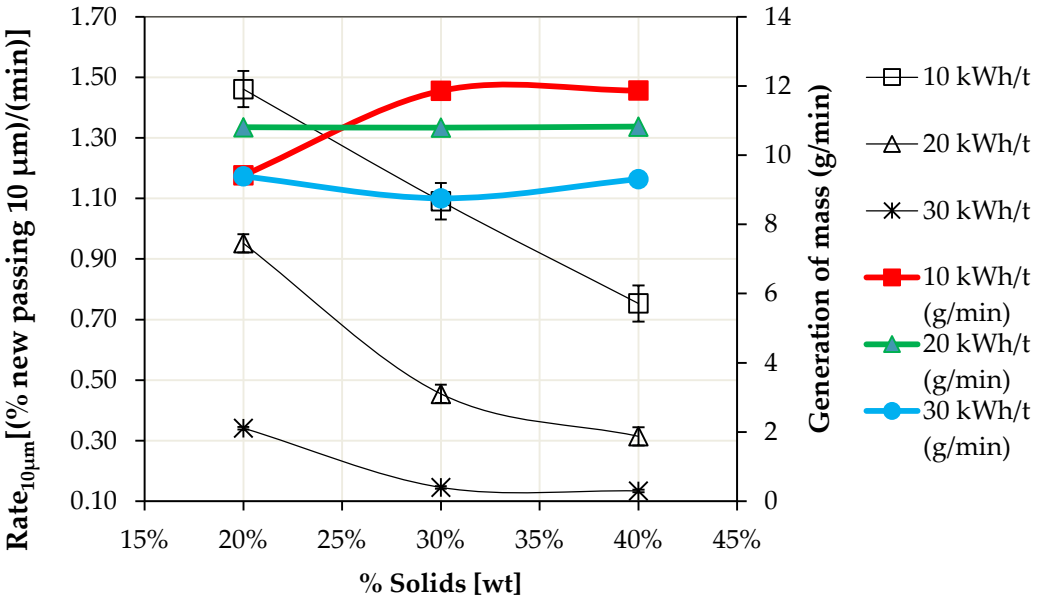

Figure 4.35: Grinding rates versus % solids (% new passing 10 µm)

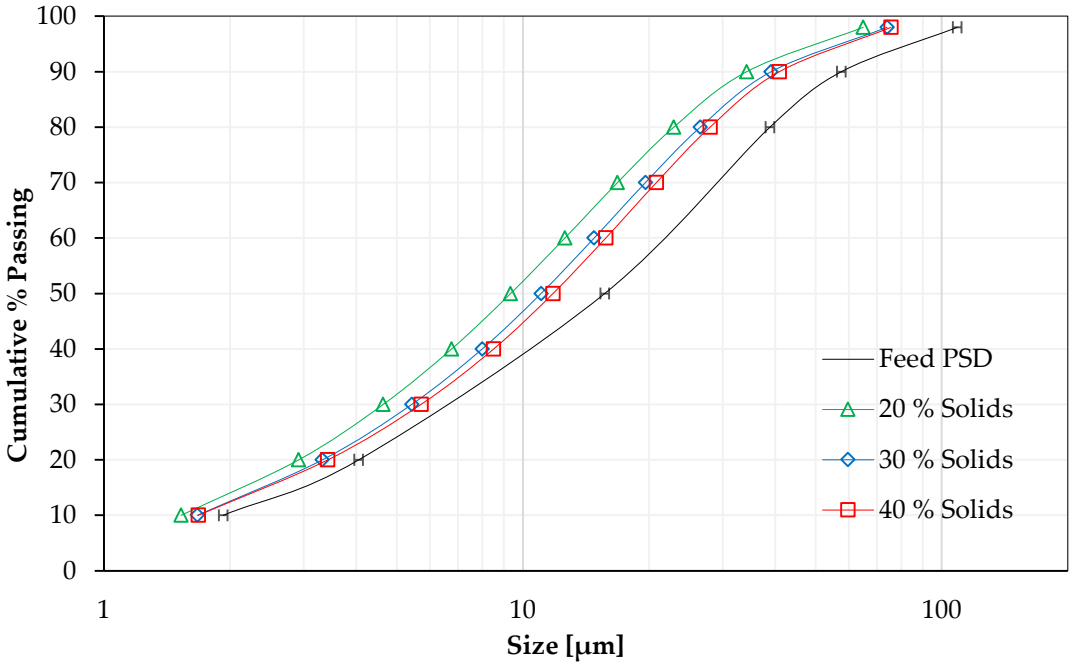

Figure 4.36: PSD's at varying % solids after pass 4

The best efficiency in this study occurred at 40 % solids for all energy inputs. It is known from past studies (Mankosa et al., 1989; Yue and Klein, 2004; He et al., 2004) that a maximum efficiency point occurs where after the efficiency decreases, it is speculated that an optimum efficiency would arise if higher concentrations were used in this study. The best rate occurred at the lowest solids concentration of 20%, for all energy inputs. The rate is proportional to the power draw, this is why the best rate coincides with the highest power draw.

4.3.3 The effect of grinding media size on efficiency, power and rate

The correct selection of grinding media can greatly reduce the energy consumption and improve energy efficiency. The selection of grinding media sizes is dependent on the feed PSD and target grind size (Zheng et al., 1996). The media provides the contact surface area needed for grinding and is the primary limitation for the fineness of the grind. From equation 2.5 it is seen that the grinding media size, d_{GM}, has the largest influence on the stress energy of the grinding media. 1.5 mm, 2.0 mm and 3.0 mm monosized grinding media were used in this study. The stirrer speed, % solids and % mill filling were kept constant at centre point conditions of 10 m/s, 30 % solids and 75 % mill filling respectively. Figure 4.37 and Figure 4.38 shows the signature plots (P80 versus E_{CS}) and PSD's at varying grinding media sizes at 10 kWh/t at varying grinding media sizes respectively.

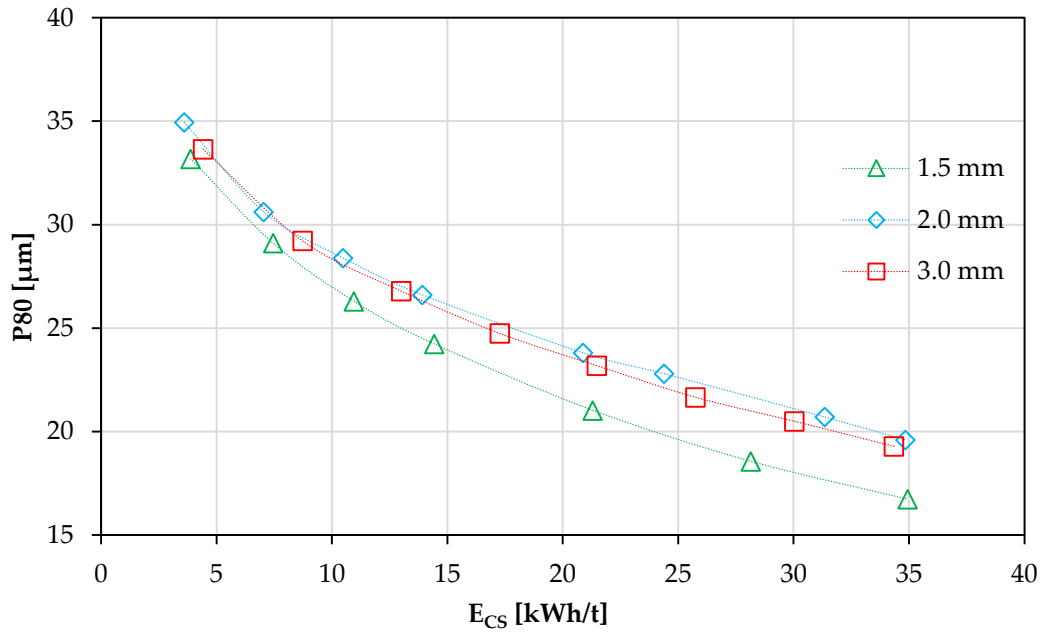

Figure 4.37: P80 versus specific energy input at varying media sizes

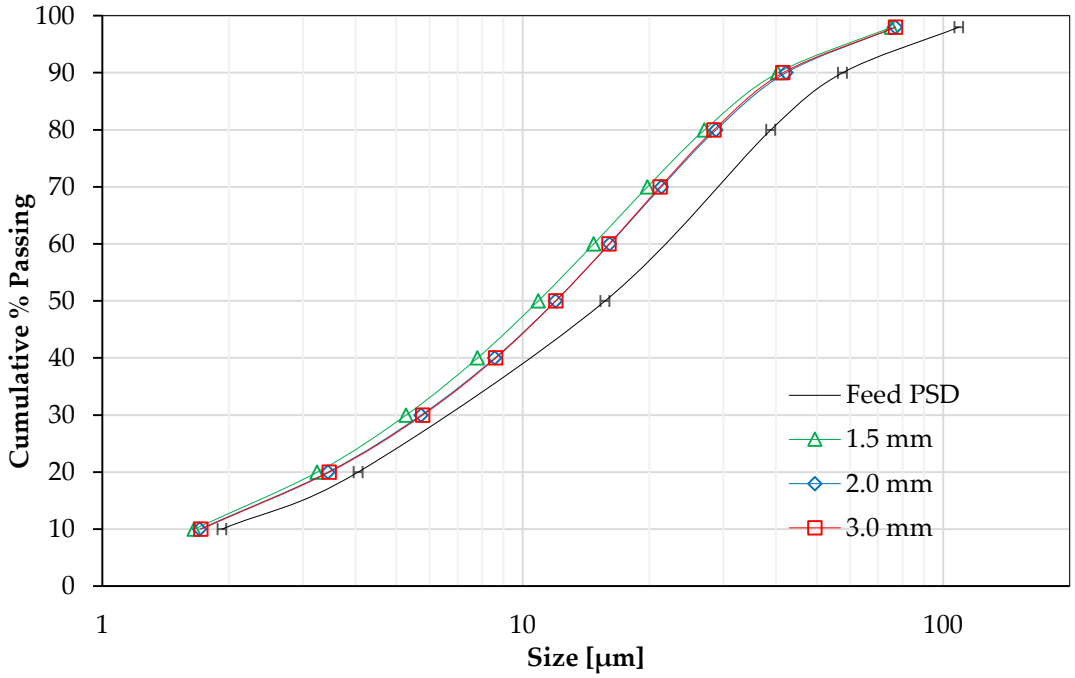

Figure 4.38: PSD's of 10 kWh/t energy input at varying media sizes

4.3.3.1 Efficiency

Figure 4.39, Figure 4.40 and Figure 4.41 shows grinding media size at energy inputs of 10 kWh/t, 20 kWh/t and 30 kWh/t versus grind size and efficiencies respectively. The figures show that the smallest media size is the most efficient for all energy inputs. When looking at media there are typically two factors to consider that affect grinding:

1. How much energy is transferred between the media and particles i.e. is the stress energy sufficient to propagate a fracture?
2. The number of grinding media in the system which is influenced by media size. Smaller media will always have more media in the system for a constant media filling than larger grinding media i.e. this is the stress number in the stress energy model.

Larger media have a higher transferrable energy due to a larger mass than smaller media at a constant media density. In this study the 2 mm and 3 mm have a larger transferrable energy than the 1.5 mm media. This higher transferrable energy might be more than is needed for breakage at this fine grind and energy is wasted, leading to less efficient grinding. In addition the effective contact surface area for grinding of the 2 mm and 3 mm media is less than the 1.5 mm contact surface area, leading to less media – particle collisions (lower stress number). From the results it is observed that the efficiency decreases as larger media is used. Jankovic (2003) using a low speed

vertical stirred mill with pins, shows that as media size increases the P80 grindsize increases (Figure 4.42). The P80 grindsize increases with larger media and decreasing energy input. The results of this study shows similar trends to that of Jankovic's (2003) on media size and is shown in Figure 4.38.

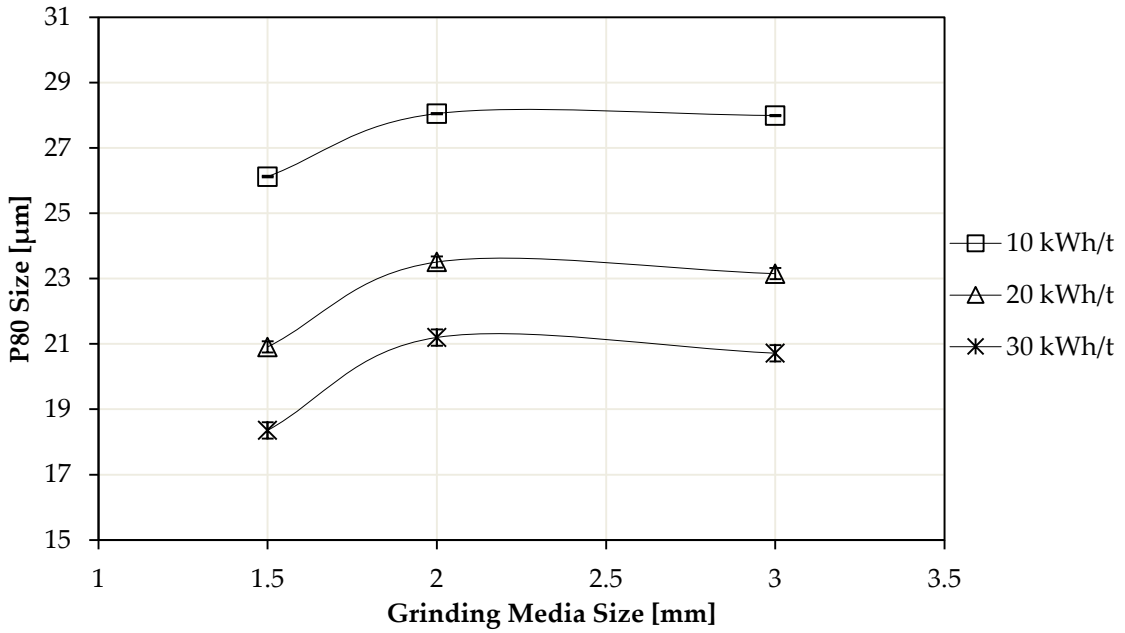

Figure 4.39: P80 size versus grinding media size

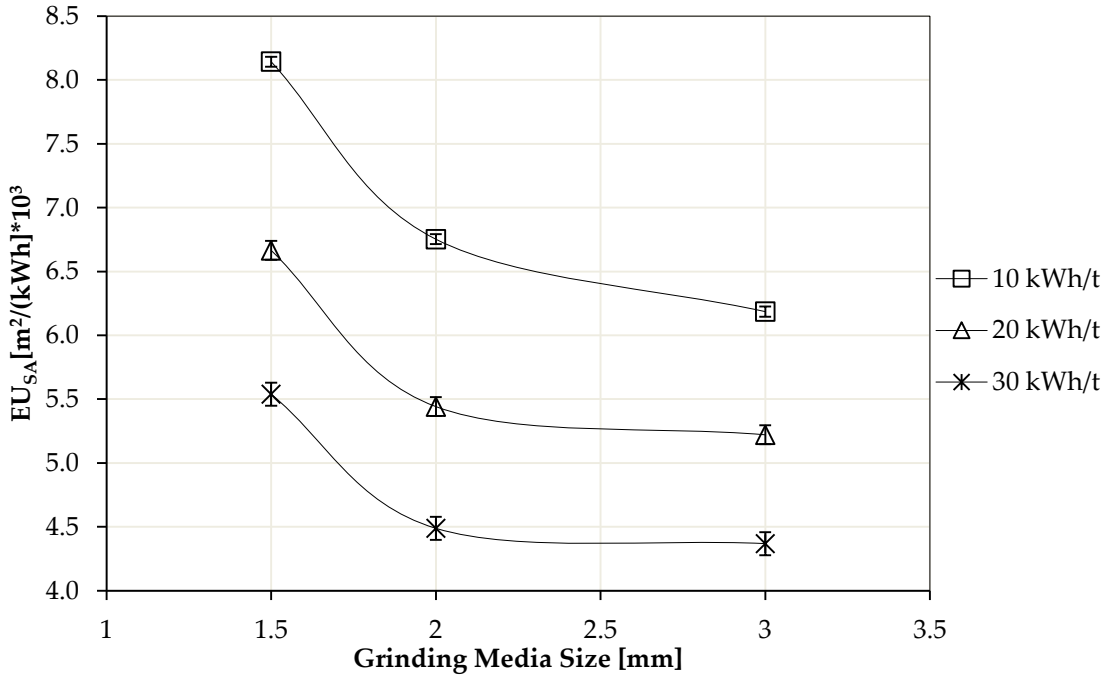

Figure 4.40: EUSA (Energy Utilisation) versus grinding media size

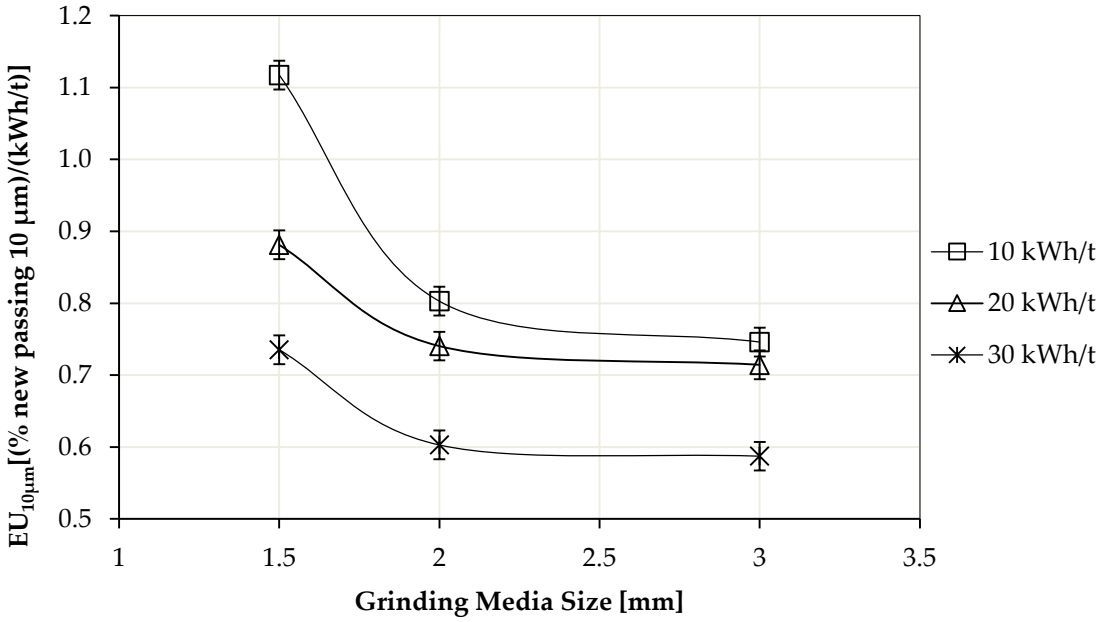

Figure 4.41: $EU_{10\mu m}$ (Energy Utilisation) versus grinding media size (% new passing 10 µm)

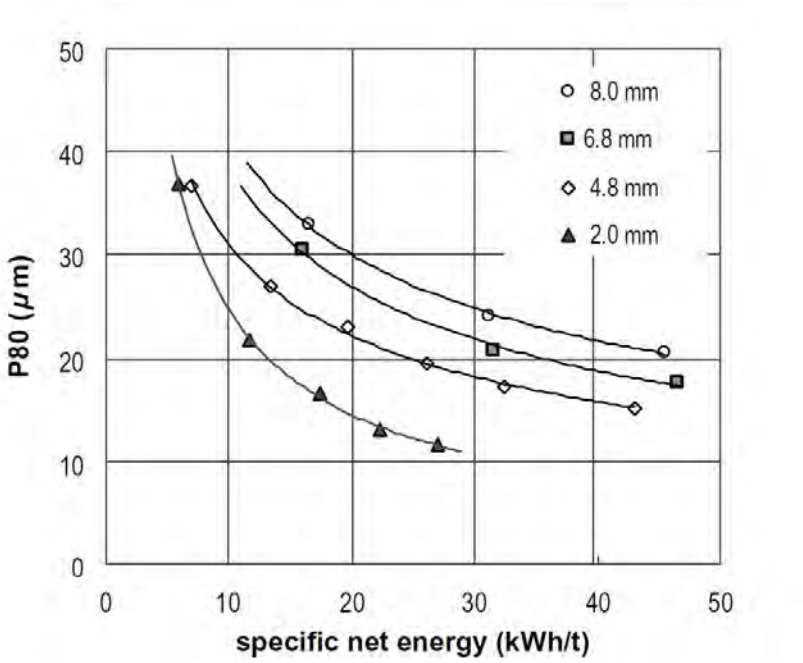

Figure 4.42: Grindsize versus specific energy input at different media sizes in a low speed vertical pin mill (Jankovic, 2003)

It is observed that at the smallest media size obtains the finest grind and there is no distinguishable differences between the 2 mm and 3 mm media sizes. This complements the previous figures in that it shows that the 1.5 mm media is the most efficient used. All grinding media size PSD's are shown in Figure B.3 in Appendix B. The signature plots (Figure A.27) confirm what is seen in Figure 4.39 and Figure 4.40 in that the smallest media size is the most energy efficient used during this study.

It is easy to see why the smaller media is more energy efficient during these experiments. Smaller grinding media have less transferrable energy than larger sized grinding media of the same density but the surface area available for grinding is larger than larger sized media. This is especially important in fine grinding, such as this study when grinding to sizes of P80's < 30 µm. The number of stress events that occur when smaller media is used is always greater than that of larger media, due to the higher number of media present in the stirred mill leading to a high number of media contacts. However if too small media is used, little or no grinding will occur due to the low energy the small grinding media possess. This result is seen in the works of Kwade et al (1996), shown in Figure 4.43. The main outcomes from Figure 4.43 is that it shows the impact the media size has on the grind size, very small media has no effect on grinding, and there is an optimum media size for an energy input.

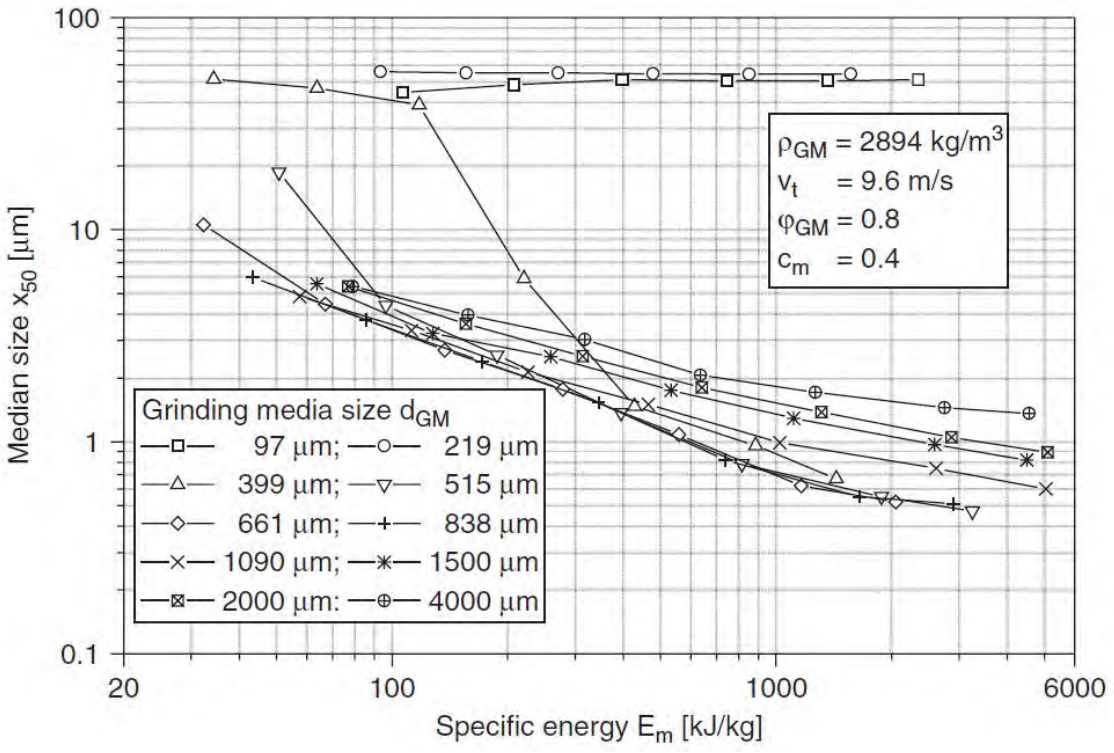

Figure 4.43: Grindsize versus specific energy input at different media sizes in a horizontal stirred mill (Kwade et al., 1996)

If too large media is used, more energy will be lost on media – media collisions and media deformations. This result is seen in the works of Kwade et al (1996) and Jankovic (2003) (Figure 4.43 and Figure 4.42) as well as in this study.

Mankosa et al (1986) and Zheng et al (1996), both found an optimum monosize grinding media for their particular feed PSD's, and stirred mill configurations. Finding the optimum grinding media size for a particular feed PSD is important to improve energy efficiencies. From the results it is shown that in this study, it is more beneficial to use smaller media (< 2 mm) when a target P80 is less than 30 μm. The optimum grinding media size in this study was the smallest grinding media used (1.5 mm). It is however noted here that as the particles are ground in the stirred mill the optimum media size would change. Using a media size distribution would be beneficial to the system as seen in industrial scale mills. In industrial scale processes, stirred mills are commissioned with a mono-sized charge, however over time due to media wear a media charge distribution is formed. This is because top size media is continually added to the stirred mill to replace the worn media and to maintain a constant charge volume in the stirred mill.

4.3.3.2 Power

Figure 4.44 shows power draw versus media size and that smaller media has a lower power draw than larger media. The power drawn by the stirred mill increases as media size increases. This could be due to the fact that the contents in the mill is more fluid-like when using smaller media leading to a reduced energy input (Zheng et al, 1996). More power is therefore needed to generate a better fluidised slurry – media suspension when using larger grinding media.

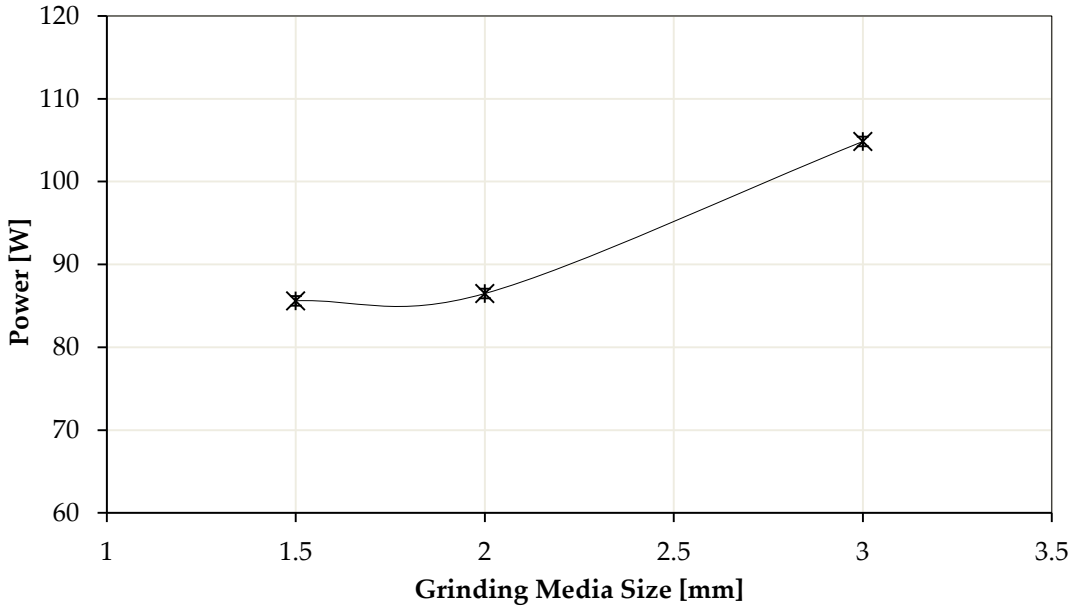

Figure 4.44: Power draw versus media size

4.3.3.3 Rate

The effect of media size on grinding rate was also evaluated. From Figure 4.45 it is seen that the highest grinding rate occurs at 1.5 mm for all energy inputs, based on the surface areas. The rate is fastest when 1.5 mm media is used due to the high surface contact area the 1.5 mm media provides over the 2.0 mm and 3.0 mm. A non-optimal point is found at the 2 mm grinding media (Figure 4.45), this is an interesting observation and could mean that at this point the energy transfer (stress energy) and number of grinding media in the system (stress number) is not sufficient. An increase in rate is seen from 2.0 mm to 3.0 mm, this can be attributed to the fact that the 3.0 mm grinding media has a higher transferable energy available for particle fracture. Figure 4.46 shows the rate based on the % new passing 10 μm, this figure shows the same trend as Figure 4.45 for the 10 kWh/t energy input only. The rates at 20 kWh/t increases as the media size is increased, and the rates at 30 kWh/t is relatively constant. Figure 4.47 shows the PSD's at varying media size after four passes (constant residence time). The PSD figure after four passes complements Figure 4.45 and Figure 4.46, it is observed that the 1.5 mm media provides the fastest grind followed by the 3 mm, with the 2 mm being the slowest grind.

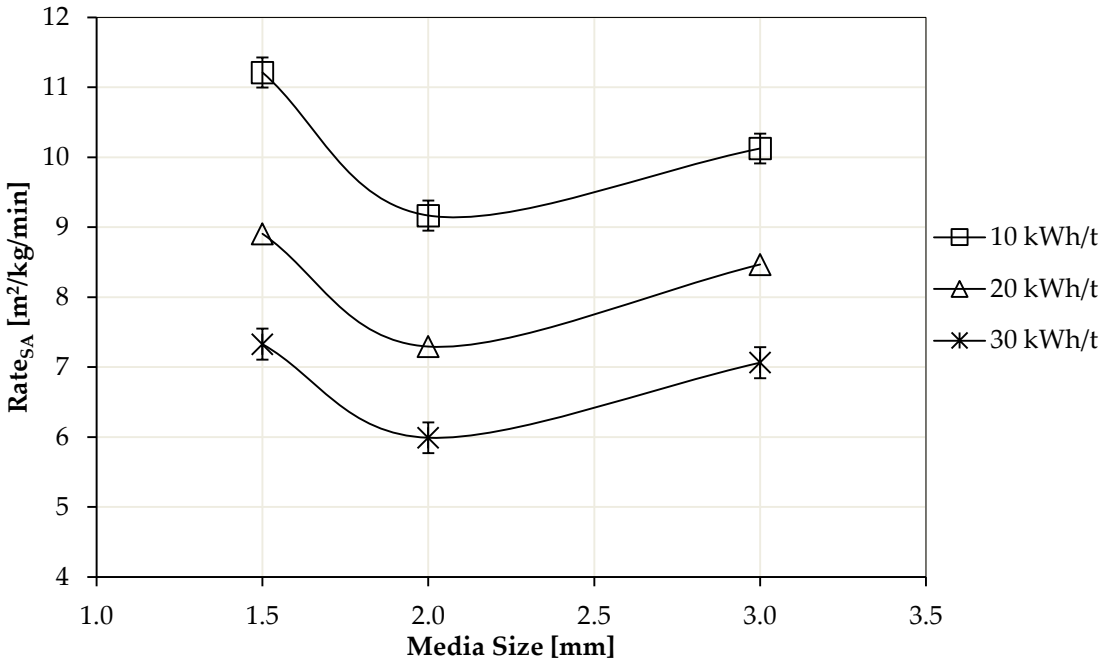

Figure 4.45: Grinding rates versus media size at varying E_{cs}

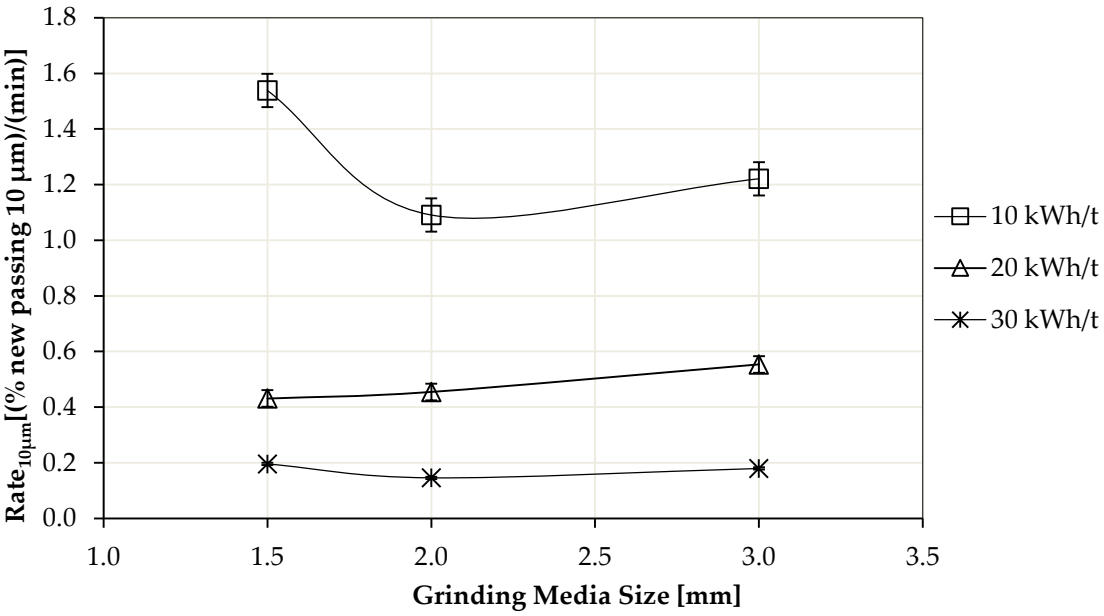

Figure 4.46: Grinding rates versus grinding media size (% new passing 10 μm)

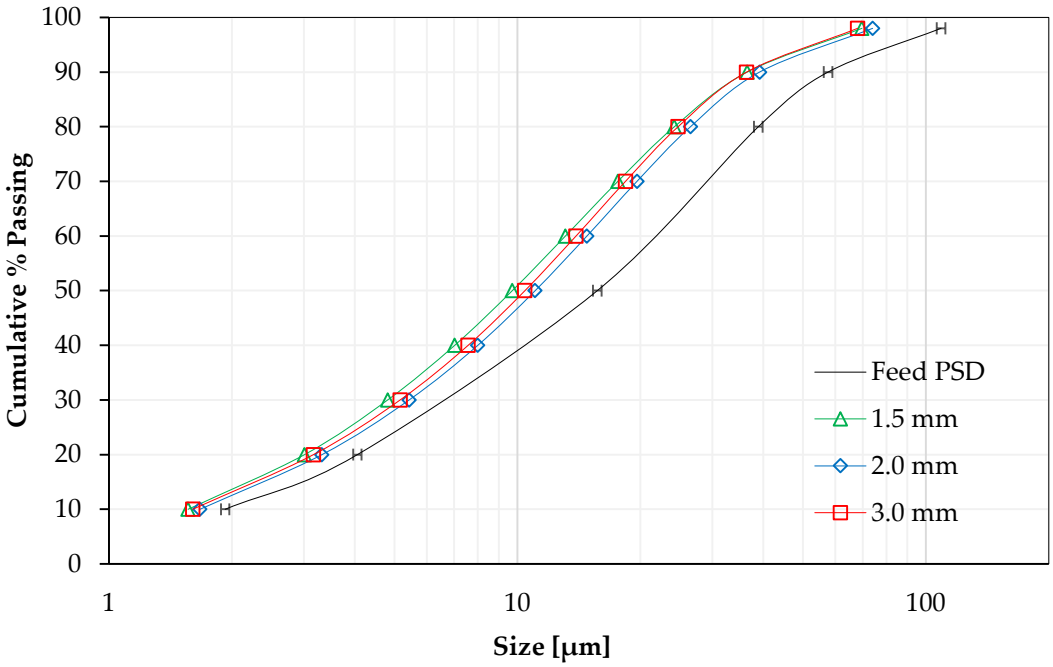

Figure 4.47: PSD's at varying media size after pass 4

The main outcomes from the media size results illustrates that there has to be a sufficient number of stresses for a higher rate (1.5 mm media – high contact surface area) or the breakage energy needs to be sufficiently high to fracture the particle at a high rate (3.0 mm media – high transferrable energy), as shown in Table 4.1.

Table 4.1: Stress number versus stress energy

Media Size (mm)	Stress Number	Stress Energy
1.5	***High***	Low
2.0	Med	Med
3.0	Low	***High***

From the results the 1.5 mm provided both the best efficiency and rate in this study.

4.3.4 The effect of grinding media filling on efficiency, power and rate

The grinding media filling is also an important variable in fine grinding. It directly affects the media motion in a stirred mill. In horizontal mills the energy utilisation increases as the media filling is increased, however an optimum media filling exists where after the energy utilisation decreases (van der Westhuizen et al., 2011). It is believed that this phenomenon also occurs in vertical stirred mills. The media loadings tested are 65 % (low), 75 % (intermediate) and 85 % (high). The range of grinding media loadings (65 % - 85 %) was selected based on literature (Rahal et al., 2011), and it is believed that an optimum media filling occurs within this range. In these tests, the stirrer speed, % solids and grinding media size were kept constant at centre point conditions of 10 m/s, 30 % solids and 2.0 mm respectively. Figure 4.48 and Figure 4.49 shows the P80 versus E_{CS} plots at varying % mill fillings and the PSDs of 65 %, 75 % and 85 % mill filling at an energy input of 10 kWh/t.

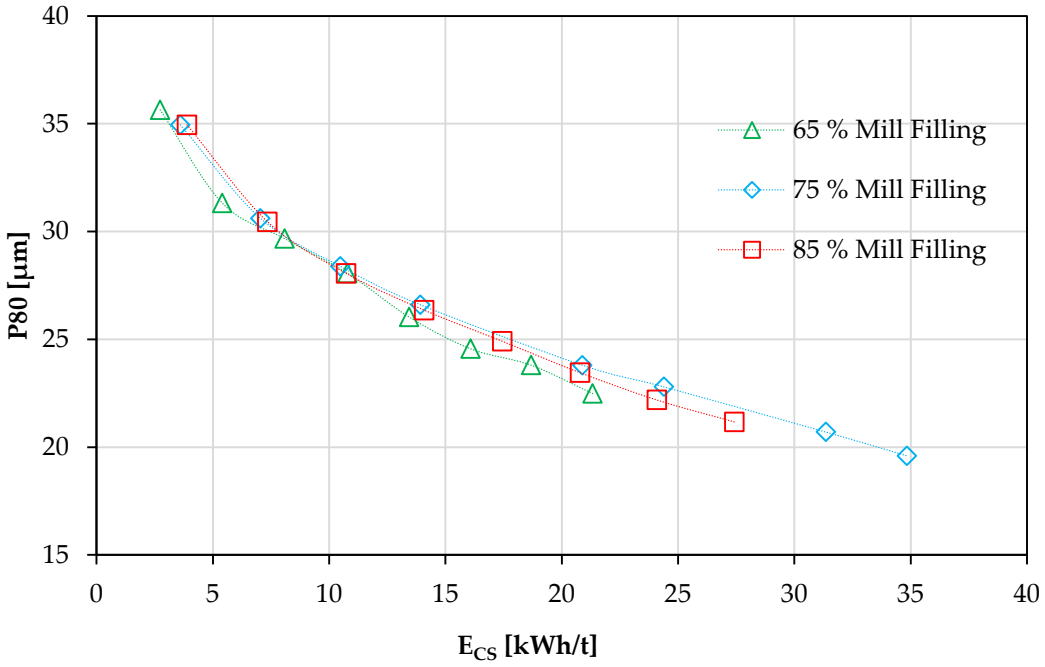

Figure 4.48: P80 size versus specific energy input

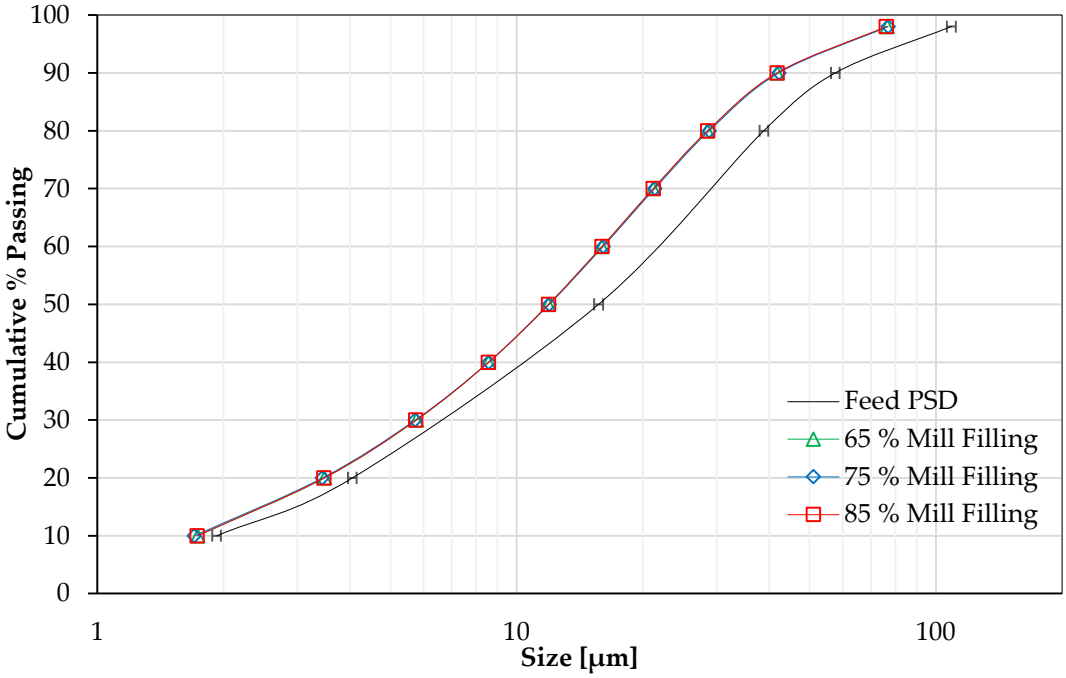

Figure 4.49: PSD's at 10 kWh/t energy input at varying mill fillings

4.3.4.1 Efficiency

From Figure 4.49 it is seen that there is no clear distinction between the PSD's. However it is seen from Figure 4.48 that the curves are only identical at 10 kWh/t, with the 65 % curve the most efficient elsewhere. Figure B.1, in the appendix shows the full PSD's at all mill fillings. Figure A.28 shows the signature plots at varying mill fillings.

Figure 4.50 shows the grinding media mill filling versus P80 size. From these results, the % mill filling does not seem to affect the efficiency. The % mill filling does not influence the P80 grind size to a large extent. However from Figure 4.48 it is observed that the 65 % mill filling is the most efficient condition. From Figure 4.51 and Figure 4.52 it is observed that 65 % mill filling is the best efficiency. It is also noted that as the energy input is increased the energy utilisation decreases due to a finer product grind.

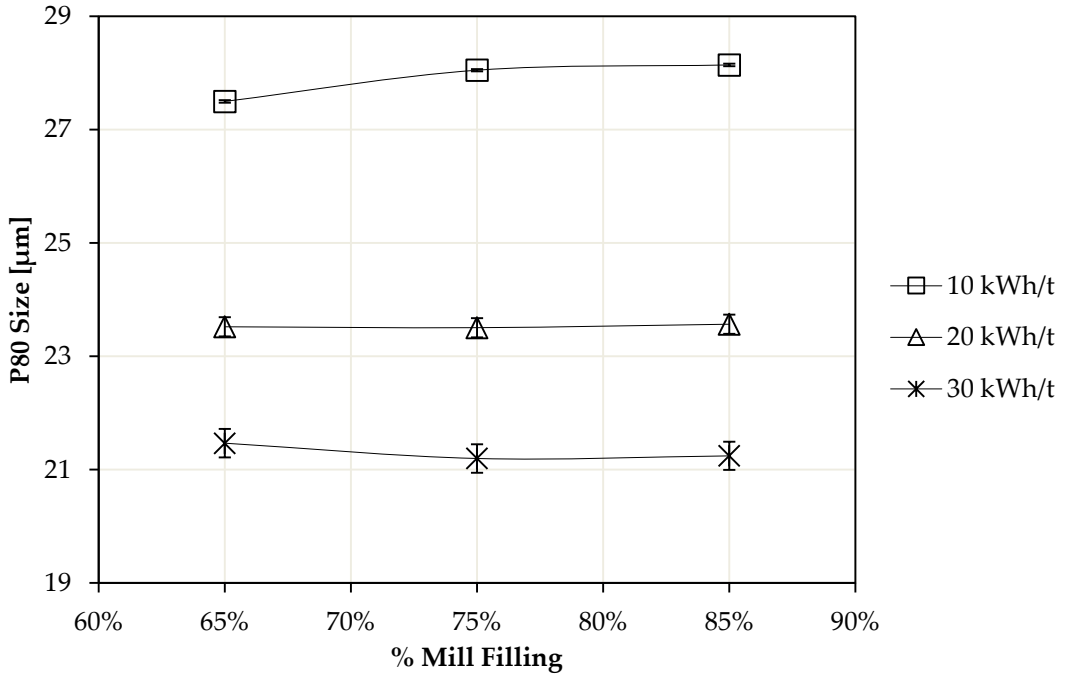

Figure 4.50: P80 versus % mill filling

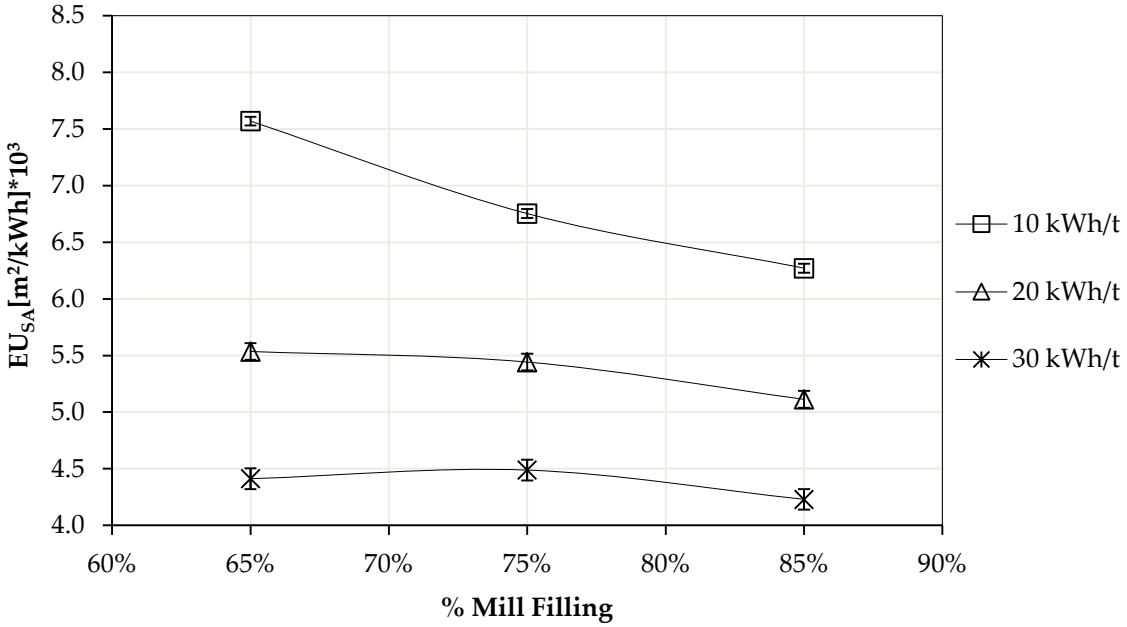

Figure 4.51: EUSA (Energy Utilisation) versus % mill filling

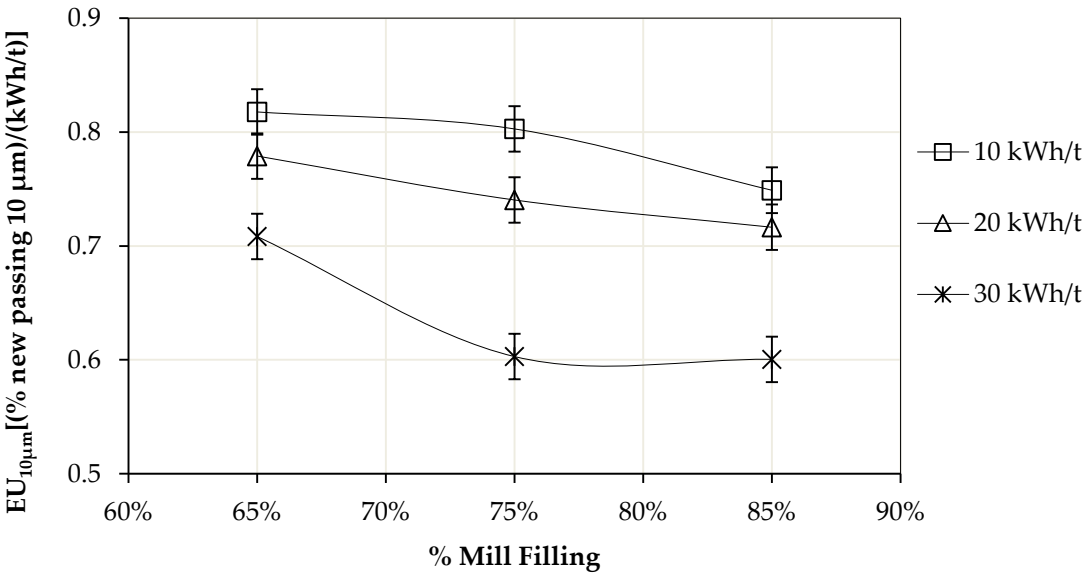

Figure 4.52: $EU_{10\mu m}$ (Energy Utilisation) versus % mill filling (% new passing 10 µm)

At much lower mill fillings (< 65 %) there are fewer media – particle collisions, and fewer progeny particles are generated through these collisions leading to a coarser product or target grind. Where a coarser grind size is targeted at low energy inputs, it is beneficial for the process to have a lower mill filling because less energy will be used on the unwanted movement of the extra grinding media. From a stress energy viewpoint, less stress events are required between the media and particles to produce the desired grind result and more stressing events would result in over grinding

More particles will be generated through a high specific energy input and a larger grinding volume is required to achieve a desired comminution result more efficiently. An increase in mill filling would supply this extra grinding volume by increasing the media – particle collisions, i.e. an increase in the number of stress events and provide a larger contact surface area for grinding. The number of media contacts is proportional to the number of stresses, so as the mill filling is increased, the number of media contacts increases and so too the number of stresses leading to a finer grind. Jayasundara et al. (2010) showed using DEM in a horizontal stirred mill, that although higher mill fillings have higher impact energy intensities a large portion of this energy is dissipated without being used for grinding and there exists is an optimal mill filling below 90%. In the case of vertical stirred mills, Barley et al (2004) showed using PEPT that 60% mill filling was the optimal filling during their experiments. An optimum mill filling therefore exists in stirred mills.

4.3.4.2 Power

Figure 4.53 shows the % grinding media mill filling versus the power drawn. The power draw increases from 65 % mill filling to 75 %, where it is approximately constant to 85 % mill filling. An explanation for this trend can be that at 65 % mill filling the grinding media is not above the last disc in the vertical stirred mill and requires less power to keep the media fluidised. An increase in mill filling would generate a higher power draw due to keeping the grinding media fluidised. The relatively constant power draw between 75 % and 85 % can possibly be explained due to the fact the grinding media is being fluidized above the top disc in the vertical stirred mill, and does not require a larger power input. Figure 4.54 shows the media height at 75 % mill filling. It is seen that the media is just below the top disk stirrer. It is assumed that when the media is agitated and fluidised the media would rise above the top stirrer. At 85 % mill filling the media would also be fluidised above the last stirrer.

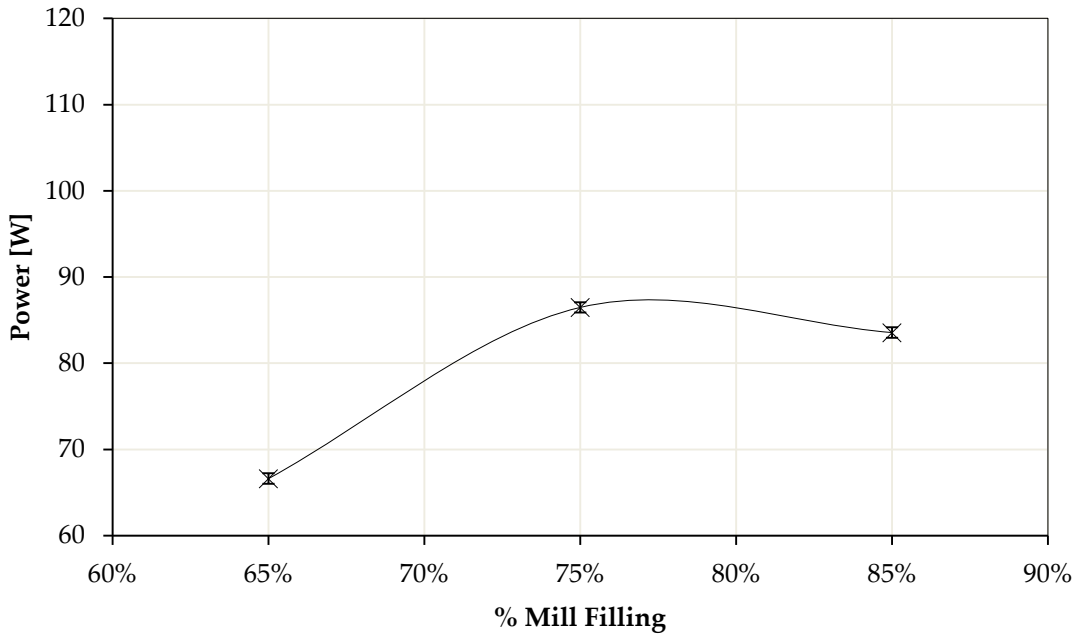

Figure 4.53: Power draw versus % mill filling

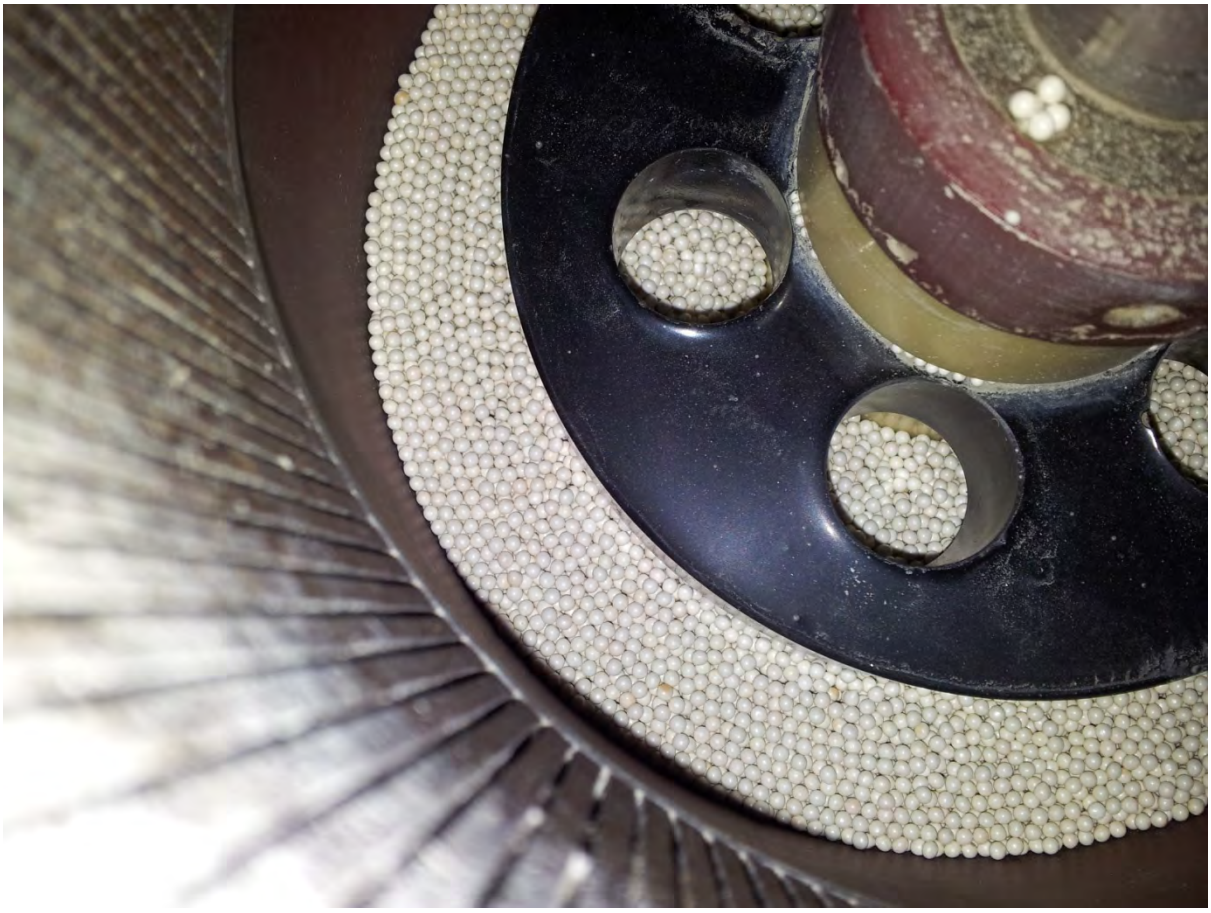

Figure 4.54: Picture showing 75 % mill filling

4.3.4.3 Rate

Figure 4.55 and Figure 4.56 shows the effect of mill filling on the grinding rate. The effect of grinding rate was evaluated at 65%, 75 % and 85 % mill filling by volume. An optimum grinding rate occurred at 75 % mill filling for all energy inputs when a surface area basis was used (Figure 4.55). As the grinding volume increases with an increase in mill filling, there are more media – particle interactions leading to a faster grinding rate i.e. an increased frequency of stress events. When the mill filling is too high, more media – media interactions take place, leading to a slower grinding rate. Looking at Figure 4.56, it can be seen that at higher energy inputs the optimum grinding rates become less distinguishable. Figure 4.57 shows the PSD's of mill filling after four passes through the mill. It is observed that at constant residence time (four passes), 75 % and 85 % mill filling grinds faster than 65 % mill filling. This figure compliments Figure 4.55 and Figure 4.56 in showing that the optimum grinding rate lies between 75 % - 85 % mill filling.

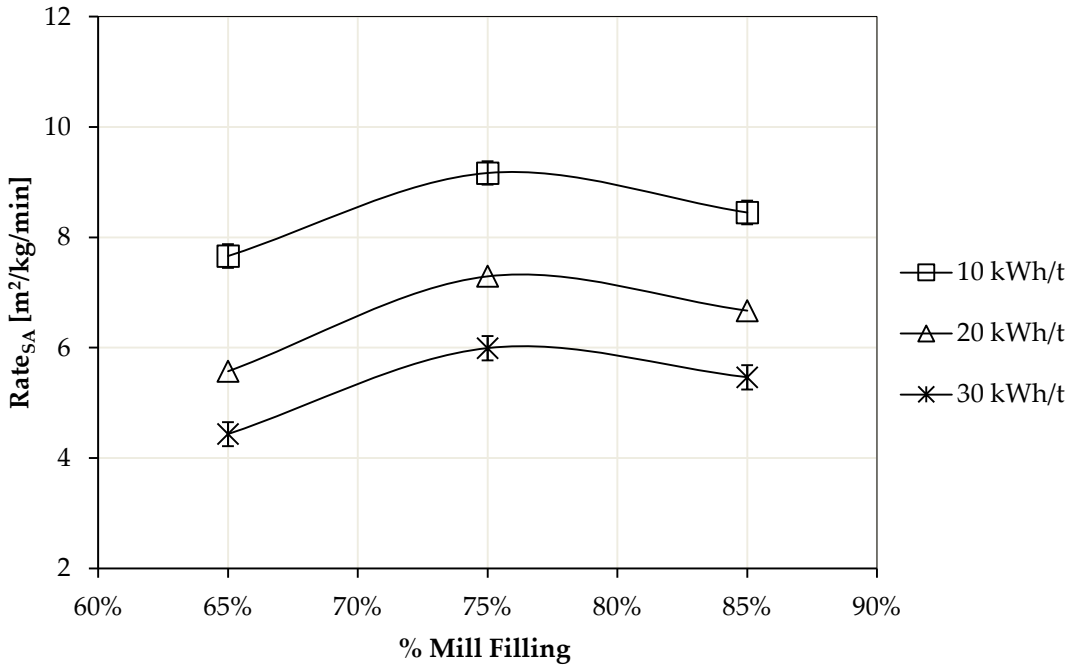

Figure 4.55: Grinding rates (surface area) versus % mill filling at different E_{cs}

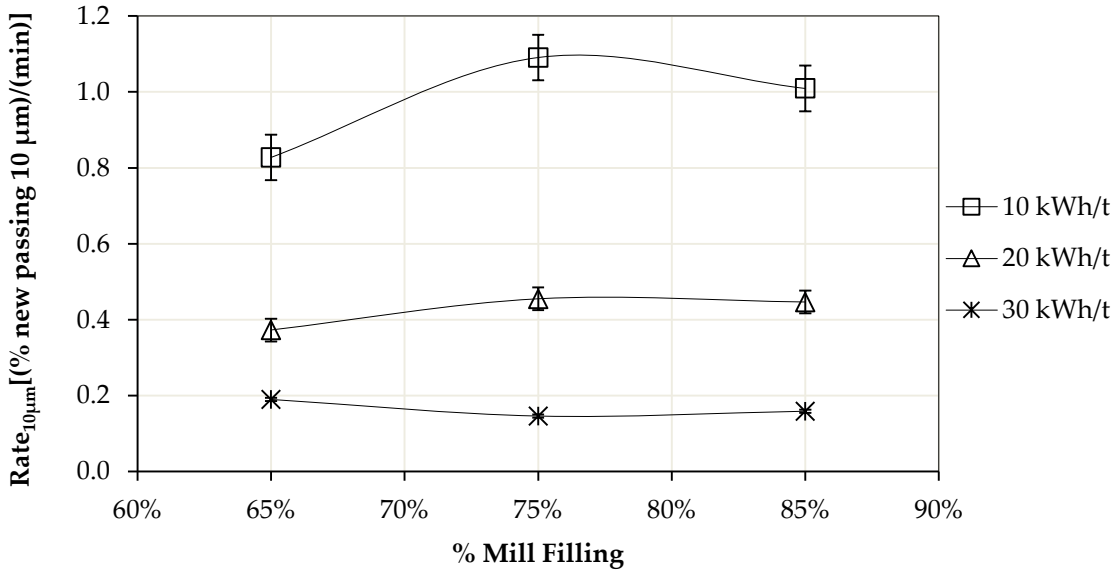

Figure 4.56: Grinding rates versus % mill filling (% new passing 10 μm)

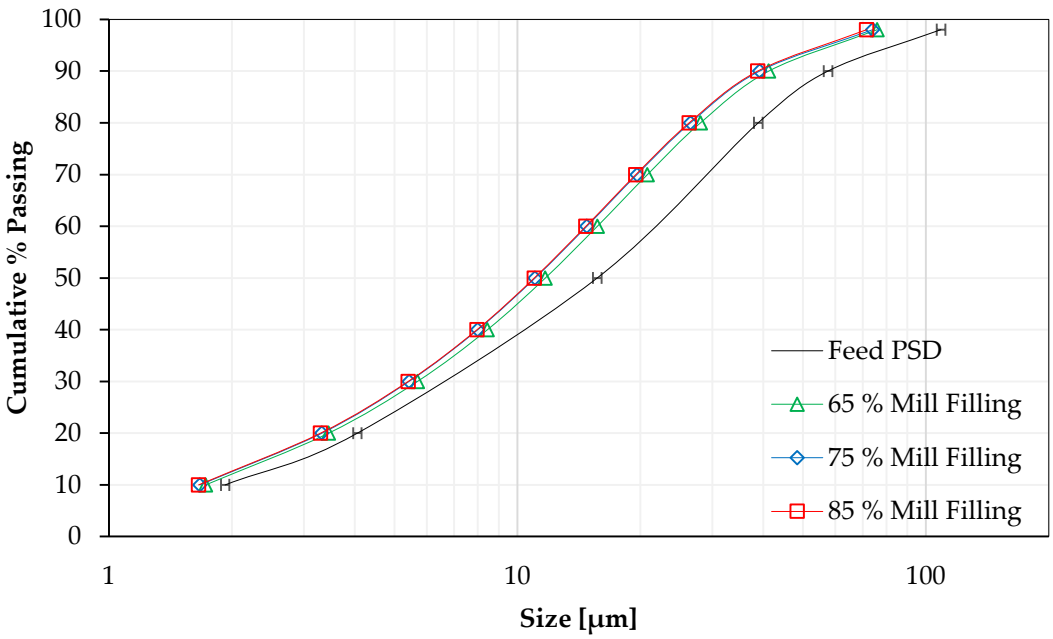

Figure 4.57: PSD's at varying mill filling after pass 4

From the results it can be seen that the mill filling during these experiments has minor effects on overall energy efficiency. The best efficiencies for this study lies at 65 %. The power draw increases as the mill filling is increased from 65 % - 75 %, the mill filling is constant from 75 % - 85 % mill filling possibly due to media fluidising above the last disc stirrer. The best grinding rate occurs at 75 % mill filling, which coincides with the power draw results, where a high rate occurs at a high power draw.

4.4 Assessing operating parameters using statistical analysis

The aim of using a design of experiments approach was to build multiple linear regression models, where a regression model can be used to optimise a system.

The relationships and interactions between the parameters were investigated and regression models of P80's and rates were built at different energy inputs of 10 kWh/t, 20 kWh/t and 30 kWh/t. The 10 kWh/t regression model can be found in this chapter while the 20 kWh/t and 30 kWh/t empirical models can be found in Appendix C. The energy inputs were chosen so that it covers the broad range of energy inputs of all the completed experiments. A power model was also developed by regression analysis to predict the power draw of the vertical stirred mill. Using these models the system was optimised and a combination of efficiency and rate optimum conditions was determined.

The analysis of variance (ANOVA) results for the energy input models are presented in Appendix C, with the parity charts presented in Appendix D. The ANOVA table includes the p-values of the variables, if the p-value of a variable is less than 0.05 the variable is significant. This means that the probability that the variable is significant to the model is ≥ 95%. Where parameters with p-values greater than 0.05 are included in the statistical model, these were included to improve the overall model adequacy, and maintain model hierarchy. If an interaction term is significant, whilst one of the single factor terms is not significant, the single factor term is included in the model to maintain the model hierarchy and leading to a well formulated model and prediction.

The R^2 value of the model shows how well the model fits the data while the $R^2_{adjusted}$ value is adjusted for the "size" of the model. If the $R^2_{adjusted}$ and R^2 differ considerably, non-significant variables have been included in the model. The $R^2_{adjusted}$ value of the model will explain the percent of the variability in new data.

4.4.1 Efficiency and rate regression model – 10 kWh/t

Table 4.2 and Table 4.3 shows the R^2 values of the efficiency model and rate model respectively. For the efficiency model the R^2 value is 0.96 and the $R^2_{adjusted}$ value is 0.94, this means that the model will explain 94% of the variability in new data. For the rate model the R^2 value is 0.88 and the $R^2_{adjusted}$ value is 0.83, explaining 83% of variability in the new data. The model equations for efficiency and rate is shown in Table 4.4 and Table 4.5 respectively and can be used to explore the design space where only significant variables, and variables that contribute to model hierarchy are included. Table C.1 and Table C.2 (Appendix C) shows the full ANOVA results for the 10 kWh/t energy input. The parity charts, which show the predictive capabilities of the models are shown in Figure 4.58 and Figure 4.59 and are in good agreement. The colour scale on the parity charts gives an indication of low and high values with blue being low and red being high.

Table 4.2: R-Squared values - 10 kWh/t efficiency model

R-Squared	0.96
Adj R-Squared	0.94

Table 4.3: R-Squared values - 10 kWh/t rate model

R-Squared	0.88
Adj R-Squared	0.83

Table 4.4: Regression model equation - 10 kWh/t efficiency model

P80 at 10 kWh/t	=
27.7	(intercept)
0.96	* Stirrer speed
-1.31	* % Solids
0.7	* Media size
-0.37	* Stirrer speed * % Solids
0.32	* Stirrer speed * Media size
0.85	* % Solids^2
-1.01	* Media size^2

Table 4.5: Regression model equation - 10 kWh/t rate model

Rates at 10 kWh/t	=
9.20	(intercept)
1.79	* Stirrer speed
-2.95	* % Solids
0.60	* Media size
0.88	* % Mill filling
0.97	* Stirrer speed * % Mill filling
1.13	* Media size * % Mill filling

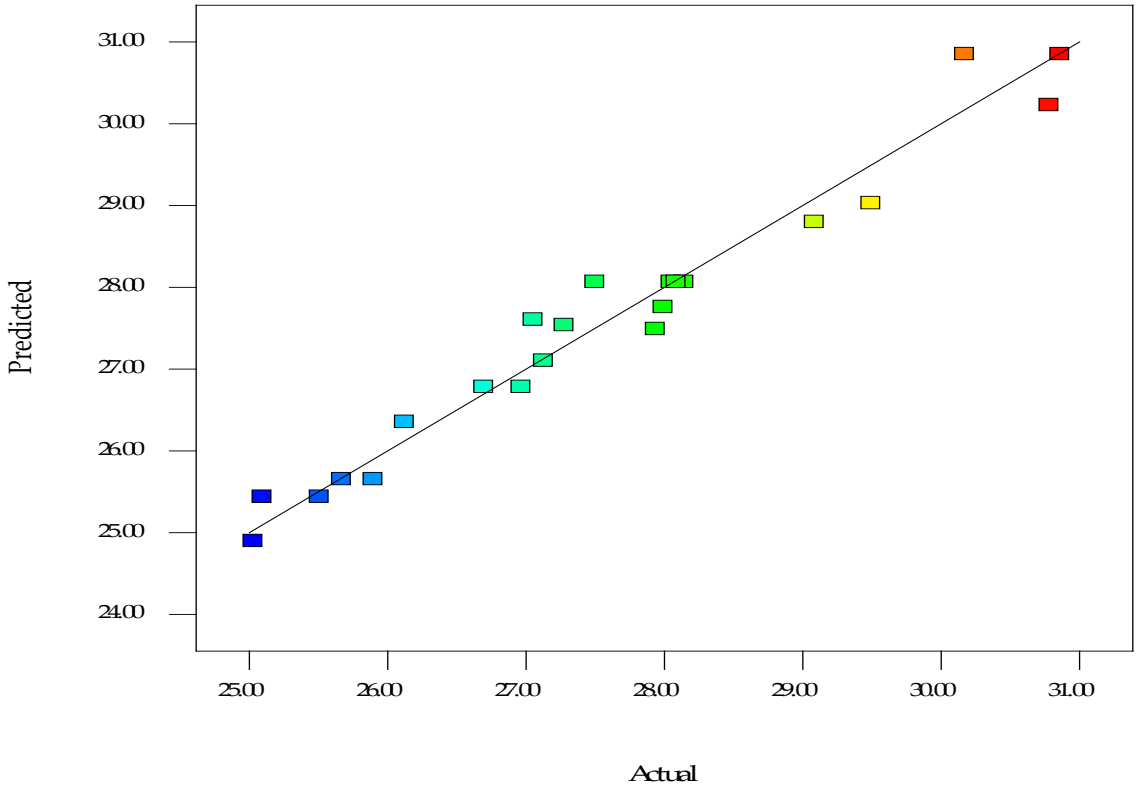

Figure 4.58: Predicted vs actual parity chart - 10 kWh/t efficiency

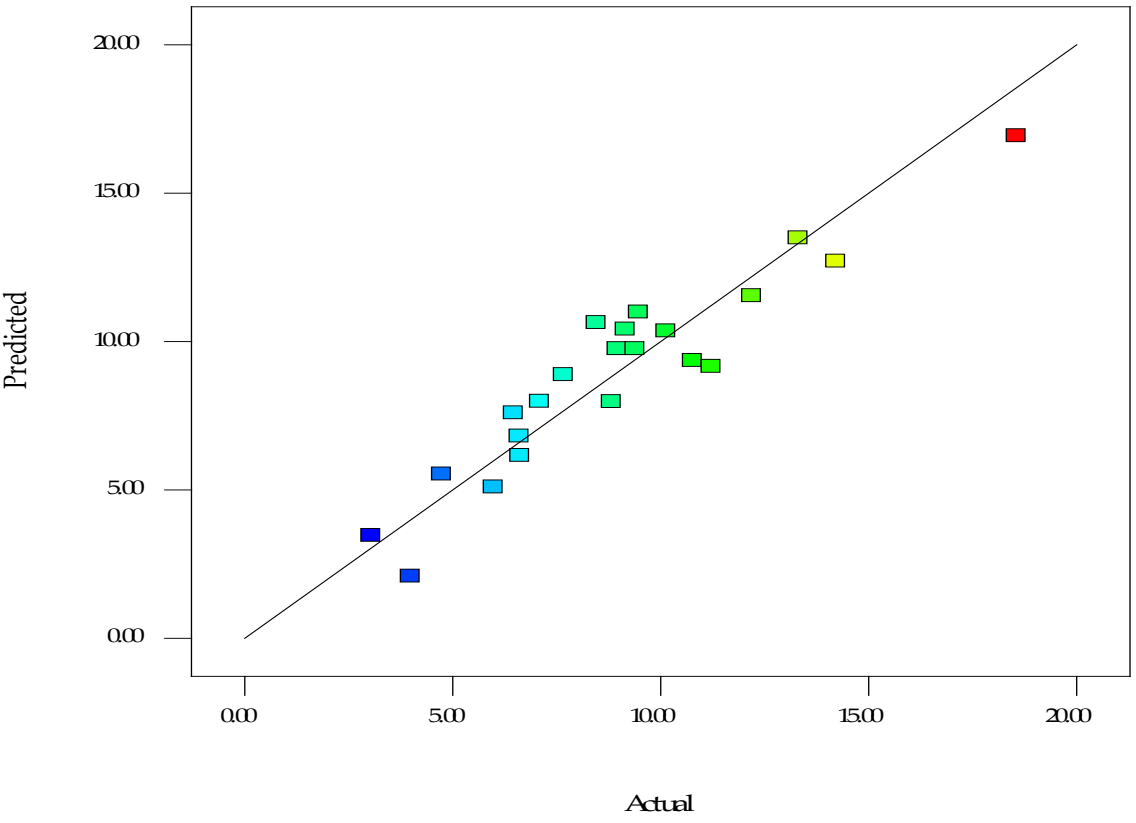

Figure 4.59: Predicted vs actual parity chart - 10 kWh/t rate

Figure 4.60 and Figure 4.61 show the significant interactions of the 10 kWh/t efficiency regression model, and Figure 4.62 and Figure 4.63 show the significant interactions of the 10 kWh/t rate regression model.

Figure 4.60 shows the interaction of stirrer speed and % solids, and it is observed that the best efficiency occurs at high % solids and low stirrer speed (lowest P80), which coincides with the best efficiency when looking just at the single variables efficiency of these variables. The reader is directed to section 4.3.1.1 and 4.3.2.1 for a full explanation and reasoning why this occurs. Figure 4.61 shows the interaction of stirrer speed and media size, and it is observed that the best efficiency occurs at low stirrer speed and a small media size. The reader is directed to section 4.3.1.1 and 4.3.3.1 for a full explanation.

Figure 4.62 shows the significant rate interaction between stirrer speed and mill filling at 10 kWh/t. it is observed that at high stirrer speed and a high mill filling the rate is the best. The reader is directed to section 4.3.1.3 and 4.3.4.3 for a full explanation for this occurrence. Figure 4.63 shows the rate interaction of media size and mill filling, and it is observed that the best rate occurs at a high mill filling and large media size. The reader is directed to section 4.3.3.3 and 4.3.4.3 for a full explanation.

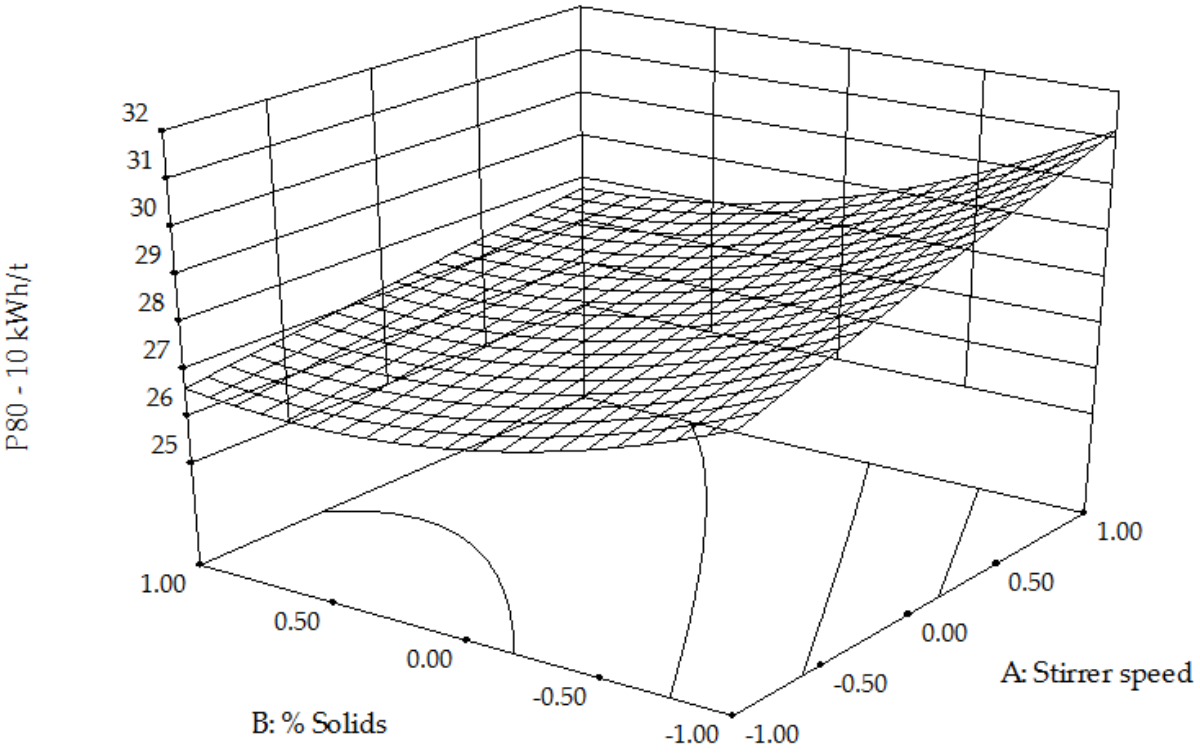

Figure 4.60: Surface plots – P80 10 kWh/t (AB)

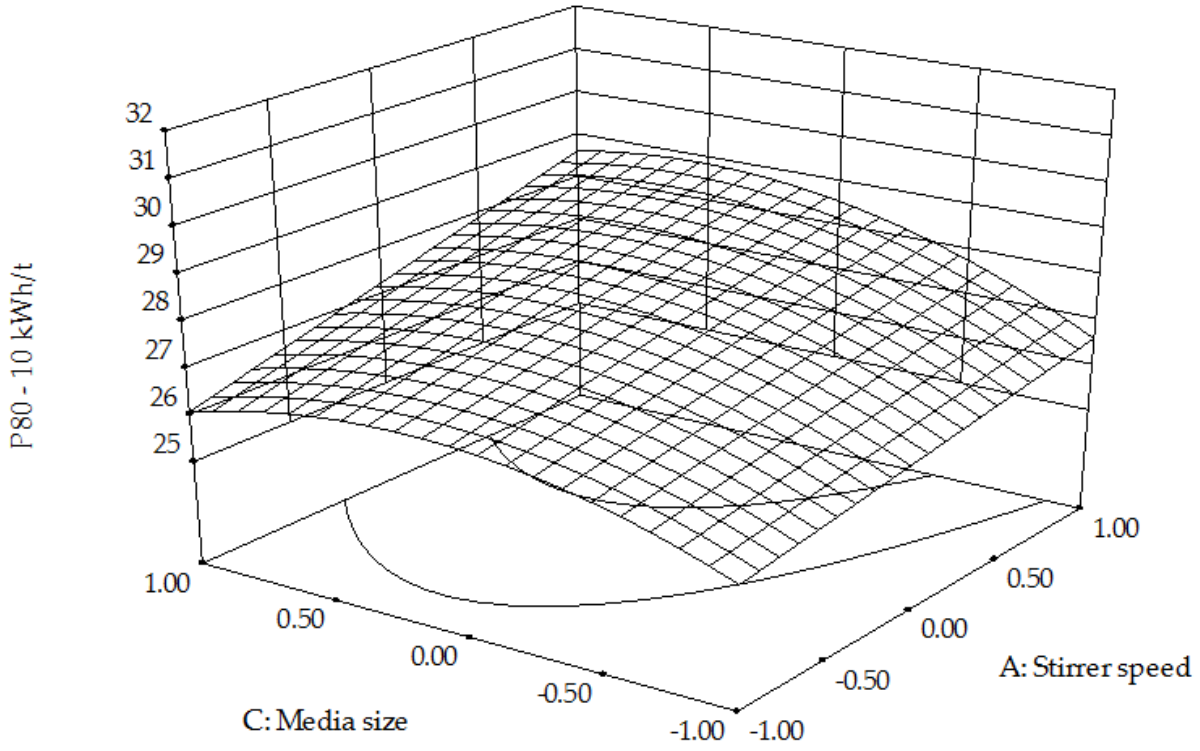

Figure 4.61: Surface plots – P80 10 kWh/t (AC)

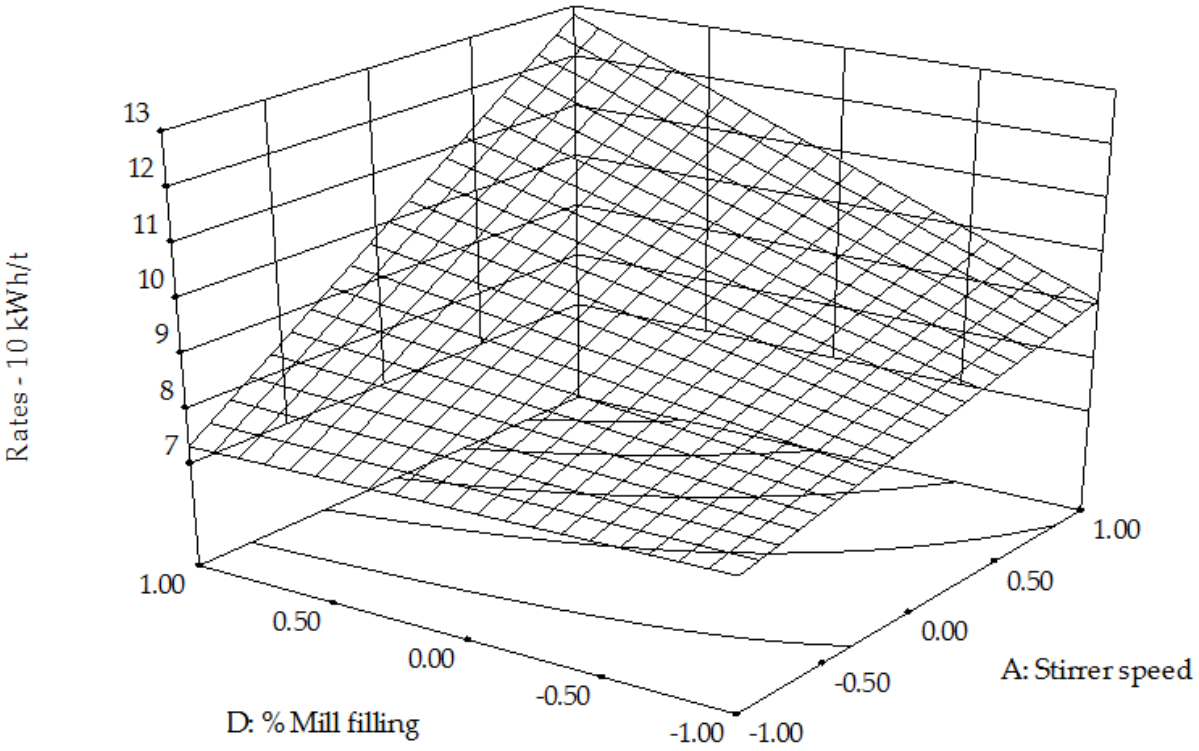

Figure 4.62: Surface plots – rates 10 kWh/t (AD)

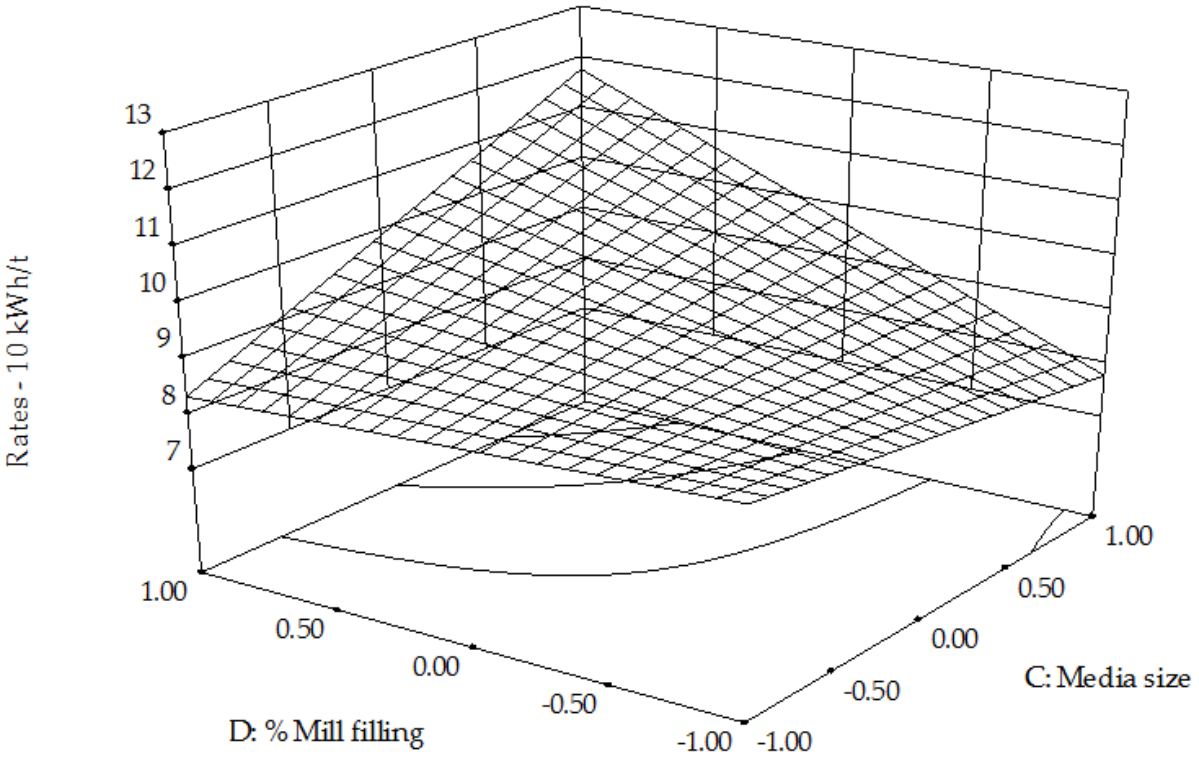

Figure 4.63: Surface plots – rates 10 kWh/t (CD)

4.4.2 A regression power model

A regression based power model was developed to be able to predict the power draw of the process based on the operating variables used in the design space. The R^2 values are shown in Table 4.6 and are in reasonable agreement with each other. The power model for this work is shown in Table 4.7. The parity chart is shown in Figure 4.64, which shows a good agreement between the actual and predicted values, and a full ANOVA table is shown in Appendix C. It is observed from the regression model and ANOVA data that the stirrer speed has the largest impact on power draw followed by mill filling, media size and % solids.

Table 4.6: R- Squared values – power model

R-Squared	0.94
Adj R-Squared	0.93

Table 4.7: Regression power model

Power (W)	=
95.39	(Intercept)
22.47	* Stirrer speed
-4.58	* % Solids
5.97	* Media size
12.32	* % Mill filling
-16.92	* % Mill filling^2

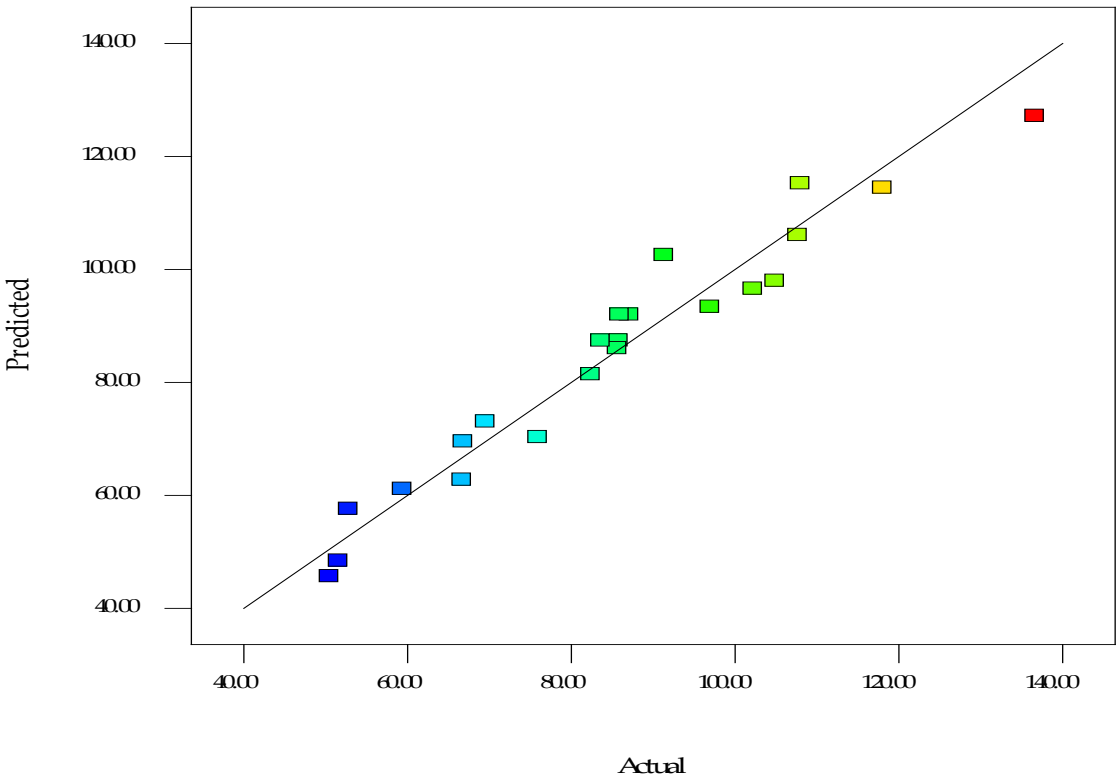

Figure 4.64: Predicted vs actual parity chart – power model

4.4.3 Optimisation of efficiency and rate

All the variables investigated have an influence on efficiency, rate and power. A variable can have minimal effects on the efficiency but have larger effects on the rate and power draw. Since efficiency and rates are linked, the combined effects of efficiency and rate was optimised, where the efficiency and rate was ranked by importance out of 5. This was done to optimise the process with the focus of prioritising the efficiency and rate. Table 4.8 shows the results of this optimisation when the process is run in combinations minimising and maximising both efficiency and rate for energy inputs of 10 kWh/t.

Table 4.8: 10 kWh/t optimisation

	Importance	Power (W)	Stirrer speed	% Solids	Media size	% Mill filling	P80	Rates
Efficiency	5/5	37.12	8 m/s	31.3 %	1.5 mm	65 %	25.24	7.65
Rates	1/5		-1.00	0.13	-1.00	-1.00		

	Importance	Power (W)	Stirrer speed	% Solids	Media size	% Mill filling	P80	Rates
Efficiency	1/5	120.32	12 m/s	27.6 %	3 mm	85 %	29.14	15.27
Rates	5/5		1.00	-0.24	1.00	1.00		

From the optimisation results it is clear that the variables have an effect on both the rate and efficiency to different degrees depending on the energy input into the process. To obtain varying degrees of rates and efficiencies for an energy input, the stirred mill can be run between the variables listed for a high rate or efficiency and a low rate or efficiency. To run the mill at a high rate and low efficiency, the mill must be run at 12 m/s, the % solids must be 27.6 %, the media size must be 3 mm and the mill filling must be 85 %. When running the mill with a low rate and high efficiency at 10 kWh/t, the stirrer speed must be 8 m/s, the % solids must be 31.3 %, the media size must be 1.5 mm and the mill filling must be 65 %.

The power draw for both options is shown in Table 4.8, from this it is observed that when the rate is high (15.27 m^2/kg/min) the power draw is high (120.32 W), and when the rate is low (7.65 m^2/kg/min) the power draw is low (37.12 W). From this it can be concluded that the higher the power draw the faster the grinding rate. It is noted that at a high power draw, a higher P80 size is obtained meaning that the efficiency is low (a high [watt/micron] grind). At a low power draw, a low P80 size is obtained meaning the efficiency is high (a low [watt/micron] grind). The reader is directed to the power

sections of each variable in Chapter 4.3 for more in depth explanations of power draw relations in this study.

Using the *regression models* the variables can be ranked on the sensitivity to change. The variables were ranked based on the change in efficiency (P80), rate and power (with respect to efficiency) from best efficiencies and rates to worst efficiencies and rates in the design space. The variables not being changed were kept at the mid points. Table 4.9 shows the overall ranking for efficiency, rate and power draw.

Table 4.9: Variables ranking "sensitivity analysis"

Variable Ranking	Δ P80 (Efficiency) [μm]	Δ Rate [m²/kg/min]	Δ P [W]
Stirrer Speed	1.93 **(2)**	3.57 **(2)**	44.94 **(1)**
Solids concentration	2.62 **(1)**	5.89 **(1)**	9.16 **(4)**
Grinding media size	1.40 **(3)**	1.19 **(4)**	11.93 **(3)**
Mill filling	0.00 **(4)**	1.75 **(3)**	24.63 **(2)**

This section shows that efficiency, grinding rate and power draw are linked and are all influential in the optimisation of the grinding process in stirred mills.

5. CONCLUSIONS & RECOMMENDATIONS

5.1 Conclusions

The following operating parameters were investigated in a vertical stirred mill using discs during this project: the stirrer speed, the solids concentration, the grinding media size, and the volume % of grinding media in the mill. The stress energy model was also investigated in a vertical stirred mill, where most previous stress energy studies have been conducted in a horizontal stirred mill. MG2 cleaner tails was used as the feed and is a South African platinum/chromite bearing reef in the bushveld igneous complex.

The results show that the Kwade stress energy model can be applied to a vertical stirred mill. In this ultrafine grinding application an optimum stress energy range of $1 \cdot 10^{-3}$ Nm – $3 \cdot 10^{-3}$ Nm was determined. The existence of an optimum stress energy is in agreement to previous studies conducted by Kwade et al. (1996) and Jankovic (2003). It is noted that to obtain this optimum, many combinations of operating variables values can be pursued.

Based on the hypotheses set out the following was observed and can be concluded:

1. Stirrer speed hypothesis:
    - An increase in stirrer speed would result in an increase in mill efficiency, followed by an optimum, then decrease in mill efficiency.
    - The power draw will increase as the mill speed is increased.
    - The grinding rate would increase as the mill speed is increased.

    Explanation:
        - The mill speed controls media motion and this in turn affects the collision rate and energy transfer between media and particles in the stirred mill. The frequency and energy of collisions in the mill increases as the speed increases until a point is reached where more energy is used to break particles than is necessary, and energy is wasted. There is an optimum mill efficiency.
        - Increasing the stirrer speed would increase the mechanical energy consumption.
        - The rate continues to increase due to the increase in collision frequency and energy at high speeds.

Conclusion:

- Within the conditions tested (8 m/s – 12 m/s), the best efficiency occurred at the lowest setting of 8 m/s. This indicates an optimum efficiency may exist below 8 m/s.
- The power draw increases as the stirrer speed is increased as expected.
- The grinding rate increases as the speed increases, with the fastest grinding rate at 12 m/s as hypothesized, but the efficiency drops as the stirrer speed is increased.
- In terms of stirrer speed there exists is a trade-off between efficiency and rate

2. Solids concentration hypothesis:
   - An increase in solids concentration would result in an increase in grinding efficiency, followed by an optimum, then a decrease in efficiency.
   - An increase in solids concentration would result in an increase in power draw.
   - An increase in solids concentration would result in an increase in grinding rate, followed by an optimum, then a decrease in rate.

   Explanation:
   - At low slurry densities there are more media on media collisions due to a low solid particle content (low efficiency and low rate). At high slurry densities there are more particle on particle collisions and a dampening effect occurs between media and particles causing a loss in energy. The suspension viscosity also increases which leads to more viscous heat losses and the media velocity is limited due to this increase in viscosity. By this reasoning there is an optimum performance in terms of efficiency and rate between low and high slurry densities.
   - As the stirred mill load increases due to an increase in solids concentration, the power draw will increase.

   Conclusion:

   - Within the conditions tested (20 % solids – 40 % solids), the best efficiency occurred at the highest solids concentration of 40 % solids by mass. The efficiency increased as the solids increased from 20 % - 40 % solids. It is

expected that the efficiency will drop if the solids concentration is further increased.

- The power draw decreased and this was not expected
- The fastest grinding rate occurred at a solids concentration of 20 % by mass. The rate decreased as the solids concentration increased.
- There exists a trade-off between efficiency and rate for solids concentration.

3. Media size hypothesis:
    - At low energy inputs larger media are more energy efficient, while at high energy inputs smaller media are more energy efficient, because the optimum media size decreases as the product particle size decreases

    Conclusion:

    - Within the conditions tested the best efficiency occurred at a grinding media size of 1.5 mm. It can be concluded that the 1.5 mm media is the most efficient media used because of the fine feed PSD, and that for a higher energy inputs an even smaller media size may have been more efficient.
    - The fastest grinding rate occurred at a media size 1.5 mm. It can be concluded that at 1.5 mm the number of media in the stirred mill (high stress number) overrides the lower stress energy, than the 3.0 mm larger media which have higher stress energies but a lower number of media in the mill.
    - No trade-off between efficiency and rate was observed for media size, and the best efficiency and rate occurs at 1.5 mm media.

4. Mill filling hypothesis:
    - An increase in mill filling would result in an increase in efficiency, followed by an optimum, then decrease in efficiency, because the grinding media mill filling affects the media – particle collision rate.
    - An increase in mill filling would result in an increase in power draw, because the mass in the mill increases.
    - An increase in mill filling would result in an increase in rate, followed by an optimum, then decrease in rate, because the grinding media mill filling affects the media – particle collision rate.

Explanation:

- An increase in the frequency of media on particle collisions would result when increasing the media load, but if the media load is too high (>80%), more media on media collisions would take place and energy is wasted.
- There is an optimum for both energy efficiency and grinding rate.

Conclusion:

- The results for mill filling (65 % - 85 %) show the best efficiency occurred at 65 % mill filling. The mill efficiency decreased as the mill filling was increased and there was a slight shift in optima to 75 % mill filling at higher energy inputs.
- The grinding rate shows an optimal point at 75 % mill filling, as hypothesized. The optimum was attributed to the fact that the media was fluidised over the last stirrer and made use of the full grinding volume available.
- A trade-off between efficiency and rate was not found in terms of mill filling. A similar optimum mill filling exists for both a high efficiency and high rate.

General observations from the study include:

- Variables can have smaller or a larger effects on the overall efficiency and rate depending on the level of specific energy input of the system.
- The best efficiency conditions does not always translate into having the best rate conditions for all the variables investigated and there is a trade-off between the overall efficiency and grinding rate.
- The regression models were developed to predict the efficiency, rate and power in the design space making the design space easier to explore and determine the optimum operating variables.

Table 5.1 shows a summary of the best conditions for efficiency and rate, where the lowest power corresponds with the best efficiency and the highest power corresponds with the best rate with the exception of grinding media size. From this it can be concluded that generally at low power draws the grinding will be efficient, and at a high power draw the grinding rate is high.

Table 5.1: Best Efficiencies and best rates for the study

Variable	Best Efficiency	Lowest Power	Fastest Rate	Highest Power
Stirrer speed	8 m/s	8 m/s	12 m/s	12 m/s
Solids concentration	40 % Solids	40 % Solids	20 % Solids	20 % Solids
Mill filling	65 % (shifting to 75 % at higher E_{CS})	65 %	75 %	75 %
Grinding media size	1.5 mm	1.5 mm	1.5 mm	3.0 mm

5.2 Recommendations

Based on the results and conclusions, the following recommendations can be outlined to gain further insights into the operation of stirred mills:

- Horizontal stirred mills are more prevalent in the South African minerals processing industry and a comparative study between a vertical and horizontal stirred mill using a South African ore can be investigated using a stress energy approach. The effect the process variables have on the grinding performance can also be compared. Vertical stirred mills are normally run at low speeds while horizontal stirred mills are run at much higher speeds. The flow regimes in the two mills would thus behave differently affecting the performance.
- Based on the range of the variables investigated in this study and the lack of optimum turn around points, a broader range of the operating parameters is recommended as shown by Table 5.2.

Table 5.2: Recommended ranges for process variables

	Investigated	**Recommended**
Stirrer speed	8 m/s – 12 m/s	4 m/s – 16 m/s
% Solids	20 % - 40 %	10 % - 80 %
Media size	1.5 mm – 3.0 mm	1 mm – 6 mm
% Mill filling	65 % - 85 %	40 % - 90 %

- Mono – sized media charge was used in this study, it is recommended that a graded media charge be used and compared to a mono – sized media charge.
- The effect of media density was not investigated in this study. The media density is an important parameter to the Kwade stress energy model and should be investigated in future studies.
- A fine feed PSD was used for this study (P80 ≈ 40 μm). It is recommended that a coarser feed size distribution be investigated in a vertical stirred mill.
- The effects that the rheology has on performance in stirred mills should be investigated.

REFERENCES

Barley, R. W., Conway-Baker, J., Pascoe, R. D., Kostuch, J., McLoughlin, B. & Parker, D. J., 2004. Measurement of the motion of grinding media in a vertically stirred mill using positron emission particle tracking (PEPT) Part II. Minerals Engineering, 17: 1179 – 1187.

Becker, M., Kwade, A. & Schwedes, J., 2001. Stress intensity in stirred media mills and its effect on specific energy requirement. International Journal of Mineral Processing, 61: 189 – 208.

Bel Fadhel, H. & Frances, C., 2001. Wet batch grinding of alumina hydrate in a stirred bead mill. Powder Technology, 119: 257 – 268.

Bernhardt, C., Reinsch, E. & Husemann, K., 1999. The influence of suspension properties on ultra-fine grinding in stirred ball mills. Powder Technology 105: 357–361.

Blecher, L., Kwade A. & Schwedes, J., 1996. Motion and stress intensity of grinding beads in a stirred media mill. Part I: Energy density distribution and motion of single grinding beads. Powder Technology, 86: 59 – 68.

Burford, B. D. & Clark, L. W., 2007. Isamill technology used in efficient grinding circuits. VIII International conference on non-ferrous ore processing, Poland.

Gao, M. W., Forssberg, K. S. E. & Weller, K. R., 1996. Power predictions for a pilot scale stirred ball mill. International Journal of Mineral Processing, 44 – 45: 641 – 652.

Graves, G. A. & Boehm, T., 2007. Mill media considerations for high energy mills. Minerals Engineering, 20: 342 – 347.

He, M., Wang, Y. & Forssberg, E., 2004. Slurry rheology in wet ultrafine grinding of industrial minerals: a review. Powder Technology, 147: 94 – 112.

He, M., Wang, Y. & Forssberg, E., 2006. Parameter effects on wet ultrafine grinding of limestone through slurry rheology in a stirred media mill. Powder Technology, 161: 10 – 21.

Hennart, S. L. A., Wildeboer, W., van Hee, P. & Meesters, G., 2009. Identification of the grinding mechanisms and their origin in a stirred ball mill using population balances. Chemical Engineering Science 64: 4123 – 4130.

Hogg, R., 1999. Breakage mechanisms and mill performance in ultrafine grinding. Powder Technology, 105: 135 – 140.

Jankovic, A., 2001. Media stress intensity analysis for vertical stirred mills. Minerals Engineering, 14(10): 1177 - 1186.

Jankovic, A., 2003. Variables affecting the fine grinding of minerals using stirred mills. Minerals Engineering, 16: 337 - 345.

Jayasundara, C. T., Yang, R. Y., Yu, A. B. & Curry, D., 2006. Discrete particle simulation of particle flow in the Isamill process. Ind. Eng. Chem. Res., 45: 6349 – 6359.

Jayasundara, C. T., Yang, R. Y., Yu, A. B. & Curry, D., 2008. Discrete particle simulation of particle flow in IsaMill – Effect of grinding medium properties. Chemical Engineering Journal, 135: 103 - 112.

Jayasundara, C. T., Yang, R. Y., Guo, B. Y., Yu, A. B. & Rubenstein, J., 2009. Effet of slurry properties on particle motion in Isamills. Minerals Engineering, 22: 886 – 892.

Jayasundara, C. T., Yang, R. Y., Yu, A. B. & Rubenstein, J., 2010. Effects of disc rotation speed and media loading on particle flow and grinding performance in a horizontal stirred mill. International Journal of Mineral Processing, 96: 27 – 35.

Jayasundara, C. T., Yang, R. Y. & Yu, A. B., 2011. Effect of the size of media on grinding performance in stirred mills. Minerals Engineering.

Kwade, A., Blecher, L. & Schwedes, J., 1996. Motion and stress intensity of grinding beads in a stirred media mill. Part II: Stress intensity and its effect on comminution. Powder Technology, 81: 69 – 76.

Kwade, A., 1999. Wet comminution in stirred media mills - research and its practical application. Power Technology, 105: 14 – 20.

Kwade, A., 2004. Mill selection and process optimization using a physical. International Journal of Mineral Processing, 74: 93 – 101.

Mankosa, M. J., Adel, G. T. & Yoon, R. H., 1986. Effect of Media Size in Stirred Ball Mill Grinding of Coal. Powder Technology, 49: 75 – 82.

Mankosa, M. J., Adel, G. T. & Yoon, R. H., 1989. Effect of Operating Parameters in Stirred Ball Mill Grinding of Coal. Powder Technology, 59: 255 – 260.

Metso, 2015. Brochure vertimill and stirred media detritors. Available online: www.metso.com

Ouattara, S. & Frances, C., 2013. Grinding of calcite suspensions in a stirred media mill: Effect of operational parameters on the product quality and the specific energy. Powder Technology.

Partyka, T. & Yan, D., 2007. Fine grinding in a horizontal ball mill. Minerals Engineering, 20, 320 – 326.

Pease, J., Curry, D. & Young, M., 2006. Designing Flotation Circuits for High Fines Recovery. Centenary of Flotation Symposium, (pp. 905-912). Brisbane.

Rahal, D., Erasmus, D. & Major, K., 2011. Knelson – Deswik Milling Technology: Bridging the Gap between Low and High Speed Stirred Mills. Proceedings of the 43rd Annual Canadian Mineral Processors Conference. Ontario. pp. 557 – 587.

Rule, C. M., 2011. Stirred milling – new comminution technology in the PGM industry. The Journal of the South African Institute of Mining and Metallurgy. 111: 101 – 107.

Ruwona, W., 2015. Rheology test work during undergraduate project.

Sinnott, M., Cleary, P. W., & Morrison, R., 2006. Analysis of stirred mill performance using DEM simulation: Part 1 – Media motion, energy consumption and collisional environment. Minerals Engineering, 16, 1537 – 1550.

Stender, H.H., Kwade, A. & Schwedes, J. 2004. Stress energy distribution in different stirred media-mill geometries. International Journal of Mineral Processing, 74S: S103 – S117.

Tuzun, M. A., Loveday, B. K. & Hinde, A. L., 1995. Effect of pin tip velocity, ball density and ball size on grinding kinetics in a stirred ball mill. International Journal of Mineral Processing, 43: 179 – 191.

Van Der Westhuizen, A. P., Govender, I., Mainza, A. N. & Rubenstein, J., 2011. Tracking the motion of media particles inside an Isamill using PEPT. Minerals Engineering. 24: 195 – 204.

Wang, Y. & Forssberg, E., 2007. Enhancement of energy efficiency for mechanical production of fine and ultra-fine particles in comminution. China Particuology, 5: 193 – 201.

Weller, K. & Gao, M., 1999. Ultra-fine grinding. AJM Crushing and Grinding Conference, Kalgoorlie.

Yue, J. & Klein, B., 2004. Influence of rheology on the performance of horizontal stirred mills. Minerals Engineering, 17: 1169 – 1177.

Zheng, J., Harris, C. C. & Somasundaran, P., 1996. A study on grinding and energy input in stirred media mills. Power Technology, 86: 171 – 178.

APPENDICES

Appendix A – Signature plots

The P80 values used in this thesis were interpolated and extrapolated using the signature plots presented below and are compared to linear interpolations between the experimental data points. The absolute % differences between the linear interpolation and the signature plot interpolation is always less than 5 % (shown below). The extrapolated data has more uncertainty in that it falls outside the experimental range. However the extrapolated data does not stray too far from the signature plot lines, this is confirmed by the results plots where extrapolated data (50 kWh/t) show the same trend as the interpolated data (10 kWh/t) at the same conditions. In this thesis only 10 kWh/t, 20 kWh/t and 30 kWh/t energy inputs were used.

The Surface Area values used in this thesis were interpolated and extrapolated using Figure 4.13

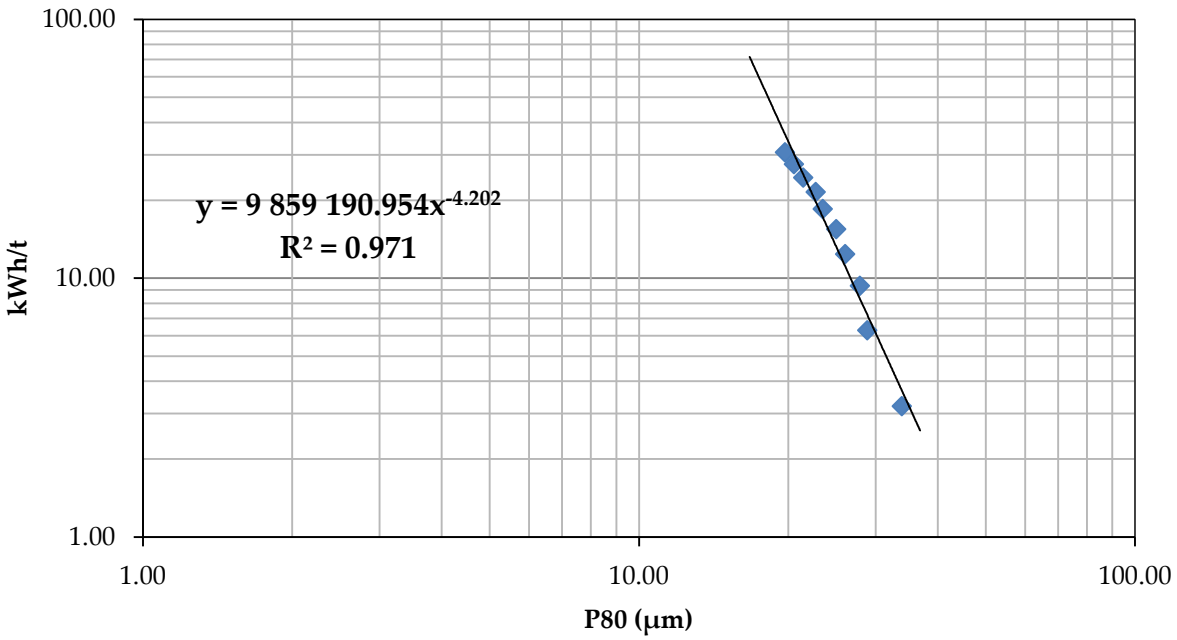

Figure A.1: Signature plot run 1

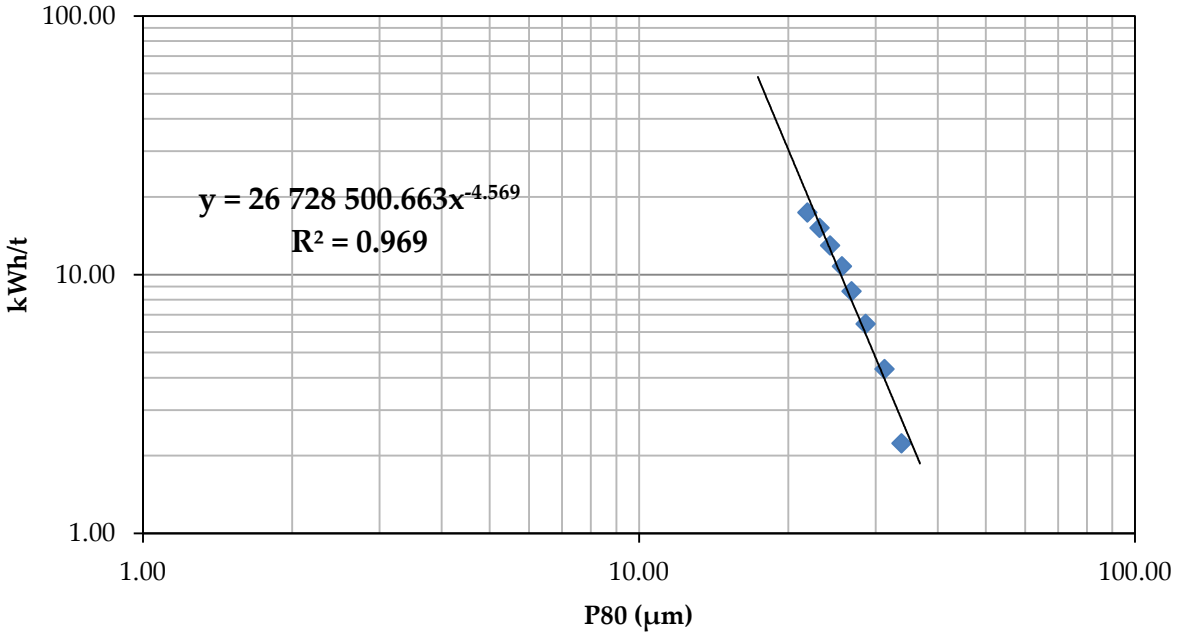

Figure A.2: Signature plot run 2

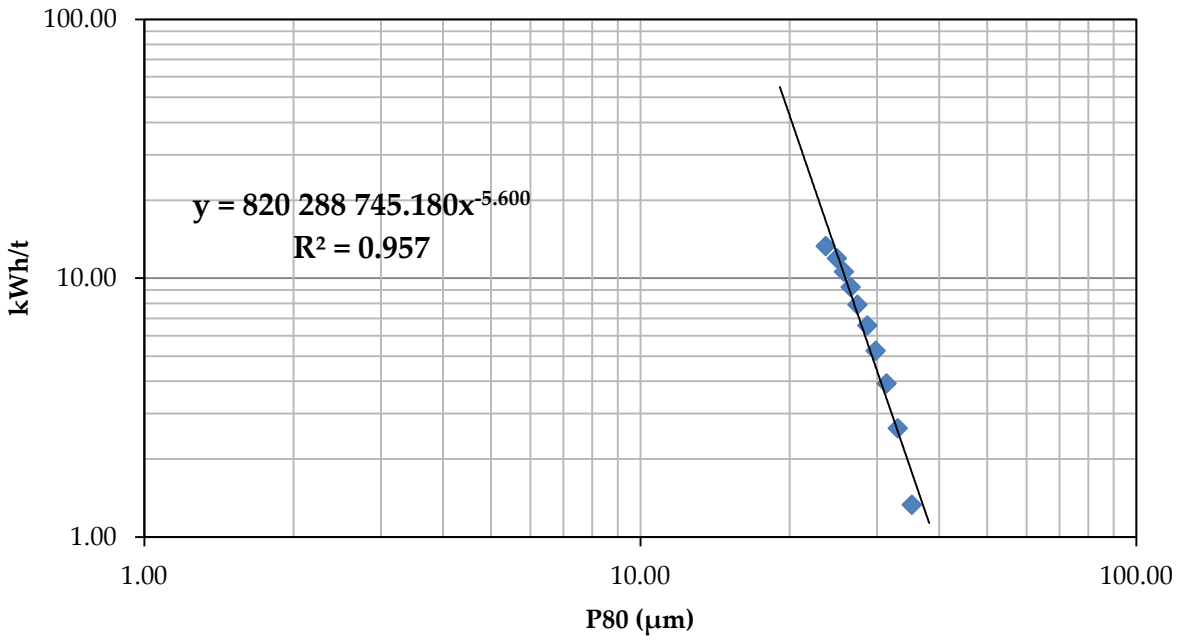

Figure A.3: Signature plot run 3

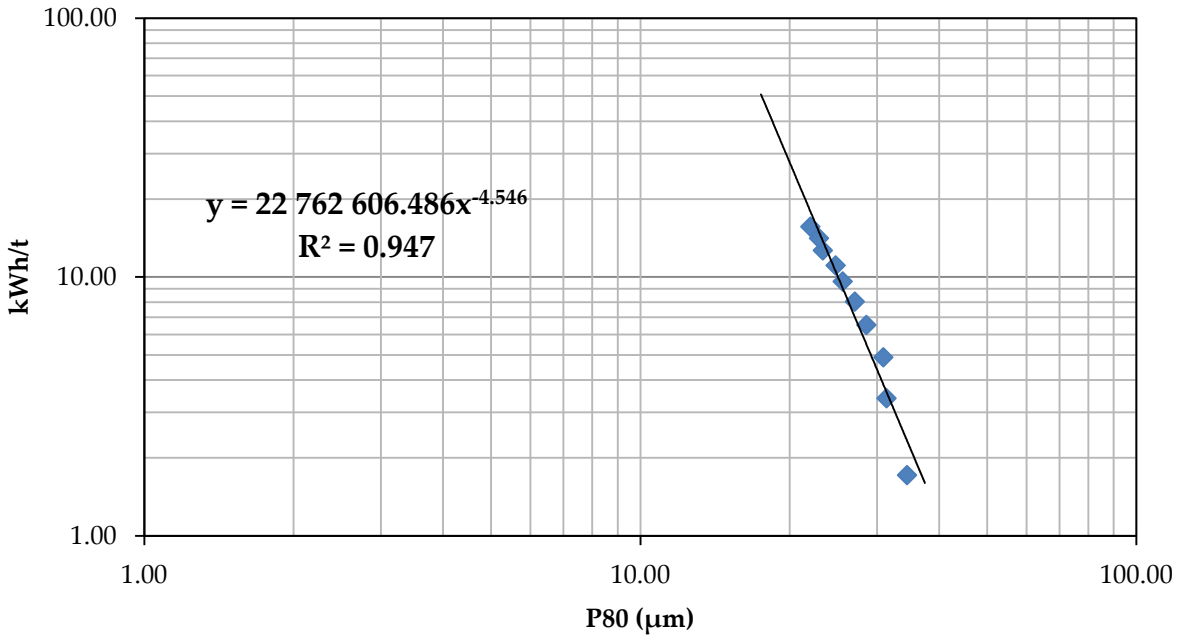

Figure A.4: Signature plot run 4

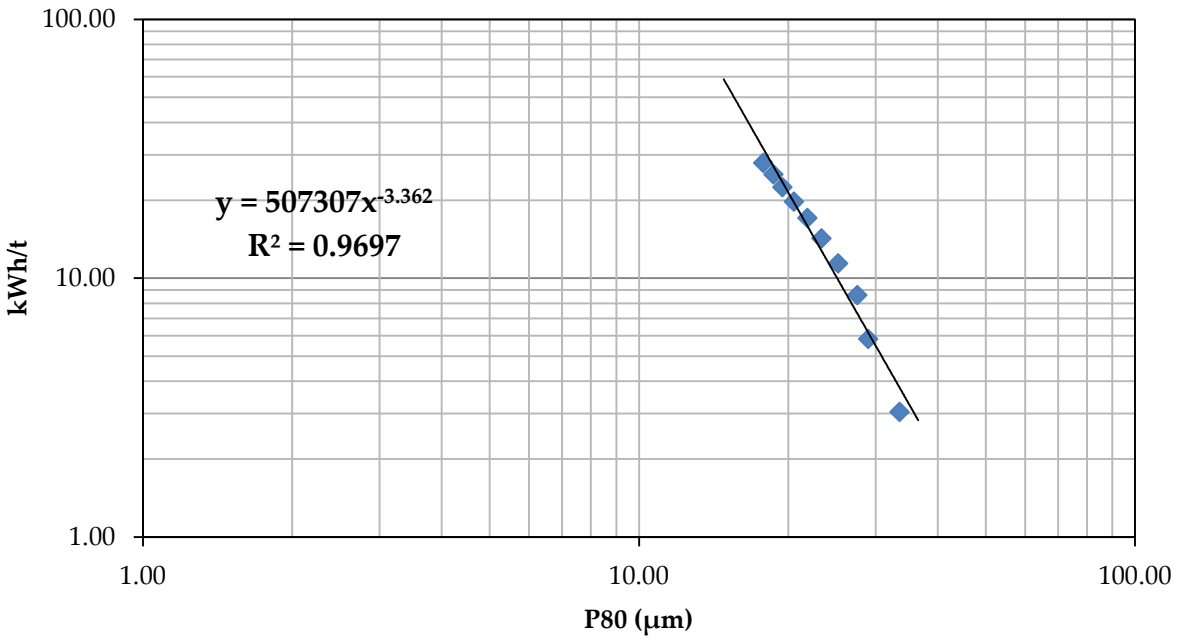

Figure A.5: Signature plot run 5

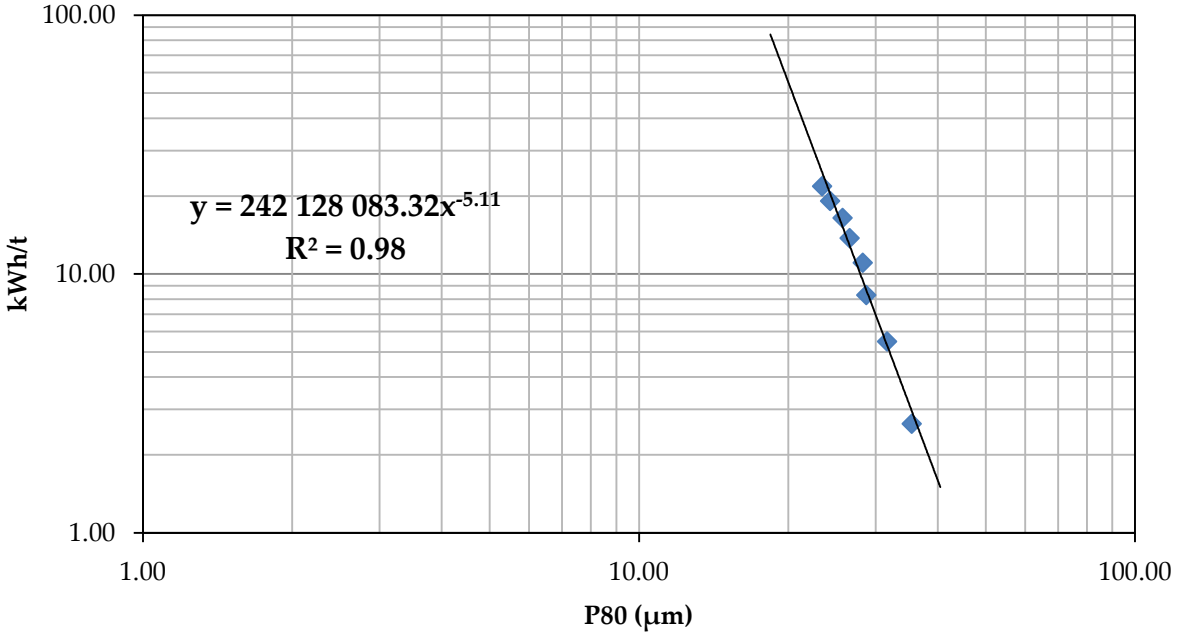

Figure A.6: Signature plot run 6

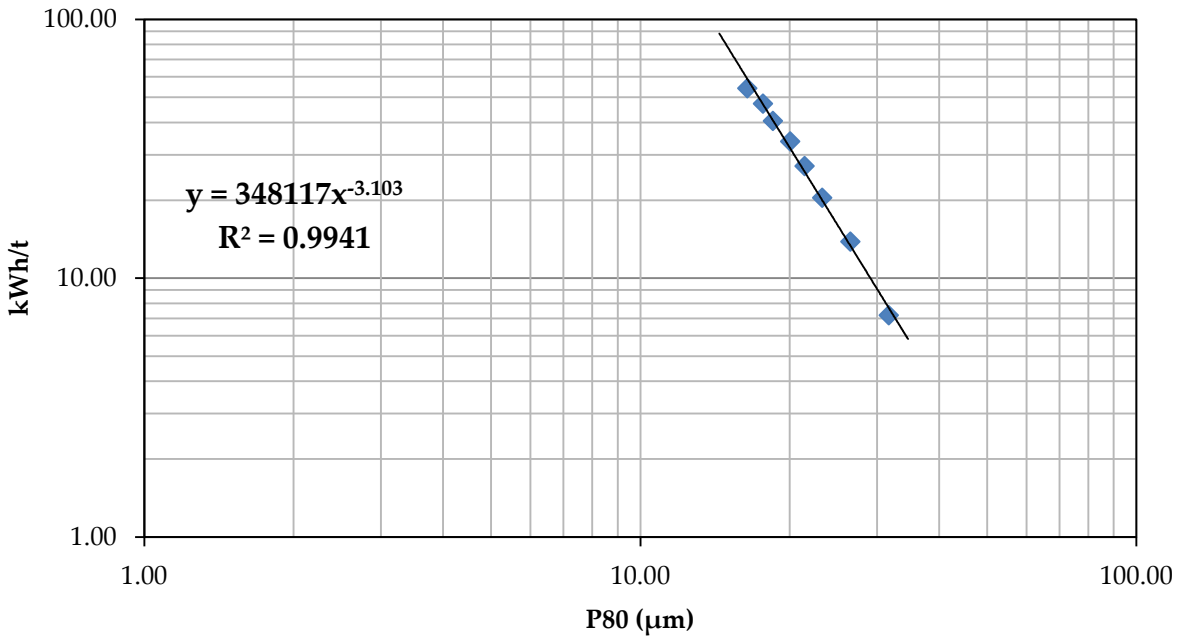

Figure A.7: Signature plot run 7

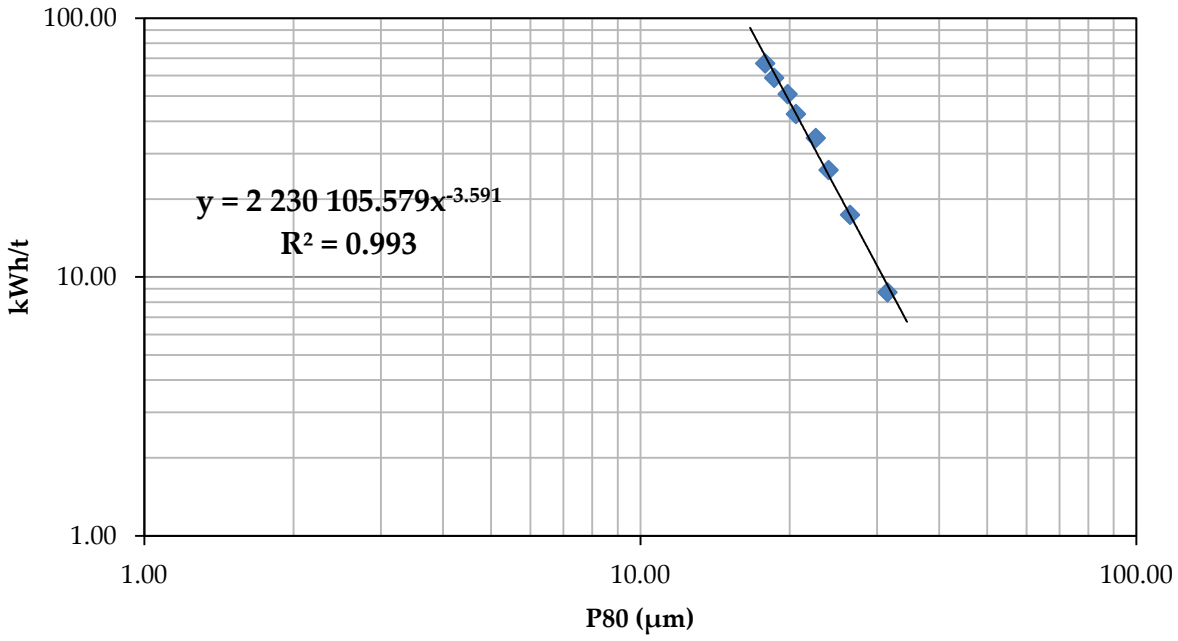

Figure A.8: Signature plot run 8

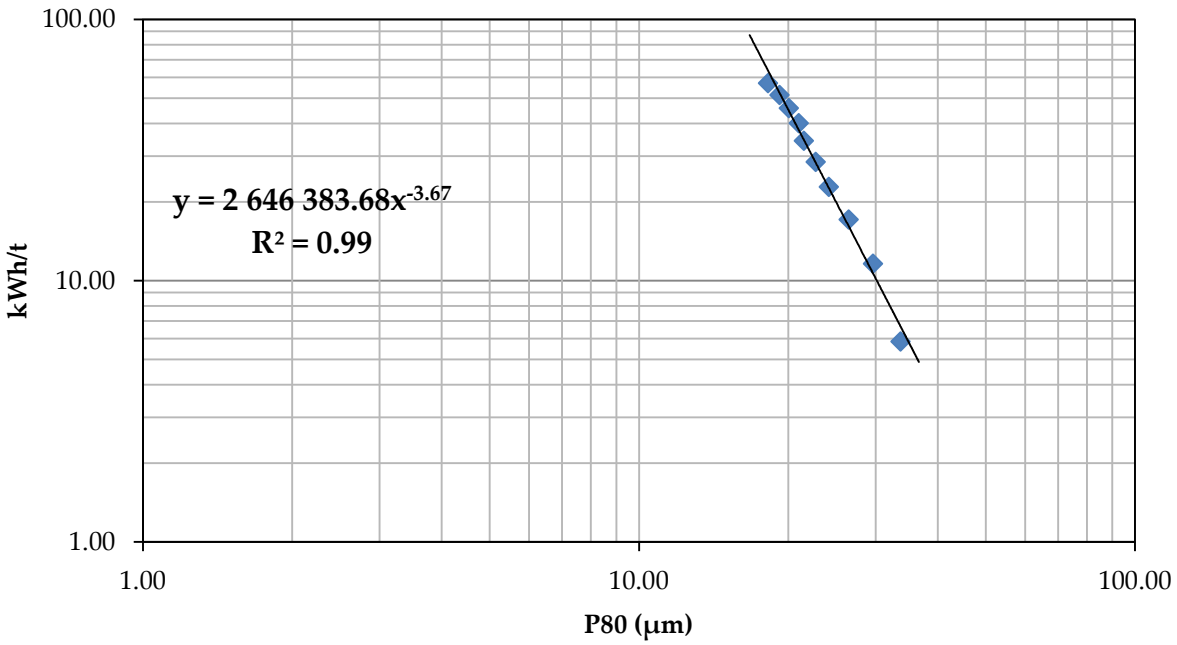

Figure A.9: Signature plot run 9

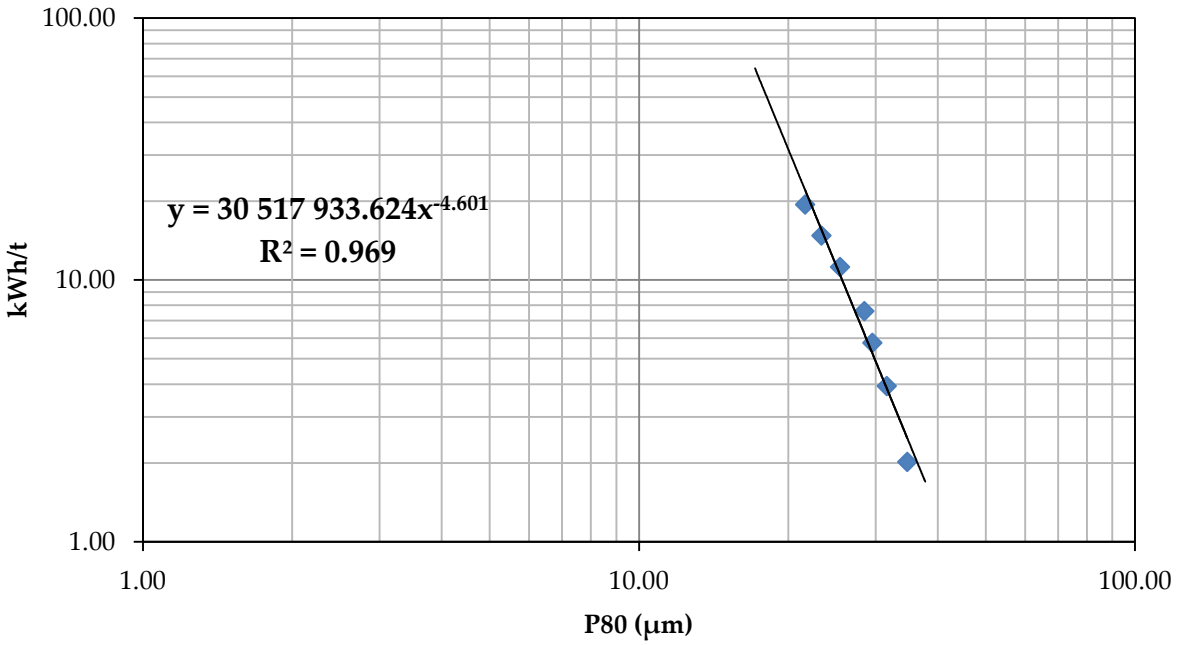

Figure A.10: Signature plot run 10

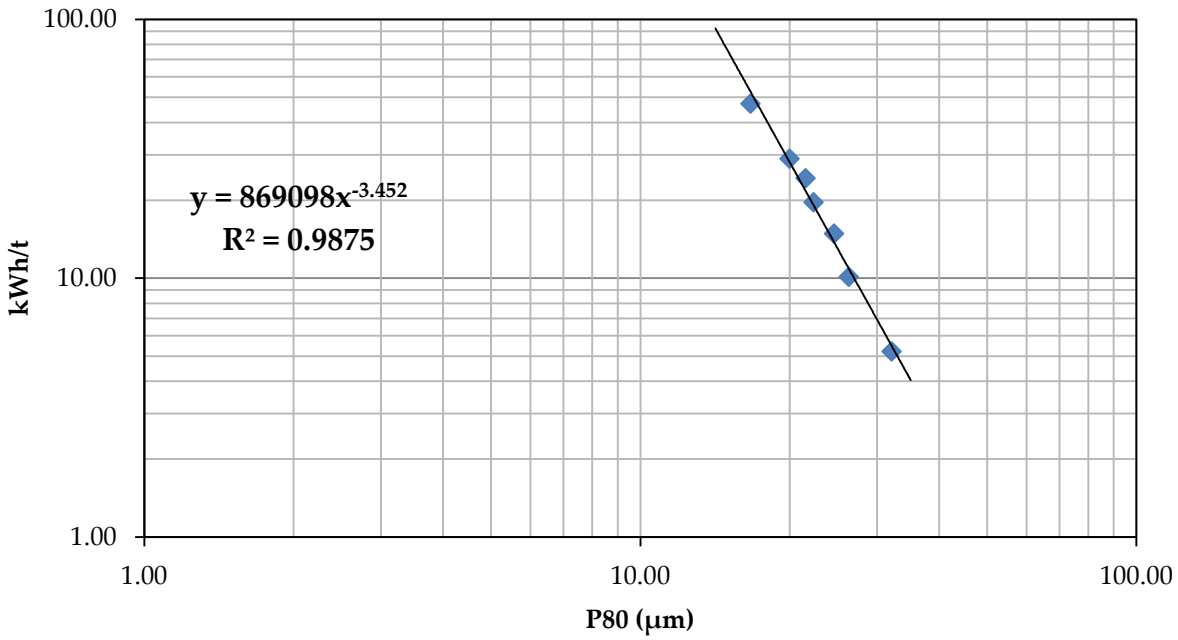

Figure A.11: Signature plot run 11

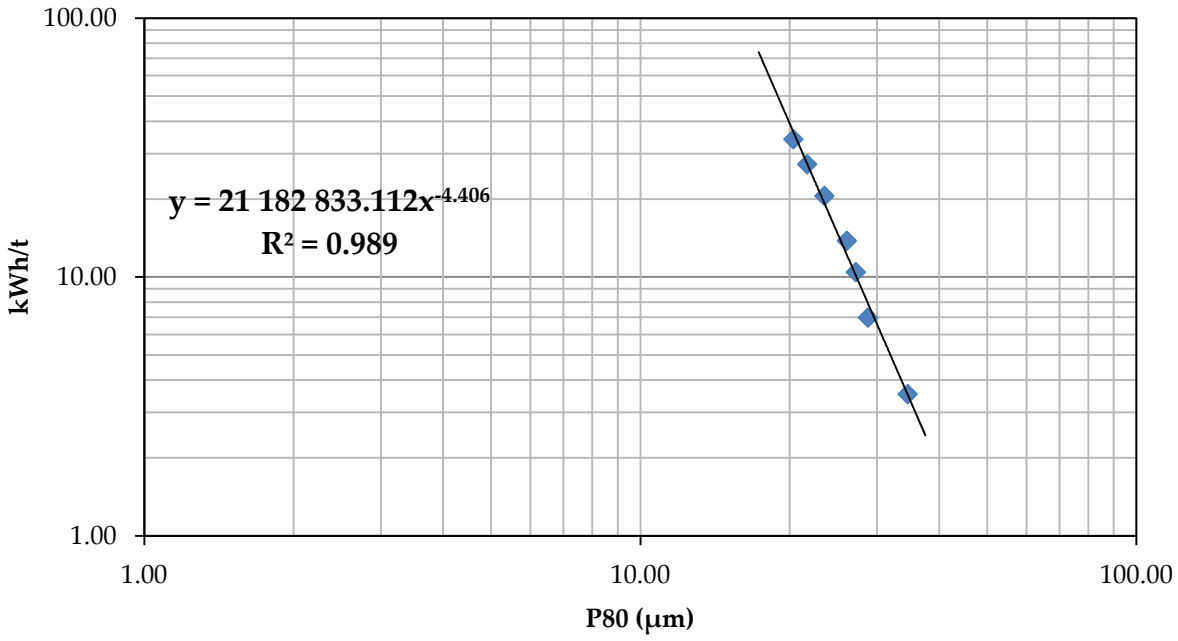

Figure A.12: Signature plot run 12

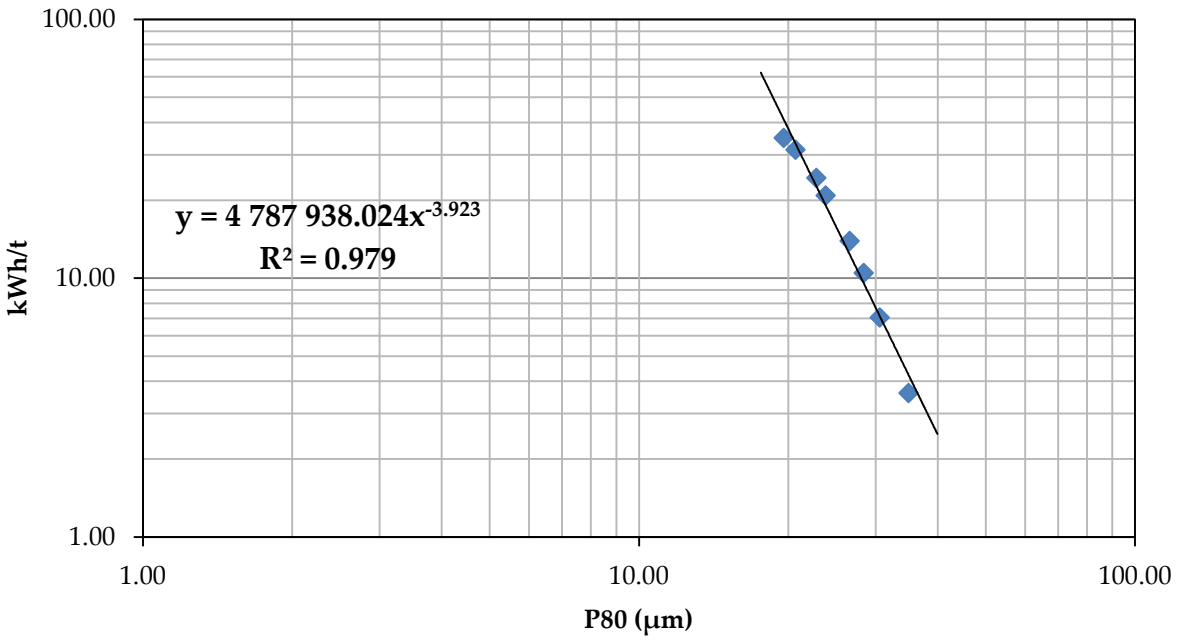

Figure A.13: Signature plot run 13

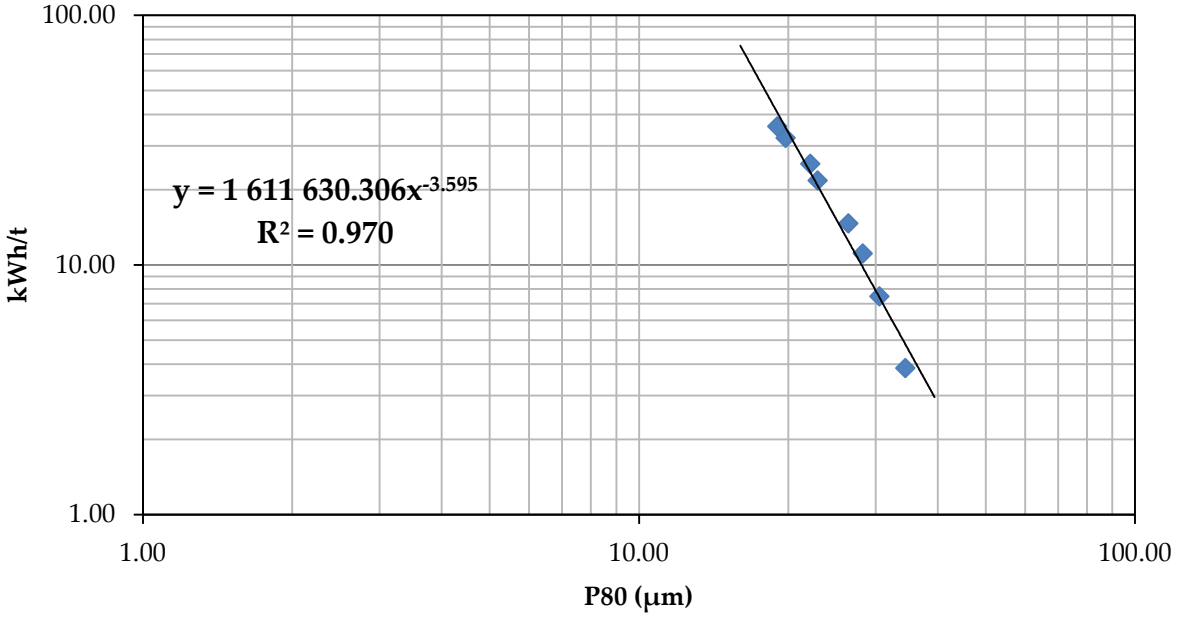

Figure A.14: Signature plot run 14

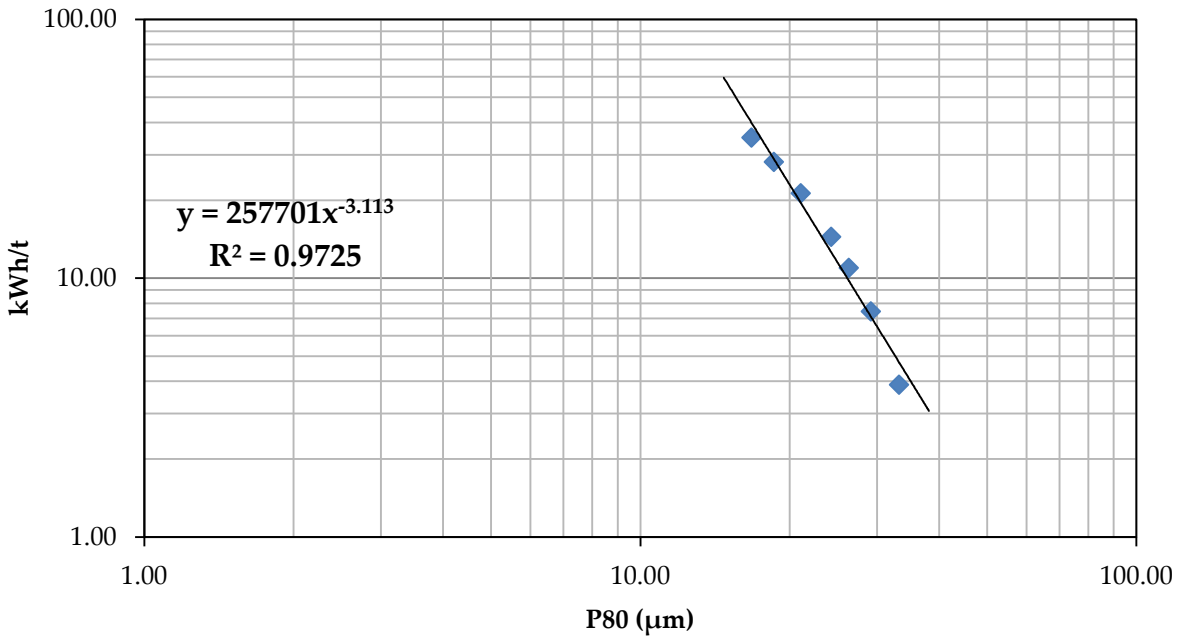

Figure A.15: Signature plot run 15

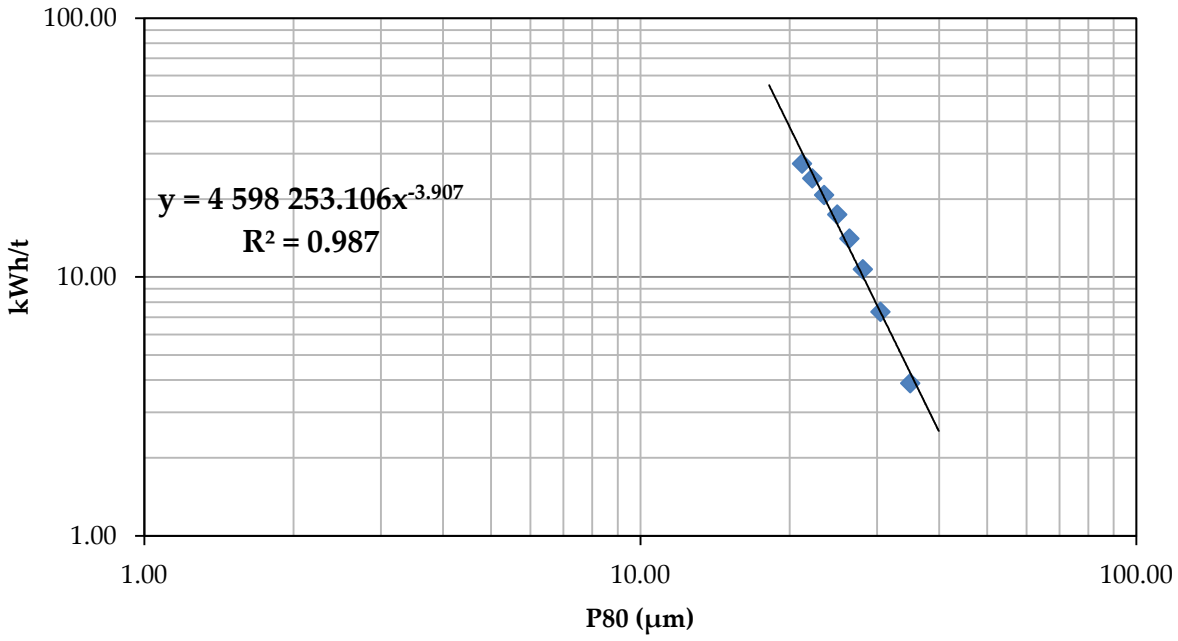

Figure A.16: Signature plot run 16

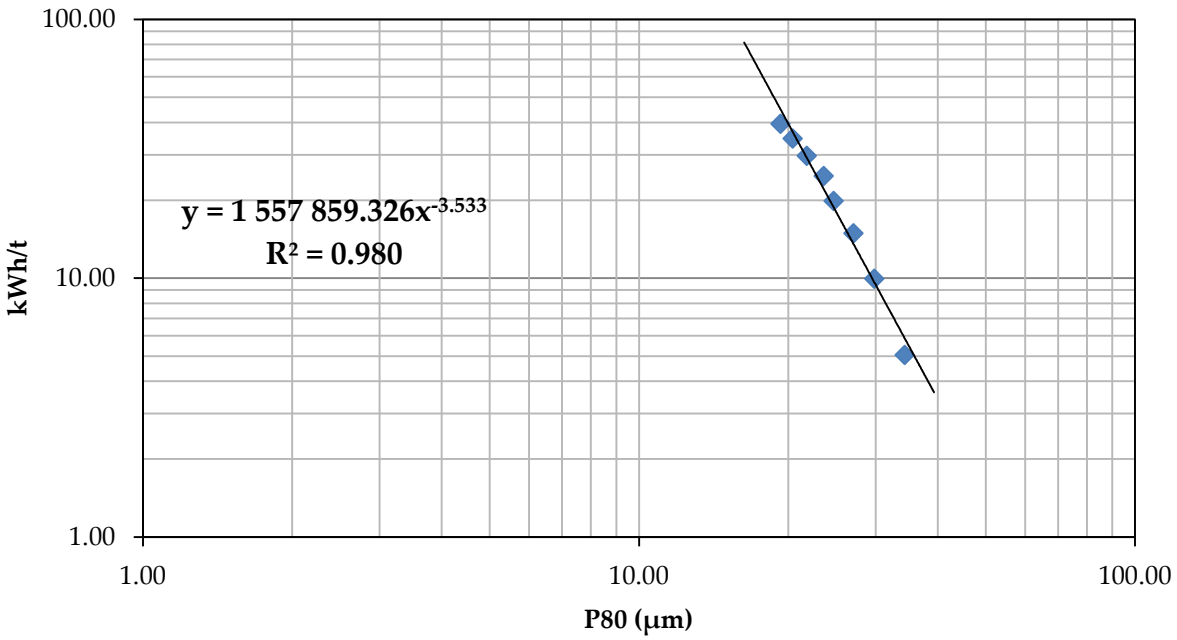

Figure A.17: Signature plot run 17

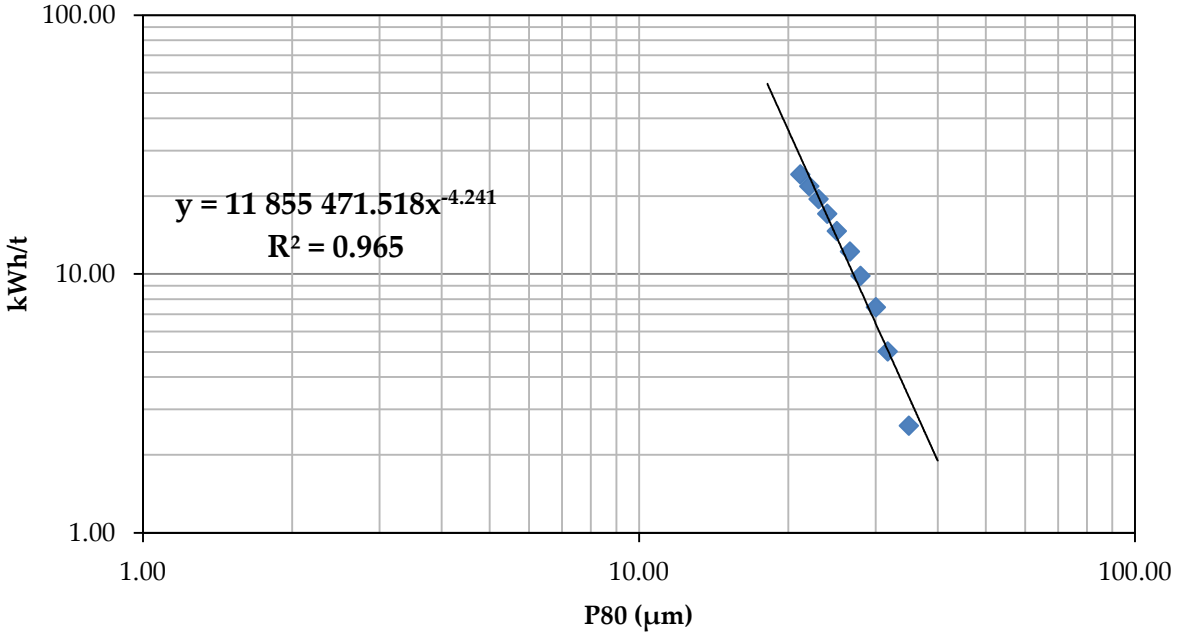

Figure A.18: Signature plot run 18

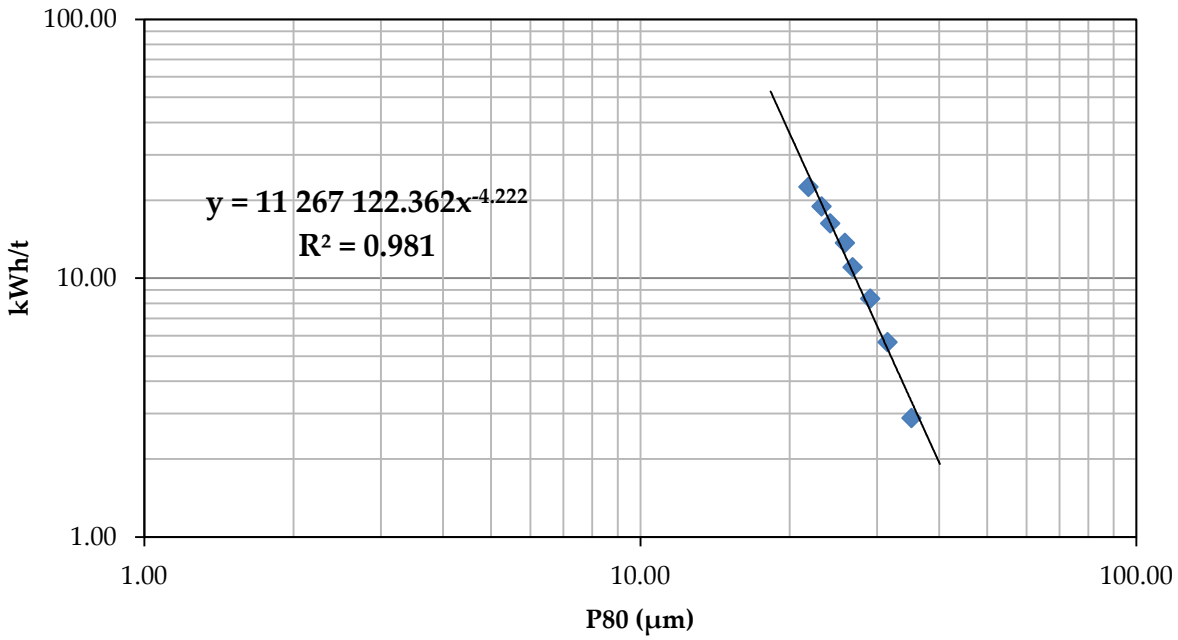

Figure A.19: Signature plot run 19

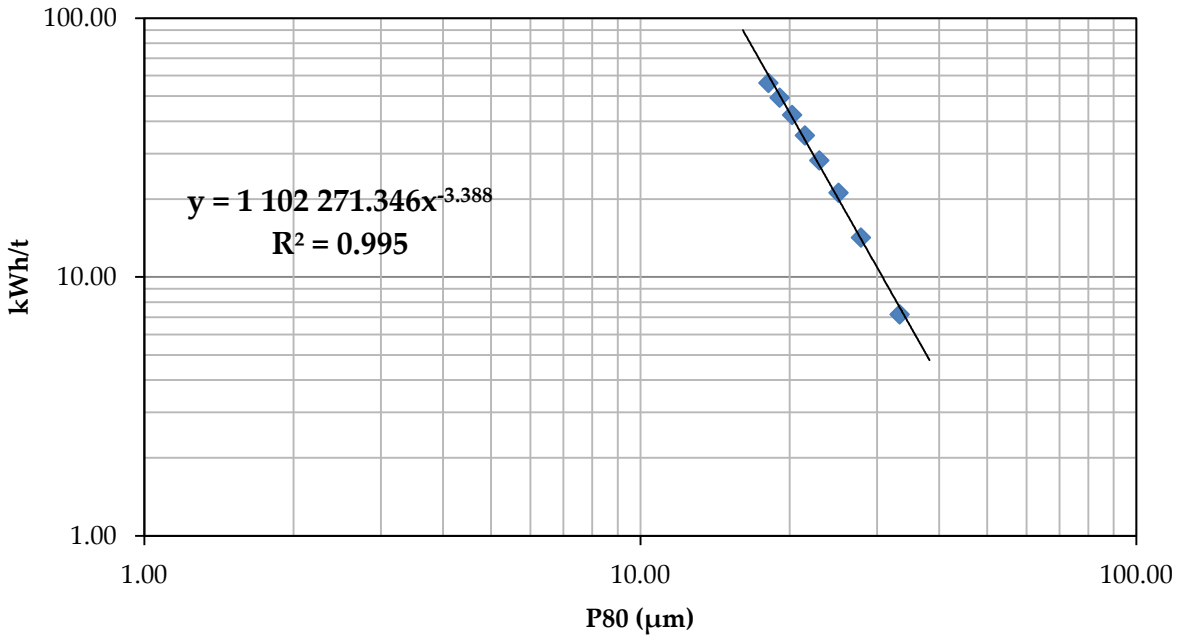

Figure A.20: Signature plot run 20

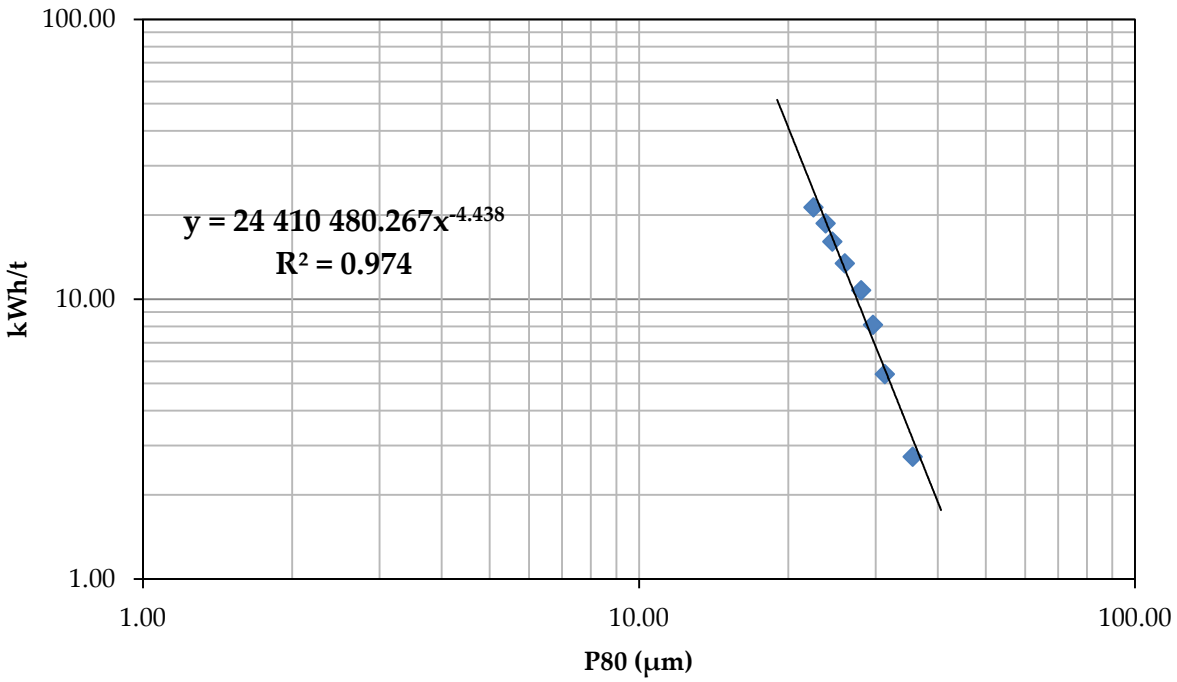

Figure A.21: Signature plot run 21

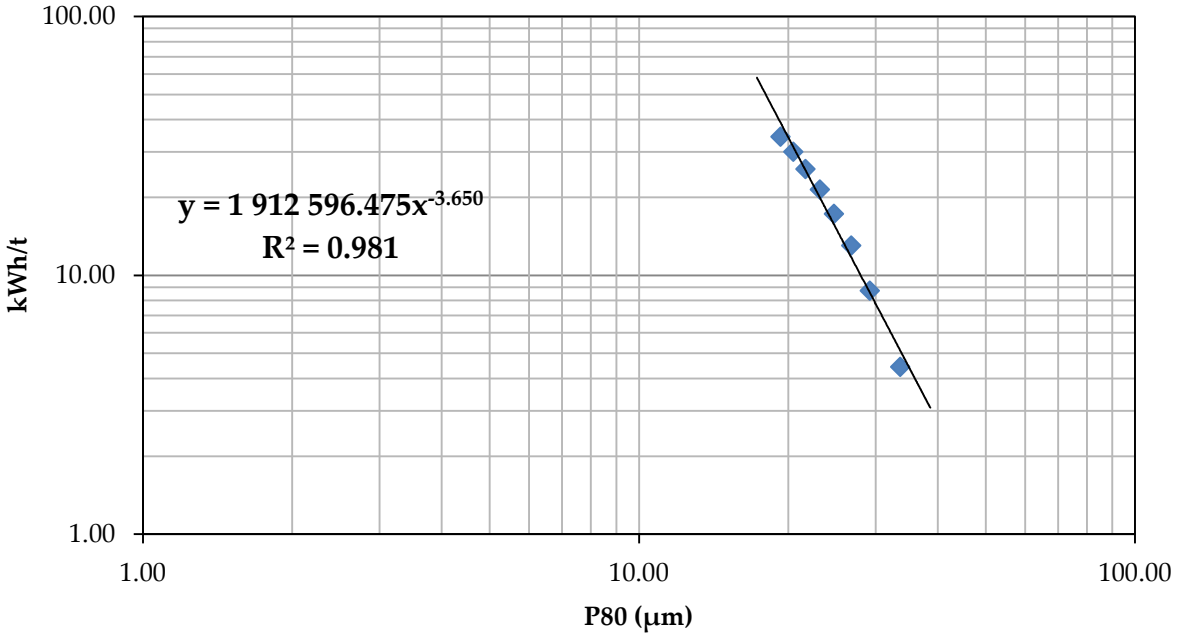

Figure A.22: Signature plot run 22

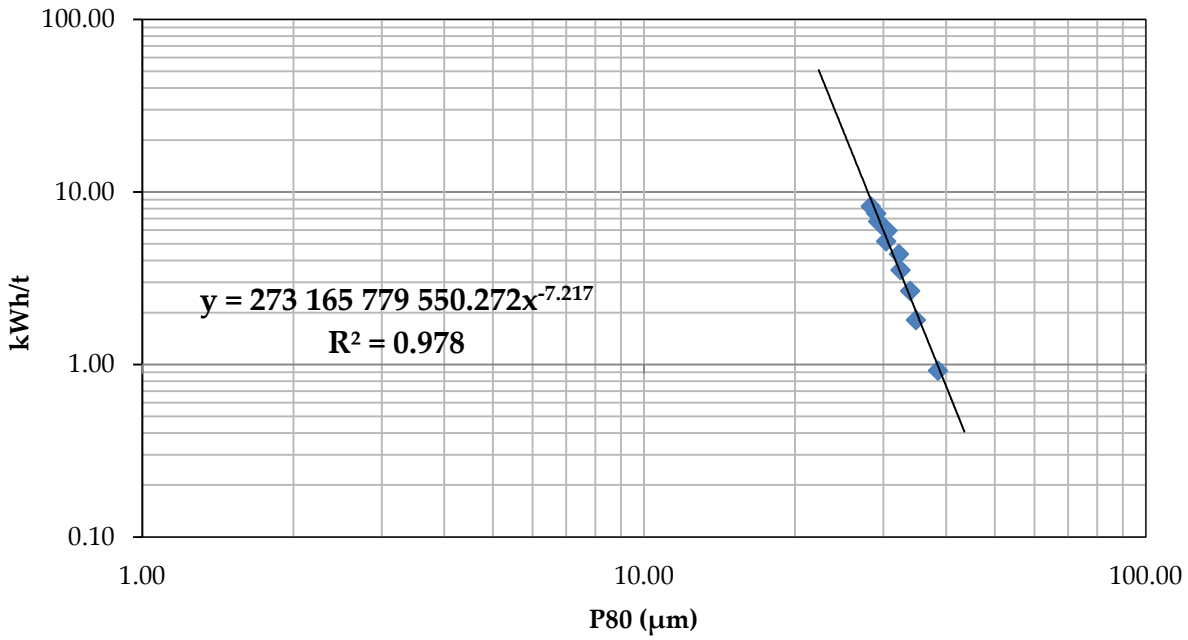

Figure A.23: Signature plot low stress energy

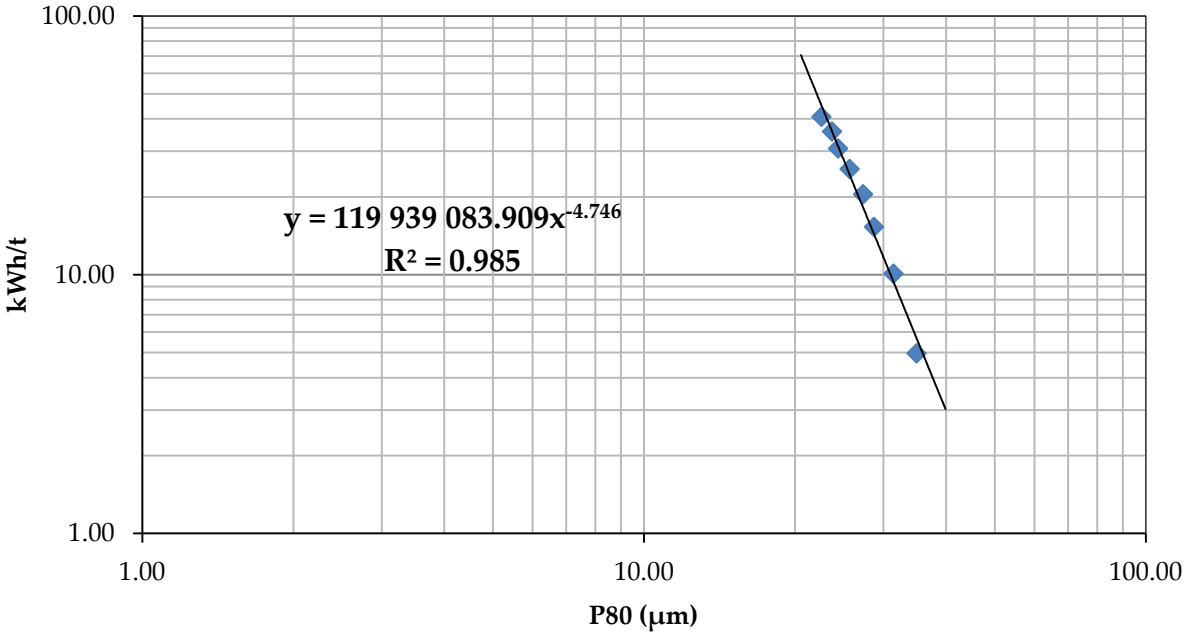

Figure A.24: Signature plot high stress energy

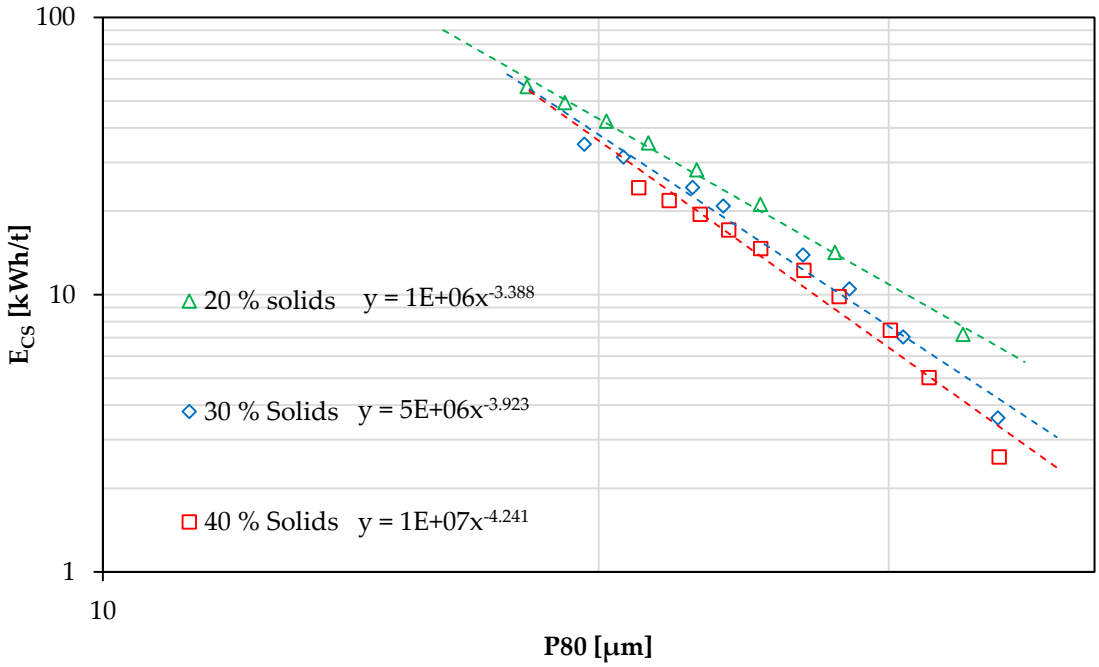

Figure A.25: Signature plots at varying % solids

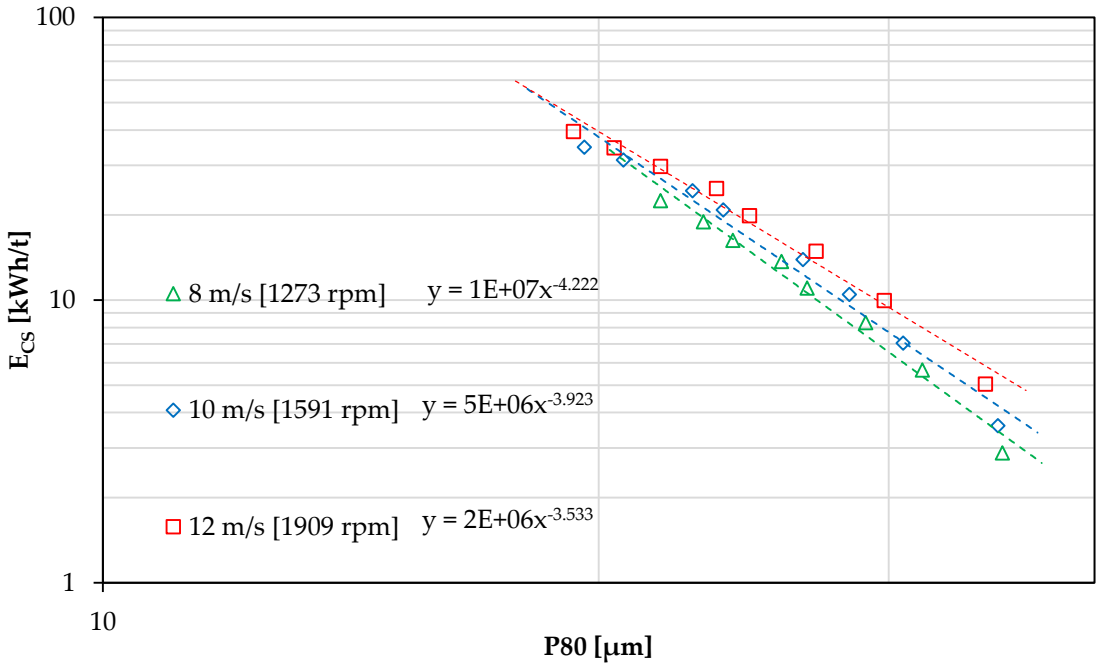

Figure A.26: Signature plots at varying stirrer speeds

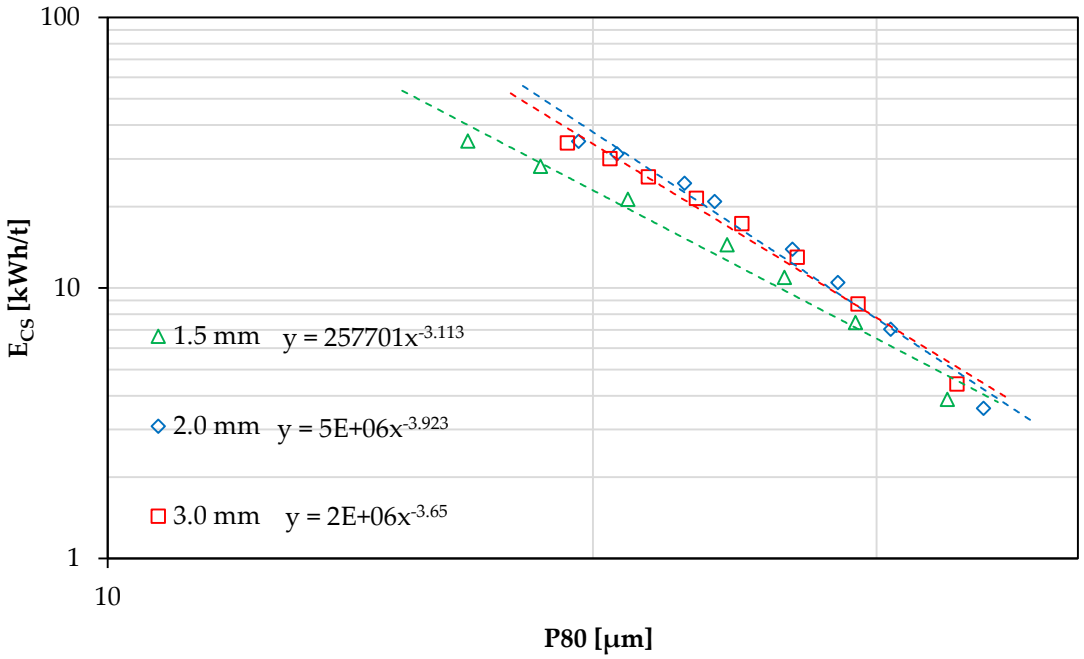

Figure A.27: Signature plots at varying grinding media sizes

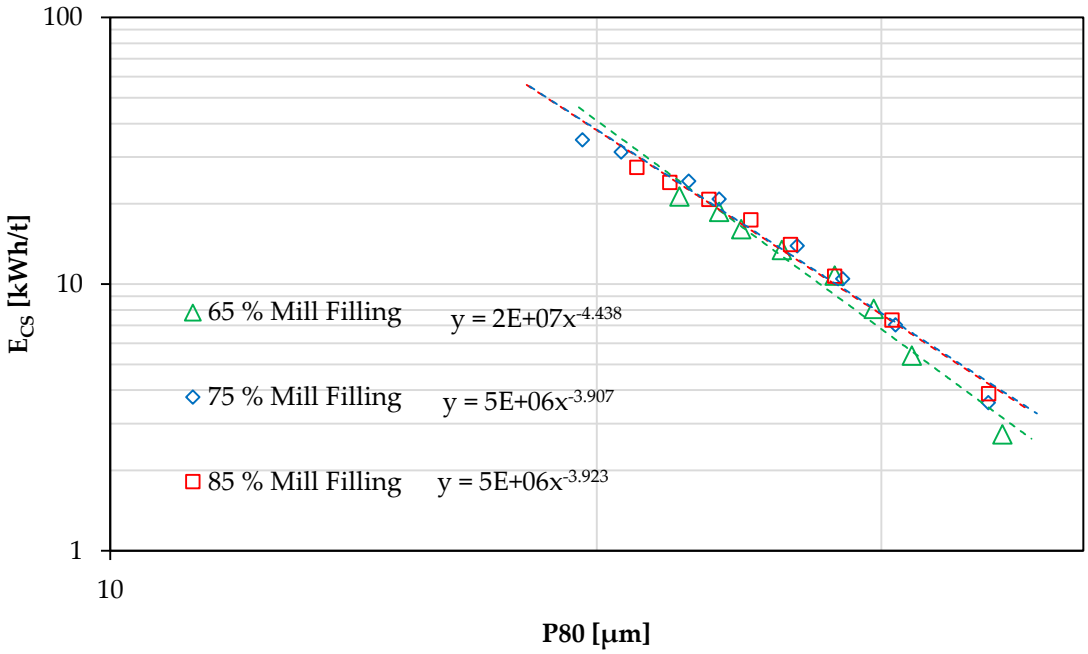

Figure A.28: Signature plots at varying % mill fillings

Tables A.1: Interpolation differences

Run 1	P80			
kWh/t	Linear Interpolation	Signature Plot	Absolute Difference	% Difference
10.00	27.50	26.69	0.80	0.03
20.00	23.11	22.64	0.47	0.02
30.00	19.89	20.55	0.67	0.03
50.00	Extrapolate	18.20		

Run 2	P80			
kWh/t	Linear Interpolation	Signature Plot	Absolute Difference	% Difference
10.00	26.10	25.51	0.59	0.02
20.00	Extrapolate	21.92		
30.00	Extrapolate	20.05		
50.00	Extrapolate	17.93		

Run 3	P80			
kWh/t	Linear Interpolation	Signature Plot	Absolute Difference	% Difference
10.00	26.06	25.89	0.17	0.01
20.00	Extrapolate	22.88		
30.00	Extrapolate	21.28		
50.00	Extrapolate	19.43		

Run 4	P80			
kWh/t	Linear Interpolation	Signature Plot	Absolute Difference	% Difference
10.00	25.35	25.03	0.32	0.01
20.00	Extrapolate	21.49		
30.00	Extrapolate	19.65		
50.00	Extrapolate	17.57		

Run 5	P80			
kWh/t	Linear Interpolation	Signature Plot	Absolute Difference	% Difference
10.00	26.39	25.09	1.29	0.05
20.00	20.45	20.42	0.03	0.00
30.00	Extrapolate	18.10		
50.00	Extrapolate	15.55		

Run 6	P80			
kWh/t	Linear Interpolation	Signature Plot	Absolute Difference	% Difference
10.00	28.44	27.86	0.58	0.02
20.00	24.01	24.33	0.32	0.01
30.00	Extrapolate	22.47		
50.00	Extrapolate	20.33		

Run 7	P80			
kWh/t	Linear Interpolation	Signature Plot	Absolute Difference	% Difference
10.00	29.46	29.08	0.38	0.01
20.00	23.45	23.26	0.19	0.01
30.00	20.81	20.41	0.39	0.02
50.00	17.18	17.31	0.14	0.01

Run 8	P80			
kWh/t	Linear Interpolation	Signature Plot	Absolute Difference	% Difference
10.00	30.73	30.86	0.12	0.00
20.00	25.66	25.44	0.22	0.01
30.00	23.26	22.72	0.54	0.02
50.00	19.87	19.71	0.16	0.01

Run 9	P80			
kWh/t	Linear Interpolation	Signature Plot	Absolute Difference	% Difference
10.00	30.76	30.03	0.73	0.02
20.00	25.32	24.86	0.46	0.02
30.00	22.42	22.26	0.16	0.01
50.00	19.43	19.37	0.06	0.00

Run 10	P80			
kWh/t	Linear Interpolation	Signature Plot	Absolute Difference	% Difference
10.00	26.45	25.67	0.78	0.03
20.00	Extrapolate	22.08		
30.00	Extrapolate	20.22		
50.00	Extrapolate	18.09		

Run 11	P80			
kWh/t	Linear Interpolation	Signature Plot	Absolute Difference	% Difference
10.00	26.43	26.96	0.54	0.02
20.00	22.27	22.06	0.21	0.01
30.00	19.79	19.61	0.18	0.01
50.00	Extrapolate	16.92		

Run 12	P80			
kWh/t	Linear Interpolation	Signature Plot	Absolute Difference	% Difference
10.00	27.35	27.28	0.08	0.00
20.00	23.71	23.30	0.40	0.02
30.00	21.14	21.26	0.12	0.01
50.00	Extrapolate	18.93		

Run 13	P80			
kWh/t	Linear Interpolation	Signature Plot	Absolute Difference	% Difference
10.00	28.70	28.05	0.65	0.02
20.00	24.16	23.51	0.65	0.03
30.00	21.11	21.20	0.09	0.00
50.00	Extrapolate	18.61		

Run 14	P80			
kWh/t	Linear Interpolation	Signature Plot	Absolute Difference	% Difference
10.00	28.96	28.08	0.88	0.03
20.00	23.82	23.16	0.66	0.03
30.00	20.56	20.69	0.13	0.01
50.00	Extrapolate	17.95		

Run 15	P80			
kWh/t	Linear Interpolation	Signature Plot	Absolute Difference	% Difference
10.00	27.06	26.12	0.94	0.03
20.00	21.63	20.91	0.73	0.03
30.00	18.06	18.35	0.29	0.02
50.00	Extrapolate	15.58		

Run 16	P80			
kWh/t	Linear Interpolation	Signature Plot	Absolute Difference	% Difference
10.00	28.57	28.14	0.43	0.02
20.00	23.80	23.57	0.23	0.01
30.00	Extrapolate	21.24		
50.00	Extrapolate	18.64		

Run 17	P80			
kWh/t	Linear Interpolation	Signature Plot	Absolute Difference	% Difference
10.00	29.80	29.49	0.30	0.01
20.00	24.66	24.24	0.43	0.02
30.00	21.73	21.61	0.12	0.01
50.00	Extrapolate	18.70		

Run 18	P80			
kWh/t	Linear Interpolation	Signature Plot	Absolute Difference	% Difference
10.00	27.89	27.05	0.84	0.03
20.00	22.83	22.97	0.14	0.01
30.00	Extrapolate	20.88		
50.00	Extrapolate	18.51		

Run 19	P80			
kWh/t	Linear Interpolation	Signature Plot	Absolute Difference	% Difference
10.00	27.63	27.13	0.51	0.02
20.00	22.76	23.02	0.26	0.01
30.00	Extrapolate	20.91		
50.00	Extrapolate	18.53		

Run 20	P80			
kWh/t	Linear Interpolation	Signature Plot	Absolute Difference	% Difference
10.00	31.10	30.78	0.32	0.01
20.00	25.54	25.09	0.45	0.02
30.00	22.55	22.26	0.29	0.01
50.00	18.98	19.14	0.17	0.01

Run 21	P80			
kWh/t	Linear Interpolation	Signature Plot	Absolute Difference	% Difference
10.00	28.54	27.50	1.04	0.04
20.00	23.15	23.52	0.37	0.02
30.00	Extrapolate	21.47		
50.00	Extrapolate	19.13		

Run 22	P80			
kWh/t	Linear Interpolation	Signature Plot	Absolute Difference	% Difference
10.00	28.50	27.99	0.51	0.02
20.00	23.73	23.15	0.58	0.02
30.00	20.50	20.72	0.21	0.01
50.00	Extrapolate	18.01		

SE 001	P80			
kWh/t	Linear Interpolation	Signature Plot	Absolute Difference	% Difference
10.00	Extrapolate	27.93		
20.00	Extrapolate	25.37		
30.00	Extrapolate	23.99		
50.00	Extrapolate	22.35		

SE 002	P80			
kWh/t	Linear Interpolation	Signature Plot	Absolute Difference	% Difference
10.00	31.44	31.01	0.42	0.01
20.00	27.43	26.80	0.63	0.02
30.00	24.53	24.61	0.08	0.00
50.00	Extrapolate	22.09		

Appendix B – PSD's

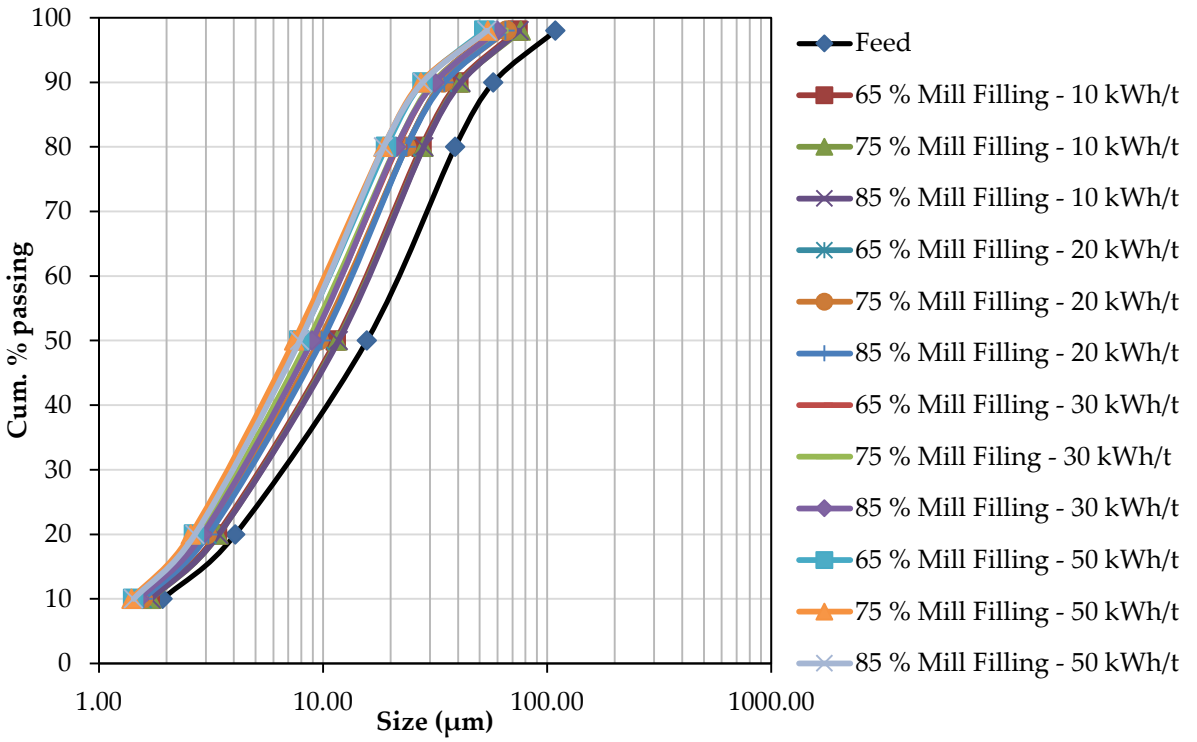

Figure B.1: PSD's of % mill filling versus specific energy input

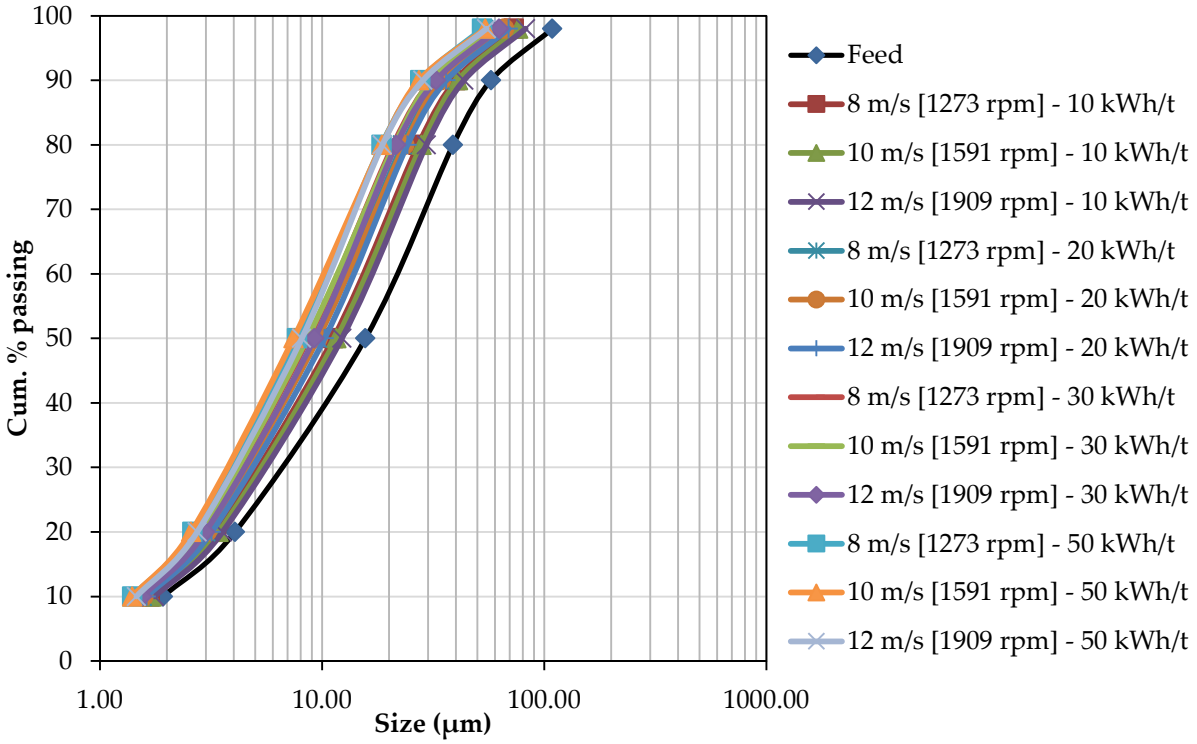

Figure B.2: PSD's of stirrer speed versus specific energy input

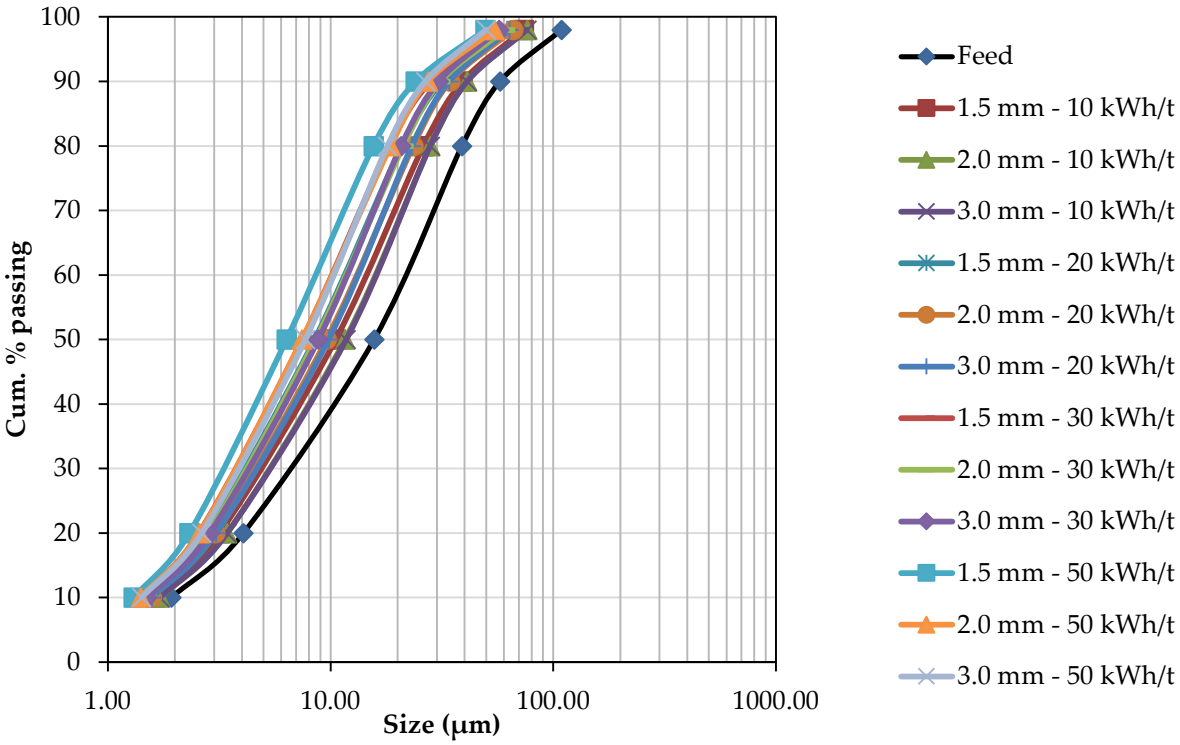

Figure B.3: PSD's of media size versus specific energy input

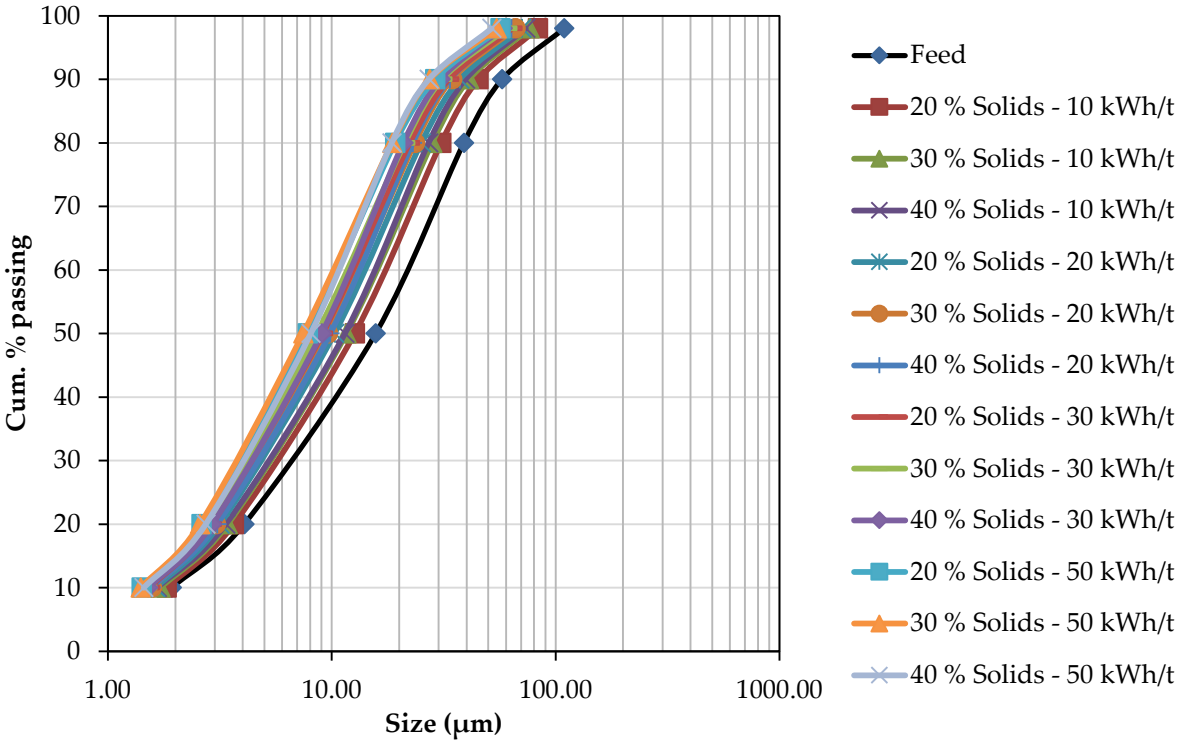

Figure B.4: PSD's of solids concentration versus specific energy input

Appendix C – ANOVA tables

Regression model – 10 kWh/t:

Table C.1: ANOVA table – P80 10 kWh/t

Source of variation	Sum of squares	Degrees of freedom	Mean square	F-value	P-value
Block	3.97	1	3.97		
Model	55.79	7	7.97	44.70	< 0.0001
A-Tip Speed	13.00	1	13.00	72.89	< 0.0001
B-% Solids	21.78	1	21.78	122.13	< 0.0001
C-Media Size	6.24	1	6.24	34.98	< 0.0001
AB	1.48	1	1.48	8.29	0.0129
AC	1.14	1	1.14	6.38	0.0253
B^2	1.09	1	1.09	6.09	0.0283
C^2	1.53	1	1.53	8.57	0.0118
Residual	2.32	13	0.18		
Lack of Fit	2.32	12	0.19	289.70	0.0459
Pure Error	0.00	1	0.00		
Cor Total	62.08	21			

Table C.2: ANOVA table - rates 10 kWh/t

Source of variation	Sum of squares	Degrees of freedom	Mean square	F-value	P-value
Block	12.26	1	12.26		
Model	225.38	6	37.56	17.09	< 0.0001
A-Stirrer speed	44.62	1	44.62	20.30	0.0005
B-% Solids	110.03	1	110.03	50.07	< 0.0001
C-Media size	4.57	1	4.57	2.08	0.1711
D-% Mill filling	9.90	1	9.90	4.50	0.0521
AD	10.17	1	10.17	4.63	0.0494
CD	13.53	1	13.53	6.16	0.0264
Residual	30.77	14	2.20		
Lack of Fit	30.67	13	2.36	25.66	0.1535
Pure Error	0.09	1	0.09		
Cor Total	268.41	21			

Regression model – 20 kWh/t:

Table C.8 shows the ANOVA results for the 20 kWh/t energy input. Table C.3 shows the R^2 values at 20 kWh/t. The R^2 values are in reasonable agreement with each other. Figure D.2 shows the parity chart for this model.

Table C.3: R-Squared values - 20 kWh/t efficiency model

R-Squared	0.90
Adj R-Squared	0.86

Table C.4: R-Squared values - 20 kWh/t rate model

R-Squared	0.90
Adj R-Squared	0.88

The 20 kWh/t model equations are shown in Table C.5 and Table C.6.

Table C.5: Regression model equations - 20 kWh/t efficiency model

P80 – 20 kWh/t	=
24.07	(Intercept)
0.51	* Stirrer speed
-0.65	* % Solids
0.97	* Media size
0.38	* Stirrer speed * Media size
-1.61	* Media size^2

Table C.6: Regression model equations - 20 kWh/t rate model

Rates – 20 kWh/t	=
8.69	(Intercept)
1.84	* Stirrer speed
-3.12	* % Solids
1.05	* % Mill filling
-2.16	* % Mill filling^2

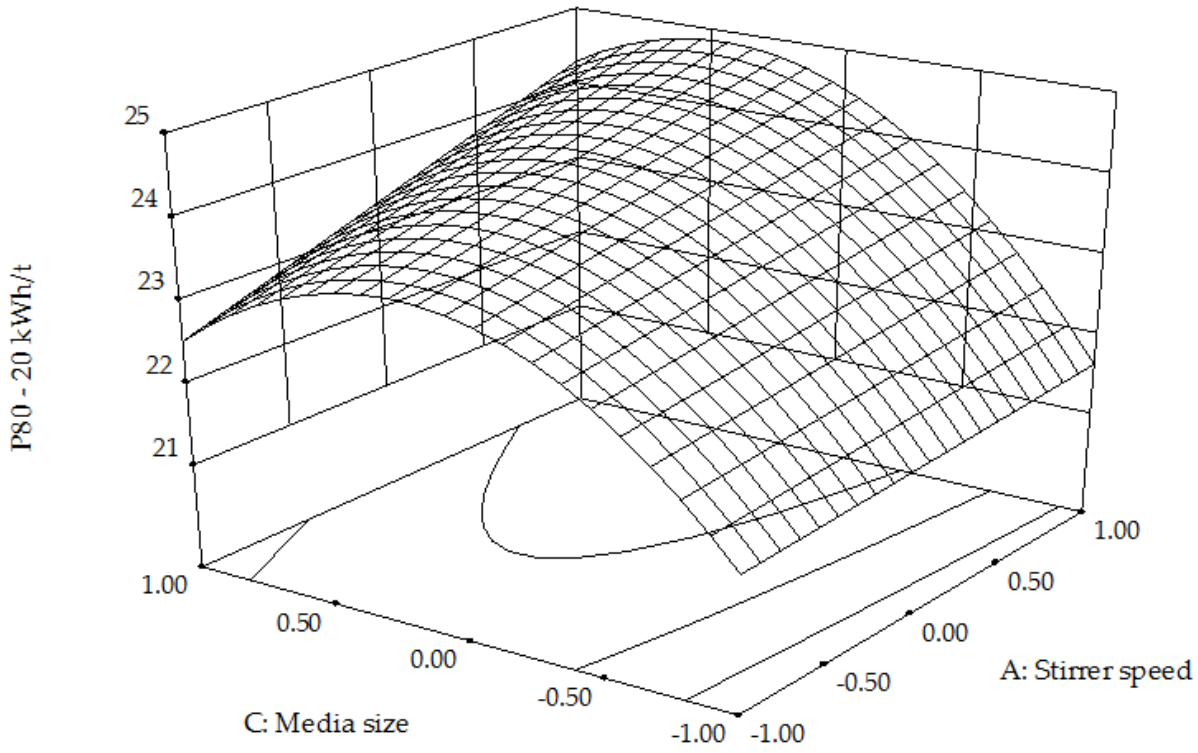

Figure C.1: Surface plots – P80 20 kWh/t (AC)

Table C.7: ANOVA table – P80 20 kWh/t

Source of Variation	Sum of Squares	Degrees of Freedom	Mean Square	F-value	P-value
Block	0.91	1	0.91		
Model	30.47	5	6.09	25.70	< 0.0001
A-Tip Speed	3.67	1	3.67	15.50	0.0013
B-% Solids	5.36	1	5.36	22.62	0.0003
C-Media Size	13.07	1	13.07	55.13	< 0.0001
AC	1.54	1	1.54	6.51	0.0222
C^2	4.12	1	4.12	17.39	0.0008
Residual	3.56	15	0.24		
Lack of Fit	3.50	14	0.25	4.18	0.3677
Pure Error	0.06	1	0.06		
Cor Total	34.94	21			

Table C.8: ANOVA table – rates 20 kWh/t

Source of Variation	Sum of Squares	Degrees of Freedom	Mean Square	F-value	P-value
Block	4.36	1	4.36		
Model	206.46	4	51.62	37.94	< 0.0001
A-Stirrer speed	47.35	1	47.35	34.80	< 0.0001
B-% Solids	136.32	1	136.32	100.19	< 0.0001
D-% Mill filling	15.35	1	15.35	11.28	0.0040
D^2	7.45	1	7.45	5.47	0.0326
Residual	21.77	16	1.36		
Lack of Fit	21.65	15	1.44	12.18	0.2216
Pure Error	0.12	1	0.12		
Cor Total	232.59	21			

Regression model – 30 kWh/t:

Table C.13 and Table C.14 shows the ANOVA results for the 30 kWh/t energy input. Table C.9 and Table C.11 shows the R^2 values at 30 kWh/t. The R^2 values are in reasonable agreement with each other. The parity chart for this model is shown in Figure D.4.

Table C.9: R-Squared values - 30 kWh/t efficiency model

R-Squared	0.91
Adj R-Squared	0.87

Table C.10: R-Squared values - 30 kWh/t rate model

R-Squared	0.92
Adj R-Squared	0.90

The 30 kWh/t model equation is shown in Table C.11.

Table C.11: Regression model - 30 kWh/t efficiency model

P80 - 30 kWh/t	=
21.88	(Intercept)
0.22	* Stirrer speed
-0.35	* % Solids
0.95	* Media size
-0.27	* % Mill filling
0.39	* Stirrer speed * Media size
-0.30	* % Solids * % Mill filling
-1.75	* Media size^2

Table C.12: Regression model - 30 kWh/t rate model

Rates - 30 kWh/t	=
7.28	(Intercept)
1.62	* Stirrer speed
-2.71	* % Solids
0.99	* % Mill filling
-1.90	* % Mill filling^2

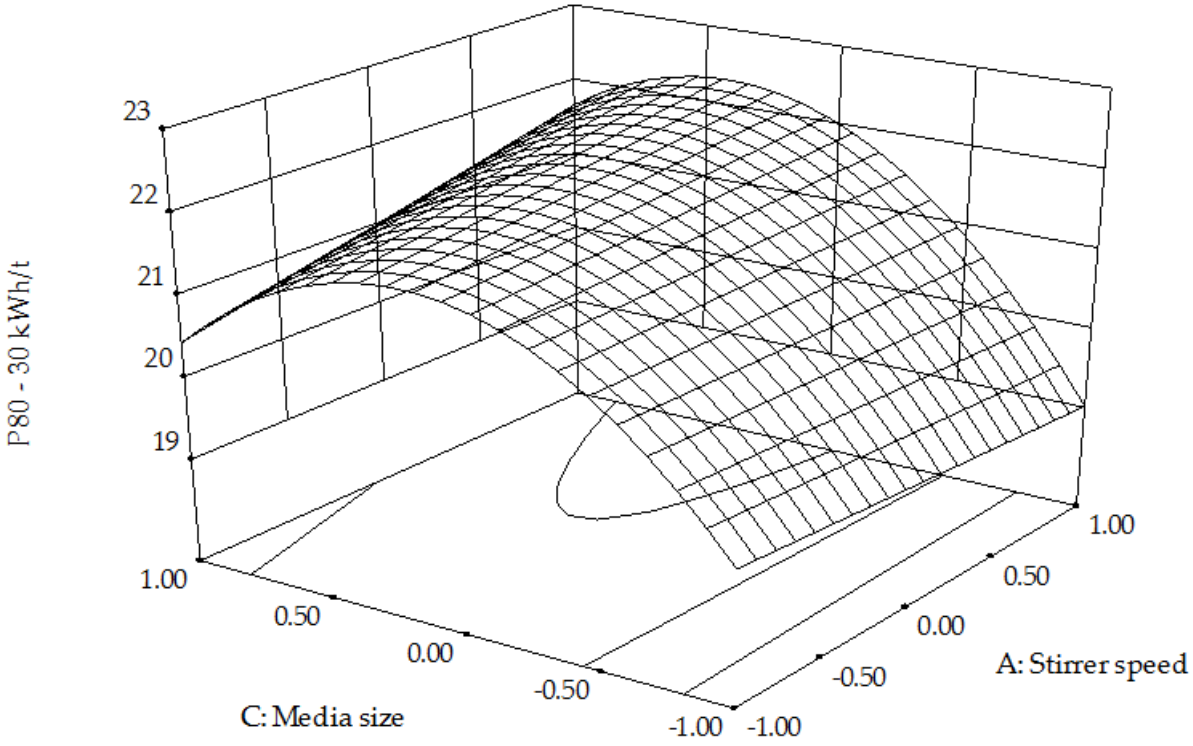

Figure C.2: Surface plots - P80 30 kWh/t (AC)

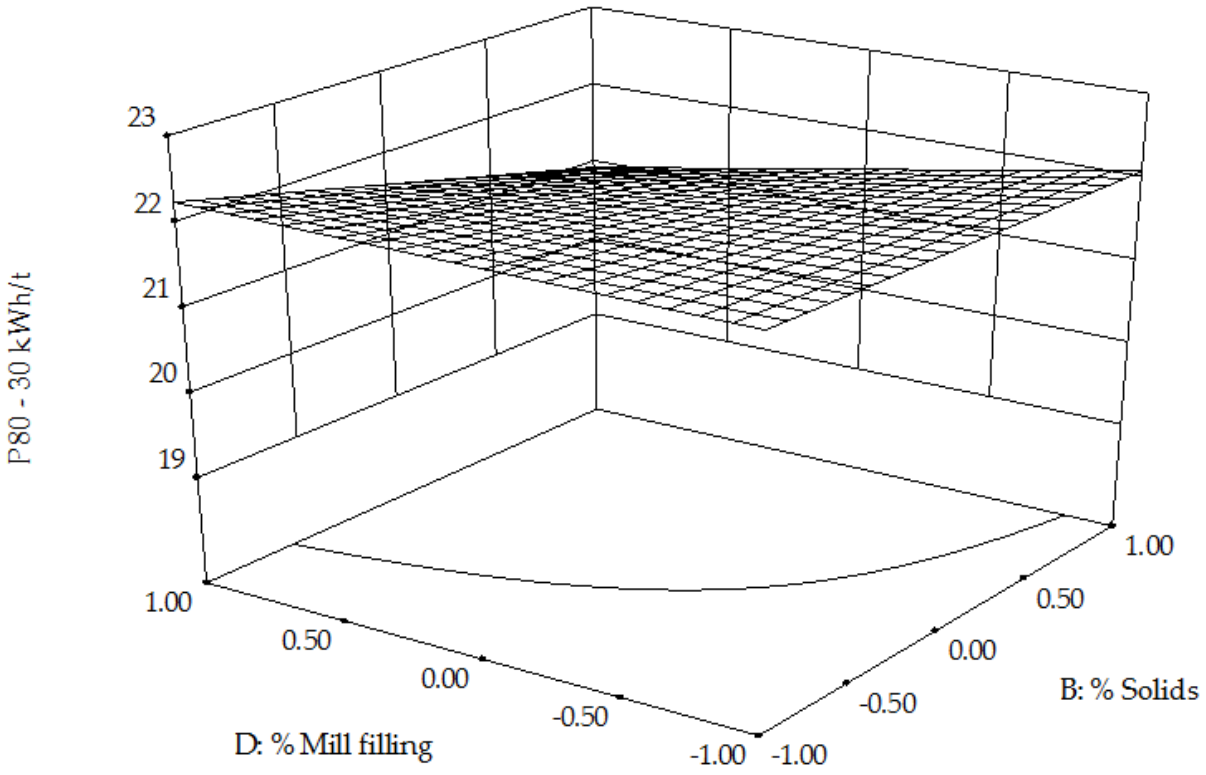

Figure C.3: Surface plots – P80 (BD)

Table C.13: ANOVA table – P80 30 kWh/t

Source of Variation	Sum of Squares	Degrees of Freedom	Mean Square	F-value	P-value
Block	0.23	1	0.23		
Model	27.44	7	3.92	19.56	< 0.0001
A-Tip Speed	0.62	1	0.62	3.10	0.1019
B-% Solids	1.55	1	1.55	7.72	0.0157
C-Media Size	11.54	1	11.54	57.62	< 0.0001
D-% Mill Filling	0.92	1	0.92	4.59	0.0517
AC	1.68	1	1.68	8.36	0.0126
BD	0.98	1	0.98	4.87	0.0459
C^2	4.88	1	4.88	24.37	0.0003
Residual	2.60	13	0.20		
Lack of Fit	2.48	12	0.21	1.60	0.5555
Pure Error	0.13	1	0.13		
Corrected Total	30.27	21			

Table C.14: ANOVA table – rates 30 kWh/t

Source of Variation	Sum of Squares	Degrees of Freedom	Mean Square	F-value	P-value
Block	2.39	1	2.39		
Model	159.19	4	39.80	45.13	< 0.0001
A-Stirrer speed	36.92	1	36.92	41.87	< 0.0001
B-% Solids	102.81	1	102.81	116.59	< 0.0001
D-% Mill filling	13.67	1	13.67	15.50	0.0012
D^2	5.79	1	5.79	6.56	0.0209
Residual	14.11	16	0.88		
Lack of Fit	14.01	15	0.93	9.55	0.2493
Pure Error	0.10	1	0.10		
Cor Total	175.69	21			

Power:

Table C.15: ANOVA table – power model

Source	Sum of Squares	Degrees of Freedom	Mean Squares	F - Value	P - Value
Block	250.50	1	250.50		
Model	9853.50	5	1970.70	51.01	< 0.0001
A-Stirrer speed	7067.25	1	7067.25	182.92	< 0.0001
B-% Solids	293.43	1	293.43	7.59	0.0147
C-Media size	457.85	1	457.85	11.85	0.0036
D-% Mill filling	1950.67	1	1950.67	50.49	< 0.0001
D^2	458.25	1	458.25	11.86	0.0036
Residual	579.54	15	38.64		
Lack of Fit	578.85	14	41.35	60.07	0.1008
Pure Error	0.69	1	0.69		
Cor Total	10683.54	21			

Appendix D – Residual and parity charts

20 kWh/t:

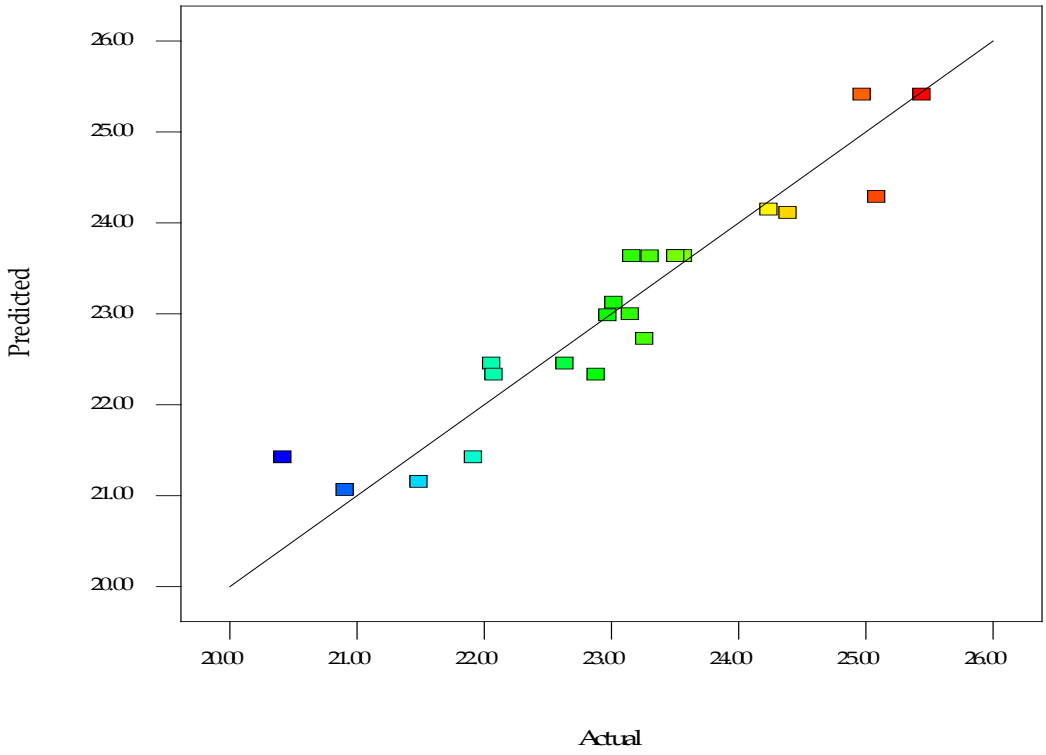

Figure D.1: Predicted vs Actual parity chart – P80 20 kWh/t

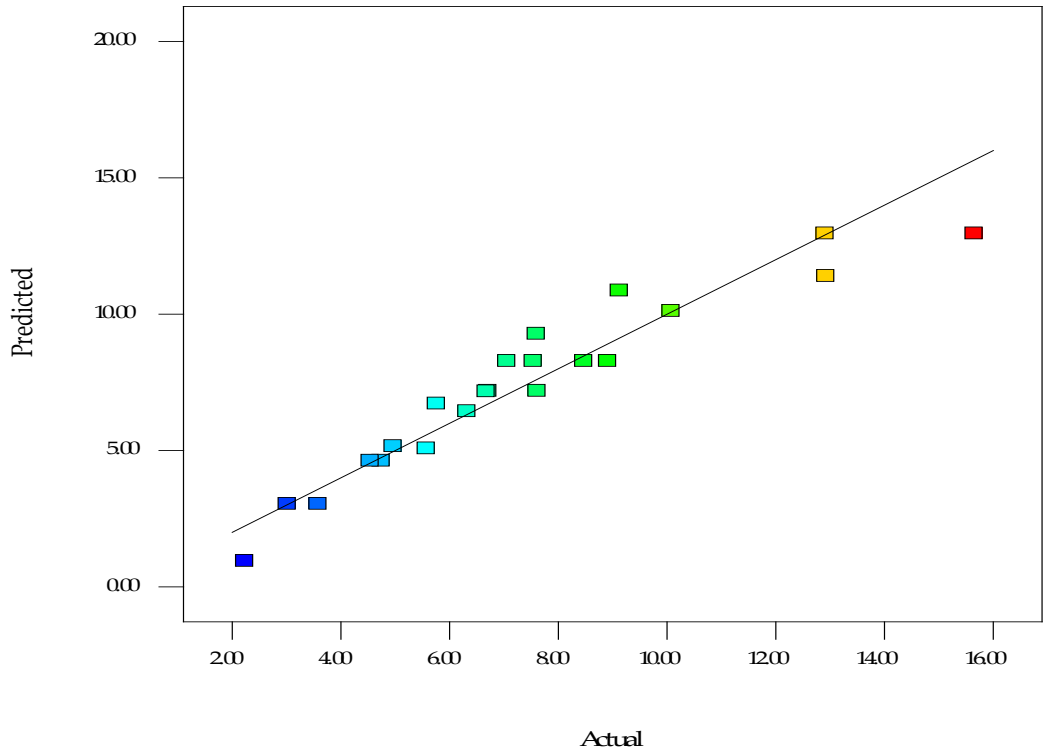

Figure D.2: Predicted versus Actual parity chart – rates 20 kWh/t

30 kWh/t:

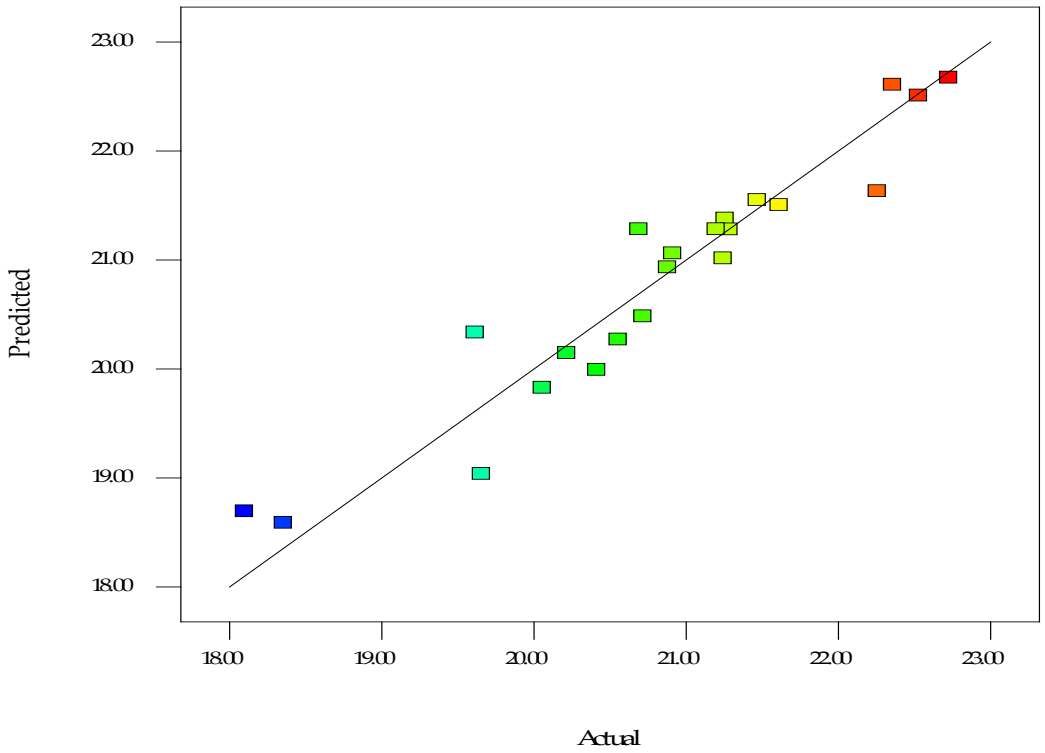

Figure D.3: Predicted vs Actual parity chart – P80 30 kWh/t

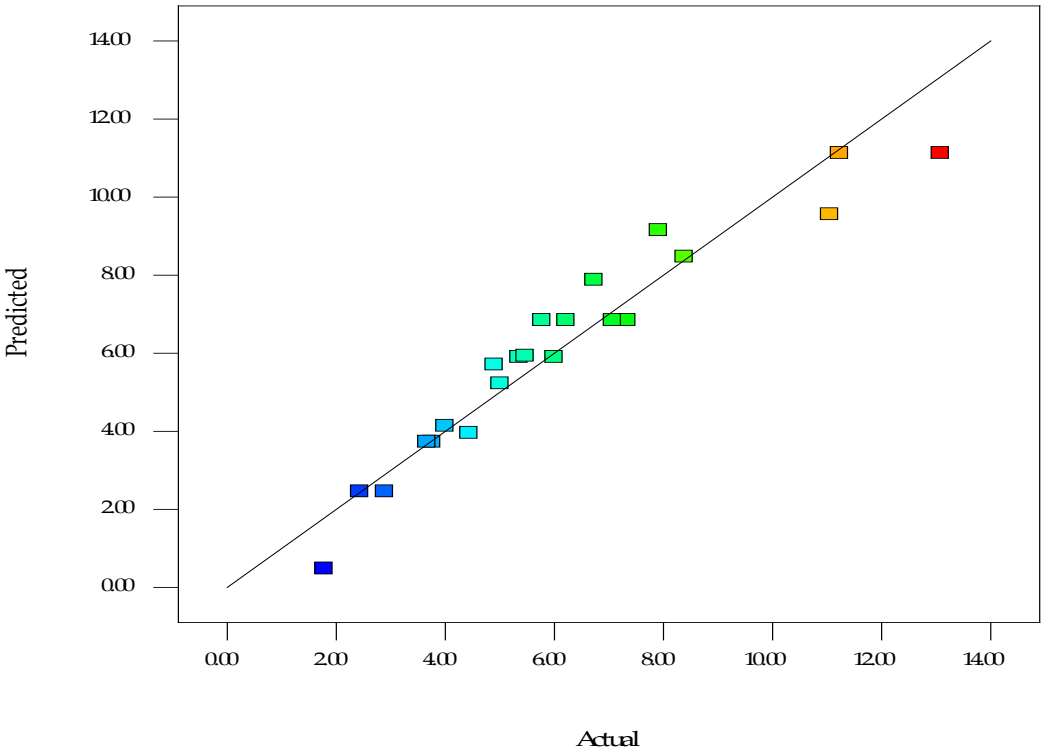

Figure D.4: Predicted versus Actual parity chart – rates 30 kWh/t

Appendix E – Residence time vs E_{cs} curve interpolation plot

The residence time data used in this thesis were interpolated using the curves shown in Figure E.1.

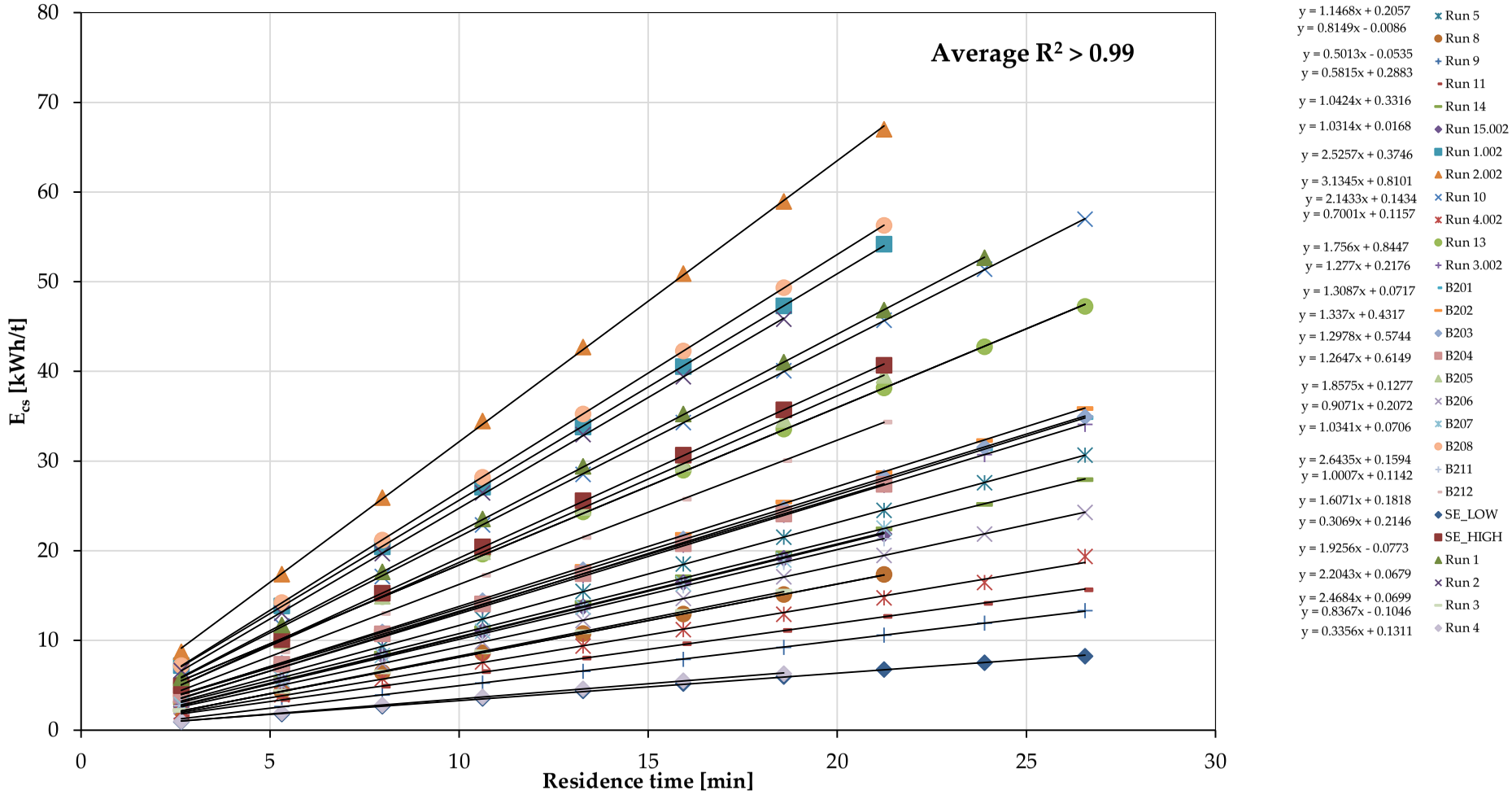

Figure E.1: Residence time vs Specific energy input

Appendix F – Examples of raw data sheets

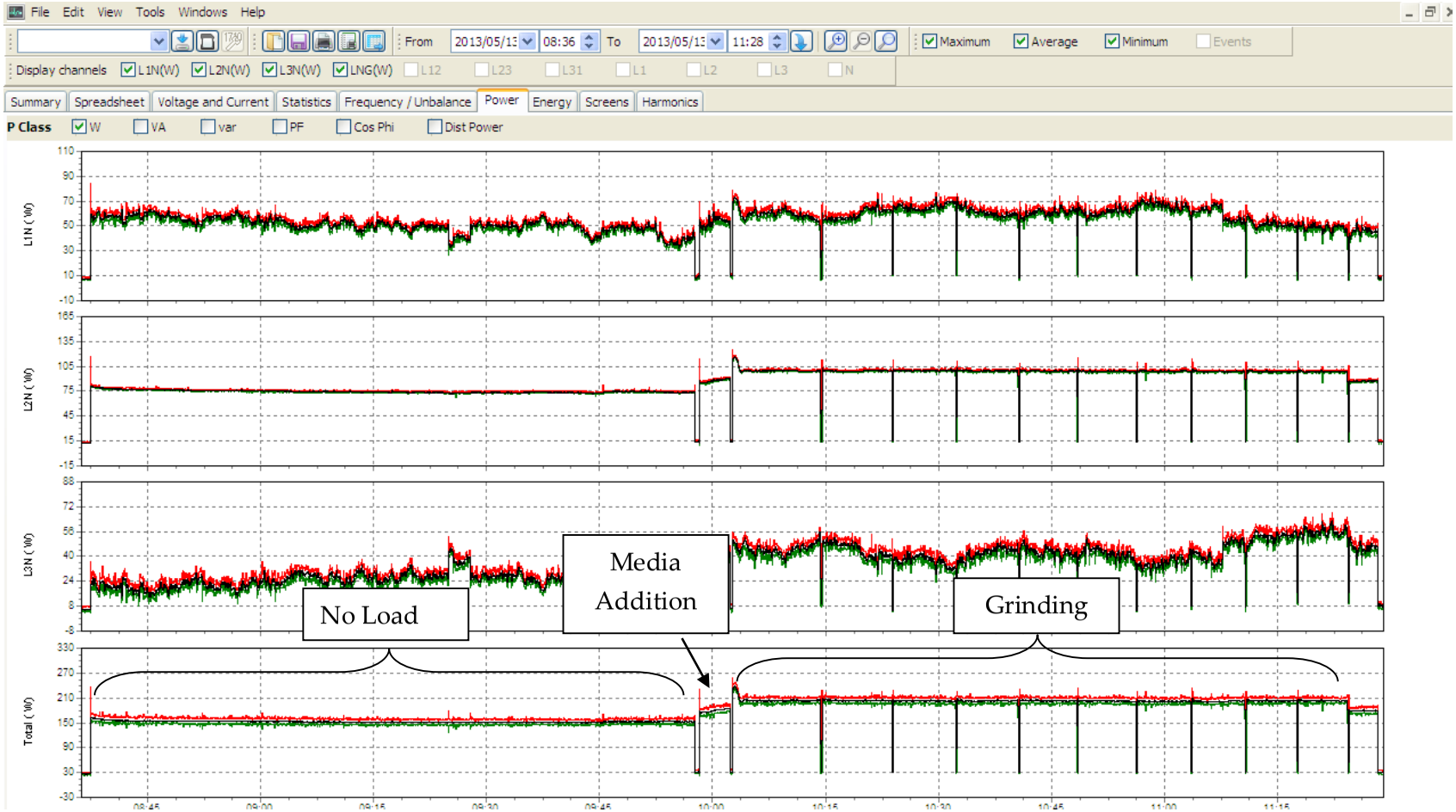

Figure F.1: Example of fluke power data logger output

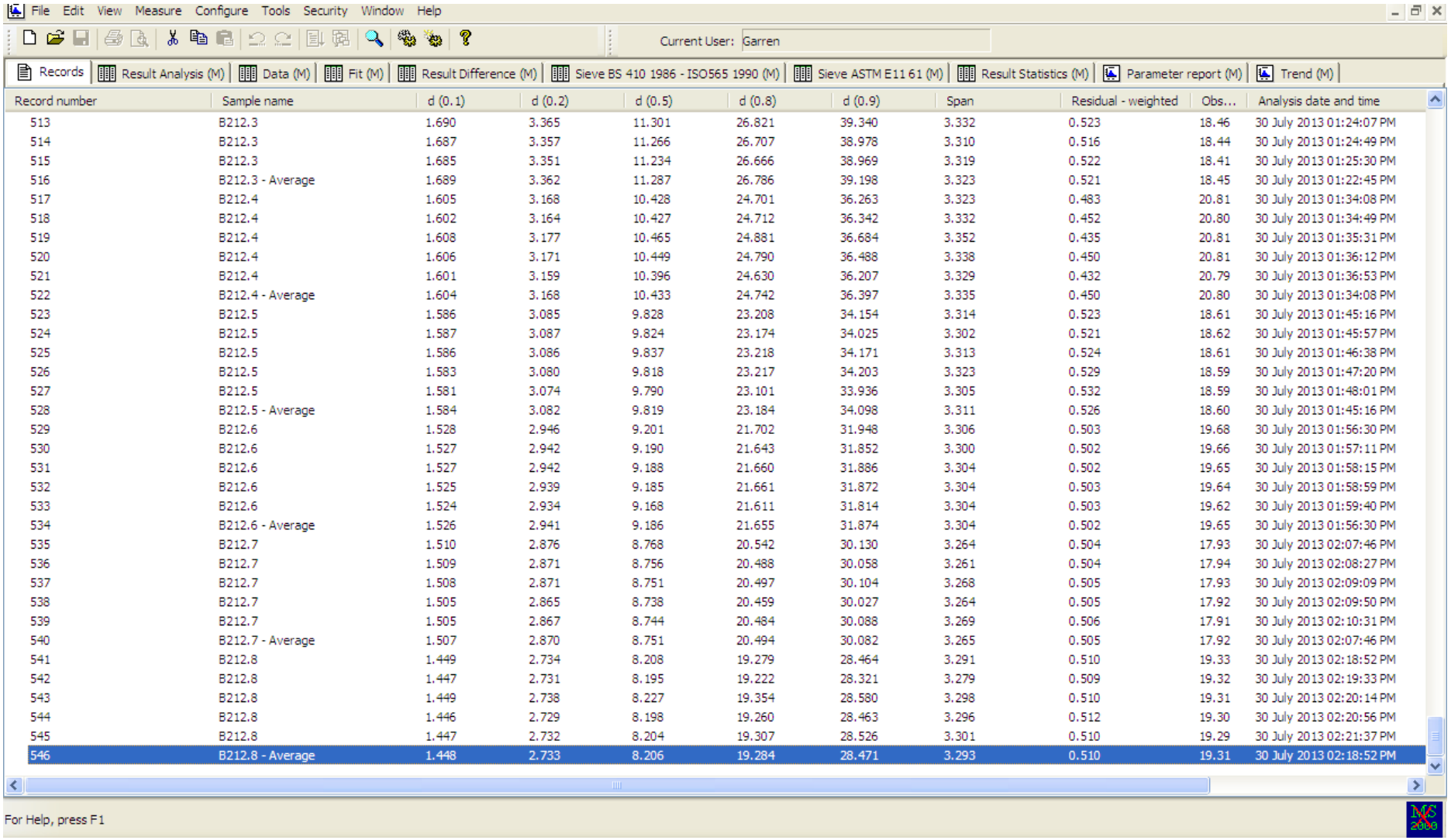

Record number	Sample name	d (0.1)	d (0.2)	d (0.5)	d (0.8)	d (0.9)	Span	Residual - weighted	Obs...	Analysis date and time
513	B212.3	1.690	3.365	11.301	26.821	39.340	3.332	0.523	18.46	30 July 2013 01:24:07 PM
514	B212.3	1.687	3.357	11.266	26.707	38.978	3.310	0.516	18.44	30 July 2013 01:24:49 PM
515	B212.3	1.685	3.351	11.234	26.666	38.969	3.319	0.522	18.41	30 July 2013 01:25:30 PM
516	B212.3 - Average	1.689	3.362	11.287	26.786	39.198	3.323	0.521	18.45	30 July 2013 01:22:45 PM
517	B212.4	1.605	3.168	10.428	24.701	36.263	3.323	0.483	20.81	30 July 2013 01:34:08 PM
518	B212.4	1.602	3.164	10.427	24.712	36.342	3.332	0.452	20.80	30 July 2013 01:34:49 PM
519	B212.4	1.608	3.177	10.465	24.881	36.684	3.352	0.435	20.81	30 July 2013 01:35:31 PM
520	B212.4	1.606	3.171	10.449	24.790	36.488	3.338	0.450	20.81	30 July 2013 01:36:12 PM
521	B212.4	1.601	3.159	10.396	24.630	36.207	3.329	0.432	20.79	30 July 2013 01:36:53 PM
522	B212.4 - Average	1.604	3.168	10.433	24.742	36.397	3.335	0.450	20.80	30 July 2013 01:34:08 PM
523	B212.5	1.586	3.085	9.828	23.208	34.154	3.314	0.523	18.61	30 July 2013 01:45:16 PM
524	B212.5	1.587	3.087	9.824	23.174	34.025	3.302	0.521	18.62	30 July 2013 01:45:57 PM
525	B212.5	1.586	3.086	9.837	23.218	34.171	3.313	0.524	18.61	30 July 2013 01:46:38 PM
526	B212.5	1.583	3.080	9.818	23.217	34.203	3.323	0.529	18.59	30 July 2013 01:47:20 PM
527	B212.5	1.581	3.074	9.790	23.101	33.936	3.305	0.532	18.59	30 July 2013 01:48:01 PM
528	B212.5 - Average	1.584	3.082	9.819	23.184	34.098	3.311	0.526	18.60	30 July 2013 01:45:16 PM
529	B212.6	1.528	2.946	9.201	21.702	31.948	3.306	0.503	19.68	30 July 2013 01:56:30 PM
530	B212.6	1.527	2.942	9.190	21.643	31.852	3.300	0.502	19.66	30 July 2013 01:57:11 PM
531	B212.6	1.527	2.942	9.188	21.660	31.886	3.304	0.502	19.65	30 July 2013 01:58:15 PM
532	B212.6	1.525	2.939	9.185	21.661	31.872	3.304	0.503	19.64	30 July 2013 01:58:59 PM
533	B212.6	1.524	2.934	9.168	21.611	31.814	3.304	0.503	19.62	30 July 2013 01:59:40 PM
534	B212.6 - Average	1.526	2.941	9.186	21.655	31.874	3.304	0.502	19.65	30 July 2013 01:56:30 PM
535	B212.7	1.510	2.876	8.768	20.542	30.130	3.264	0.504	17.93	30 July 2013 02:07:46 PM
536	B212.7	1.509	2.871	8.756	20.488	30.058	3.261	0.504	17.94	30 July 2013 02:08:27 PM
537	B212.7	1.508	2.871	8.751	20.497	30.104	3.268	0.505	17.93	30 July 2013 02:09:09 PM
538	B212.7	1.505	2.865	8.738	20.459	30.027	3.264	0.505	17.92	30 July 2013 02:09:50 PM
539	B212.7	1.505	2.867	8.744	20.484	30.088	3.269	0.506	17.91	30 July 2013 02:10:31 PM
540	B212.7 - Average	1.507	2.870	8.751	20.494	30.082	3.265	0.505	17.92	30 July 2013 02:07:46 PM
541	B212.8	1.449	2.734	8.208	19.279	28.464	3.291	0.510	19.33	30 July 2013 02:18:52 PM
542	B212.8	1.447	2.731	8.195	19.222	28.321	3.279	0.509	19.32	30 July 2013 02:19:33 PM
543	B212.8	1.449	2.738	8.227	19.354	28.580	3.298	0.510	19.31	30 July 2013 02:20:14 PM
544	B212.8	1.446	2.729	8.198	19.260	28.463	3.296	0.512	19.30	30 July 2013 02:20:56 PM
545	B212.8	1.447	2.732	8.204	19.307	28.526	3.301	0.510	19.29	30 July 2013 02:21:37 PM
546	B212.8 - Average	1.448	2.733	8.206	19.284	28.471	3.293	0.510	19.31	30 July 2013 02:18:52 PM

Figure F.2: Example of Malvern raw data

EBE Faculty: Assessment of Ethics in Research Projects

Any person planning to undertake research in the Faculty of Engineering and the Built Environment at the University of Cape Town is required to complete this form before collecting or analysing data. When completed it should be submitted to the supervisor (where applicable) and from there to the Head of Department. If any of the questions below have been answered YES, and the applicant is NOT a fourth year student, the Head should forward this form for approval by the Faculty EIR committee: submit to Ms Zakiya Chikte (Zakiya.chikte@uct.ac.za); New EBE Building, Ph 021 650 5739). Students must include a copy of the completed form with the dissertation/thesis when it is submitted for examination.

Name of Principal Researcher/Student: GARREN EDWARDS **Department:** Chemical Engineering

If a Student: **Degree:** MSc. (chem eng) **Supervisor:** Andre vd Westhuizen

If a Research Contract indicate source of funding/sponsorship:

Research Project Title: Investigation of operating parameters in a vertical stirred mill.

Overview of ethics issues in your research project:

Question 1: Is there a possibility that your research could cause harm to a third party (i.e. a person not involved in your project)?	YES	(NO)
Question 2: Is your research making use of human subjects as sources of data? If your answer is YES, please complete Addendum 2.	YES	(NO)
Question 3: Does your research involve the participation of or provision of services to communities? If your answer is YES, please complete Addendum 3.	YES	(NO)
Question 4: If your research is sponsored, is there any potential for conflicts of interest? If your answer is YES, please complete Addendum 4.	YES	(NO)

If you have answered YES to any of the above questions, please append a copy of your research proposal, as well as any interview schedules or questionnaires (Addendum 1) and please complete further addenda as appropriate.

I hereby undertake to carry out my research in such a way that

- there is no apparent legal objection to the nature or the method of research; and
- the research will not compromise staff or students or the other responsibilities of the University;
- the stated objective will be achieved, and the findings will have a high degree of validity;
- limitations and alternative interpretations will be considered;
- the findings could be subject to peer review and publicly available; and
- I will comply with the conventions of copyright and avoid any practice that would constitute plagiarism.

Signed by:

	Full name and signature	Date
Principal Researcher/Student:	GARREN EDWARDS	08/03/2016

This application is approved by:

Supervisor (if applicable):		08 Dec '16
HOD (or delegated nominee): Final authority for all assessments with NO to all questions and for all undergraduate research.		8/12/2016
Chair : Faculty EIR Committee For applicants other than undergraduate students who have answered YES to any of the above questions.		